DEVELOPMENT OF A REALISTIC SOIL-STRUCTURE INTERACTION SYSTEM

BY

MD. SHAFIQUL BARI

A thesis submitted to the Department of Civil Engineering of Bangladesh University of Engineering and Technology, Dhaka in partial fulfillment of the requirement for the degree

of

MASTER OF SCIENCE IN CIVIL ENGINEERING

July, 1996

DEVELOPMENT OF A REALISTIC SOIL-STRUCTURE INTERACTION SYSTEM

BY

MD. SHAFIQUL BARI

A thesis approved as to the style and content by:

Dr. Salek M. Seraj
Asstt. Professor,
Department of Civil Engineering,
BUET, Dhaka 1000

: Chairman
(Supervisor)

Dr. Md. Saiful Alam Siddiquee
Asstt. Professor
Department of Civil Engineering,
BUET, Dhaka 1000

: Member
(Co-Supervisor)

Dr. M. Azadur Rahman
Professor & Head
Department of Civil Engineering,
BUET, Dhaka 1000

: Member

Dr. Alamgir Habib
Professor,
Department of Civil Engineering,
BUET, Dhaka 1000

: Member

Dr. Ahsanul Jalil Khan
Managing Director
Construction and Development Co.
44, Dhanmondi, Road No. 4A
Dhaha.

: Member

DECLARATION

I hereby certify that the research work reported in this thesis has been performed by me and that this work has not been submitted elsewhere for any other purpose (except for publication).

July, 1996

মো: শফিকুল বারী

(Md. Shafiqul Bari)

ACKNOWLEDGEMENT

The author wishes to express his deepest gratitude to Dr. Salek M. Seraj, Assistant Professor, Department of Civil Engineering, BUET for his continuous guidance, invaluable suggestions and affectionate encouragement at every stage of this study.

The author wishes to express his profound gratitude to Dr. Md. Saiful Alam Siddiquee, Assistant Professor, Department of Civil Engineering, BUET for the interest taken by him in this research and for his constant encouragement and guidance.

The author is grateful to Professor M. Azadur Rahman, Head, Department of Civil Engineering, BUET for his encouragement and co-operation.

Acknowledgement is also made to Professor A.M.M. Safiullah and Mr. Md. Shahjahan Khan for rendering their helping hands during the course of this study.

The author expresses his thanks to Dr. A. B. M. Badruzzaman for his co-operation in using the computer facility. The author is thankful to Mr. M. A. Malek for the care he has taken in typing the manuscript.

ABSTRACT

In this study attempts have been made to construct an analytical model that closely resembles the real field behaviour of Dhaka soil. In developing the model, the critical state program - CRISP - has been used in its core and the formulation of interface element has been incorporated into its computer code. Whereas the ensuing model is expected to work well with various types of soil-structure interaction systems, the model has been developed and tested against deep (pile) foundations and shallow (footing) foundations. Availability of reliable data of pile load tests performed in- and interaction of piles with both clayey and sandy layers of Dhaka soil prompted a detailed study of pile-soil systems. Here, apart from proposing a methodology for fixing various mesh parameters, a study concerning the sensitivity of various input parameters of pile-soil system has been conducted. A design formula has been developed, after an extensive parametric study, for predicting the load at the onset of nonlinearity in the pile-soil system. The interaction system has been applied to square footings resting on Dhaka soil at various depths and the load-displacement relationship of footings of various sizes has been studied.

The guidelines proposed and implemented for mimicking various structure-soil systems have been found to be very effective. It has been understood that special care should be taken in specifying *in-situ* stresses in soil prior to the installation of the structural member, in order to simulate field behaviour faithfully. While studying the interaction of pile-soil and footing-soil systems, it has been revealed that the horizontal and vertical extent of soil to be included in the finite element idealization has a pronounced effect on the satisfactory prognosis of the system. Although the performance of the finite element model is affected by the thickness of the interface element, for a width-to-breadth ratio of 0.1 for the interface element, such an effect has been found to be minimal. Prior to the final analysis of any soil-structure system, the loading rate has to be determined individually for the case concerned. In case of interaction analysis involving consolidation, it has been observed that excess pore water pressure does not dissipate much during the time span considered in case of pile load testing in the field. The onset of nonlinearity of pile-soil system has been found to be sensitive to the variation of parameters like the unit weight of soil, depth of clay layer, the angle of friction of soil and, of course, the pile size. On the other hand, the responses have been found not to be very sensitive to the variation of cohesion, critical void ratio and the slopes of the virgin compression and swelling lines. Although the displacement predictions were affected by the variation in the value of the initial tangent modulus of structural- and soil-elements, the failure load of deep (pile) foundations remained independent of such variations. The design rationale suggested in this study for designing pile foundations has been found to match the finite element predictions satisfactorily. Although some deviations from the results obtained from a traditional design method were detected, such divergence could be explained. The load-displacement relationship of square footings has been found to be related by a hyperbolic function; the ensuing load-displacement equation traced the finite element predictions faithfully. The resulting load-displacement relationship of square footings may be conveniently used for calculating expected settlements of such footings of a superstructure. Apart from assessing differential settlements, footing sizes and depths may be chosen, albeit approximately, using the equation developed, via settlement equalization of footings.

CONTENTS

LIST OF FIGURES

LIST OF TABLES

NOTATIONS

A,B	Constants in Eq. (6.1)
A_b	Area of pile base
A_c	Contact area
As, A_D, Bs, B_D	Factor in Eq. (6.2)
BD_1	Boundary 1 in Fig. 4.4
BD_2	Boundary 2 in Fig. 4.4
C	Cohesion of soil
C_1	Radial extent of mesh from the pile edge
C_2	vertical extent of mesh from the pile tip
C_a	Adhesion
C_c	Slope of (ln p',e) curve
C_p	Pile perimeter
C_r	Remolded strength
C_u	Undrained cohesion
D	Diameter of pile
D_F	Depth of footing
E	Modulus of elasticity
e	Void ratio
E_c	Modulus of elasticity for concrete
e_{cs}	Critical void ratio
e_o	Initial void ratio for
E_o	Modulus at depth y_o of soil
E_s	Modulus of elasticity for sand
F_ϕ , f_c, $f_{c,max}$	Factor of Potyondy equations (Eq.5.6)
f'_c	cylinder strength of concrete
$F_{c\phi}$	Factor for ϕ of clay in Eq. 5.11
$F_{c\gamma}$	Factor for γ of clay in Eq. 5.11
F_D	Factor for D of pile in Eq. 5.11
F_{DCL}	Factor for DCL of clay in Eq. 5.11
F_H	Factor for H of pile in Eq. 5.11
$F_{s\phi}$	Factor for ϕ of sand in Eq. 5.11
$F_{s\gamma}$	Factor for γ of sand in Eq. 5.11
G	Shear modulus
Gres	Residual shear modulus
G_s	Shear modulus of interface element
H	Length of pile
K_h, K_s	Coefficient of lateral pressure
K_n	Modulus in normal direction of interface elements
K_o	Static lateral earth pressure
K_x	Co-efficient of permeability in x direction
K_y	Co-efficient of permeability in y direction
L_i	Loading rate
M	Soil constant (Eq. 2.12)
m_1	Rate of increase of young's modulus with depth

m_r	Rate of change of element size with distance from pile
N	Soil constant (Eq. 2.10)
N′	Standard penetration number
N_1	Number of elements along pile length
N_2	Number of elements within a distance of twice diameter of pile form pile tip
N_c, N_q, $N\gamma$	Bearing capacity factors
ND_1	Direction 1 in Fig. 4.4
ND_2	Direction 2 in Fig. 4.4
ND_3	Direction 3 in Fig. 4.4
p'	Mean normal effective pressure
p'_c	Isotropic pre-consolidation pressure
P_{bu}	Ultimate base resistance
P_M	Failure load of model pile
P_{su}	Ultimate shaft capacity
Pu	Ultimate load capacity
q	Deviator stress
S_F	Size of footing
T_i	Thickness of interface element
u, u_0	Pore water pressure
V	Specific volume of soil
v	volume
$V\lambda$	Specific volume of recompression line at $p'=1$
$V\kappa$	Specific volume of Virgin compression line at $p'=1$
W	Weight of pile
Z_c	Critical depth
σ, σ_n	Normal stress of soil
σ_1	Major principal stress
σ_3	Minor principal stress
σ_a, σ_b, σ_c	Normal stress in axes a, b, c
σ_v	Vertical stress
σ_{vb}	Vertical stress at pile base
σ_h	Horizontal stress
σ_{sn}	Stress-norm (Eq. 4.1)
σ_r	Stress in the radial direction
κ	Slope of swelling or recompression line
λ	Slope virgin compression line
η	Stress ratio = q/p'
υ	Volumetric strain
ε	Deviator strain
ε_a	Normal strain
ε_r	Radial strain
ν	Poisson's ratio
ϕ	Angle of internal friction of soil
ϕ_a	Angle of friction between structure and soil
ϕ_c	Angle of friction of clay
ϕ_s	Angle of friction of sand

τ	Shear stress
τ_L	Limiting shear stress
γ_{bulk}	Bulk density
γ_c	Bulk unit weight of clay
γ_s	Bulk unit weight of sand
α	Reduction factor of Berensentsez equation
δ	Displacement of footing
Γ	Soil constant (Eq. 2.13)
$[K]_i$	Stiffness matrix of interface element
$[B]$	Transformation matrix
$[C]_i$	Constitutive matrix
$\{q\}$	Vector of nodal displacement
$\{Q\}$	Vector of nodal forces
$[D]_i$	Inverse of $[C]_i$
$\{F\}$	Vector equivalent nodal loads
$\{\sigma\}$	Stress matrix

ABBREVIATIONS

CPT	Cone penetration test
CSL	Critical state line
DCL	Depth of clay layer
DTIME	Toatal time increment in consolidation analysis
FE	Finite element
MCC	Modified Cam-Clay
OCR	Over consolidation ratio
P.W.P	Pore water pressure
SCHO	Schofield soil model
SPT	Standard penetration test
SSBS	Stable state boundary surface
YR	Yield ratio

CHAPTER 1

INTRODUCTION

1.1 GENERAL

Almost all the structures that can be built have to be supported by the earth in the end through foundations- shallow or deep. There are also some structures which are buried in the soil. Structural engineering usually deals with the analysis and design of structures while Geotechnical engineering deals with the soil which supports and/or surrounds these structures. It is worth mentioning that the mode in which structure and soil interact with one another is different from their individual mode of behaviours and has to be dealt with exclusively.

Soil is a complex composite material with anisotropy and non-homogeneity. Thus, when structures interact with soil as a whole, it becomes really a daunting task for engineers to understand their interactive behaviour. While the need of an interactive analysis is appreciated, few exhaustive methods are available. Most of these simplify the behaviour of the structure or the soil or both and give insufficient or inaccurate results. The traditional concept attacks the problem as a two phase system. The structure is one and the soil is the other. Attempts are then made to account for the interaction between these two phases by some simplified approach. Either the structure is supported by a fictitious soil or the soil is analyzed, with the structure being represented by an artificial model.

The structural behaviour of any superstructure is largely dependent on the behaviour of sub-structures underneath. The conventional methods for computing deformations and bearing capacities of shallow or deep foundations, on the other hand, can not generally account for such factors as *in-situ* stresses and its spatial variation, stresses and disturbances caused during installations, variation in strength of soil and interfaces, size and length of embedment, geometrical changes, consolidation and negative skin friction, group action, excavation or filling, realistic interface behaviour, etc. The finite element method, however, has shown considerable promise in handling many of these factors.

In order to get faithful prognoses from a numerical procedure like finite elements (FE) method, realistic representation of the soil-structure system in the FE mesh idealization as well as proper specification of various material parameters are essential. Naturally, when a FE model deals with soil-structure interaction, the proper portrayal of various soil properties in the model poses more importantance than its structur counterpart as soil is a natural and composite material with spatial variation in behaviour.

Whereas, most of the computer codes available do not cater for real soil properties, a computer code, CRISP which is available in the public domain is an exception. This code has been selected in this study as the basis for developing a realistic soil-structure interaction system. The existing version of CRISP does not include special interface element for dealing with different modes of response that are expected to occur at the interface of soil and structural elements. However, subroutines for a interface element (Desai et. al, 1984) were available and subsequently incorporated into the program making it yet more realistic.

CRISP is a powerful FE program specially developed for dealing with critical state soil mechanics i.e. plastic state of soil in which nonlinearity of stress-strain behaviour becomes predominant. Here, the nonlinear stress-strain behaviour of clay can be modeled as to follow the Modified Cam-clay (MCC) constitutive law. The MCC model is expected to work well for Dhaka clay and attempts have been made in this study to incorporate the Dhaka clay parameters in the MCC model to mimic Dhaka soil. Besides, elastic-perfectly plastic model, inhomogeneous elastic model, linear elastic model, etc. are other the soil models available in CRISP which have been effectively used for soils or materials other than clay.

In this study attempts have been made to construct an analytical model, with CRISP in its core, that closely resembles the real field behaviour of Dhaka soil. Whereas the ensuing model is expected to work well with various types of soil-structure interaction systems, the model has been developed and tested against deep (pile) foundations and shallow (footing) foundations. Availability of reliable pile load test data performed in Dhaka soil and interaction of piles with both clayey and sandy layers of Dhaka soil prompted a detailed study of the pile soil systems. Apart from proposing a methodology for fixing various mesh parameters, a study concerning the sensitivity of various input parameters of pile soil system has also been conducted. A design formula has been developed, after an extensive parametric study, for predicting the load at the onset of nonlinearity in the pile soil system. The interaction system has been applied to footings resting on Dhaka soil at various depths. The load-displacement relationship of footings of various sizes has also been studied and related by a hyperbolic function. The ensuing load-displacement relationship of footings may be conveniently used for calculating expected settlements of various footings of a superstructure; the differential settlements, thus found, may be used as inputs to frame analysis. Alternatively, footing sizes and depths may be chosen, using the equation developed, for frame analysis via settlement equalization of footings.

This thesis describes the objectives, the methodology and the findings of the research.

1.2 PRESENT STATE OF ART OF RESEARCH TOPIC

At present no soil-structure interaction system is available which has been specially developed for Bangladesh. Although considerable amount of work in the area of soil-structure interaction is being done at various overseas research installations, details of systems including the computer codes are not readily available or expensive and may not be applicable to Bangladesh soil, as these systems are calibrated against data which are rather widely varying in comparison to its Bangladesh counterpart. Of course, some attempts have been made to simulate soil structure interaction system numerically by researchers like Karim(1985), Nazneen(1986), Seraj(1986), Siddique (1989) and Morshed (1991). Although the studies undertaken by the above mentioned researchers had thrown new dimensions to the understanding of various soil-structure systems, most of these studies did not use realistic soil parameters as their input, rather the soil had been idealized either as a spring with certain modulus of subgrade reaction comparable to the soil conditions or represented by octahedral shear-stress and shear strain diagrams for various confining pressures. Thus, the numerical models so far developed and used locally do not cater for realistic soil or structure properties and may not be applied readily to real life situations faithfully. In contrast, the present model considers real structure and soil parameters along-with *in-situ* conditions of soil prior to installation as their input. Thus, the present study which is first of its kind in Bangladesh, is expected to lead to reasonable simulation of various soil structure interaction problems.

1.3 OBJECTIVES OF THE RESEARCH

The principal objectives of the present research can be summarized as below:

(a) To modify an existing finite element code, CRISP, by incorporating interface element of Desai et. al (1984).

(b) To assemble guidelines for realistic input preparation and test these guidelines against available test data.

(c) To establish a methodology for determining mesh parameters for authentic portrayal of soil-structure interaction system (with special reference to pile-soil system).

(d) To use the aforementioned soil-structure interaction system in studying the sensitivity of various structure and soil parameters on the behaviour of piles and to formulate an equation connecting all the important parameters.

(e) To propose a methodology for predicting load-displacement relationship of footings.

1.4 METHODOLOGY

In the present study, an existing soil-structure interaction package, CRISP has been used after incorporating interface element and adapting the constitutive relationship of Dhaka soil characteristics. The model, thus developed, has been employed to simulate the behaviour of various soil-structure interaction problems realistically. The predicted results from this model have been compared with actual measured parameters. Pile-soil system has been used as the special interaction system in this study to test the model against actual pile-load tests conducted at a number of sites in Dhaka. The pile-soil system has been selected in this study as the model interaction problem, mainly because the variation of soil parameters with depth and the effect of multi-layered soil profile on the soil-structure interaction system can be best investigated in case of piles. Again apart from the fact that pile is a deep foundation passing through several soil layers, predominant interface behaviuor such as slippage and shear transfer are the main mode of load resisting mechanism in piles. Thus, the response of the newly incorporated interface element can be best tested by studying such a problem. Above all, actual load test results are available in case of piles for comparison.

Extensive parametric study has been conducted for fixing a guide line for reasonable proportioning of the FE mesh. A methodology for undertaking an objective parametric study to fix mesh configuration as well as loading rate has also been suggested.

A study of the sensitivity of various material parameters on the predicted response in case of piles has also been done. From the apparent trend of the variation of failure load (the load at which nonlinearity commences) of piles with the variation of different material parameters, an empirical equation for calculating failure load of axially loaded piles have been introduced. The results obtained from this empirical method have been compared with conventional design methods and also with FE predictions.

The finite element model has been further employed to study the interaction of square footings with soil. Using the model, a methodology has been presented by which load-displacement responses of any interaction problem can be formulated. Also, an empirical equation for tracing the load-displacement curve of square footings embedded in Dhaka-soil has been introduced.

The main feature of the finite element program, CRISP along with the properties of newly incorporated interface element forms the content of chapter 2. Specific guidelines for realistic input preparation pertaining to Dhaka soil and its testing against available instrumented pile load-test data have been incorporated in chapter 3. In chapter 4, in order to establish a methodology for fixing mesh parameters, an extensive parametric study has been conducted for pile-soil system; in this chapter three different pile-soil problems have been studied and compared with load test data using the mesh thus configured and following the input guidelines of chapter 3. A detailed sensitivity analysis of various material parameter on the predicted response along with an empirical rationale for obtaining failure load of axially loaded piles has been undertaken in Chapter 5. Chapter 6 deals with the application of the model on footing-soil interaction and a empirical equation for obtaining load-displacement curves for square footing embedded in Dhaka has been introduced. Conclusions derived from the present research and some recommendation for future research have been presented in Chapter 7.

CHAPTER 2

THE FINITE ELEMENT INTERACTION MODEL

2.1 INTRODUCTION

The finite element program, CRISP (Britto & Gunn,1987) used in this study has been obtained by personal communication from A.M. Britto and M.J. Gunn. The present version of the program is not available in the public domain. It contains some new features like linear strain brick element with both displacement and pore pressure unknown, 3 noded beam elements with displacement and rotations unknown, elastic perfectly plastic soil model, etc. Although, it does not contain interface elements, subroutines for incorporating interface element (Desai et al, 1984) were available from Britto and Gunn. In this study, these subroutines have been incorporated, tested and subsequently used for analysis of various soil-structure interaction problems.

Some salient features of CRISP (Britto & Gunn,1987) along with some relevant new features are discussed in the following sections.

2.2 THE PROGRAM CRISP

The critical state program, CRISP can tackle any size of problem depending on the amount of memory and processing power of the computer concerned. It contains facilities to analyze several soil-structure interaction problem provided realistic soil parameters are available. A brief summary of facilities provided by CRISP is presented below.

2.2.1 Summary of Facilities

a) *Types of analysis*: Undrained, drained or fully coupled consolidation analysis of two dimensional plain strain or axisymmetric (with axisymmetric loading) or three dimensional bodies.

b) *Soil models*: Isotropic and anisotropic elasticity, inhomogenous elasticity (properties varying with depth, critical state soil models (Cam-clay and Modified Cam-clay), elastic perfectly plastic models (with yield criterion by Von Mises, Tresca, Druckel Prager, Mohr-Coalom), the Schofield soil model (SCHO).

c) *Element types*: Linear strain triangle and cubic strain triangle (with extra pore pressure degrees of freedom for consolidation analysis), linear strain quadrilateral (with extra pore pressure degrees of freedom), linear strain brick (with extra pore pressure degrees of freedom), 3-noded bar and beam elements with displacement and rotations unknown.

d) *Non-linear techniques*: Incremental (tangent stiffness) approach. Options for updating nodal co-ordinates with progress of analysis. For integration in time, $\theta = 1$ (consolidation analysis).

e) *Boundary conditions:* Element sides can be given prescribed incremental values of displacements or excess pore pressures. Loading applied as nodal loads or pressure loading on element sides. Automatic calculation of loads simulating excavation, or construction when elements are remarked or added.

f) *Miscellaneous:* Stop-restart facility allows analysis to be continued from a previous run.

2.2.2 Solution Techniques

The small-displacement, small-strain approach is used throughout CRISP. Hence one can avoid the extra complexity of using the strain and stress tensors appropriate to large deformations and strains. The program does, however, contain the option of updating the co-ordinates of nodal points as the analysis proceeds.

There are a number of techniques for analyzing non-linear problems using finite element. CRISP uses the incremental or tangent stiffness approach, i.e. the user divides the total load acting into a number of small increments (say 50 or 100 in a typical analysis) and the program applies each of these incremental loads in turn. During each increment the stiffness properties appropriate for the current stress levels are used in the calculations. If only a few increments are used, this method produces a solution which tends to drift away from the true or exact solution. This means a stiffer response results for a strain-hardening model and the displacement are always under-predicted.

This approach is in contrast to that adopted in the elasto-plastic programs used in the analysis of mechanical engineering components or steel structures. In these applications it is usual to use larger size of increments (say 10 in a complete analysis) and to correct the error described above by performing iterations within each increment until convergence to the non-linear load-displacement curve is obtained. Experience with this technique with critical state models has been rather mixed. Some claim to have applied the technique with no particular difficulty (e.g. Zienkiewicz et al., 1975), but Britto and Gunn's experience, in common with that of Naylor (1975), is that sometimes there can be problems with convergence, and that sometimes the known (analytical) solution cannot be recovered from the numerical procedure. Perhaps this is not surprising; in structural mechanics problems the zone of plastic behaviour is often restricted to a small part of the structure, whereas in geotechnical problems the zone of plastic deformation frequently occupies the majority or even the whole mesh.

The program incorporates an equilibrium check to ensure that equilibrium is satisfied at the end of each increment. In this equilibrium check the stresses in the elements currently in the mesh are integrated over the volume to calculate the equivalent nodal loads and these are then compared with the external loadings. The difference is then expressed as a percentage of the applied loading, and is called the error in equilibrium or the out-of-balance load. This out-of-balance load is then applied as correcting load in the next increment.

2.3 CRITICAL STATE SOIL MECHANICS

The theories of soil behaviour, known as 'critical state soil mechanics', are developed from the application of the theory of plasticity to soil mechanics. The plastic behaviour of soil allows a rational treatment of bearing capacities of foudations and the failure of slopes, excavations and tunnels. It also allows complete description of the stress-strain behaviour of soils so that soil deformations can be predicted right up to the failure.

In order to predict the behaviour of engineering structures when plastic behaviour is involved, the first step is to choose an appropriate idealization of plasticity. Figure 2.1(a) shows the idealization known as elastic-perfectly plastic. Here the first part of the stress-strain curve is linear and elastic until the material yields. The material then continues to deform at a constant

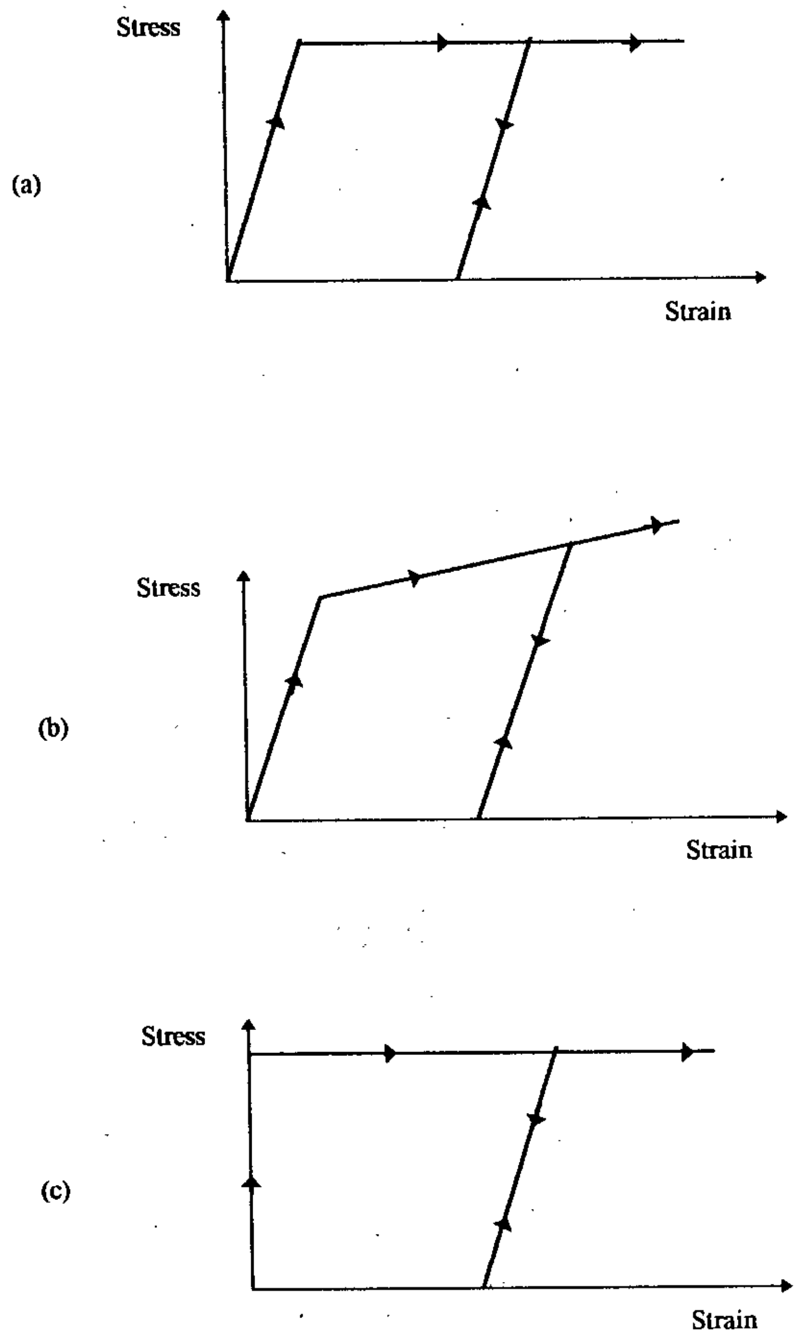

Fig. 2.1 Idealization of plastic behavior; a) Elastic-perfectly-plastic, b) Elastic, strain-hardening plastic, c) Rigid, perfectly plastic

yield stress. In the terminology of plasticity the material exhibit no strain-hardening. Figure 2.1(b) shows the simplest way of incorporating strain-hardening into an idealization. When the material yields, although the stress-strain curve still remains linear, the slope gets reduced. This type of behaviour is referred to as elastic-linear-strain-hardening. Sometimes (when only collapse loads are to be considered in a calculation) it is convenient to idealize the behaviour as rigid-plastic (see Fig. 2.1(c)).

To completely describe the stress-srain relations for an elasto-plastic material, four different types of statement are required.

(a) A yield function for the material.

(b) A relationship between the direction of the principal plastic strain increments and the principal stresses.

(c) A flow rule for the material. This specifies the relative magnitudes of the incremental plastic strains when the material is yielding.

(d) A hardening law of the material.

2.3.1 Yield Functions Appropriate for Soil

In 1773 the French engineer Coulomb introduced in his analysis of the thrust acting on a retaining wall, the failure condition for soil which is still in wide use, usually called the Mohr-Coulomb criteria

$$\tau = C' + \sigma_n{}' \tan\phi' \qquad (2.1)$$

Although this equation is normally interpreted in terms of Mohr's circle plot, it can instead represent the failure criteria in the three dimensional stress space. This can be achieved by rewriting Eq. 2.1 into Eq. 2.2 as shown below.

$$\sigma_1{}' - \sigma_3{}' = \mathrm{Sin}\phi'\left(\sigma_1{}' + \sigma_3{}' + 2C'\cot\phi'\right) \qquad (2.2)$$

Where, $\sigma_1{}'$ and $\sigma_3{}'$ are the major and minor principal effective stresses respectively. Taking into account the six possible permutations of the magnitudes of $\sigma_a{}'$, $\sigma_b{}'$ and $\sigma_c{}'$ (i.e. $\sigma_a{}'>\sigma_b{}'>\sigma_c{}'$, $\sigma_a{}'>\sigma_c{}'>\sigma_b{}'$, etc.) six planes are generated in $(\sigma_a{}',\sigma_b{}',\sigma_c{}')$ space.

Thus, the Mohr-Coulomb yield criteria is equivalent to the irregular pyramid in principal effective stress space (shown in Fig. 2.2).

For some metal plasticity conditions, Von Miss yield criteria is more convenient than Tresca as the former is round in shape. So Drucker and Prager believed that it might be useful to round off the Mohr-Coulomb yield surface to give conical surface for soils as shown in Fig. 2.3.

2.3.2 Modified Cam-clay (MCC)

Cam-clay is the name given to an elasto-plastic model of soil behaviour. Thus Cam-clay is not a real soil in the sense that one cannot find deposits of it at some location in the ground. However, the Cam-clay equations can be used to describe many real soils if appropriate material parameters are chosen. Cam-clay model in its modified form is called Modified Cam-clay (MCC), the brief description of which is given in this section.

Critical State Parameters for MCC

Three parameters, p', q and V, describe the state of a sample of soil during a triaxial test. The parameters are defined as:

$$p' = \frac{\sigma_a' + 2\sigma_r'}{3} = \frac{\sigma_a + 2\sigma_r}{3} - u \tag{2.3}$$

$$q = \sigma_a' - \sigma_r' = \sigma_a - \sigma_r \tag{2.4}$$

V is the specific volume, i.e., the volume of soil containing unit volume of solid material, (N.B. $V = 1 + e$, where e is the void ratio).

p' is often called the mean normal effective pressure, and q the deviator stress,. The reader should note that these three parameters varies during a test. The progress of a soil sample during a triaxial test can be represented by a series of points describing a line in a three-dimensional space with axes p', V and q. Different types of test (drained, undrained, compression, extension and so on) lead to different test paths in this (p', V, q) space. Critical state soil mechanics advocates for a set of rules for calculating test paths in (p', V, q) space;

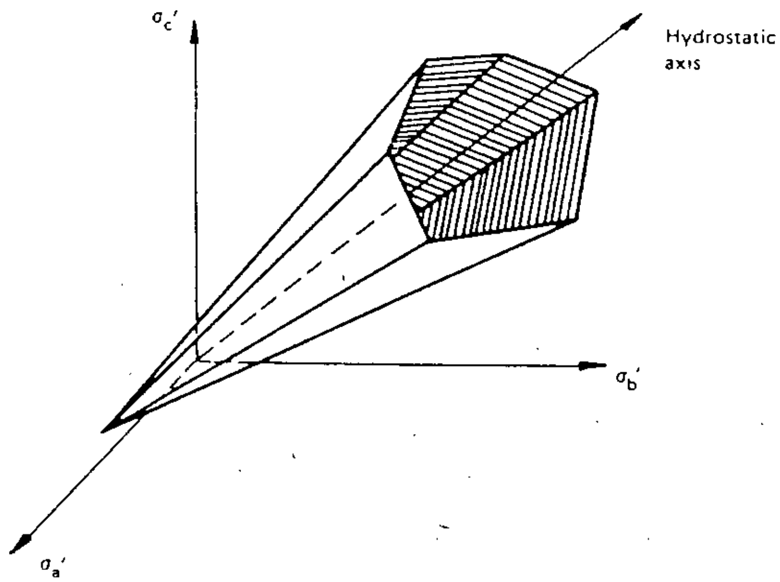

Fig. 2.2 The Mohr-Coulomb yield surface

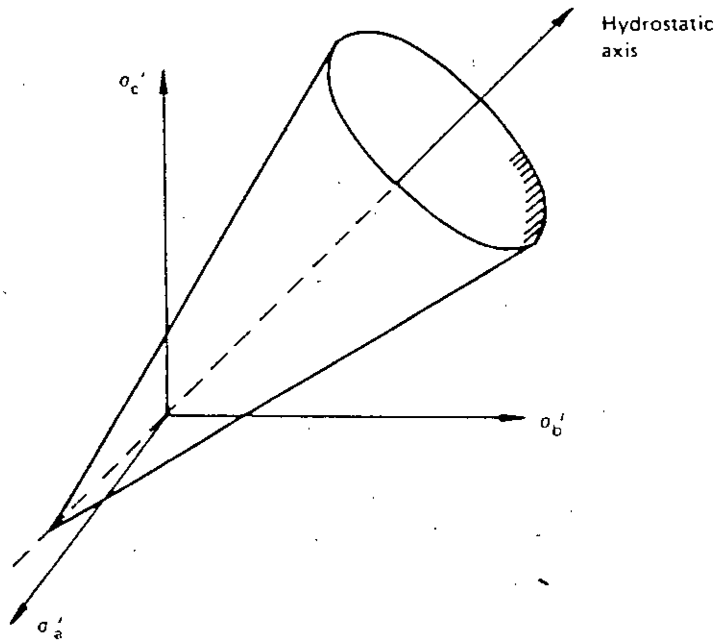

Fig. 2.3 The Drucker-Prager yield surface

usually two of (p', V, q) are determined by the type of test and there is a simple procedure for determining the third.

There are also four parameters which are soil constants: M, Γ, κ and λ. They describe the fundamental properties of soil with a given mineralogy. Other parameters are defined in terms of the seven already mentioned; for example the stress ratio $\eta = q/p'$.

Corresponding to the stress parameters p' and q are strain parameters υ (volumetric strain) and ε (deviator strain):

$$\upsilon = \varepsilon_a + 2\varepsilon_r \tag{2.5}$$

$$\varepsilon = \left(\tfrac{2}{3}\right)(\varepsilon_a - \varepsilon_r) \tag{2.6}$$

Volume pressure relationship for MCC

If a sample of soil is subjected to isotropic compression (and swelling) tests, then it follows paths in (p', V) plots as shown in Fig. 2.4. this is basically similar to the more familiar (σ_v', e) plots obtained from oedometer tests. In critical state theory the virgin compression, swelling and recompression lines are assumed to be straight in ($\ln p'$, V) plots with slopes $-\lambda$ and $-\kappa$, respectively, as shown in Figs. 2.5 and 2.6. The equation of the isotropic virgin compression line (often called the isotropic normal consolidation line) is

$$V = N - \lambda \ln p' \tag{2.7}$$

where N, a constant for a particular soil is the value of V when $\ln p' = 0$, i.e. $p' = 1$: clearly the value of N depends on the units which are used to measure pressure. The units adopted here are kN/m^2, (kPa). Although N is a soil constant, it is related to those already defined as shown below.

$$N = \Gamma + (\lambda - \kappa)\ln 2 \tag{2.8}$$

The equation of a swelling or recompression line is given by

$$V = V_\kappa - \kappa \ln p' \tag{2.9}$$

When moving up or down one of these 'κ-lines' the soil is over consolidated. The Eq. (2.9) is sometimes written as follows:

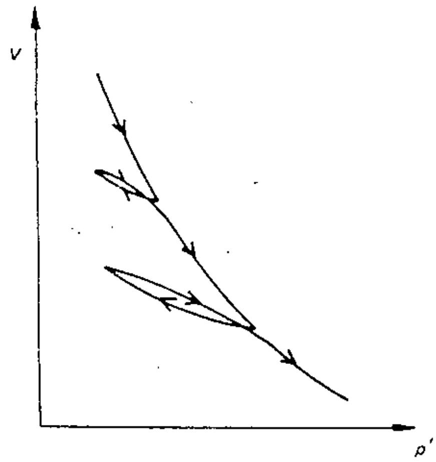

Fig. 2.4 Typical (p′ , V) plot of isotropic compression, swelling and recompression

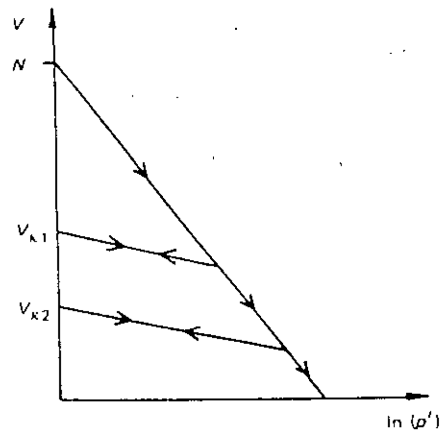

Fig. 2.5 Idealized (ln p′ , V) plots in critical state theory

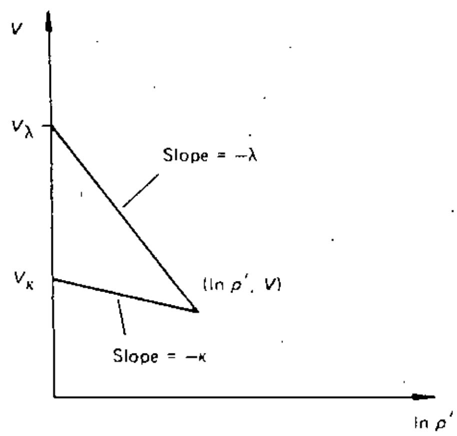

Fig. 2.6 Idealized (ln p′ , V) plots in critical state theory showing V_λ and $V\kappa$

$$V_\kappa = V + \kappa \ln p' \qquad (2.10)$$

These values of V_κ depends upon which κ-line the soil is on, but it stays constant while the soil is moving up or down the same line.

It is convenient here to introduce the parameter V_λ. The definition of V_λ is similar to that of V_κ:

$$V_\lambda = V + \lambda \ln p' \qquad (2.11)$$

One particular λ-line is the isotropic normal consolidation line, when $V_\lambda = N$.

Critical state line

When soil samples are sheared they approach the critical state line (CSL). The equations of the CSL are

$$q = Mp' \qquad (2.12)$$

$$V = \Gamma - \lambda \ln p' \qquad (2.13)$$

M and Γ are constants for a particular soil. They determine the slope of the CSL in a (p′,q) plot and the location of the CSL in the (p′,V) plot, respectively. Figures 2.7(a) and 2.7 (b) show the CSL in (p′, q) and (p′,V) plots. Note that Eq. 2.13 is the equation of a λ-line with $V_\lambda = \Gamma$. The critical state line represents the final state of soil samples in triaxial tests when it is possible to continue to shear the sample with no change in imposed stresses or volume of the soil.

Hence, at the critical state:

$$\frac{\delta \upsilon}{\delta \varepsilon} = 0; \quad \frac{\delta q}{\delta \varepsilon} = 0; \quad \frac{\delta p'}{\delta \varepsilon} = 0 \qquad (2.14)$$

Equations 2.12 and 2.13 describe a curved line in three-dimensional (p′, V, q) space as shown in Fig. 2.8.

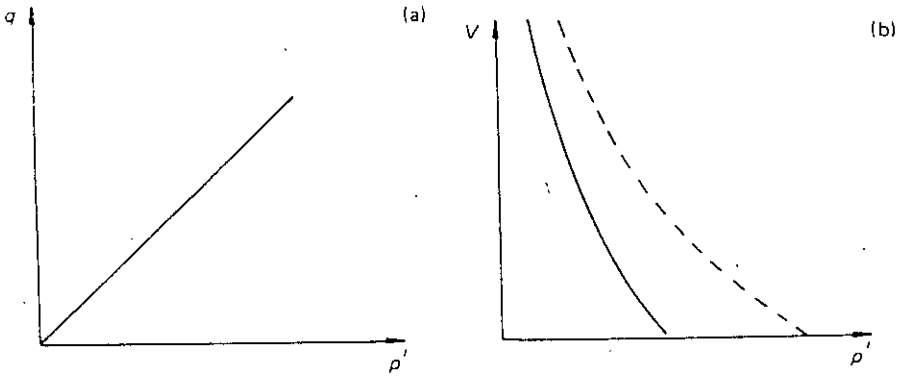

Fig. 2.7 The critical state line in (a) (p' , q) plot and (b) (p' , V) plot (isotropic normal compression line is shown dashed in (b))

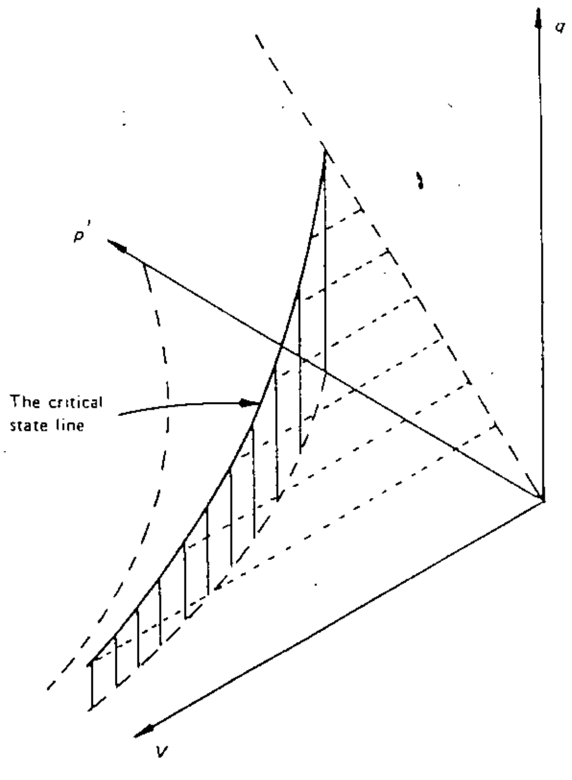

Fig 2.8 The critical state line in (p' , V, q) space is given by the intersection of two planes: $q = Mp'$ and a curved vertical; plane $V = \Gamma - \lambda \ln(p')$

Yielding of MCC:

There is a surface in (p′, V, q) space which indicates yielding of soil. When the state of a specimen of soil can be represented by a point below that surface, then the soil behaviour is elastic. Soil states on the surface indicates yielding, and it is impossible for soil samples to exist in states equivalent to points above the surface. For this reason the surface is called the Stable State Boundary Surface (SSBS). The equation of SSBS is

$$V_\lambda = \Gamma + (\lambda - \kappa)\left[\ln 2 - \ln\left\{1 + \left(\frac{\eta}{M}\right)^2\right\}\right] \tag{2.15}$$

The SSBS has been shown in Fig. 2.9.

The Flow Rule of MCC

The equation of flow rule can be written as

$$\frac{\delta v^p}{\delta \varepsilon^p} = \frac{M^2 - \eta^2}{2\eta} \tag{2.16}$$

Where δv^p and δv^p are the corresponding strain incrememts in plastic state

The flow rule can be integrated to give the Modified Cam-clay yield locus in (p′, q) plane as

$$q^2 + M^2(p')^2 = M^2 p' p'_c \tag{2.17}$$

Where p'_c is the isotropic pre-consolidation pressure lying on a particular κ-line.

The Modified Cam-clay yield locus is elliptical in shape (shown in Fig.2.10). The size of yield locus is determined by the value of p'_c.

2.4 INCORPORATION OF INTERFACE ELEMENT

Behaviour at junctions or interfaces between structure and soil elements involve relative slippage or separation of structure from soil. This may occur because of exceeding the limiting interface friction and inward movement of the structure. In order to obtain a better

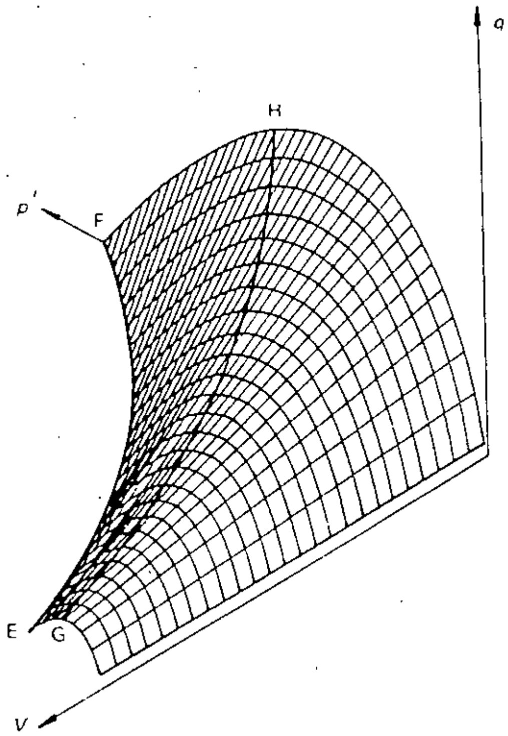

Fig 2.9 The stable state boundary surface (SSBS) in (p', V, q) space

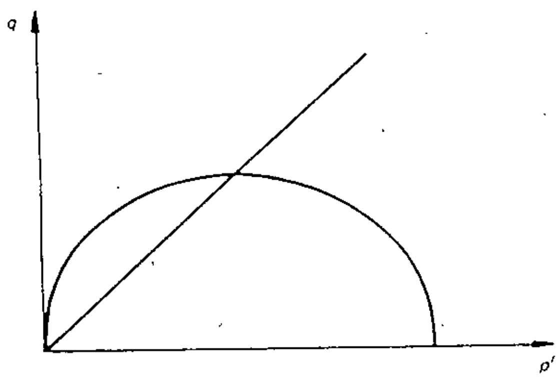

Fig. 2.10 The elliptical Modified Cam-clay yield locus

simulation of soil-structure interaction, special interface elements have to be used while using finite element method as the numerical tool.

Goodman, Taylor and Brekke (1968) developed an interface element to account for relative movements between rock joints. The element consists of two lines each with two nodal points. The two lines occupy the same position before deformation. Each node has two degrees of freedom (horizontal and vertical displacements). To simulate slippage across an interface, an arbitrary large normal stiffness and a very small tangent stiffness would be specified. Attempts have been made by a number of investigators (Ghaboussi et al., 1973; Goodman and St. John, 1977; Wong, 1977) to modify the Goodman-Taylor-Brekke interface model However, there are certain inconsistencies with the elements that are very difficult to overcome. Herrmann (1978) improved the element of Goodman et al. through the introduction of constraint conditions.

Clough and Duncan (1969) conducted direct shear interface tests in the laboratory to measure the relationship of interface shear stress and relative displacement between concrete and backfill sand. They proposed a hyperbolic functional relationship for the interface shear stiffness.

Zienkiewicz, et al. (1970) advocated the use of continuous isoparametric elements with a simple nonlinear material property for shear and normal stresses, assuming uniform strain in the thickness direction. In certain cases, ill conditioning of the stiffness matrix takes place.

Katona, et al. (1976) and Katona (1981) introduced a simple friction-contact interface element from the principle of virtual work modified by appropriate constraint conditions. Various deformation modes at the interface are incorporated in this formulation.

Desai et al. (1984) proposed a thin-layer element, for using in structure-soil interaction and rock joints. A special constitutive model is used. Various deformation modes such as stick, slip, debonding and rebonding can be handled with this element. It is capable of providing improved definition of normal and shear behaviour; hence, it can be computationally more reliable than the zero thickness element. The formulation of this element is essentially the same as other solid elements. As such it is easier to program and implement. Inclusion of a finite thickness for the interface is realistic since there is very often a thin layer of soil which participates in the interaction behaviour. The thin layer element can easily be introduced in an interface having a curved configuration. In view of the merits in the use of the thin-layer element, it has been decided to use this model in the present research.

2.4.1 Modes of Deformation at Interfaces

The physical behaviour of a sructure-soil interface may involve relative movements that are both normal and tangential to the interface surface. There are 4 basic modes of deformation that an interface element can undergo:

a) Stick or no-slip;
b) Slip or sliding;
c) Separation or debonding; and
d) Rebonding.

Figure. 2.11 shows various modes of deformation for a two-dimensional idealization. An interface element is in stick or no-slip mode when there is no relative movement between the adjoining bodies, Fig 2.11(a). Slip or sliding occurs when relative movements take place in such a manner that the contact between the mating bodies is maintained, Fig. 2.11(b). Separation or debonding mode occurs when gaps open up between two bodies that were in contact previously, Fig. 2.11(c).

An interface element in separation mode can return to stick mode in subsequent loading, which is referred to as rebonding, Fig. 2.11(d).

2.4.2 Thin Layer Element for Interfaces

Schematic diagram of the thin-layer element proposed by Desai, et al. (1984) for two dimensional idealization is shown in Fig. 2.12. The underlying idea of the thin-layer element is based on the assumption that the behaviour near the interface involves a finite thin zone as shown in Fig. 2.12, rather than a zero thickness zone as assumed in previous formulations. The behaviour of this thin zone or layer can be significantly different form the behaviour of

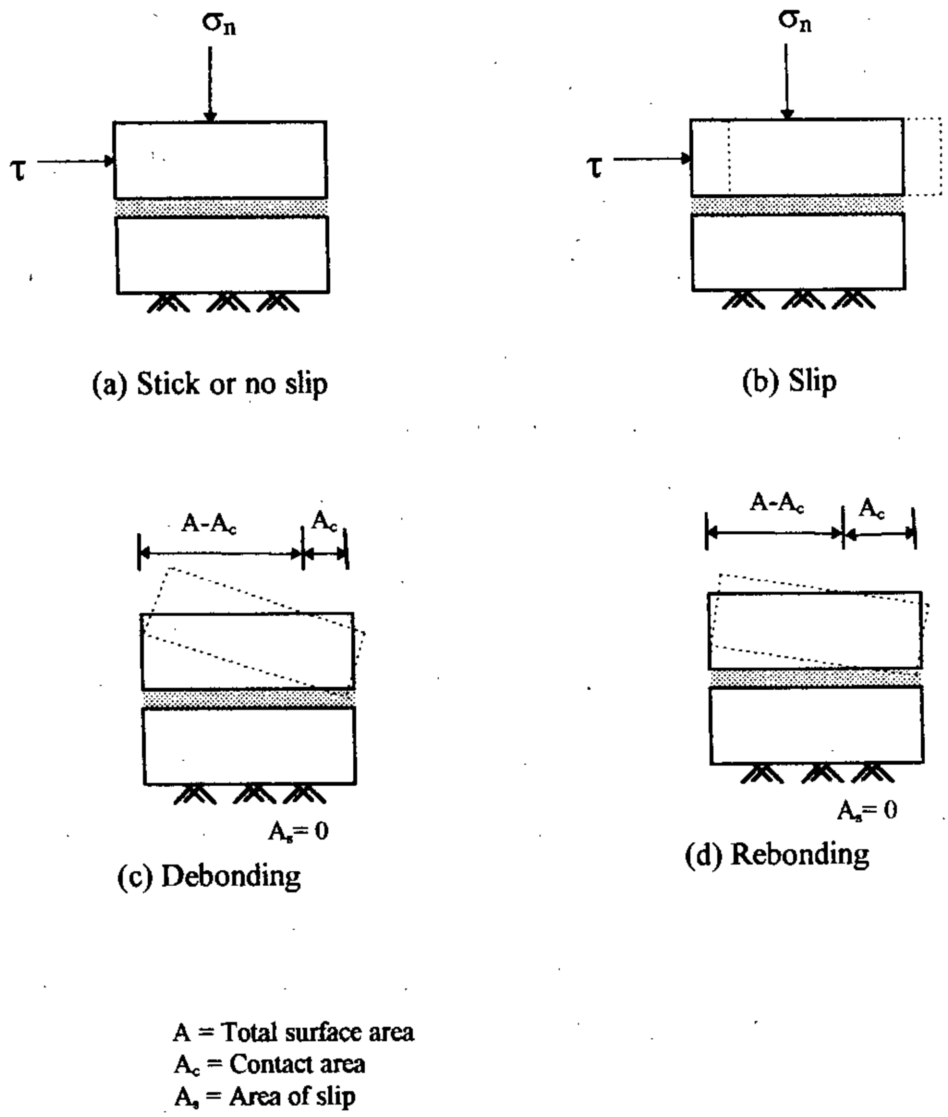

Fig. 2.11 Schematic diagrams of modes of deformation at interface

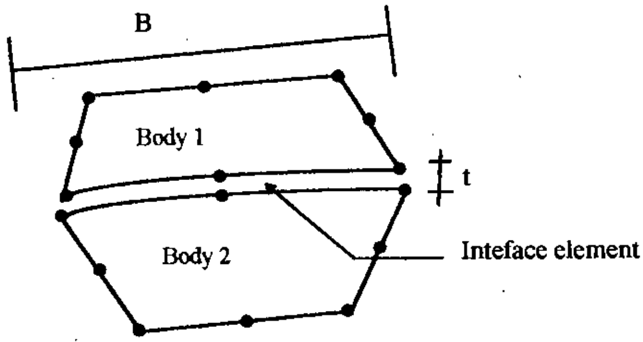

(a) Idealization of interface

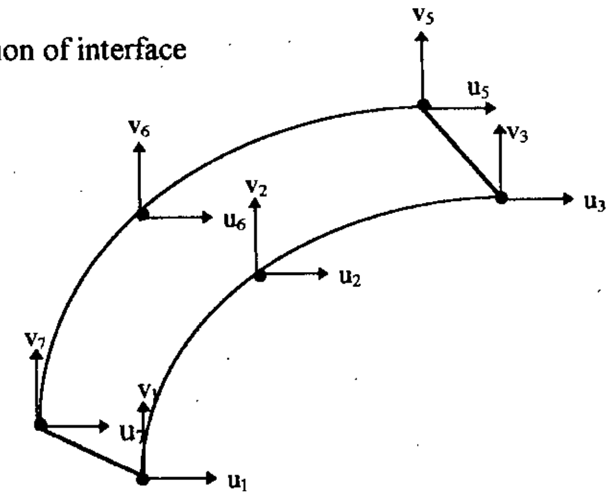

(b) Interface element

B= Average contact distance
t= Thickness of the interface

Fig. 2.12 Thin-layer interface element

surrounding structural and geological materials. However, the element can be treated like any other solid element by adopting appropriate constitutive laws.

The thin-layer interface element can be formulated by assuming it to be linear elastic, non-linear elastic or elastic-plastic. The stiffness matrix of the interface element, $[K]_i$ is written as

$$[K]_i = \int_v [B]^T [C]_i [B] dv \tag{2.18}$$

where $[B]$ = transformation matrix, v = volume and $[C]_i$ is the constitutive matrix. Then the element equations are written as

$$[K]_i \{q\} = \{Q\} \tag{2.19}$$

where $\{q\}$ = vector of nodal displacements and $\{Q\}$ = vector of nodal forces.

For two dimensional plane-strain idealization, the matrix $[C]_i$ and its inverse form $[D]_i$ are given as

$$[C]_i = \begin{bmatrix} C_1 & C_2 & 0 \\ C_2 & C_1 & 0 \\ 0 & 0 & G_i \end{bmatrix} \tag{2.20}$$

where,

$$C_1 = \frac{E(1-\nu)}{(1+\nu)(1-2\nu)}$$

$$C_2 = \frac{E\nu}{(1+\nu)(1-2\nu)}$$

and

$$[D]_i = \begin{bmatrix} \frac{1-\nu^2}{E} & \frac{-\nu(1+\nu)}{E} & 0 \\ \frac{-\nu(1+\nu)}{E} & \frac{1-\nu^2}{E} & 0 \\ 0 & 0 & \frac{1}{G_i} \end{bmatrix} \tag{2.21}$$

For non-linear elastic behaviour E, ν and G can be defined as variable moduli based on triaxial and direct shear tests.

In general, the stiffness properties of the interface elements are quite different from the properties of the adjacent continuum elements. In this study, it is assumed that the normal behaviour of the interface element is the same as regular soil elements; however the shear behaviour is quite different according to Desai (Desai, et al. 1984).

2.4.3 Simulation of Interface Modes

The quality of simulation of the interface behaviour depends on a number of factors such as physical and geometrical properties of the surrounding media, non-linear material behaviour and the thickness of the thin-layer element. If the thickness is too large in comparison with the average contact dimension (Fig. 2.12) of the surrounding elements, the thin layer element will behave essentially as a solid element. If it is too small, computational difficulties may arise. Desai, et al. (1984) have proposed that for satisfactory simulation of the interface behaviour, the ratio of thickness to average contact dimension (t/b) should lie between 0.01 and 0.1.

Various deformation modes that an interface can experience are incorporated in the thin layered element. It is assumed that before the application of load the interface elements are in stick or no-slip mode. Mohr-Coulomb criteria is used in order to identify the various modes of deformation. For a given increment of load, the normal stress, σ_n, and the total shear stress, τ, on the plane of interface elements are calculated. The modes of deformation are then checked and if the element is found to be in separation or slip mode, appropriate redistribution of stresses is performed. Details of the adopted procedure are given in the following steps.

i) The normal stress, σ_n, and shear stress, τ, due to the loading in a particular increment is calculated for the interface plane. Then, the sign of the normal stress, σ_n is checked. If it is found to be positive, the element can be either in stick mode or in slip mode (positive sign of σ_n indicates compressive stress while the negative sign indicates tensile stress). If σ_n is found to be negative, the element is considered to be in separation mode.

ii) For positive value of σ_n, the stick or slip mode is determined using the limiting shear stress of the interface place. The limiting shear stress, τ_L in the shear plane is calculated based on Mohr-Coulomb criteria as

$$\tau_L = C_a + \sigma_n \tan\phi_a \tag{2.22}$$

where, C_a is the adhesion and ϕ_a is the angle of friction between structure and soil.

iii) If $\tau_L \geq \tau$ then, element is in non-slip or stick mode. In this case, there will be no re-distribution of stresses and no change in the stiffness parameters E and G_i.

iv) If $\tau_L < \tau$, the element is in slip mode. Now, the shear stress, τ, would be made equal to the limiting shear stress, τ_L. Thus the unbalanced load due to the excess shear stress $(\tau - \tau_L)$ would be applied at the nodes of the interface elements as self-equilibrating load in the next increment. The equivalent nodal loads due to stresses in an element is calculated by using.

$$\{F\} = \int [B]^T \{\sigma\} dv \tag{2.23}$$

v) For negative value of σ_n i,e. separation mode, both the shear stress, τ and normal stress, σ_n are made to be almost zero, but with a negative sign (say $-2.7\text{x}10^{-30}$). As a result, the unbalance equivalent nodal loads, calculated using Eq. 2.23, is applied at the nodes of interface elements as self-equilibrating load in the next increment of load. The E and G_i values at this stage are actually zero. In order to avoid numerical difficulties, a very low value of E and G_i are assigned for the next step of analysis.

vi) To check the possibility of re-bonding, the sign of normal stress for each individual loading increment is checked. If it is found to be positive, the total normal stress which was negative previously is made to be equal to zero. As a result, it is no longer negative and falls into the category of stick or slip mode. Then the element would undergo the same steps as experienced by a normal interface element with positive normal stress.

2.5 REMARKS

The finite element code, CRISP, is a powerful numerical program specially for problems dealing with soil and soil-structure interaction. The MCC model is expected to work well for

Dhaka-clay when it would be calibrated against Dhaka-clay in the course of the present study. The sand layer can be modelled to follow the elastic-perfectly-plastic constitutive law using the Mohr-Coulomb yield functions. Moreover, small thickness interface elements have been incorporated to the existing program to take care of slippage, debonding, etc. As a result, the FE model is expected to work satisfactorily for the analysis of various soil-structure interaction problems and predict realistic results.

CHAPTER 3

REALISTIC INPUT PREPARATION

3.1 INTRODUCTION

The existing finite element code CRISP (Britto and Gunn,1987) which has been modified by incorporating interface and 3-noded beam element has been calibrated for Dhaka-soil. In this connection a judicious selection of problem type is of utmost importance in an effort to make this calibration exercise applicable, albeit approximately, to a wide range of soil-structure interaction problems. This selection of problem type is also dependent on the availability of reliable experimental results with which the results obtained from this model could be compared. Similarly, the availability of laboratory tested values of various soil parameters needed also plays an important role in this study. Besides the problem should have a prominent interface behaviour dependency as the currently updated model uses interface elements. In light of all these, pile foundation has been selected for calibrating the model in the present research.

Pile is a deep foundation. In Dhaka, piles having lengths 20 m to 25 m are frequently used. The length being quite large, one may encounter three or four different layers of soil having properties varying with depth. Thus a model calibrated for piles with layered soil is expected to work well for all other interaction problems like frames on footings, rafts etc. in which the effect of loading on them does not propagate to a great extend in the soil below them. The effect of variation of various soil parameters with depth on the structural behaviour is also expected to be less prominent for these structural elements in comparison to their pile foundation counterpart. Additionally, pile is a structural element which usually interacts greatly to its surrounding soil and a considerable amount of various types of deformations may take place at the interface of soil and the pile, specially towards the latter part of the pile load-test. It has also been envisaged that the performance of the newly incorporated interface element can be best determined by testing it against available pile load-test data. Needless to mention here that although results of some tests performed on piles are available alongwith detailed soil test results, field test results for cases such as footing, rafts etc. could not be obtained from local sources as such tests are usually not performed in Bangladesh. Under the circumstances, selection of the pile problem in calibration purposes has been deemed to be the most appropriate choice.

A reliable pile load test data (SSE, 1982) was available for Senakallayan Bhaban site at Motijheel, Dhaka. Detailed soil-test report on this site was also available. Thus, the calibration of the model has been conducted for the piles tested in Senakallayan Bhaban site.

Out of six numbers of piles tested, one pile (designated as pile A in this thesis) was loaded to failure. While all the piles tested have been reported in this thesis, pile A has been given additional importance as complete load deflection behaviour can be studied from its results.

Pile A had a diameter of 0.508 m and it was 19.3 m long. The soil profile at the location of pile A is characterized into distinct layers as clay and sands below the clay layer, based on the SPT value and available soil test report. Figure 3.1 shows these layers along with SPT values at various depth .

For clays, Modified Cam-clay (MCC) model is used as constitutive law. Sand layers are assumed to follow the elastic perfectly plastic constitutive law. Although, the axially loaded pile essentially represents a three dimensional problem, since the loading and geometry are symmetrical about the longitudinal axis of the pile, axisymmetric approach permit to reduce it to a two dimensional problem. Accordingly, an axisymmetric analysis has been performed for axially loaded piles.

The following sections shed some lights on the procedures which were followed in preparing the input data for CRISP. The basis of selecting the input parameters for soil and of the material parameters has also been included in these sections.

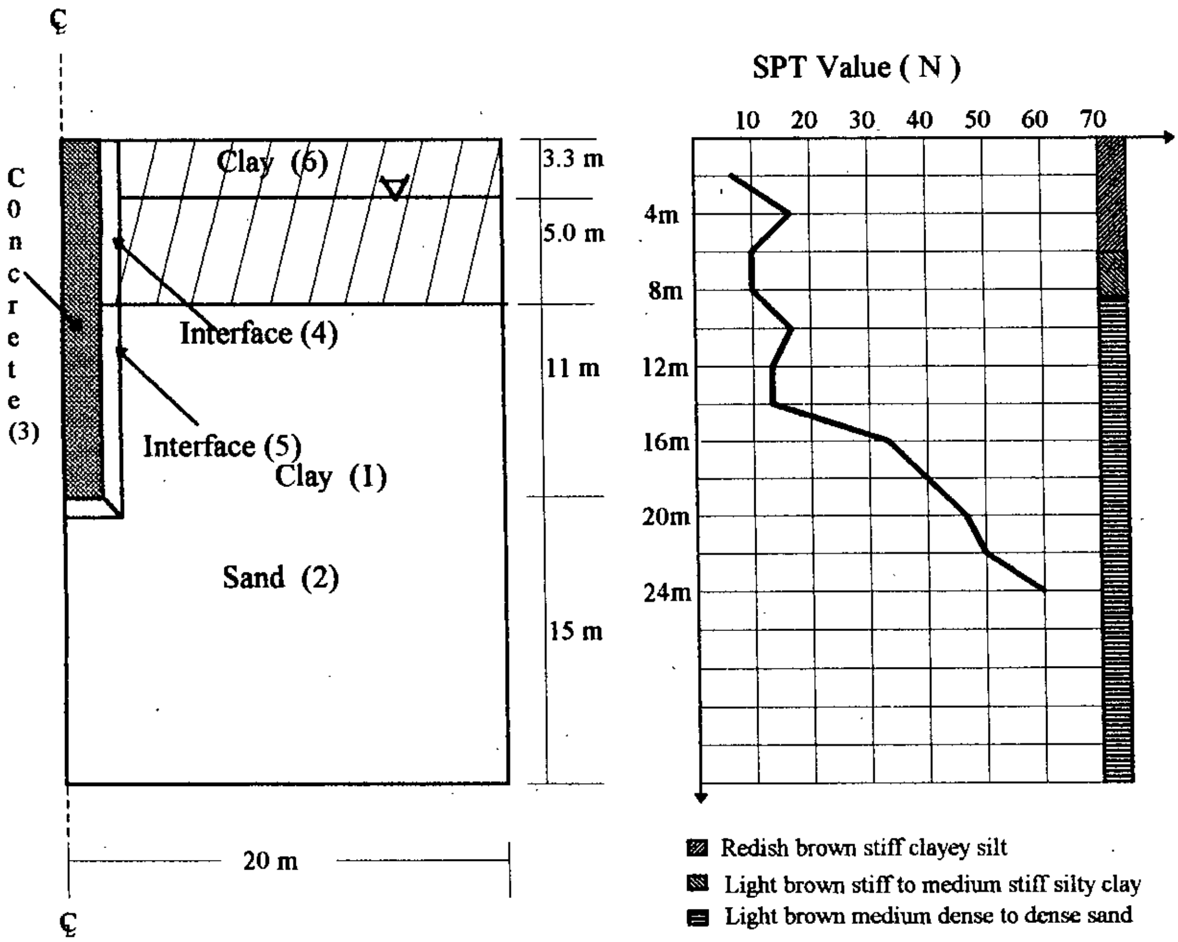

Fig 3.1 The soil profile alongwith SPT values for pile A

3.2 GEOMETRY DEFINITION BY CRISP

For clarity the geometry part i.e. the type of elements used, the nodal connectivity etc. calls for separate discussion. As this geometry part of the program can run separately, once formed accurately it can be used straightway during different runs of the main portion of the program. A number of crucial decisions have to be taken in this part of the program in order to accurately define the problem analytically.

3.2.1 Element Types

There are ten different element types available in CRISP. In addition to these elements, an interface element (Desai et al, 1984) has been incorporated in this study. In this study, linear strain quadrilateral element with displacements unknown (Element type 4, See Fig. 3.2) has been used for both pile elements and soil elements in case of drained or undrained analysis. But for consolidation analysis, soil elements under water table have been selected to be linear strain quadrilateral with displacement and excess pore pressures unknown (Element type 5, See Fig. 3.2). For interface elements, the 6 noded interface element with displacement unknown is used. All these elements are basically standard displacement finite elements (Zienkiewicz, 1977).

3.2.2 Element and Nodal Numbering

Each element and each vertex node in the finite element mesh have to be numbered with integers. There could be gaps in nodal or element numbers to facilitate the removal of elements when necessary. However, in general, they are better to be consecutive integers. In this model, there are no gaps in the numbering of nodes or elements. In specifying the nodal co-ordinates, the x-axis has been considered to be pointing to the right from the pile center and the y-axis has been considered to point upwards from the bottom of the pile (See Fig. 3.2). The origin, thus, has been the bottom center of the pile. As this analysis is axisymmetric, the y-axis must point upward so that it acts as the axis of symmetry (i.e., the x-axis is in the radial direction).

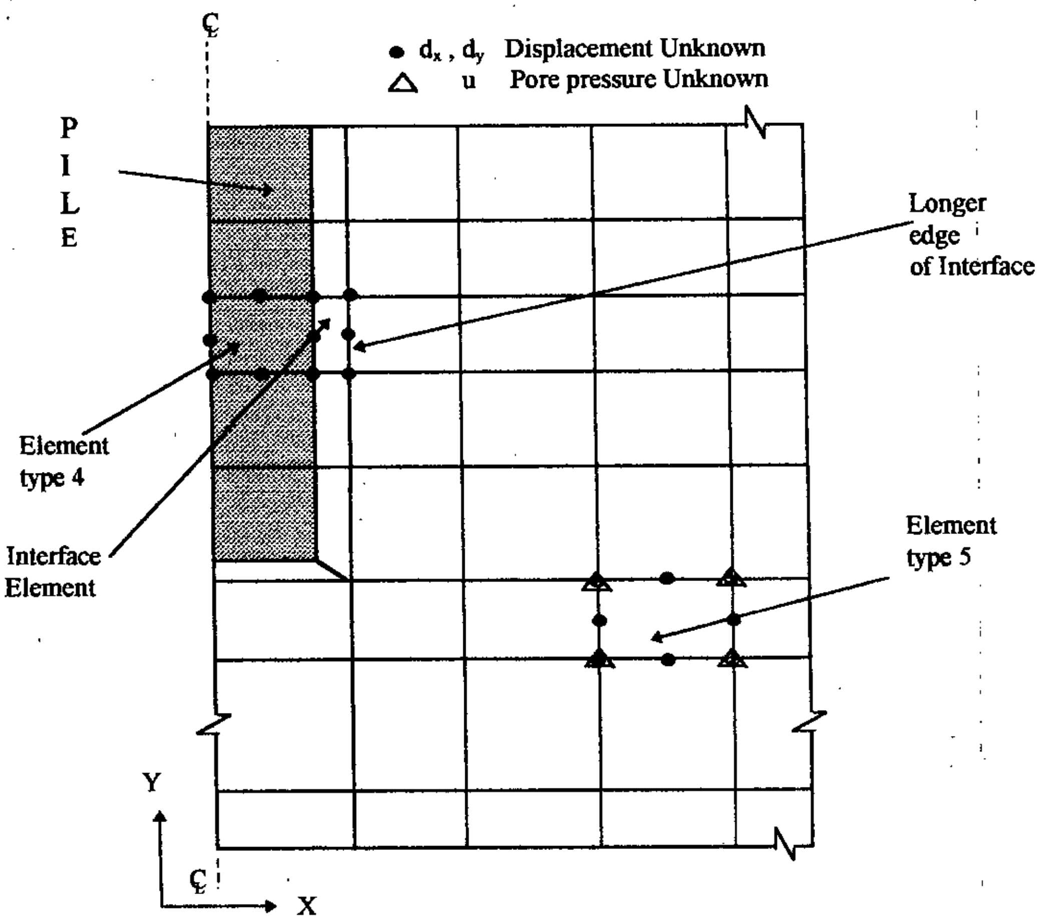

Fig 3.2 Different types of elements used in this study

When assigning the connectivity of the vertex node numbers for each element, the node numbers are to be listed in anti-clockwise direction for being congruent to the axis directions chosen. For the interface elements the nodes along the longer dimension should be input first so that the shear plane contains the longer side.

The positioning of interface elements along pile shaft specially near the tip calls for a special treatment. All along the pile shaft, the interface elements are rectangular having the longer dimension along the pile. But at the tip of pile the interface elements are set to be trapezoidal as shown in Fig. 3.2. This has been done to avoid the placement of one vertex of interface element on the side of the soil element below where is no node present. If a node is placed at that point, then the aspect ratio of all soil elements below would be too large for accurate analysis.

For finite element analysis one can choose any appropriate unit system as long as the units of all parameters are consistent. Units for only three different quantities have to be chosen and the rest are automatically determined. These three quantities are unit of length; unit of force and unit of time (for consolidation analysis). In this study the unit of length is meter (m), force is kilo-Newton (kN) and time is second (sec). All these units have been presented in Table 3.1.

Table 3.1 Unit used for various properties

Length	Force	Time	Stress	Density	Permeability
m	kN	Sec	kN/m^2	kN/m^3	m/sec

3.3 MAIN PART OF CRISP

After specifying the geometry of mesh and its element configuration, parameters have to be set for actual operation of finite element method in this part of the program. Here in the present study, axisymmetric analysis have been performed as during the course of the research implementation of interface elements for only plain strain and axisymmetric cases could be made. Options have been selected so that co-ordinates of nodes are not updated after each increment. Again, suitable option has been selected so that the out of balance loads from each increment act as correcting loads in the next increment.

3.3.1 Material Properties

Selection of various properties of soil and pile material is the most important task that has to be performed to achieve a satisfactory simulation of experimental data during the course of the numerical experiments to be undertaken in this study. Selection of material properties is not an easy task. Availability of reliable data is very scanty in our country. Detailed test results of soil from low to high depths are not readily available and all that can be obtained from different agencies are not always dependable. On the other hand, the satisfactory functioning of CRISP, like most of the numerical models, greatly depends on the elaborate and accurate assignment of these material properties. Say for example, if data could be available for every meter of soil depth on the location where the structure is interacting with soil, then the input of the analysis of soil properties may be defined more faithfully. Typical soil properties reported in different published materials usually do not give a detailed and accurate picture of actual soil characteristics. Thus, while an independent and thorough soil investigation for each site is, perhaps, most appropriate prior to conducting numerical experiments, in the present study attempts have been made to prepare input data based on readily available basic soil tests conducted by various agencies before the installation of piles. Tests conducted on Dhaka soil by various researchers have also been given due weightage in formulating ways of preparing reliable input data based on simple tests like Standard Penetration Test (SPT), Triaxial tests etc.

In Bangladesh usually a number of bore holes are dug at a site and both disturbed and undisturbed samples are taken for testing in the laboratory. Many parameters show difference in values from borehole to borehole. Consequently, when one has to select single value for all parameters reflecting the nature of the entire site, the task becomes difficult. To avoid this, test results found from boreholes near the testing piles have been given preference and sometimes average of all related values have been taken in preparing the input data. It is expected that during the course of the extensive sensitivity analyses, encompassing all important material properties which would be in Chapter 5, the relative importance of various input parameters will be understood better. It is also possible to detect a number of insensitive parameters, thus allowing the use of a typical value within a specific range.

In this study, the soil profile has been assumed to consist of two different layers, one is clay and the other is sand below it. If the typical bore chart for SPT values of the site is looked at (Fig. 3.1), it becomes clear that two layered soil profile is quite reasonable for accuracy and simplicity at the same time. Although two different clay and silty-clay layers can be seen, but they are very little different from one another. The sand layer has extended upto 30 m which is all the depth that is needed in our analysis. Altogether six different material types are used in this study. All these material zones with their respective zone numbers are shown in Fig. 3.1. Clay above the water table has been considered to be a separate layer and the clay layer has been set to obey Modified Cam-Clay model (MCC) while the sand layer is analyzed as elastic-perfectly-plastic model with modulus of elasticity increasing with depth.

Clay parameters

For Modified Cam-Clay (MCC), the important parameters that are to be assigned are λ, κ, e_{cs}, M, ν, and G. Now, λ and κ parameters can be obtained from oedometer tests or from triaxial tests on samples either isotropically or with k_0-normally-consolidated. But it is standard practice to obtain the value of λ from the slope of normally consolidated line of $(\log_{10}\sigma_v', e)$ curve using the following formula

$$\lambda = \frac{C_C}{2.303} \tag{3.1}$$

In this study, the value of C_c has been obtained from the result of one-dimensional compression test and the respective $(\log_{10}\sigma_v', e)$ curve which is available in any usual soil test report. Again, κ values are often chosen in the range of one fifth to one-third of λ (Britto and Gunn,1987). Here in this study, the value of κ has been selected to be equal to one forth of λ.

Next, location of critical straight line (CSL) in ($\ln p'$, e) plot i.e. the value of e_{cs} has to be obtained. Here, e_{cs} is defined to be the void ratio on the critical straight line for a value of $p'=1$ and e_{cs} is called the critical void ratio. For Modified Cam-clay, e_{cs} is usually obtained using Eq. 3.2.

$$e_{cs} = \Gamma - 1 \tag{3.2}$$

Now, Γ can be obtained from Eq. 2.8. The value of N in Eq. 2.8 can be found from the value of e_0 using $N=1+e_0$; where e_0 is the void ratio for $\sigma_v' = 1$ in ($\ln \sigma_v'$, e) curve. Therefore, after obtaining the value of e_o from one-dimensional compression test, the value of Γ and e_{cs} can be calculated and subsequently used in this study.

The frictional constant M can easily be found from triaxial test (drained or undrained with pore pressure measurement) on isotropically consolidated samples. If one obtains principal effective stress at failure, then the drained angle of friction ϕ' can be obtained from the geometry of a Mohr's circle plot. Then the value of M is obtained using Eq. 3.3.

$$M = \frac{6\ \mathrm{Sin}\phi'}{3 - \mathrm{Sin}\phi'} \tag{3.3}$$

In the present study, no triaxial test has been conducted and the value of ϕ' for Dhaka clay has been chosen from the data available in Kamal Uddin (1990) and Ameen (1985). The value of ϕ' reported by Kamal Uddin (1990) and Ameen (1985) are 23° and 25° respectively as shown in Fig. 3.3 (Kamal Uddin, 1990).

The computer code CRISP allows the user to specify either a constant value of Poisson's ratio (ν') or a constant value of shear modulus G. If the value of ν' is

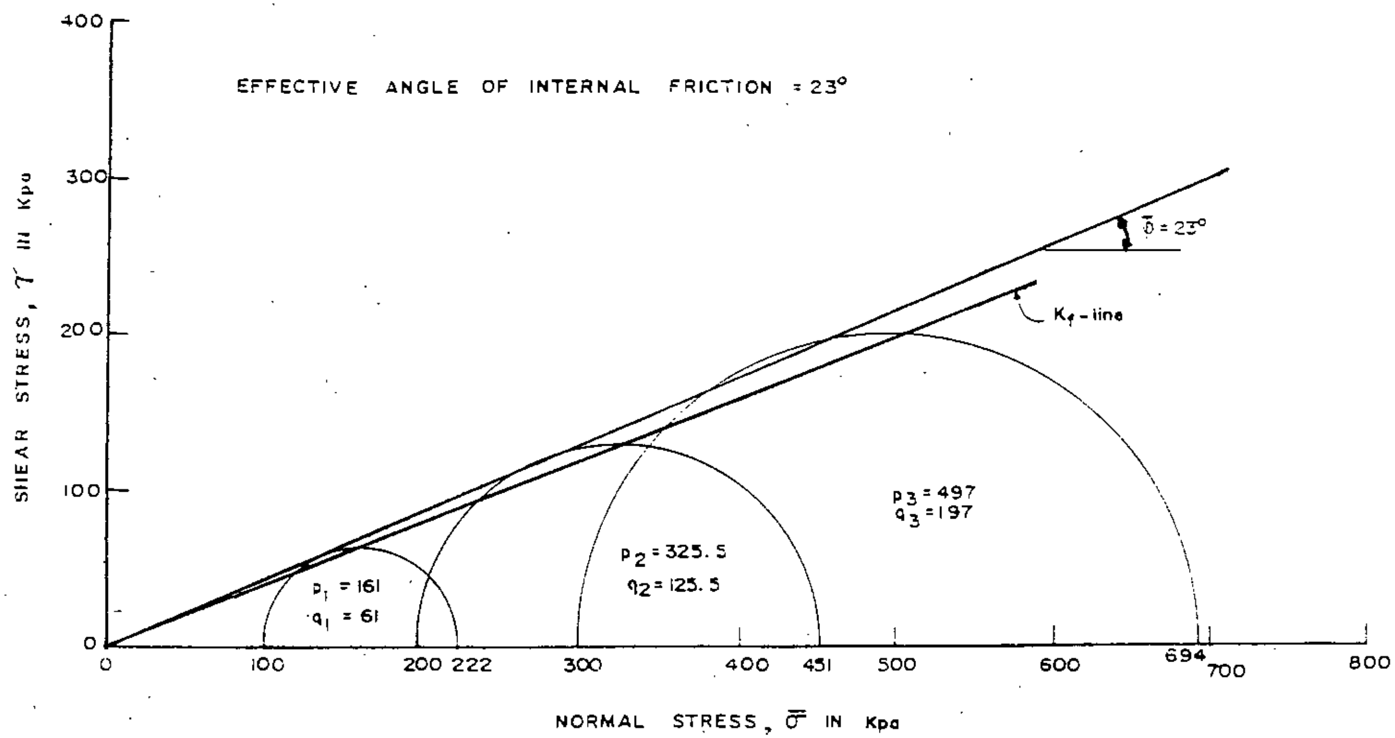

Fig. 3.3 Drained tests on K_0 INC samples of Dhaka clay (Kamal Uddin, 1990).

specified, then the value of G is allowed to vary with p' to depict the truly inelastic behaviour of soil. In contrast, G can be specified if a constant value of G is expected. In this study, the value of ν' is specified and its value has been taken as 0.25. It is worth pointing out here that the main strength of the MCC model is in the calculation of plastic strain during yielding, as opposed to the elastic strains which are calculated for over-consolidated case. Thus for many problems and practical purposes the exact assumption made for elastic properties like ν' and G is of only secondary importance.

In case of consolidation analysis, co-efficient of permeability values have to be assigned. Here, the permeability in both x and y direction are obtained from the research carried out by Siddique and Safiullah (1995) assuming that $K_X = 1.5\ K_Y$

Sand Parameters

The sand layer below the clay layer is analyzed using the elastic-perfectly-plastic model with increasing value of modulus of elasticity with depth (Material property type 5 in CRISP). For elastic perfectly plastic material type, the critical parameters that have to be assigned are E_o, C, ϕ , y_o and J. Here, E_o is the modulus of elasticity at depth y_o of soil (See the figure below). This option enables one to assign modulus of elasticity of a certain depth and a corresponding value of the rate of increase of E. All the value of E below the specified depth would be interpreted by the program using the specified increase rate. The elastic Young's modulus at any depth y is calculated by Eq. 3.4.

$$E = E_0 + m_1(y_0 - y) \qquad (3.4)$$

Here, m_1 is the rate of increase of Young's modulus.

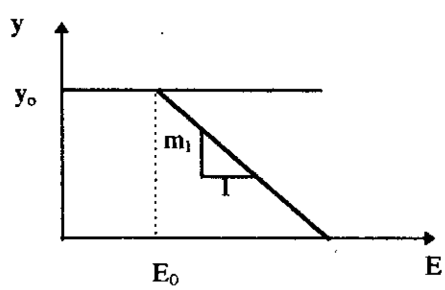

Now, the selection of representative values of E_0 is very important as the analysis is expected to be sensitive to change in values of E. Yet again, reliable data for obtaining E value are hard to find. But in general the elastic modulus can be obtained from any of the available test methods listed below:

1. Unconfined compression tests
2. Triaxial compression tests
3. *In-situ* tests
    a. Standard Penetration Test (SPT)
    b. Cone Penetration Test (CPT)
    c. Pressuremeter Test
    d. Plate-load Test
4. Other available empirical formulae.

Unconfined compression tests tend to give very conservative values for E. Triaxial tests tend to improve the value of E since any confining pressure *stiffens* the soil so that a larger initial tangent modulus is obtained. According to Craw-ford and Burn (1962) *in-situ* E values generally are 4 to 3 times as large as unconfined compression test value, and 1 to 1.5 times those obtained from triaxial values.

Since the laboratory values of E, although expensive to obtain, do not represent *in-situ* conditions well, SPT and CPT values are widely used to obtain (Stress-strain modulus) E. Moreover, extensive SPT values at any depth of sand layer of soil can be readily obtained from bore log chart and data as available from standard soil investigation reports. It becomes a rational choice to obtain the E value from empirical formulae using SPT value. These relations are presented below.

$$E_s = 18000 + 750\,N' \quad (\text{kPa}) \tag{3.5}$$

$$E_s = (15200 \text{ to } 22000)\ln N' \quad (\text{kPa}) \tag{3.6}$$

Equation (3.5) is given by D'Appolonia et al (1970) and Equation (3.6) is given by Bowles (1989). Of the two equations, former one is slightly conservative than its counterpart. While taking a decision for selecting a rational E value, it should be kept in mind that the measurement of SPT value itself is conservative. Thus, the D' Appolonia equation can be used with confidence. If the strain measurement can be done in much finer scale, then the value of initial tangent modulus of stress-strain curves in triaxial test tend to assume a value much greater than what can be obtained from conventional test method. In this respect Iwasaki and Tatsuoka (1977) put forward an equation for calculating G value using *in-situ* void ratio and p'. They established empirical equations for shear modulus G (kg/cm^2) as

$$G = 700\frac{(2.17-e)^2}{1+e}(p')^{0.5} \tag{3.7}$$

where p'= mean principal stress = $(\sigma_1 + 2\sigma_3)/3$

The value of G or E (using v) obtained from Eq. 3.7 gives value of E at least 2 to 3 times larger than the values calculated from Eq. 3.6. Therefore, the largest value of E calculated from Eq. 3.6 can be used in the FE input as it still falls within the conservative range. In this study, usually Eq. 3.6 has been used to calculate values of E and sometimes engineering judgement has been applied to arrive representative input values. But usually, somewhat smaller values than the maximum one are used.

Now, C and ϕ for sand are to be assigned. These values should be obtained from triaxial test results. Although, ϕ values could be evaluated from SPT values using empirical equations, but in this study ϕ value and C values are obtained from triaxial test results conducted by Yasin (1990). The SPT values tend to predict much larger values of ϕ and are rarely reliable; so the available empirical relations between SPT and are ϕ avoided.

Lastly, the type of yield functions may be selected from four available yield criterion, namely i) Von Mises, ii) Tresca, iii) Drucker - Prager and iv) Mohr-Coulomb yield functions. The first two yield functions are usually applicable to metals. For soils, both the Drucker-Prager or Mohr-Coulomb yield functions can be used. But as a yield surface, Drucker-Prager has some draw backs and gives the worst fit to the data of soil failure (Britto and Gunn, 1987). So the Mohr-Coulomb yield functions has been selected in this study.

Interface Parameters

For interface material properties, the parameters that are to be assigned are C_a , ϕ_a , K_n, G_s and G_{res}. The C_a and ϕ_a values of interface element should be the C and ϕ values respectively for pile and soil interface; not for soil itself. Thus, C_a is the adhesion between pile and soil while ϕ_a is the angle of friction between pile and soil. Usually ϕ_a value is slightly lower than ϕ value in case of steel piles but for bored concrete piles, the value of ϕ_a is much higher and can be set to equal to ϕ (Reese et al, 1976). Thus, in this study ϕ_a values are set to be equal to ϕ for respective soil type, i.e., for clay layer ϕ from clay and for sandy layer ϕ from sand have been used.

The modulus in the normal direction of the interface elements (K_n) and the shear modulus of interface element (G_s) can be calculated from E and ν as follows:

$$K_n = \frac{E(1-\nu)}{(1+\nu)(1-2\nu)} \tag{3.8}$$

$$G_s = \frac{E}{2(1+\nu)} \tag{3.9}$$

If values for E and G could be obtained rationally then K_n and G_s could also be easily found. As the interface element has been implemented according to the thin layered elements for interfaces and joints proposed by Desai et al (1984), the interface elastic properties should also be assigned using the method prescribed by them. In general, the stiffness properties of the interface elements are quite different from the properties of the adjacent continuum elements. In this study it is assumed that the normal behaviour of the interface elements is the same as regular soil elements; however, the shear behaviour is quite different (Desai et al, 1984). Thus, the value of E can be conveniently taken as the average value of the corresponding soil layer, whereas the shear stiffness of these elements may be set to a very low value.

The value of G_S for interface can be obtained from shear test conducted between two dissimilar materials. As this is rather expensive, in this study the value of G_S has been assumed using a very high value of ν as recommended by Jayatheran (1996).

The residual shear modulus, after the interface element has reached its limiting shear value (G_{res}), should have a very low value as it is almost equal to zero in reality. So, in this study, G_{res} has been assigned to be equal to 10 kN/m^2 arbitrarily to avert the numerical problems which may take place if such a value is set to zero.

Pile Material

In this study, the pile is made of reinforced concrete. The pile material has been assumed to be isotropically elastic. Only, one critical parameter has to be assigned for pile material. That is the modulus of elasticity of concrete (E_c). It is expected that the main components of displacement at the top of the pile is its elastic shortening. A significant difference in displacement values would occur due to this elastic shortening. Therefore, assigning a representative value of E_c is very important. The value of E_c can be obtained from the well known Eq. 3.10 shown below.

$$E_C = 57500\sqrt{f_C'} \tag{3.10}$$

If we consider 3000 psi concrete, then E_c becomes equal to $20\text{x}10^6$ kPa. But it is well known that by confining a concrete in two out of three mutually perpendicular directions, the ultimate compressive strength of the element in the third direction increases considerably and in practice, confinement is usually passive, and provided by steel which, due to the elongation imposed on it by the lateral expansion of concrete, induces compressive stresses in the element (Kinoshita et al., 1994). Figure 3.4 shows the axial stress-strain ralationship obtained from the research carried out by Kinoshita et al. (1994) for a particular mix of concrete with Cylindar strength (f_c') equal to 33 MPa when passive confinement of different thickness have been used. It is clear fron the Fig. 3.4 that the ultimate stregth of concrete increases many times than the normal cylinder strength when passive confinement is used. As the pile being analyzed has

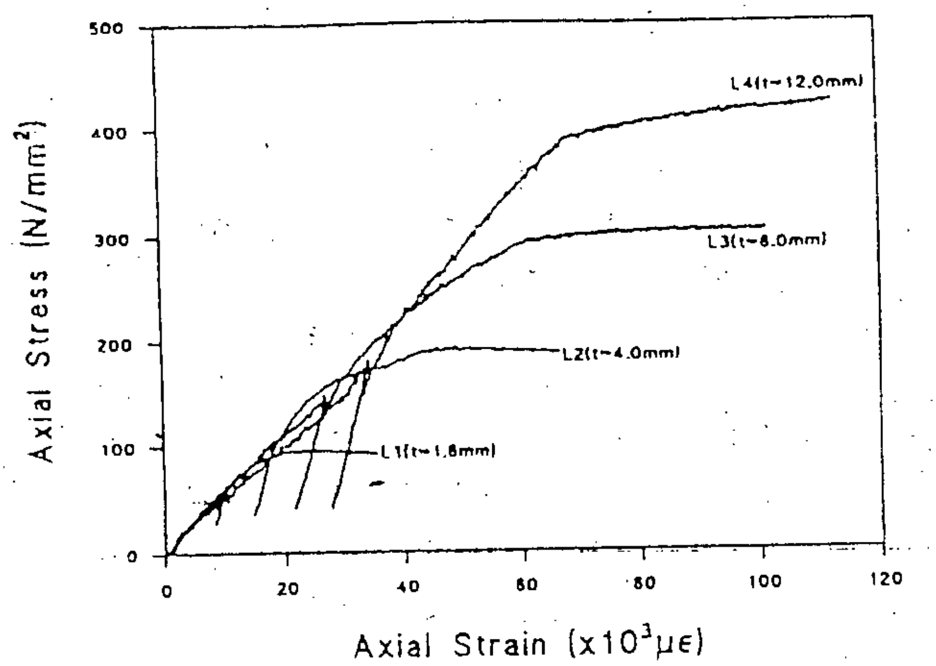

Fig 3.4 Experimental Axial stress-strain relationship for Mix 1 (Kinoshita, et al., 1994)

been constructed using spiral tie bars which is an effective form of passive confinement, the value of E_c is sure to increase considerably according to the Eq. 3.10. In light of this understanding, the value of E_c has been used, although still underestimated, as 30×10^6 kPa for 3000 psi concrete.

Tables 3.2, 3.3, 3.4 and 3.5 represent all the material properties used for pile A in this model in the light of previous discussions.

Table 3.2 Soil parameters for Clay layer (Pile A)

Depth (m)	Soil Type	Zone number	κ	λ	e_{cs}	M	ν	γ_{bulk} (kN/m^3)	K_x (m/s)	K_y (m/s)
0-3.3	Clay above W.T	6	0.01875	0.075	0.81	0.898	0.25	13.5	8.E-10	5.3E-10
3.3-8.3	Clay below W.T.	1	0.01875	0.075	0.81	0.898	0.25	19.0	8.E-10	5.3E-10

Table 3.3 Soil parameters for Sand layer (Pile A)

Depth (m)	Zone Number	E_0 (kN/m^2)	ν	C (kN/m^2)	ϕ (degree)	Y_0 (m)	γ_{bulk} (kN/m^3)	K_x (m/s)	K_y (m/s)	Rate m_1 (kN/m^2)/m
8.33-34.3	2	50E3	0.25	0	31	28.3	19.5	5.E-4	3.E-4	2.E3

Table 3.4 Interface element parameters (Pile A)

Depth (m)	Zone Number	C (kN/m^2)	ϕ (degree)	K_n (kN/m^2)	G_s (kN/m^2)	G_{res} (kN/m^2)
0-8.33	4	5	23	23.34 E4	1.01 E4	10
8.33-19.3	5	0	31	54.90 E4	2.1 E4	10

Table 3.5 Parameters for Pile Material (Pile A)

E (kN/m^2)	Zone Number	ν	γ_{bulk} (kN/m^3)
30 E6	3	0.20	23.5

3.3.2 *In-Situ* Stresses

The satisfactory performance of the FE model depends heavily on the accurate use of *in-situ* stresses which vary from point to point in the soil. The *in-situ* stresses that are to be assigned in the present model are σ_v', σ_h', U_o and p'_c for the entire region of the mesh. The parameter p'_c, which is the isotropic preconsolidation pressure, is only needed for those zones of the mesh where the Cam-clay models are used. CRISP uses this information to calculate the initial value of void ratio (e_o) over those zones as well as the size of the yield locus. For Cam-clay analysis it is important to try to establish the *in-situ* stress state as accurately as possible. This is because the displacements predicted by an analysis are quite sensitive to the amount of elastic (over-consolidated) / plastic straining that takes place.

To determine these *in-situ* stresses, an empirical method based on the data accumulated by Wroth (1975) has been used in this study. *In-situ* stresses can be specified in every integration point for each element and it could also be specified for certain horizontal layers when *in-situ* stresses for each element is interpolated from the given set of reference points representing layers. In this study, the second option has been used as this is much easier to specify and is accurate as well.

The basic steps in calculating *in-situ* stresses using Wroth's method has been summarized with an example in Appendix A.
The detailed *in-situ* stresses for pile A are shown in Table 3.6.

Table 3.6. *In-situ* Stresses for different layers (Pile A)

Depth (m)	σ_v' (kN/m^2)	σ_h' (kN/m^2)	U_o (kN/m^2)	p_c' (kN/m^2)
0-3.3	44.55	27.143	0.0	44.35
3.3-8.3	89.55	54.56	50.0	89.145
8.3-34.3	336.55	163.215	310.0	0.0

The user has to specify external loading (pressure loading along the boundary) and self weight loading (due to body force) which is in equilibrium with *in-situ* stresses. The zero displacement boundary conditions has to be specified along the boundary that is supported (or restrained). In specifying these conditions the user must consider the entire boundary of mesh and ensure that along any part of the boundary which is loaded (i.e. not free of stress) either the pressure loading or the restrain has to be specified. This specified loading or boundary condition is expected to be in equilibrium with the *in-situ* stresses.

In this study, the mesh boundary fixities have been assigned in such a way that the vertical boundaries are restrained for displacement in x-direction and the horizontal bottom boundary is restrained for displacement in y-direction as shown in Fig. 3.5.

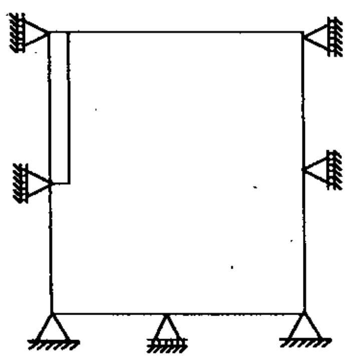

Fig 3.5 Boundary conditions for the mesh

It should be noted that any displacement fixities only need to be specified once either at the *in-situ* stage (in the presence of in-situ stresses) or in the stage when loading are specified in the first increment block of loading. Once specified, these zero displacement (or pore pressure fixities) remain in effect during the rest of the analysis. Therefore, these need not be re-specified for each and every increment block.

3.3.3 Loading

When a non-linear or consolidation analysis is performed using CRISP, it is necessary to divide either the loading or the time span of the analysis (or both if there is consolidation with non-linear material properties) into a number of increments. Thus if a total stress of 20 kPa is applied to part of the boundary of the finite element mesh, it might be divided into ten equal increments of 2 kPa, each of which is applied in turn. The total number of increments that are necessary will vary from problem to problem, but in general about 50 increments would be required in a drained or undrained analysis using one of the Cam-clay models which goes as far as collapse. CRISP calculates the incremental displacements for each increment using a tangent stiffness approach, i.e. the current stiffness properties are based on the stress at the start of each increment. While it is desirable to use as many increments as possible to obtain accurate results, the escalating computer costs that this entails will inevitably mean that some compromise is made between accuracy and cost. The recommended way of reviewing the results to determine whether enough increments have been used in an analysis is to examine the values of yield ratio (YR) at each integration point. When plastic hardening is taking place the value of YR gives the ratio of the size of yield locus following the increment to the size before the increment. Thus a value of 1.10 means that the yield locus has grown in size by 10%. Values of about 1.02 (0.98, if softening) are generally regarded as leading to sufficiently accurate calculations. If values greater than 1.05 (less than 0.95, if softening) are obtained, then the size of the load increments should be reduced. When one of the Cam-clay models is softening (i.e. yielding dry of critical), smaller increments (than the size suggested by the above discussion) may be necessary.

The time intervals for consolidation analysis (DTIME) should be chosen after giving consideration to the following factors:

i) The amount of pore pressure dissipation expected within the time step;

ii) In a non-linear analysis the increments of effective stress must not be too large (i.e. the same criteria apply as for a drained or undrained analysis);

iii) It is a good idea to use the same number of increments in each log cycle of time (thus for linear elastic analysis the same number of time increments would be used in carrying the analysis forward from one day to ten days as from ten days to one hundred days). Not less than three time steps should be used per log cycle of time (for a log base of ten). Thus a suitable scheme might be as follows:

Increment no.	DTIME	Total time
1	1	1
2	1	2
3	3	5
4	5	10
5	10	20
6	30	50
7	50	100
8	100	200
9	300	500
10	500	1000

This scheme would be modified slightly near the start and end of an analysis (see below);

iv) If a very small time increment is used near the start of the analysis then the finite element equations might become ill-conditioned.

v) When a change in pore pressure boundary condition is applied the associated time step should be large enough to allow the effect of consolidation to be experienced by those nodes in the mesh with excess pore pressure variables that are close to the boundary. If this is not done then the solution may predict excess pore pressures that show oscillations (both in time and in space).

The application of step no. v will often mean that the true undrained response will not be captured in the solution. The following procedure, however, usually leads to satisfactory results;

(a) Loads applied in the first increment (for the first few increments for a non-linear analysis); however pore pressure boundary conditions are not to be introduced;

(b) Excess pore pressure boundary conditions are introduced in the increment following the application of the loads.

In this study (in all the analysis for piles), loading has been applied in a number of incremental blocks as pressure load at the top of the first pile element. This pressure is equal to the external load on pile top divided by the cross-sectional area of pile. In consolidation analysis, time increments have been chosen in-line with the actual the pile load-test which is to be simulated during the investigation. In the following chapter, an extensive comparative study will be carried out to ascertain the loading rate that should be used to have the rational result from this model.

In case of consolidation analysis, the pore pressure fixities have to be assigned after the first incremental block as this has not been assigned in the in-situ stage. The top surface of the mesh has been considered to be zero excess pore pressure boundary in this case. The CRISP manual contains an elaborate explanation on the methodology of applying loading and boundary conditions that are needed to be followed.

Finally, a complete input data for both geometry and main part of the model has been presented in Appendix-B for reference.

3.4 USE OF THE MODEL IN UNDERSTANDING REAL PILE BEHAVIOUR

After the input parameters have been fixed, a consolidation analysis with the same time increment as used in the load test has been performed for pile A. In running the final analysis, the mesh configuration used is obtained from an extensive parametric study (Chapter 4). Loading increment and size of interface elements also have been obtained from those parametric studies. When all the geometry and element parameters along with material properties have been selected rationally, then the final model has been put to final run. This section deals with a thorough comparison of the actual pile load with response obtained from soil-structure interaction analysis.

3.4.1 Load-Displacement Response

The predicted load-displacement response obtained from the FE run using consolidation analysis is presented in Fig. 3.6 along with load displacement curve obtained from pile load-test conducted on pile A. It shows that the predicted load displacement curve resembles the load-test curve reasonably. Although the actual load-test curve shows less displacement than its numerical counterpart, this prediction could be considered as an acceptable prediction from the engineering point of view. This higher FE displacement prediction is, however, quite natural and expected keeping in mind that various material properties selected actually were on the somewhat conservative side. Accordingly, the prediction is on the safer side.

Looking carefully into the causes for this extra displacement, one can easily find that some critical parameters that were assigned conservative values in the input. Firstly, the actual initial tangent of the stress-strain plot giving the modulus of elasticity of soil is much greater than the value found from traditional triaxial testing. Here the angle of internal friction of soil has also been selected conservatively. The actual soil profile consists of many layers. In the present study, the adopted soil profile has been simplified to have only two layers, the clay layer with uniform properties and the sand layer with increasing E with depth. Whereas the Dhaka soil is actually preconsolidated, the presently adopted assumption of normally consolidated behaviour invariably predicted less *in-situ* stresses which may result in substantial increase in displacements. Above all, there are several parameters that are to be determined from laboratory testing at almost every meter of depth of soil for at least for 35 m depth, in order to faithfully prepare input data so that closer prediction of the actual pile load test could be achieved. However, for all practical purposes and after considering the variability of various parameters as well as cost involved, it is neither warranted nor possible to have an all encompassing match between physical and numerical tests.

It can be further noted here that the actual *in-situ* pore-water distribution for the whole soil depth concerned has to be found out and used for accurate prediction of consolidation settlement. Presently, the *in-situ* pore pressure has been assumed to be the same as static head distribution, i.e. linear increase of pore-pressure from water table. But actual pore pressure distribution may be quite different from the assumed profile. This would certainly affect the prediction.

In view of all these it can be stated that the presently demonstrated numerical prediction matches the real response reasonably well. The displacements predicted may be large, but the failure load, the load at which considerable non-linear displacement occurs, seems to match the actual value well. The overall trend of both curves are similar too.

The elastic shortening of pile itself is a considerable part of the total displacement at the top of the pile. If the Figure 3.7 which shows the load displacement curve at the pile tip is looked at, it becomes clear that the difference between displacement at pile tip and pile top for a particular load is considerable and is equal to the elastic shortening of the pile material. Here, Pile A is a concrete pile with closely space spiral confinement. It has been found (Kinoshita et al., 1994) that the strength of concrete (also the elastic modulus) increases significantly when subjected to confinement, both active and passive. It can increase even upto 4 to 5 times than the values of uniaxial compressive strength of concrete. Hence, the pile used in this study has much greater E_c value than the value used due to possible confinement of concrete and this would certainly account for much of the differences in displacement observed in Fig. 3.7. Had the value of E_c been increased, the curve of displacement at pile top would have moved leftwise and better correlation with the pile load test would have been obtained.

3.4.2. Pile load transfer

The predicted load transfer characteristics for pile A is shown in Fig. 3.8(a). Also, the propagation of slippage for different loads have been shown in Fig. 3.8(b). Figure 3.8(a) shows that the load transfer in sand layer is much higher than clay layer, as expected. Almost all the loads are transferred to the soil by interface shear and a very small portion of the applied load is resisted by the pile tip. This signifies that a major portion of pile load is transferred through frictional resistance. Thus, the condition in which both frictional resistance and tip bearing resistance would be attained has not reached in the case studied.

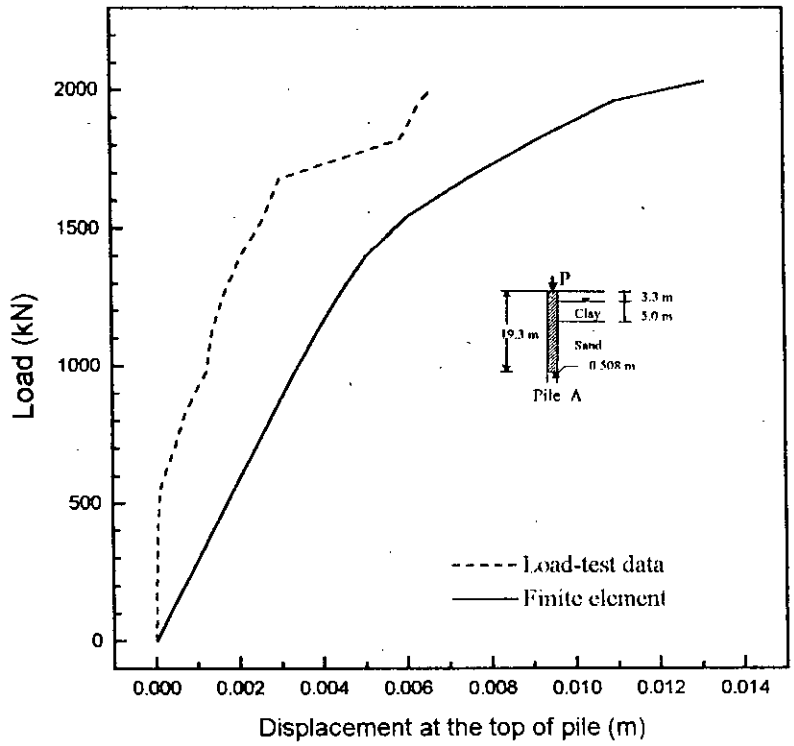

Fig. 3.6 Load-displacement response of Pile A

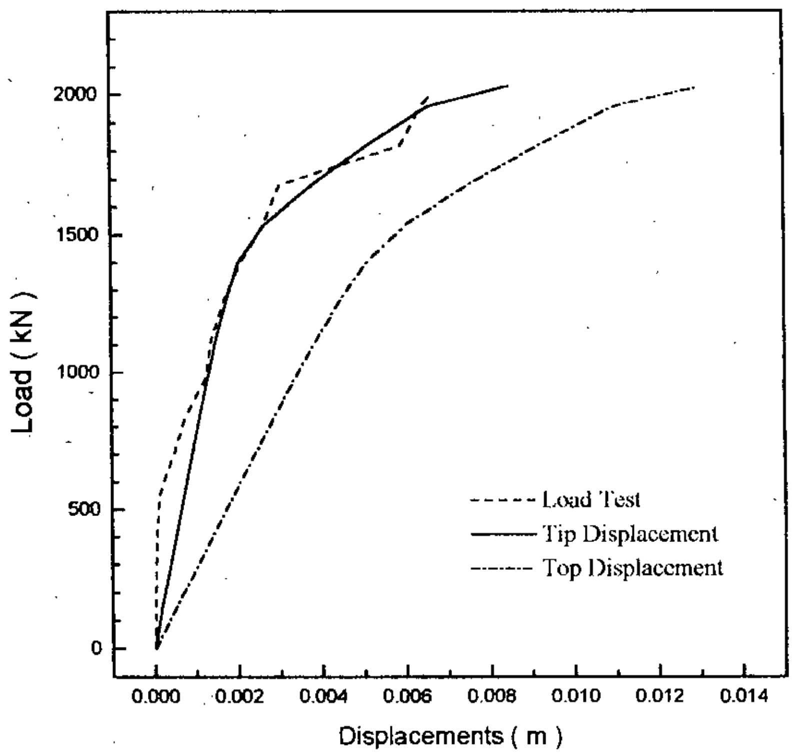

Fig. 3.7 Load-displacement responses of Pile A for displacements at pile top and pile tip.

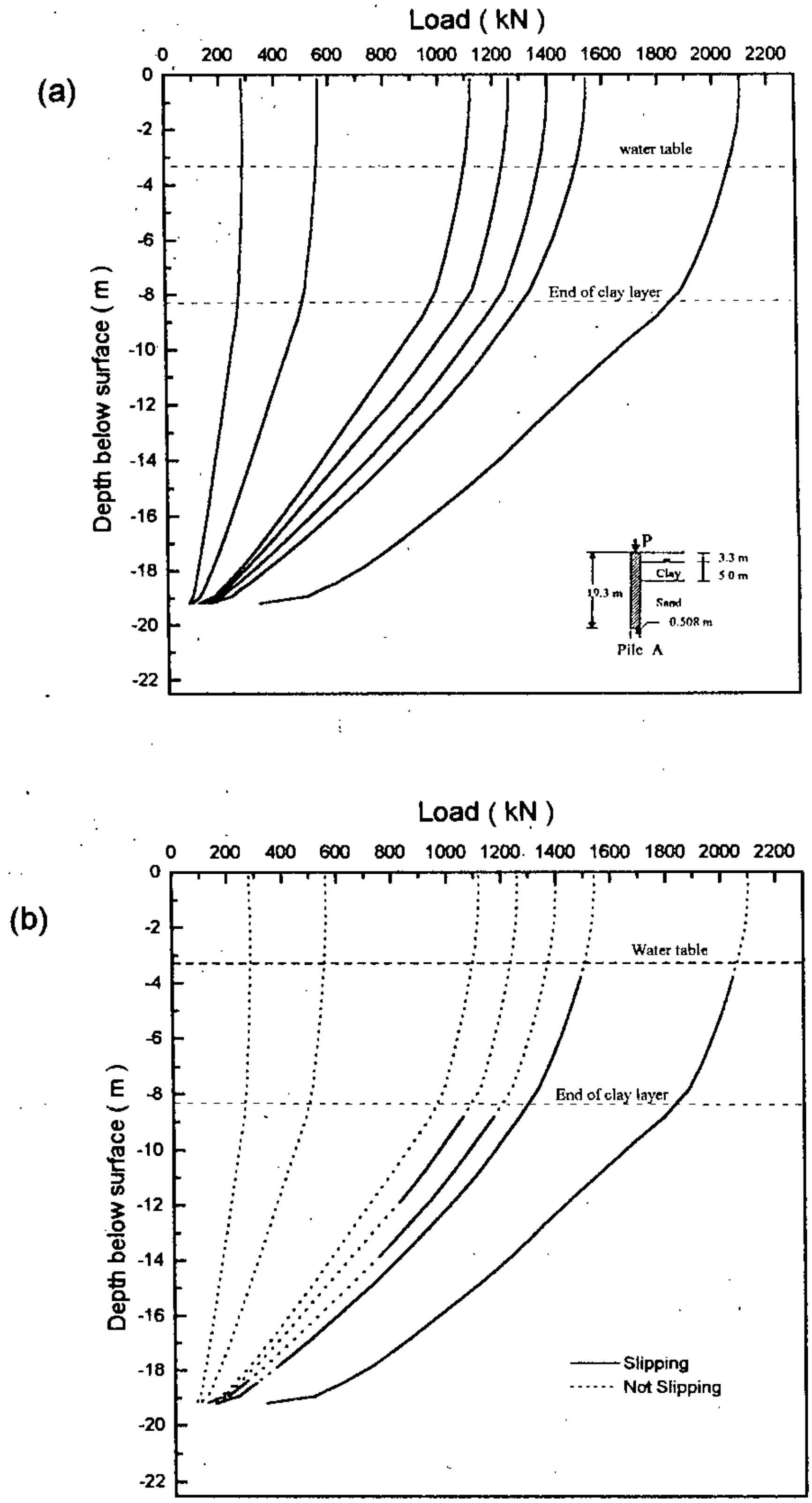

Fig. 3.8 (a) Pile load transfer with depth for different loads
(b) Pile load transfer with propagation of slippage.

Figure 3.8(b) depicts the slippage zone and its propagation with increasing load. First slippage occurs after more than 1100 kN of load and it starts in the beginning of the sand layer rather than the clay layer. With increasing load, the slippage moves both upward and downward upto 2030 kN load when almost all other zones show slippage. There is also some slippage near the pile tip. One thing should be noticed here that the initial clay layers which is above the water table has not slipped at all, as the effective *in-situ* stress is relatively greater here than the clay layer below the water table. So, the shear stresses developed in the interface of this layer have not reached its capacity.

The reason for starting of slippage first in the sand layer rather than in clay layer lies in the interface shear resisting properties of the two layers. In clay layer there is adhesion (C_a) with friction (ϕ) which resist shear, but in sand layer only frictional shear resistance comes into action. As a result, the shear capacity in the interface between pile and sand layer starts to reach limiting state first.

The interface element is formulated in such a way that it controls the slippage and the load transfer. Figure 3.9(a) shows the shear stress distribution of interface elements along the pile shaft. It is observed that the shear-stress in interface elements start to reach limiting value first at 1120 kN of load as was shown in Fig. 3.8(b) too. With increasing load, these shear stresses reach limiting values gradually along the shaft depth of pile in sand layer. When 1540 kN load is applied, the shear stress of the whole depth seem to reach limit and after that load, the shear stresses do not increase considerably.

If the shear stress distribution of soil elements adjacent to interfaces is looked at in Fig. 3.9(b), it is clear that these soil elements have shear stresses varying in the same manner as in the interface elements. When the shear stresses in interface reaches their limiting state, the shear stresses in adjacent soil elements does not increase any more.

The shear stress contours for 560 kN, 1560 kN and 2030 kN are shown in Figures. 3.10(a), (b) and (c) respectively. All these plots show that the maximum shear stresses develop near the shaft of pile with a tendency of shear stress concentration near the

(a)

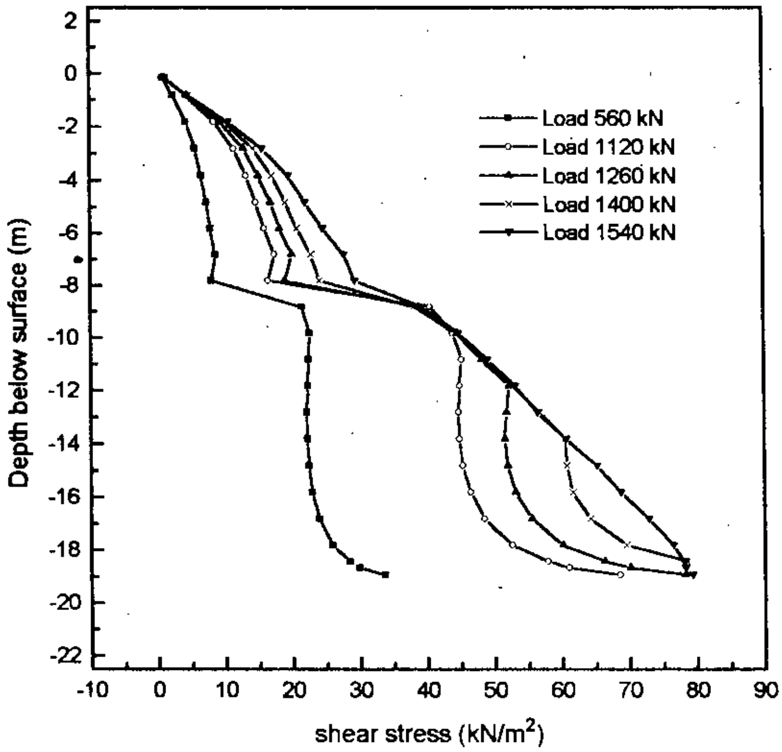

(b)

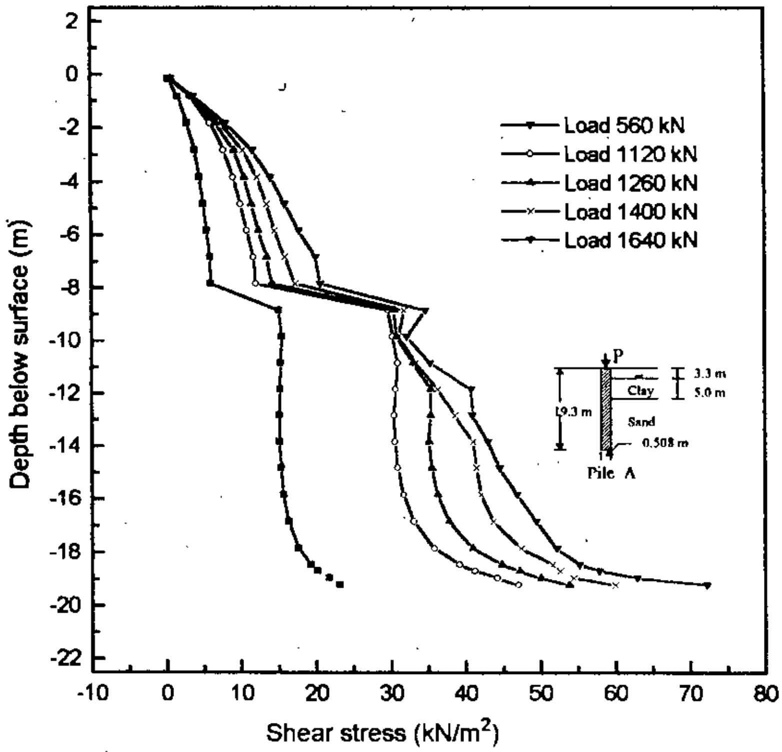

Fig. 3.9 Shear stress distribution with depth (a) for interface elements (b) for elements adjacent to interface

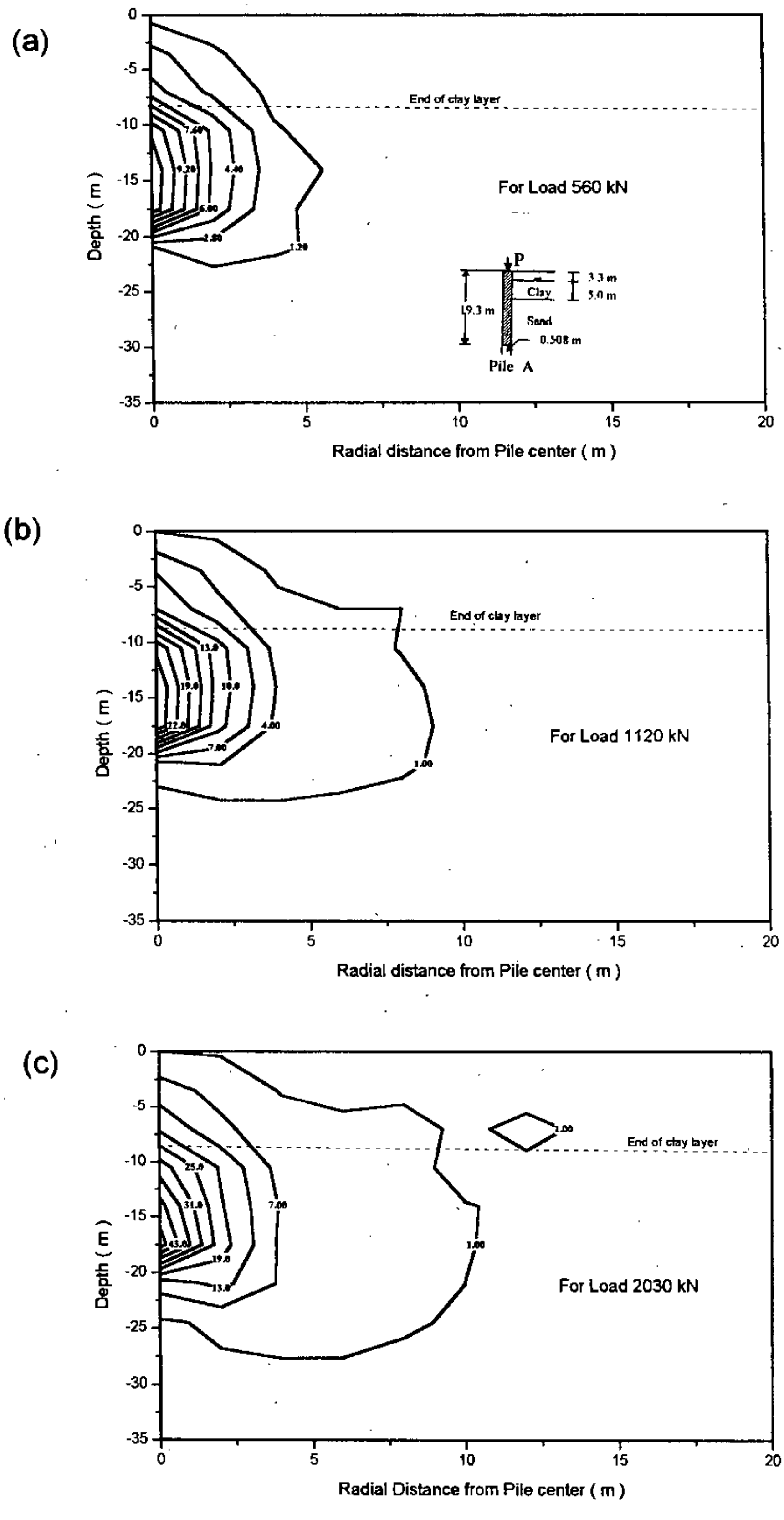

Fig. 3.10 shear stress contour for (a) 560 kN, (b) 1120 kN and (c) 2030 kN load

pile tip. As the pile transfers load predominantly as friction along the shaft, this pattern of shear stress contours is quite expected. When the tip resistance would be significant, only then maximum shear would occur below the pile tip. Besides, the contours seem to become uniformly varying in the sand layer as sand layer has greater shear strength.

3.4.3. Pore water pressure

The excess pore water pressure developed and their dissipation with time for different depth in clay layer are shown in Figures. 3.11(a), (b) and (c). For the time span shown, as used in pile load test, it is evident that very insignificant excess pore pressure has been dissipated. Hence, the subsequent displacement due to consolidation is very nominal as compared to the immediate displacement which is also the case in actual load test. For the three depth selected in these plots, 4 m and 8 m depth show more excess pore pressure dissipation than for 6 m depth. This is so because the other two depths are near the drained boundaries. But depth of 6 m is deep in the clay layer, so it is taking much greater time than the other two to dissipate the excess pore pressure.

Figures 3.12(a), (b) and (c) show the dissipation of pore pressure with radial distance from pile shaft center for all three depths discussed earlier. These figures indicate that significant pore pressure increase due to loading take place near the pile shaft. Some distance away from it, the pore water pressures assume in-situ value again. This confirms that the consolidation settlements are concentrated only close to the pile and it is insignificant some distance away from the pile.

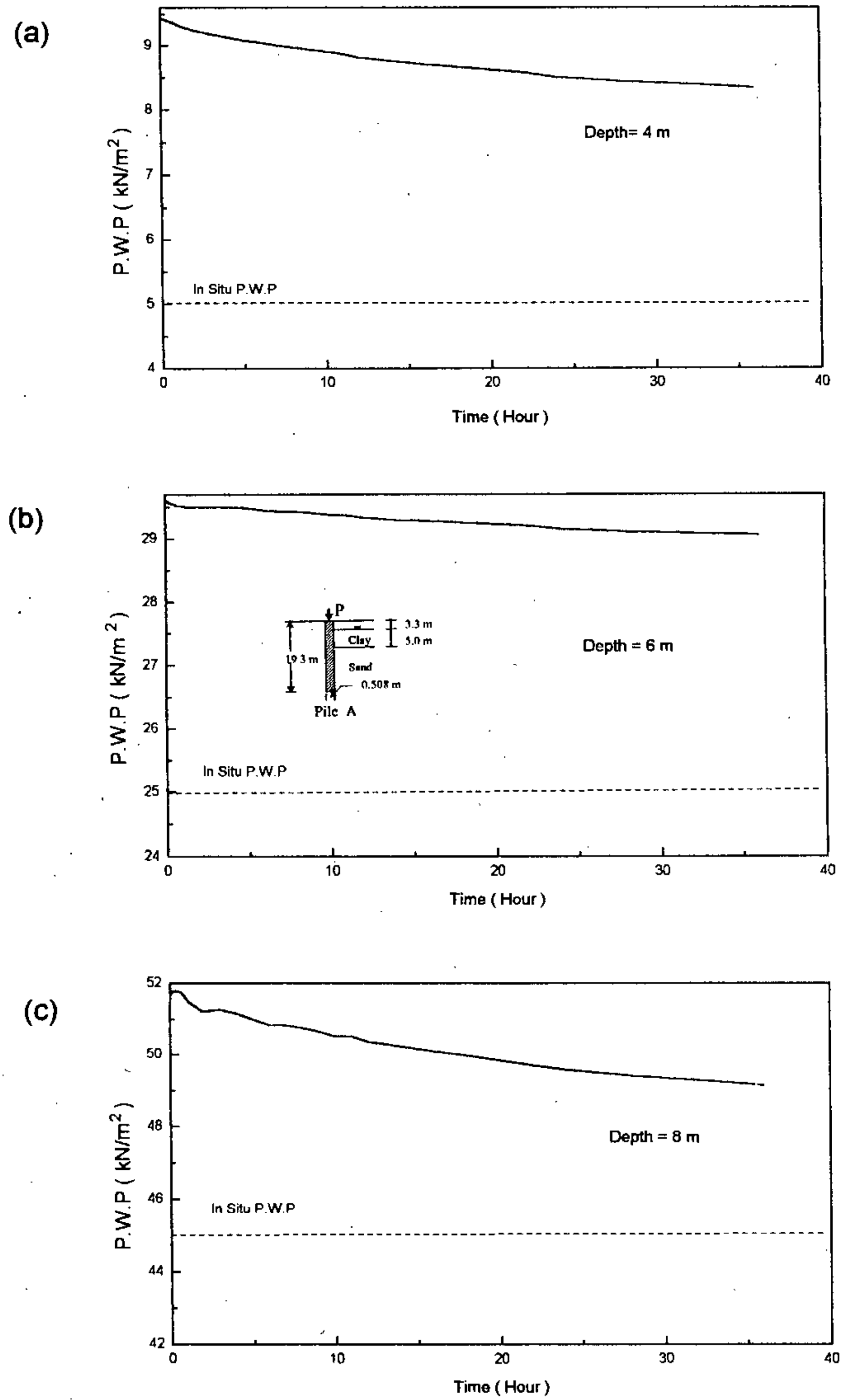

Fig. 3.11 Pore water pressure distribution with time for (a) 4 m, (b) 6 m and (c) 8 m depth

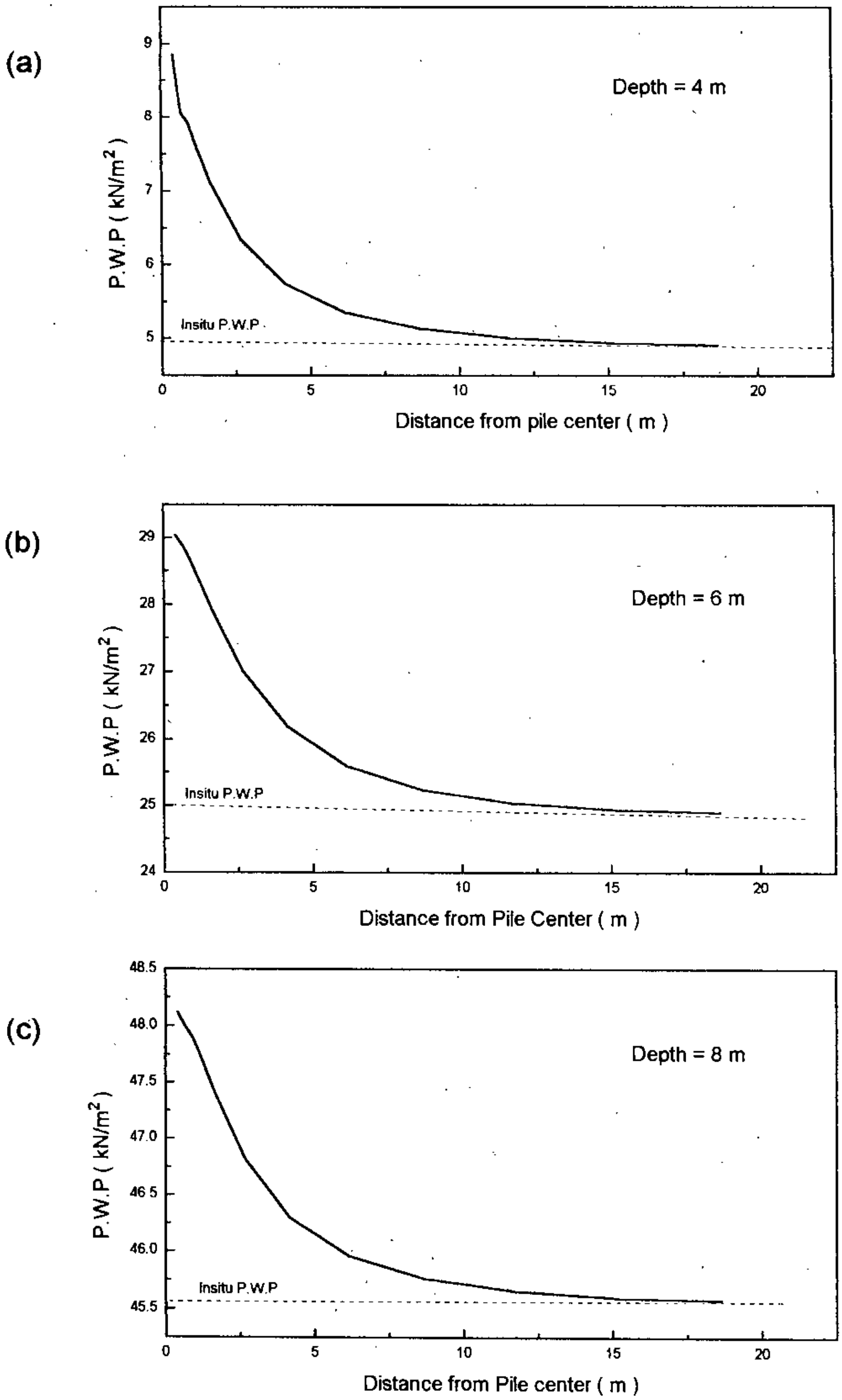

Fig. 3.12 Pore water pressure distribution with radial distance from pile center for (a) 4 m, (b) 6 m and (c) 8 m depth

CHAPTER 4

ESTABLISHMENT OF A METHODOLOGY FOR DETERMINING MESH PARAMETERS OF SOIL-STRUCTURE INTERACTION SYSTEM

4.1 INTRODUCTION

For any finite element analysis pertaining to soil-structure interaction study, the configuration of mesh has considerable influence on the subsequent predictions. Ideally, infinitely extending fine mesh gives accurate predictions when compared with coarser as well as not to extended mesh. But increase in computing time and very little improvement achieved due to this refinement make such exercise less attractive. Therefore, a pragmatic, yet sufficiently refined mesh configuration has to be found out for satisfactory predictions. Jayatheran (1996) have suggested parameters for selecting reasonable mesh configurations as applicable to the soil-structure analysis, with special reference to piles. In this chapter, an extensive comparative study on mesh configuration, with respect to deep (pile) foundation, is presented. This study has been carried out in order to arrive at a more objective mesh configuration as applicable to Dhaka-soil. The study circles around pile foundations mainly because reliable data of load-tests performed on full scale bored piles cast-in-situ in Dhaka soil were available. More importantly, it was thought that the detailed nature of soil strata of Dhaka soil can be best incorporated into the mesh by studying the interaction of pile with soil, both extending to a considerable amount to soil. It is believed that the adopted methodology as well as the sensitivity of various mesh parameters as understood from this chapter will also give some guidelines for the study of other interaction problems.

4.2 DETERMINATION OF VARIOUS PARAMETERS OF MESH CONFIGURATION

4.2.1 Scheme

Several parameters play important roles for satisfactory performance of any finite element idealizations. Their degree of importance also depends on the objective and type of system on which the analysis is carried out. In this study, seven very crucial parameters are selected (see Fig. 4.1). The parameters are, the radial extent of mesh from the pile edge (C_1); the vertical extent of mesh from pile tip (C_2); the rate of change of element size with horizontal distance from pile edge and vertical distance from pile tip (m_r), the loading rate (L_i); the number of elements along the pile length and its interface with soil (N_1); the number of elements within a distance of twice the diameter of pile from pile tip (N_2) and the thickness of interface element (T_i).

Usually triangular elements are used as a transition from fine to coarse mesh. However, in the present study triangular elements have not been adopted for such practice. This allowed the fixing of the parameter m_r, which relates the dimensions of various elements of the FE mesh. Once the sensitivity of this parameter (m_r) is sorted out from this study, it would act as a criterion for selecting the distance from pile where triangular element could be used as a measure of transition from small- to large-sized elements. Besides, modern day computers, with enormous memory and speed, pose lesser problem in running time and cost as they used to do in the past. Therefore, a gradual increase of quadrilateral element dimensions without using triangular element is justifiable.

Although the element dimensions are increasing with distance from the pile edge or tip, the sizes of the elements along the pile length have been considered to be constant as it is a good practice to keep the dimensions of all the elements that connects the interface elements, constant (Jayatheran, 1996). Moreover, the high stressed zone such as the zone near the pile tip should have very finer mesh. The size of the elements within a radial distance of 2D have been kept to a smaller and constant dimension following the guidelines of Jayatheran (1996).

The thickness of interface elements have been selected using the criteria of t/b ratio within 0.01 to 0.1 as suggested by Desai (1984). Again, the rate of load increment has a significant effect on incremental finite element analysis. The rate of load increment is selected in such a way that the yield ratio (YR) be within 0.95 to 1.05. Larger increments are used for linear portion of analysis and finer increments are used for non linear portion of analysis.

Drained analysis has been done for all the cases investigated here to fix mesh configuration. As it is expected that the impacts of various parameters in shaping the mesh may not be dependent on the type of analysis - drained or undrained. Drained analysis has been performed which is very pragmatic for sandy soil and predicts larger displacement (i.e. conservative response) than any other analysis for clayey soil. Finally, consolidation analysis has been performed on the mesh configured following the guidelines as obtained from this study by drained analysis. The effect of time increment is also investigated and selected subsequently in the final consolidation analysis.

The pile used in this study has a length of 19.3 m and diameter of 0.504 m. The site in which the pile is bored is Senakallayan Bhaban site for which case, extensive soil and pile load test data were available. The various relevant soil and pile material parameters for this pile (Pile A) have been listed in Tables 3.2, 3.3, 3.4, 3.5, 3.6 and in Fig. 3.1.

4.2.2 Determination of C_1

The lateral extent of mesh (C_1) is a very important parameter. To investigate the effect of the variation of C_1 on the accuracy of analysis, other parameters have to be kept unchanged. Table 4.1 shows the values of various parameters used in this study for determining C_1.

Table 4.1 Parameters used in fixing C_1

m_r (m/element)	C_1 (m)	C_2 (m)	L_i	N_1	N_2	T_i (m)
0.25 0.5 1	5 10 15 20 25 30	12	L_1 (see Fig. 4.2 for detail)	20	2	0.05

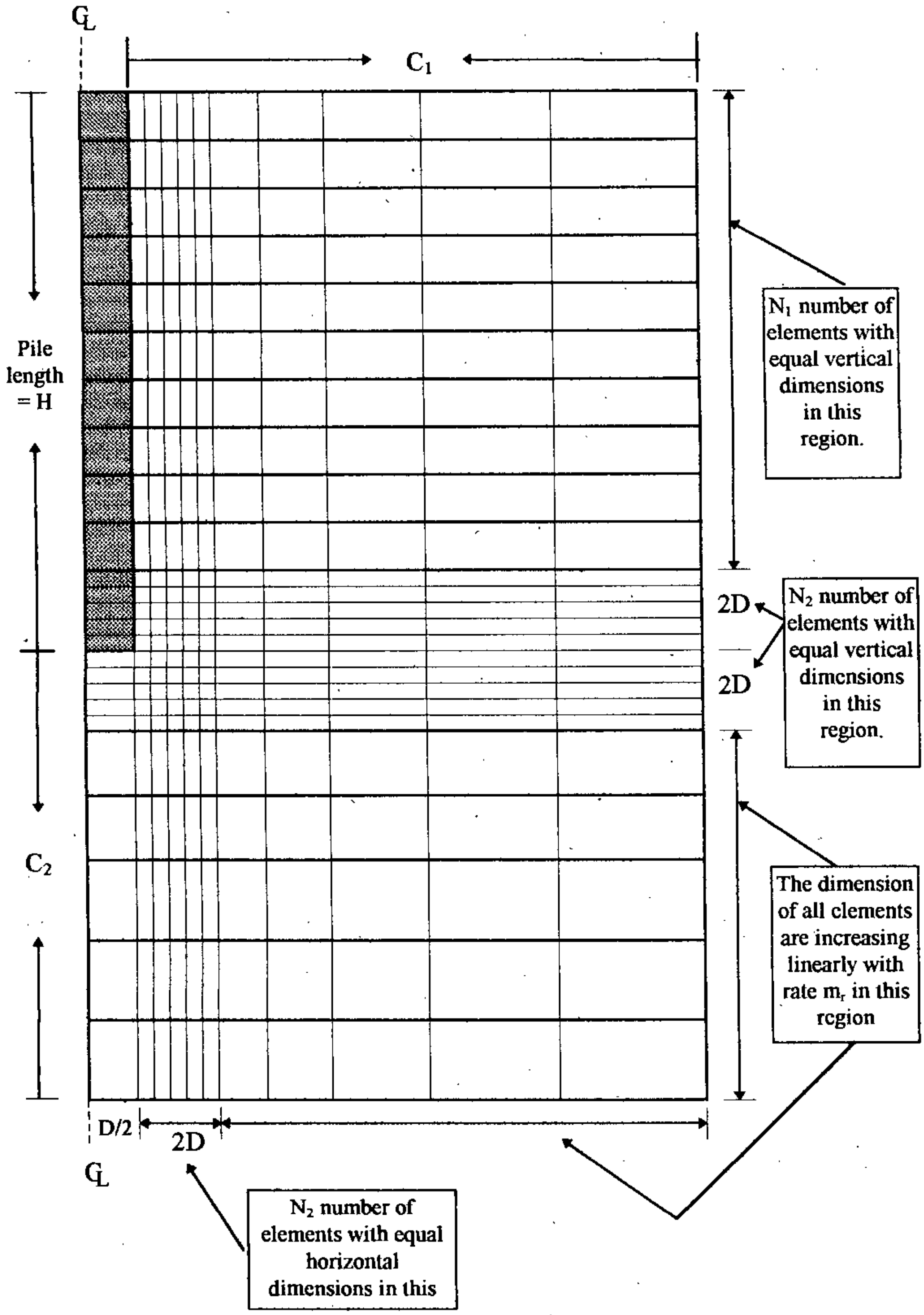

Fig. 4.1 Various critical mesh configuration parameters.

Load Range (kN)	Increment Size	No of Increment
0-1500	100	15
1500-1800	20	15
1800-2000	10	20

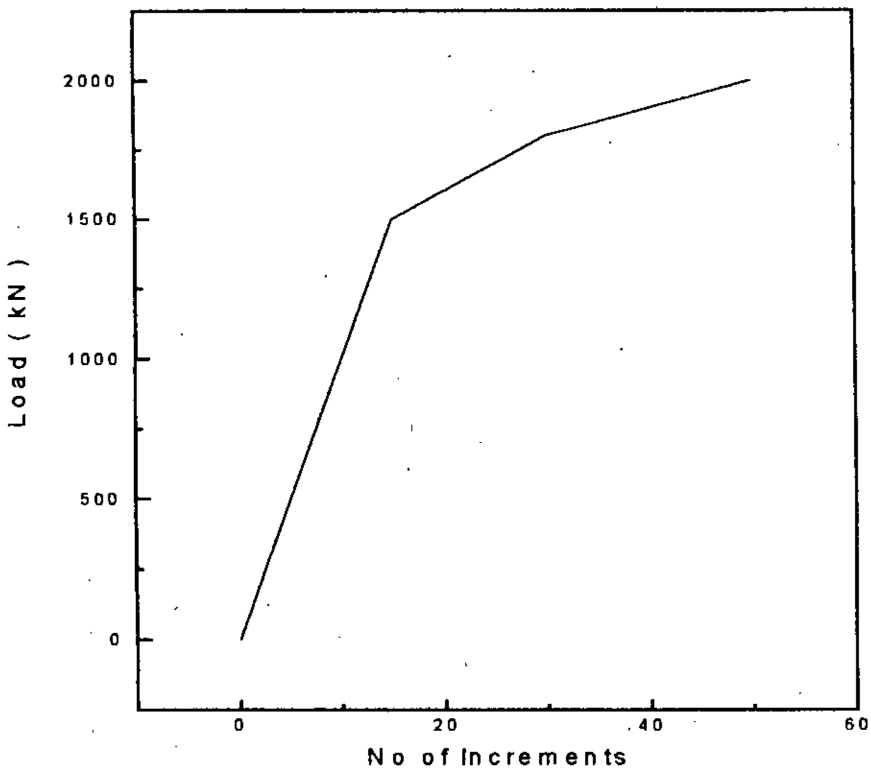

Fig. 4.2 The load increment rate L_1

Firstly, the effect of variation of C_1 in the load-displacement curve is investigated which is shown in Fig. 4.3. It shows that for all values of C_1 other than for C_1 equal to 5 m and 10 m, the load-displacement curves have very insignificant or no difference. For C_1 equal to 10 m, the curve deviates from the others slightly and for C_1 equal to 5 m, the curve deviates considerably from the convergent group. Therefore, as far as load-displacement behaviour is concerned, a value of 15 m for C_1 may be considered to be an acceptable value for predictions without impairing accuracy.

For understanding of the effect of C_1 better, it is understood that the radial boundary of a mesh has to be extended upto that point where stress caused by load on pile top becomes very negligible. In view of this understanding, a new parameter of stress which represents the overall stress conditions of any element has been introduced. This is called the Stress-norm (σ_{sn}) which can be calculated as follows:

$$(\sigma_{sn})_i = \left| \sqrt{(\sigma_x)^2 + \left(\sigma_y\right)^2 + (\sigma_z)^2 + \left(\tau_{xy}\right)^2} \right| \qquad (4.1)$$

Where,

$(\sigma_{sn})_i$ = stress-norm of element i
σ_X = normal stress of element i in x direction caused by extra load on pile top only
σ_y = normal stress of element i in y direction caused by extra load on pile top only
σ_z = normal stress of element i in z direction caused by extra load on pile top only
τ_{xy} = shear stress of element i in xy plane caused by extra load on pile top only

Here all the stresses have been calculated by subtracting the corresponding stress caused by *in-situ* stress only from the stress caused by load and *in-situ* stress combined.

The σ_{sn} for every element along the boundary 1 (BD_1), as shown in Fig. 4.4, has been calculated. These stress-norms for each element along BD_1 is then summed up to have $\sum(\sigma_{sn})_i$. Now, this $\sum(\sigma_{sn})_i$ for each value of C_1 is calculated and plotted in Fig. 4.5 for various values of m_r. It can be seen from Fig. 4.5 that $\sum(\sigma_{sn})_i$ for all elements along BD_1 decreases with increasing values of C_1. It is also clear that for all values of

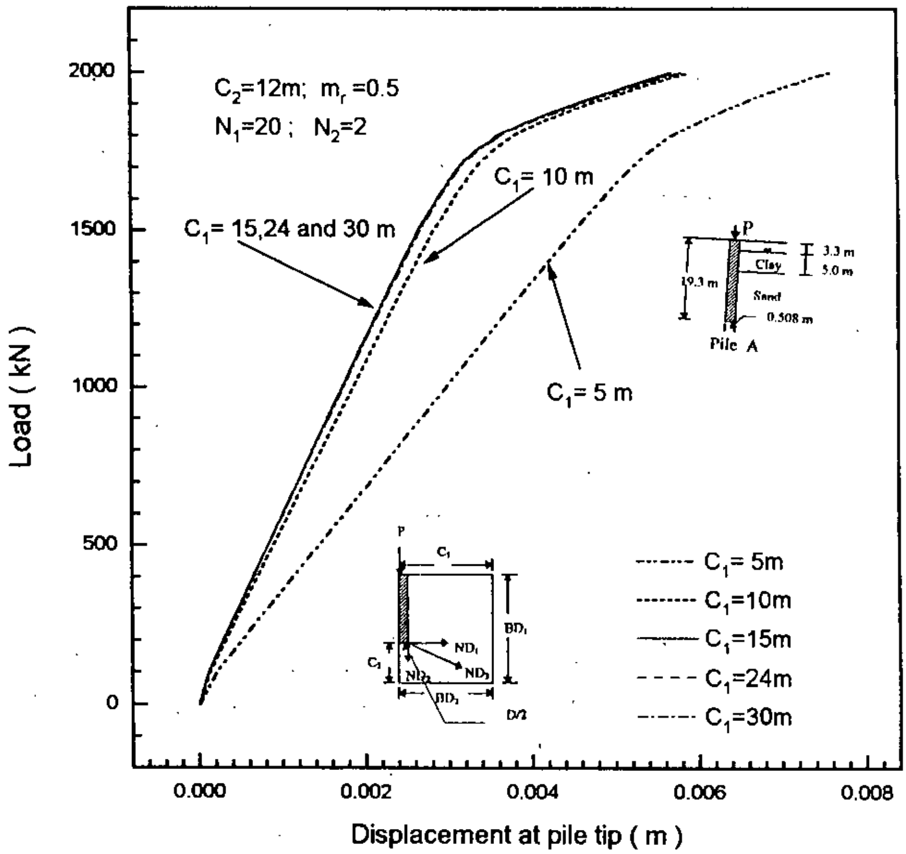

Fig.4.3 Load-displacement curves for various radial extent of mesh

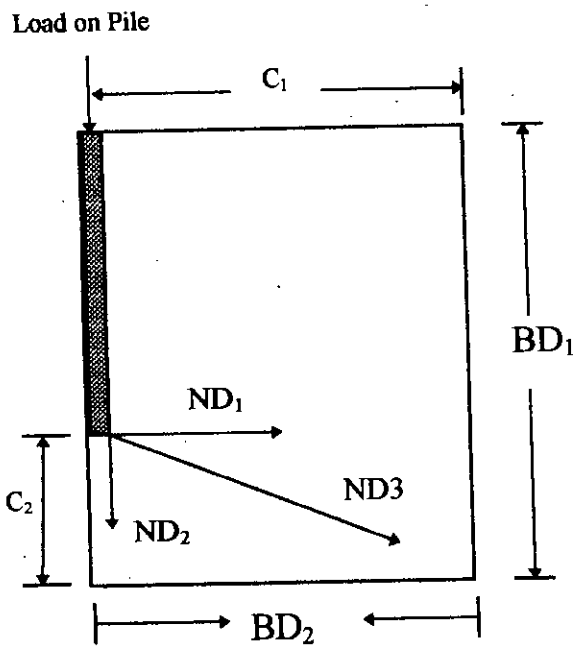

Fig 4.4 various boundaries and direction considered

m_r analyzed, the trend is similar and all curves converge as C_1 takes larger values. Starting from a value as high as more than 10 kN./m^2, $\sum(\sigma_{sn})_i$ reaches a value as low as below 0.4 kN/m^2. For C_1 ranging from 5 to 15 m, the value of $\sum(\sigma_{sn})_i$ decreases sharply, but after that decreases very slowly with increasing C_1. Therefore, the convergence of load-displacement curves for C_1 equal to 15 m or greater (Fig. 4.3) is justified as the values of $\sum(\sigma_{sn})_i$ for them are very insignificant. Although C_1 equal to 15 m gives reasonable results, C_1 equal to 20 m has been selected in this study as the radial distance upto which the mesh should be extended in order to mimic the actual soil-structure system more faithfully.

One can argue that the effect of C_1 on $\sum(\sigma_{sn})_i$ may not depict the whole picture as it does not cater for the variation of individual element stress along BD_1. To overcome this, a plot of variation of stress-norm for each element along the line ND_1 (see Fig. 4.4) is given in Fig. 4.6. Here, the stress-norm of these elements are plotted along the y-axis while the distance of corresponding elements are plotted along x-axis. Figure 4.4 shows that the highly stressed elements are those which are within 3 to 4 m of pile tip. For other elements along ND_1 , the value of stress-norm decreases very slowly with increasing C_1. Therefore the selection of the value of C_1 as 20 m is justified again, as the stress-norm becomes negligible beyond this value of C_1.

From all these comparative analyses, the value of C_1 has been selected to be 20 m. In this case the value of C_1 equals to the length of pile (H). In the subsequent analysis, C_1 has been taken to be equal to H; the ensuing findings as well as cross-checks proved that the use of C_1 equal to H is justifiable in all respect.

4.2.3 Determination of C_2

A comparative analysis, similar to the one undertaken for C_1, has been performed in order to fix C_2. The parameters used in this exercise is presented in Table 4.2

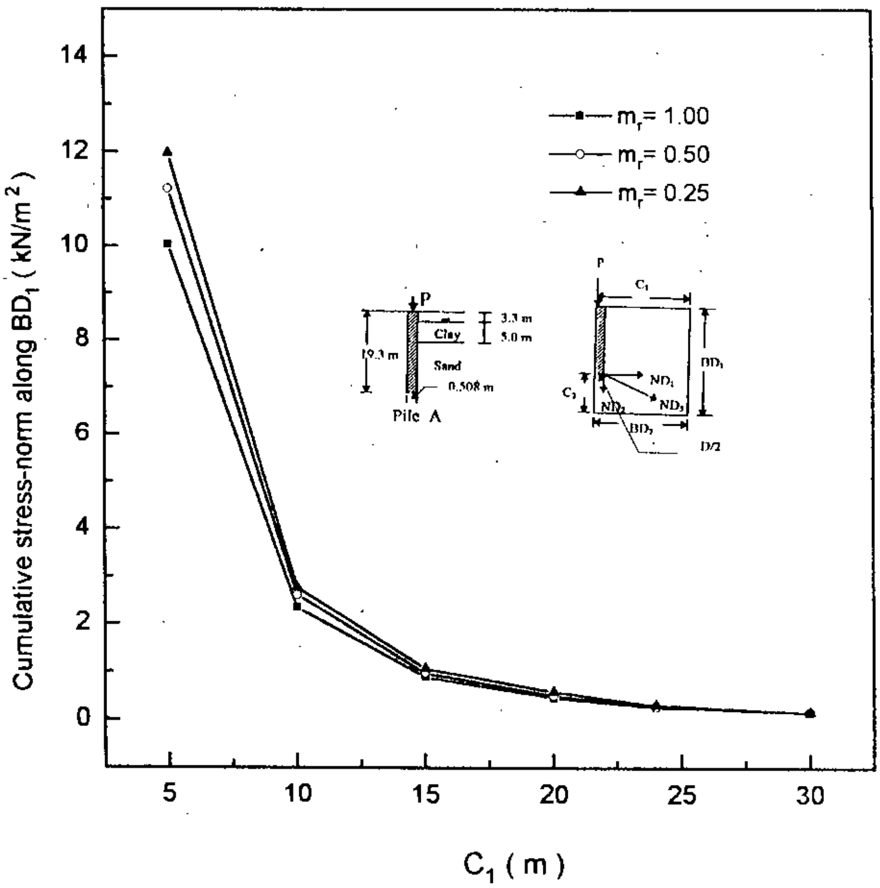

Fig.4.5 Variation of cumulative stress-norm along boundary BD_1 with radial distance from pile

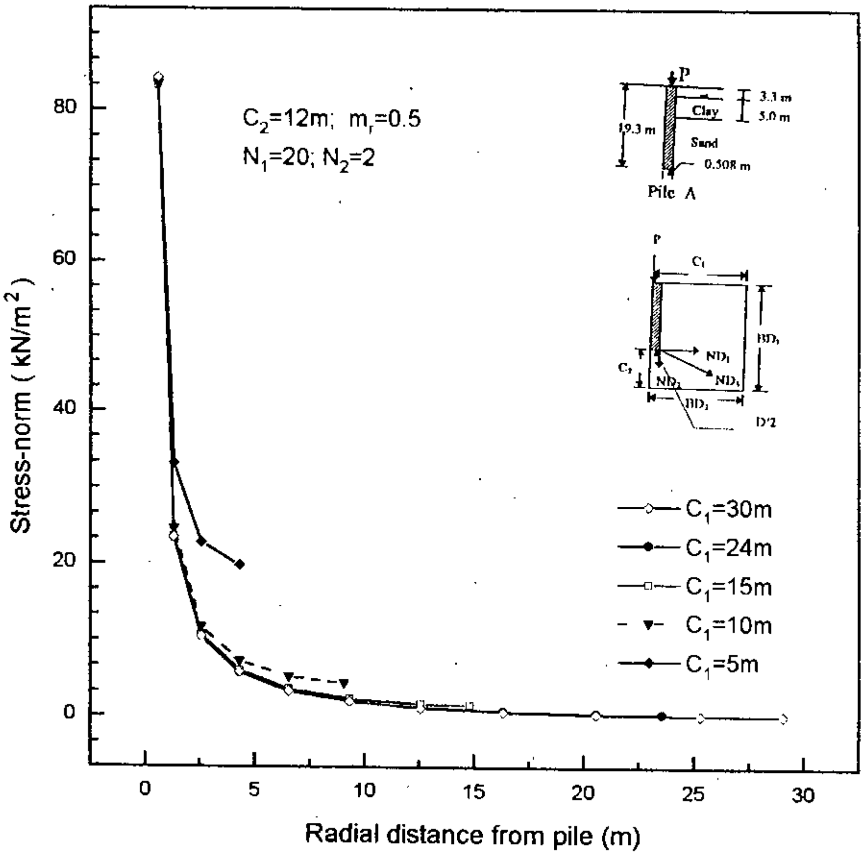

Fig. 4.6 Variation of stress-norm with radial distace (along ND_1) from pile center

Table 4.2 Parameters used in analysis for fixing C_2

m_r (m/element)	C_1 (m)	C_2 (m)	L_i	N_1	N_2	T_i (m)
0.25 0.5 1	20	5 10 15 20 25 30	L_1	20	2	0.05

The effect of variation of C_2 on the load-displacement curve of pile is shown in Fig. 4.7. The figure shows that for increasing values of C_2, the curves tend to shift rightways slightly. At the region, where transition from linear state to nonlinear state occurs, the rightward shifts are most significant. After that region, curves start converging. From engineering point of view, the values of C_2 equal to 15 m, 20 m or 25 m are equally good as they represent very little difference in the load at the onset of significant nonlinearity. It can be expected that for very large values of C_2, the load-displacement curves will converge completely. But increase in the running time cost, would make the use of a very large value of C_2 less attractive as reasonable results could easily be obtained by using a smaller value of C_2.

Figure 4.8 shows the variation of $\sum(\sigma_{sn})_i$ for boundary 2 i.e. BD_2 (Fig. 4.4, Eq. 4.1) with increasing value of C_2. As expected, the values of $\sum(\sigma_{sn})_i$ decreases exponentially with increasing value of C_2. For values C_2 between 5 to 15 m, the curves show significant decline, but after that the rate of decrease becomes sluggish and use of a very large value of C_2 (say C_2 equal to 30 m) would result in very little improvement in the load deflection behaviour. It should be noted here that the value of $\sum(\sigma_{sn})_i$ in the present case did not converge to an insignificant quantity as was the case with C_1.

Likewise, the stresses caused by load on pile top did not attain a negligible value in BD_2 either. This explains the non-convergence of load deflection curves with increasing C_2 for the range of C_2 used. Understandably for those values of C_2 when

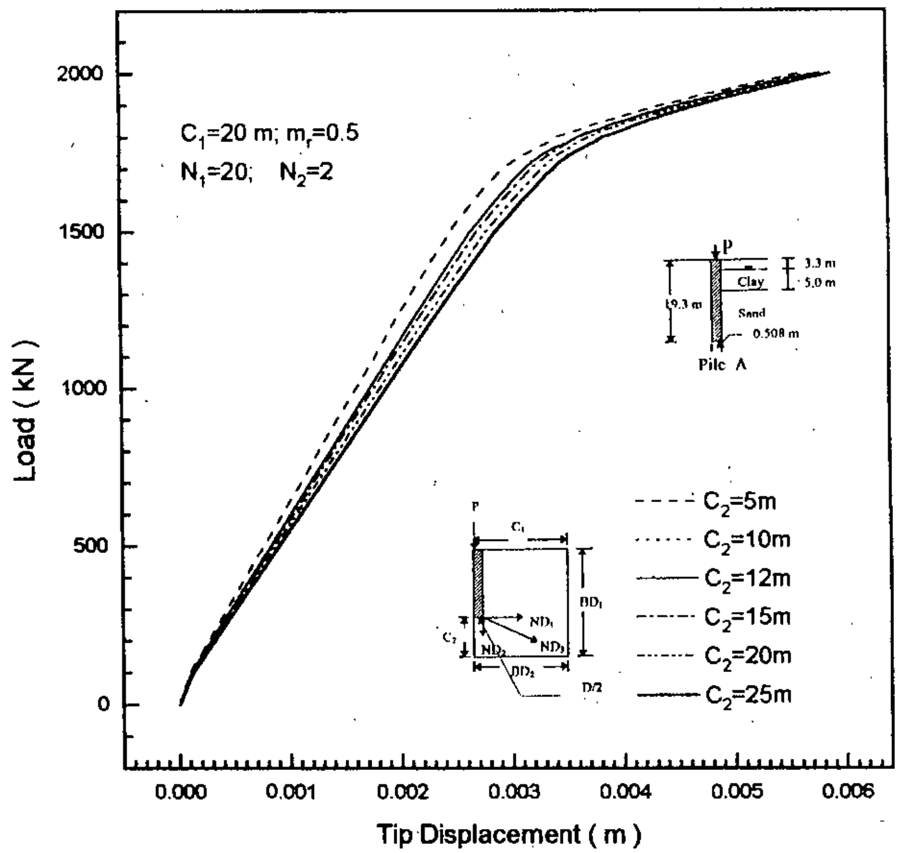

Fig.4.7 Load-displacement curves for various depth of mesh below pile tip

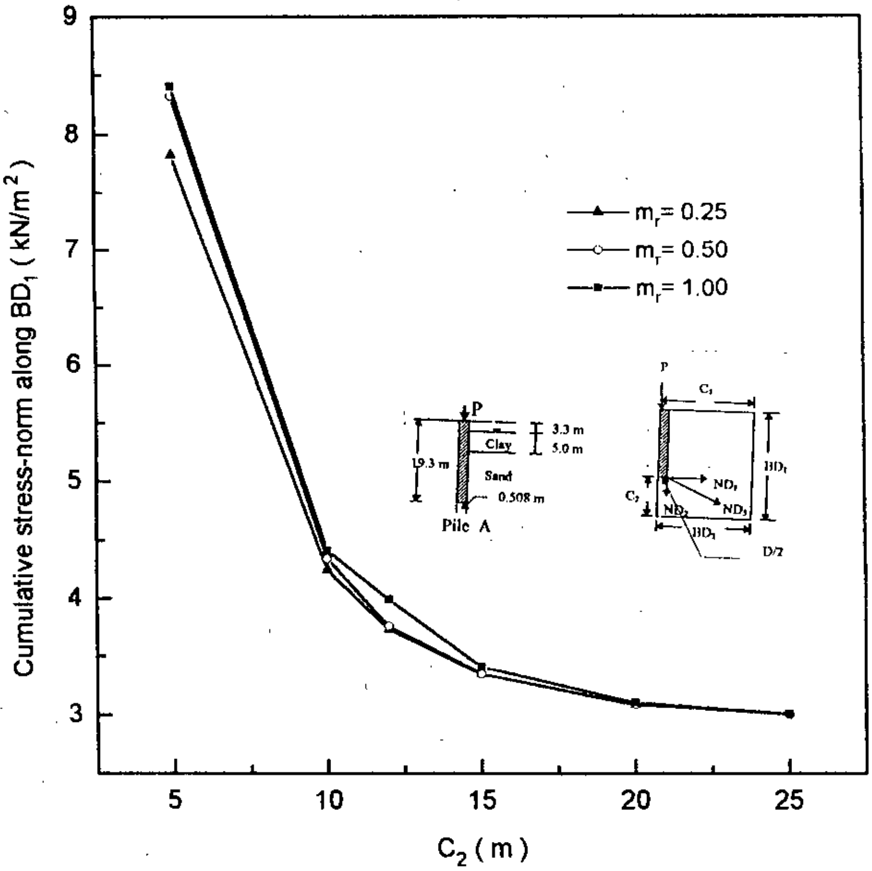

Fig. 4.8 variation of cumulative stress-norm along BD_2 with radial distance from pile center

$\sum(\sigma_{sn})_i$ for BD_2 would be near to zero, the load deflection curves are expected to converge. But, drastic increase in running time and cost, yet very little tangible benefit compels us to select smaller value of C_2. The effect of m_r on the relation of $\sum(\sigma_{sn})_i$ of BD_2 with C_2 has also been shown in Fig. 4.8. For all the values of m_r, curves show the same trend. But for values of m_r equal to 0.5 and 0.25, they almost give the same result at value of C_2 equal to 15 m or higher. Thus, although the use of m_r equal to 1.0 may lead to a slightly coarser mesh, the other two values lead to reasonable mesh refinements.

As in the case of C_1, the variation of stress-norm in every elements along ND_2 line (Fig. 4.4) is shown in Fig. 4.9. It can be seen from Fig. 4.9 that the stress-norm declines very sharply within the first 5 m below the pile tip. After that depth, σ_{sn} almost becomes asymptote to $\sigma_{sn} = 0$ line. If the scale used in σ_{sn} axis is looked at, it becomes clear that this figure does not do justice to the relative variation of σ_{sn} with depth from pile tip as the scale is very large when compared to the scale used in Fig. 4.6. To overcome this, the Fig. 4.9 has been blown up and is shown in Fig. 4.10. It is apparent that for C_2 equal to 15 m or more, the values of σ_{sn} decreases very slowly with increase in depth.

Therefore, from all these comparative analyses, it can be stated, admittedly tentatively, that the use of C_2 equal to 3/4 H (i.e. 15 m in the present case) may lead to satisfactory prognosis in all cases with m_r equal to 0.5 or less.

Finally, the plot of σ_{sn} with radial distance from pile tip, i.e. along ND_3 (Fig. 4.4) is presented in Fig. 4.11 to justify both the selection of C_1 and C_2. It clearly shows that for C_1 equal to 20 m and C_2 equal to 15 m (the radial distance being equal to 25 m), σ_{sn} becomes almost equal to zero. Thus there is no point in increasing the size of the mesh as the stresses caused by load on pile top become negligible indeed at the boundaries of the mesh selected.

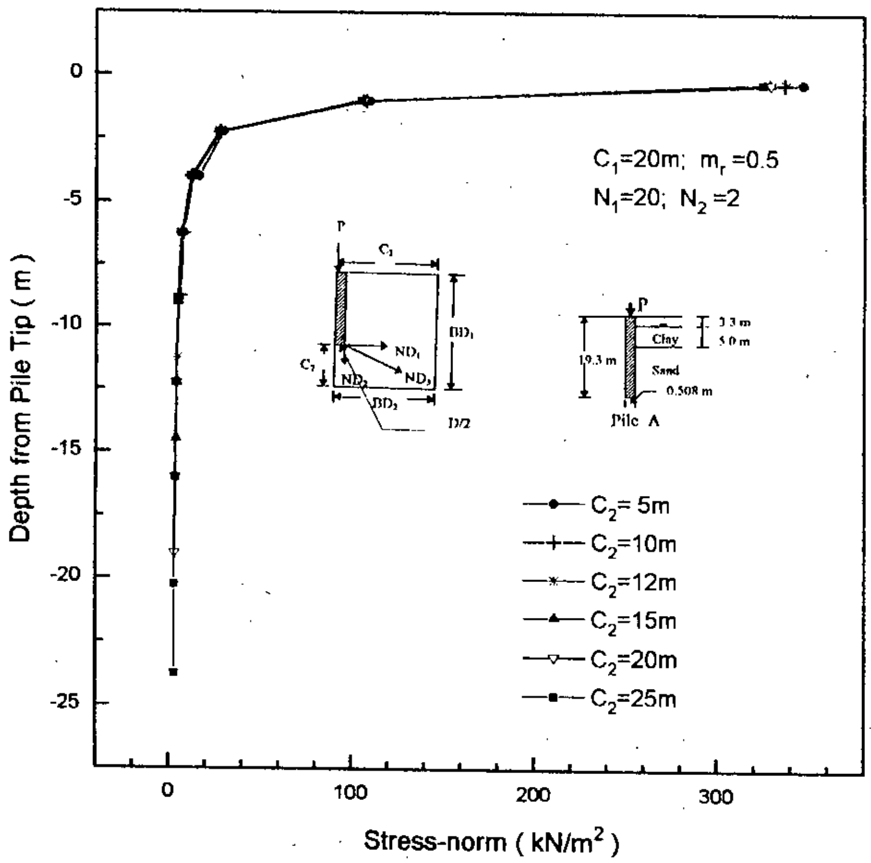

Fig. 4.9 Variation of stress-norm with depth (along ND_2) from pile tip

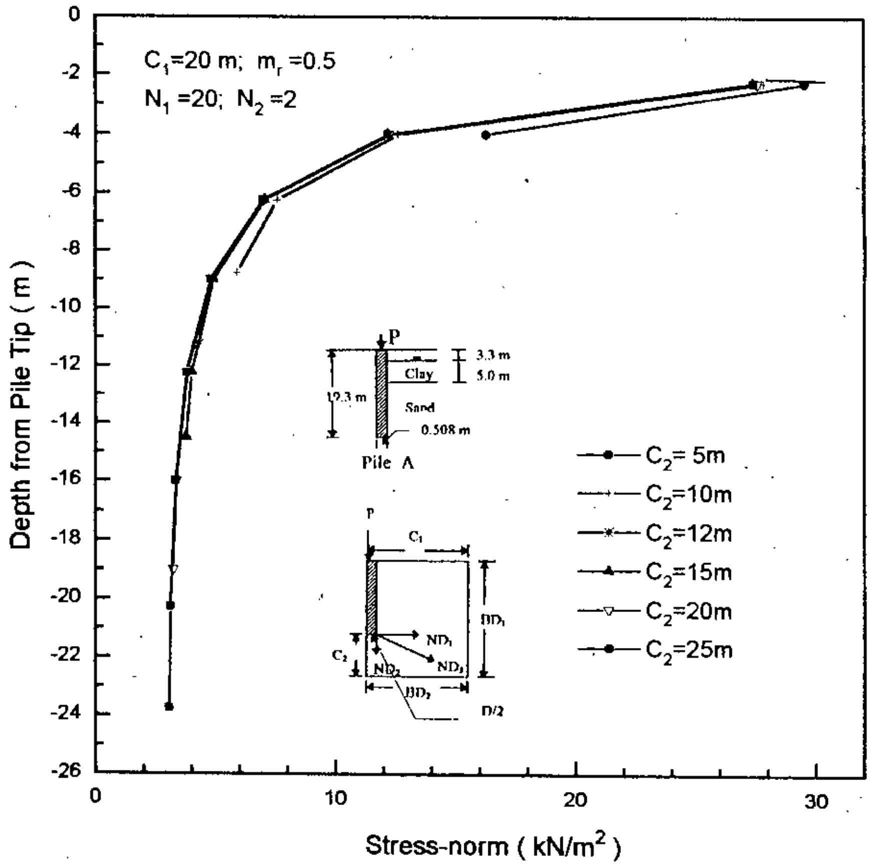

Fig. 4.10 Variation of stress-norm with depth (along ND_2) from pile tip

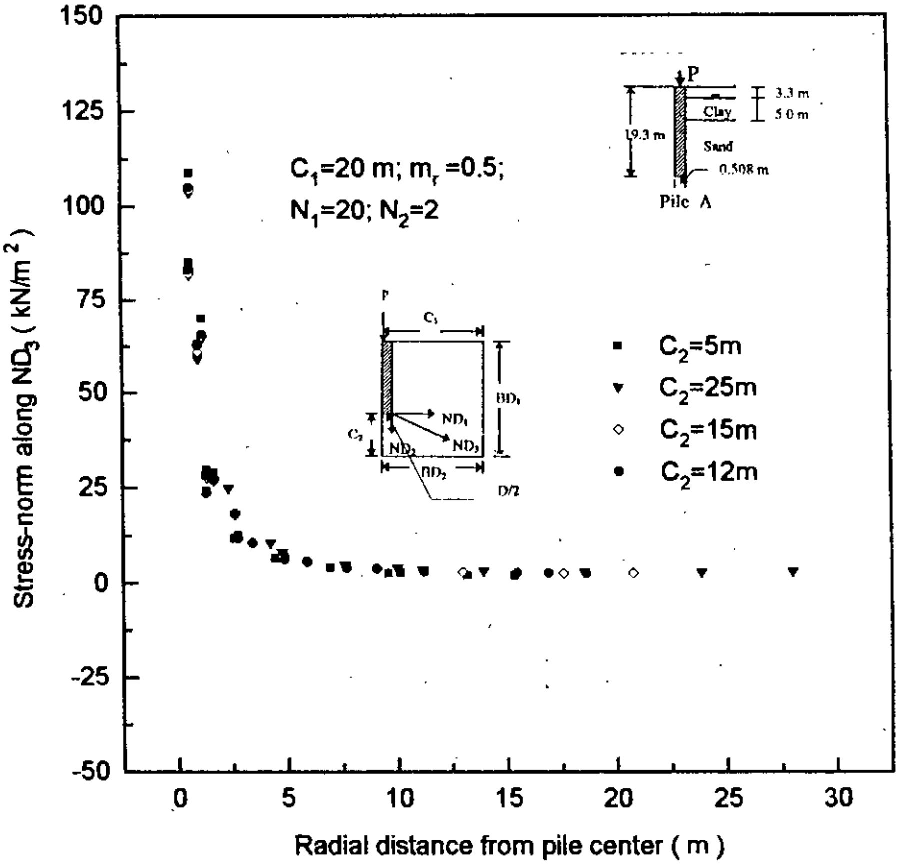

Fig. 4.11 Variation of stress-norm with distance along ND_3

4.2.4 Determination of m_r

Till now, three different values for rate of increase of element dimension have been investigated for fixing C_1 and C_2. This article deals exclusively with the effect of m_r on the predicted response and a fourth value of m_r has also been investigated here for better understanding and improving confidence. Other parameters have been fixed in the light of section 4.2.2 and 4.2.3, and they are presented in Table 4.3

Table 4.3 Parameters used in analysis for fixing m_r

m_r (m/element)	**C_1 (m)**	**C_2 (m)**	**L_i**	**N_1**	**N_2**	**T_i (m)**
1.000 0.500 0.250 0.125	20	15	L_1	20	2	0.05

Figure 4.12 shows the effect of varying m_r on load-displacement curves. It is clear form Fig. 4.12 that for the three values of m_r used in this analysis, the load-displacement curves completely converge into one. Therefore, there is no practical benefit in using much finer mesh than the meshes adopted in this study. However, since the use of m_r equal to 1.0 results in too high value of aspect ratio for some elements distant from pile, for satisfactory finite element analysis a value of m_r equal to 0.5 appears to be reasonable.

To have a better understanding of the effect of varying m_r, the variation of stress-norm for every element along ND_1 and ND_2 directions (Fig. 4.4) are plotted in Fig. 4.13 and Fig. 4.14, respectively. Both the figures show that for m_r equal to 1.0, the variation of stress-norm within 5 m of pile tip is more or less discrete and discontinuous. But for m_r equal to 0.5 and 0.25, the variation of norm is more continuous. Besides for m_r having a value of 1.0, the curves show clear deviation from the other two cases while for m_r equal to 0.5 or 0.25, curves reasonably converge into a single continuous

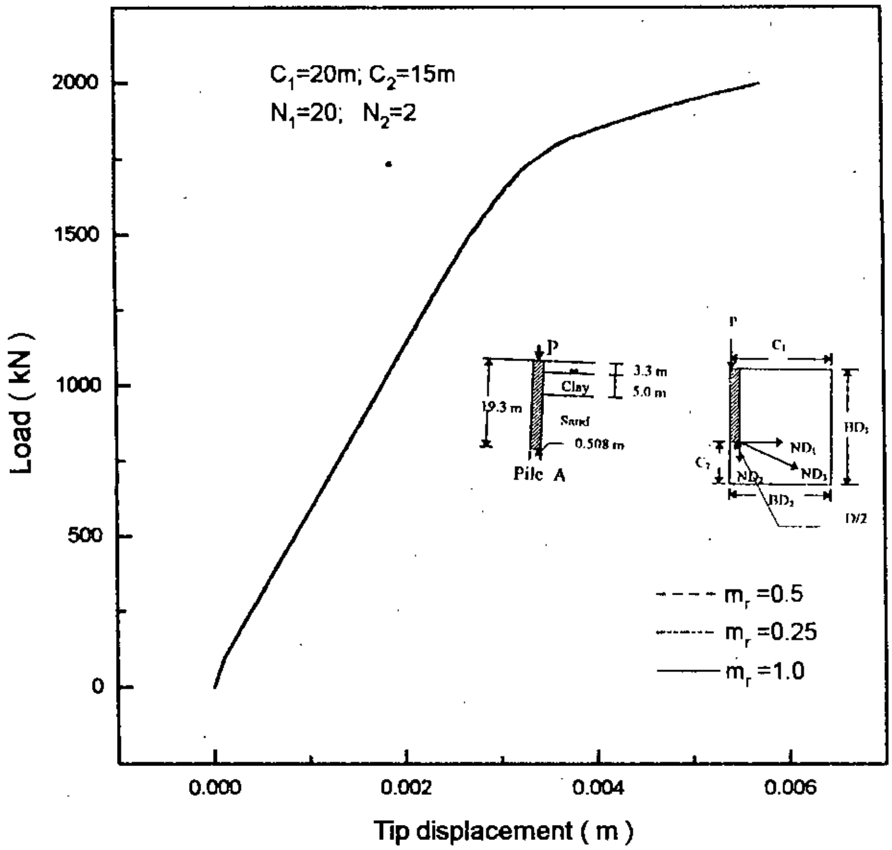

Fig. 4.12 Load-displacement curves for various m_r

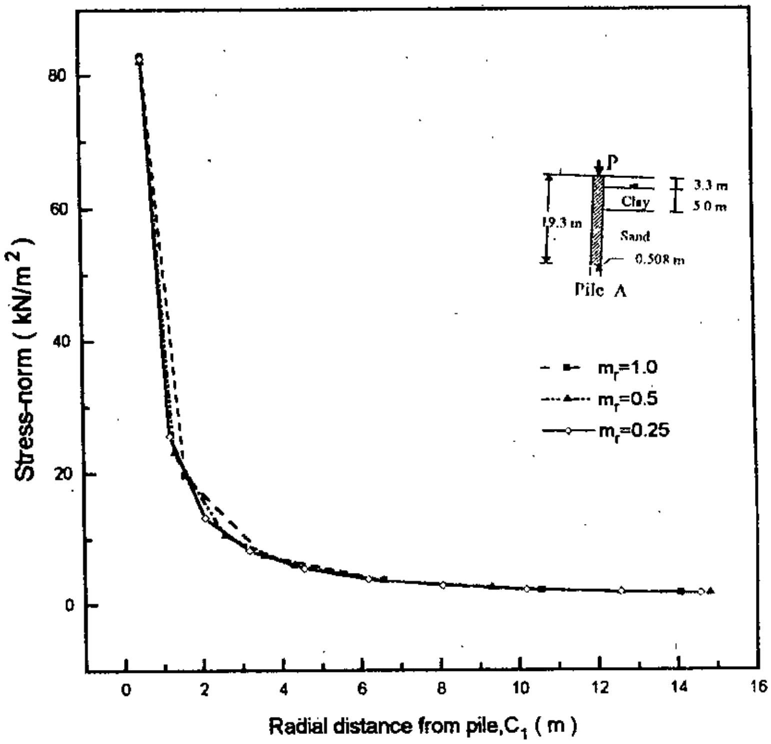

Fig. 4.13 Variation of stress-norm with radial distance from pile center

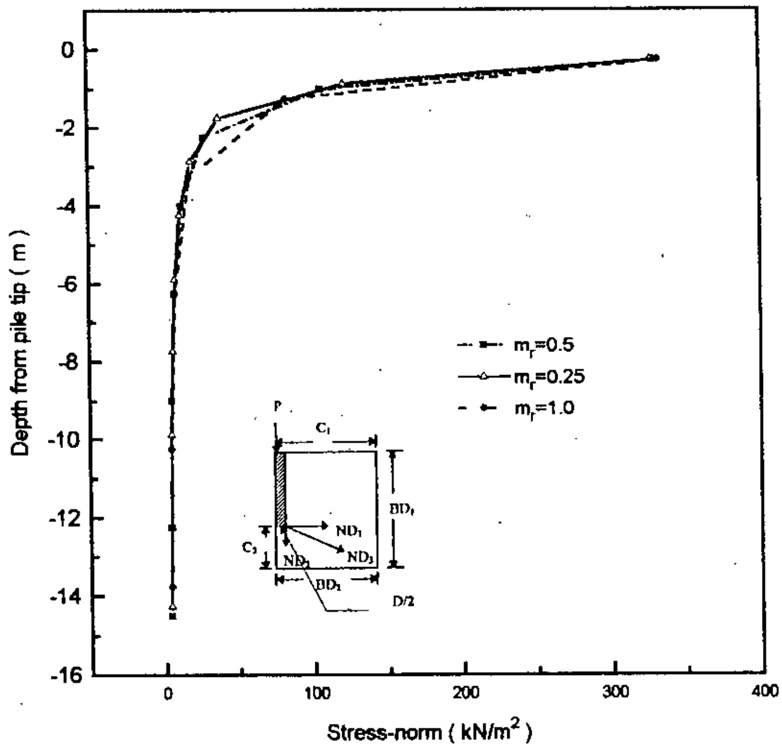

Fig. 4.14 Variation of stress-norm with depth from pile tip

curve. Therefore, the selection of m_r equal to 0.5 is quite reasonable as a value of m_r equal to 0.25 does not improve the trend.

There is another thing worth mentioning here. Figures 4.13 and 4.14 show that the effect of increasing dimensions of elements is more pronounced within say 5 m of pile tip and beyond that point, higher rate of increase of mesh size can be adopted. Therefore, it appears to be a better approach to select smaller increase rate for first 5 m or (H/4 in the present case) distance from pile and a larger increase rate for elements beyond that region.

In this analysis, the number of elements within a distance of 2D from pile tip (N_2) has been taken to equal to 2. If finer mesh is adopted in that region (say N_2 equal to 4), the effect of m_r on load-displacement curves may slightly differ from those shown in Fig. 4.12. Here, the value of N_2 may be selected as 4 in some of the analyses to be carried out later in section 4.2.7. The effect of varying m_r for the case of N_2 equal to 4 is worth investigating. Figure 4.15 show the load-displacement curves for varying m_r in case of N_2 equal to 4. Once again these curves converge into one curve pointing out that the selection of m_r equal to 0.5 is satisfactory. Here, even a smaller value of m_r (= 0.125) has been investigated with others. It is clear that this value of m_r does not improve the practical aspect of the analysis a bit.

This nonchalancy of load deflection behaviour with variation of m_r is quite expected as the dimension of element along interface is unchanged and a finer mesh is used in the region within 2D of pile tip. Only the dimension of elements which are away from pile for at least 2D are changing with varying m_r and those elements happen to be in the low stress zone. Therefore, the variation of m_r is not sensitive enough as long as the aspect ratio be within reasonable limits. After all these analysis, the value of m_r has been selected to be 0.5 or equal (the diameter, D) of the pile.

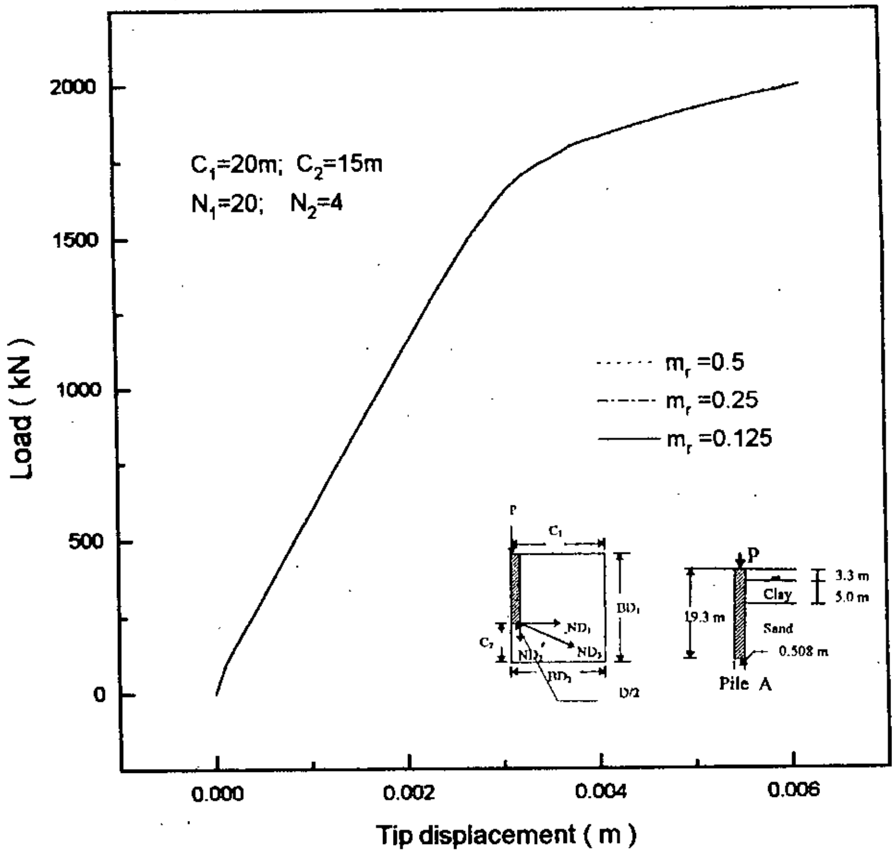

Fig. 4.15 Load-displacement curves for various m_r

4.2.5 Determination of load increment, L_i

Load-increment is very important in nonlinear finite element analysis. This analysis uses incremental loading method rather than iterative loading method which makes the selection of proper loading-increment even more important. The CRISP manual says that for accurate analysis, the loading increment should be selected in a way so as to keep the yield ratio (YR) within 0.95 to 1.05.

In the present analysis, six different load-increments are investigated and the load-increments are reduced gradually using the understanding gained from the previous higher load increment analysis. Other parameters used here are presented in Table 4.4.

Table 4.4 Parameters used in analysis for fixing Li

C_1 (m)	C_2 (m)	L_i	N_1	N_2	T_i (m)
20	15	L_1,L_2 L_3,L_4 L_5,L_6 (see Fig. 4.16 and 4.17)	20	2	0.05

The load-displacement curves for different load-increment ratios are shown in Fig. 4.18. It can be stated from the figure that for the linear portion of load-displacement curves the size of load increments do not have any effect. But, as expected, in the non-linear portion of the curves, displacements at the pile tip for any particular load increases with decreasing load-increment sizes. The load-increment rate, L_1 had been being used for the all previous analysis. For L_1, the increment size upto 1500 kN load is high (@ 100 kN/load step), but for L_2 and L_4, the increment size upto 1200 kN is high (@ 100 kN/load step), but the increment size from 1200 to 1500 kN is considerably low (@ 30 kN/load step). In spite of this decrease in increment size, the load deflection behaviour for all the cases of L_1, L_2 and L_4 are identical in linear portion of curves which signifies that there is no need to lower the increment size upto 1500 kN.

L_i	Load Range (kN)	Increment size (kN)	No of increment
L_1	0-1500	100	15
	1500-1800	20	15
	1800-2000	10	20
L_2	0-1200	100	12
	1200-1500	30	10
	1500-1700	20	10
	1700-1900	10	20
	1900-2000	5	20
L_3	0-1500	100	15
	1500-1800	30	10
	1800-2000	20	10

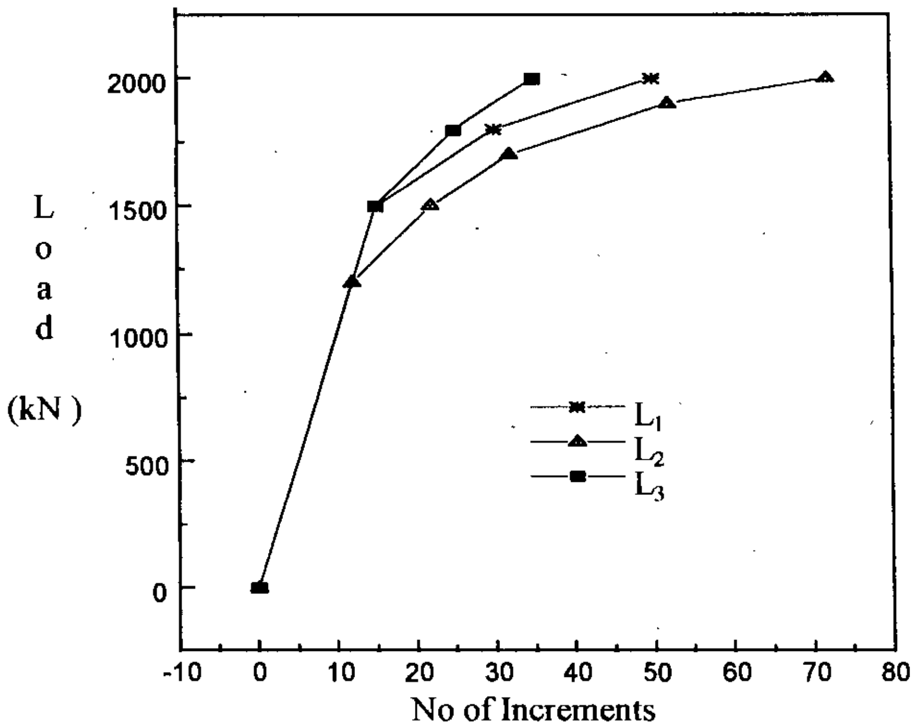

Fig. 4.16 Load Increment Rate L_1,L_2 and L_3

L_i	Load Range (kN)	Increment size (kN)	No of increment
L_4	0-1200	100	12
	1200-1500	30	10
	1500-1650	15	10
	1650-1800	10	15
	1800-2000	5	40
L_5	0-1500	100	15
	1500-2000	5	100
L_6	0-1500	100	15
	1500-2000	2.5	200

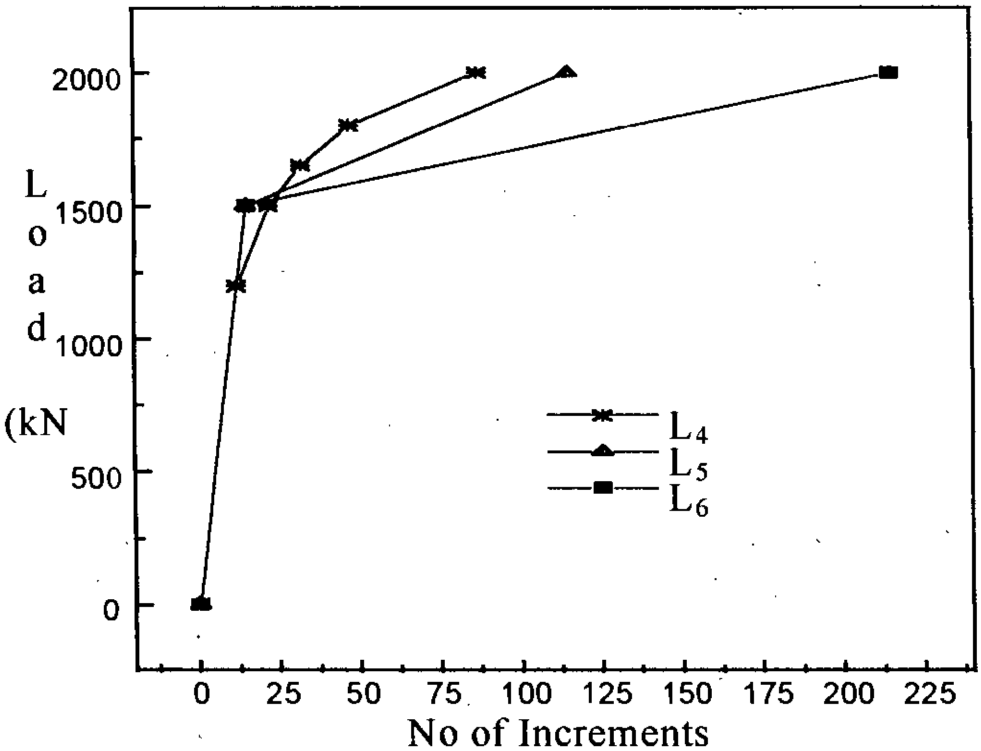

Fig.4:17 Load Increment Rate L_4, L_5 and L_6

With this understanding, the load increment size for L_5 and L_6 are selected which use high increment size upto 1500 kN load and very low increment size for rest of the load. As expected, the load-displacement curve for the case of L_5 shift rightway further from the case of L_4 due to the presence of increment size as low as 5 kN. For the case of L_6, the increment size is lowered even further to 2.5 kN after the application of 1500 kN load. The load-displacement curve for the case of L_6 traces the curve for L_5 upto 1990 kN load and after that, the former curve shifts rightways a little causing more tip displacement for the 2000 kN applied load.

If the trend of all curves are observed in Fig. 4.18, a realistic and reasonably accurate load increment rate can be suggested. For 0 to 1500 kN load, an increment size of 100 is acceptable. Then for 1500 to 1900 load, an increment size of 5 kN and for 1900 to 2000 kN load, an increment size of 2.5 kN can be selected. But if running time is of less importance, then the load-increment rate of L_6 may be used.

Although load-increment rate of L_1 is used for all subsequent analyses in this chapter, a new loading rate L_7 would be used in the final consolidation analysis. The selected loading rate L_7 is shown in Table 4.5

Table 4.5 Load-increment Rate , L_7

L_i	Load Range (kN)	Increment Size	No of Increment
	0-1500	100	15
L_7	1500-1900	5	80
	1900-2000	2.5	40

It should be noted that the suitable load increment rate varies from problem to problem as the commencement of nonlinearity in load-displacement behaviour depends on many factors including the soil type in which the pile is bored. Therefore, the load-increment rate should be determined individually for every problem keeping the yield ratio (YR) within the specific limit.

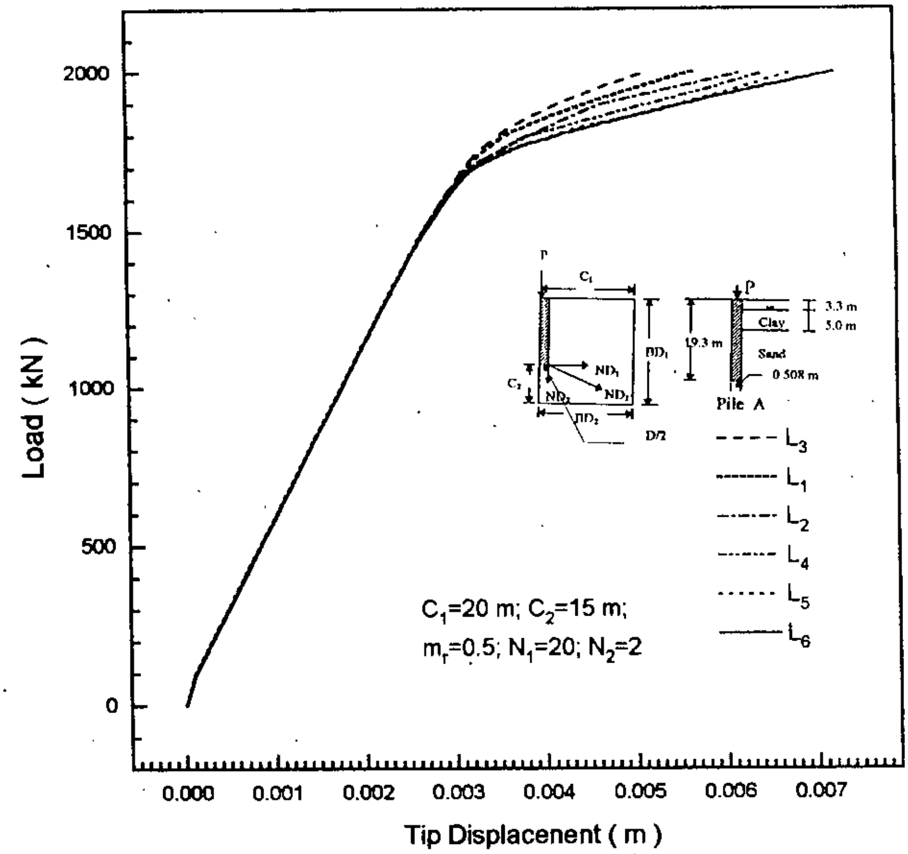

Fig. 4.18 Load-displacement curves for various loading rates

4.2.6 Determination of N_l

The size of elements connecting interface elements should be equal as otherwise, it would be difficult, in the present case, to keep the aspect ratio of interface elements within specified limit (Desai et al,1984). In this analysis, it has been tried to keep the size of elements adjacent to interface elements constant and subsequently, vertical dimension of all elements within the soil surface and pile tip have been kept constant. Here N_l is the number of these equal length elements along the pile length.

All other parameters fixed in previous articles and used in this comparative study are presented in Table 4.6 along with the different values of N_l used here.

Table 4.6 Parameters used in the analysis for fixing N_l

m_r (m/element)	C_1 (m)	C_2 (m)	L_i	N_l	N_2	T_i (m)
0.5	20	15	L_1	12 16 20 40	2	0.05

The effect of the variation of N_l on load-displacement behaviour is investigated and shown in Fig. 4.19. It can be seen from Fig. 4.19 that the increase of the number of elements along pile shaft over 20 does not produce any benefit as both the curves for N_l equal to 20 and 40 almost converge to one. Other lower values of N_l such as N_l equal to 16 or 12, produce gradual deviation from the converged group, as expected. But these deviations are small enough to be of any tangible significance.

One should notice that the effect of the variation of N_l as investigated in Fig. 4.19 dealt with tip displacement of pile and did not cater for elastic shortening of the pile itself. To incorporate this effect, curves of load vs. displacement at pile top have been plotted for different values of N_l and presented in Fig. 4.20. This figure shows an interesting effect of N_l on the displacement at pile top. In Fig. 4.19, the displacement

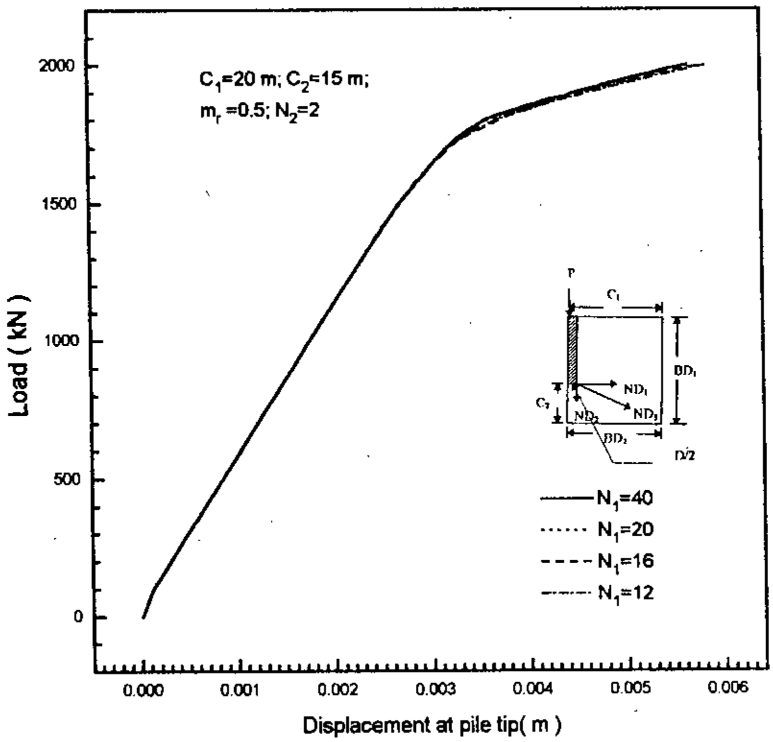

Fig. 4.19 Load-displacement (tip) curves for various N_1

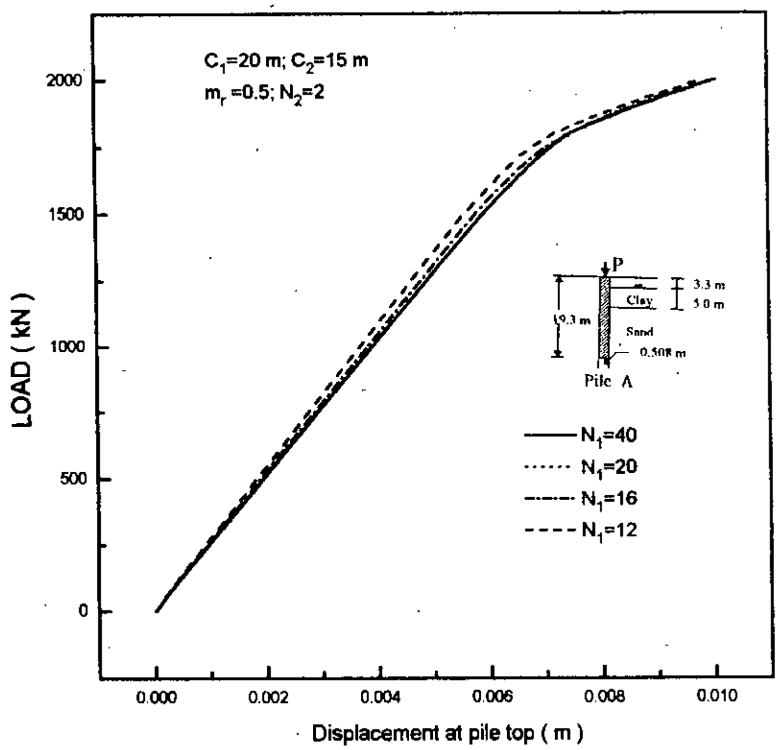

Fig. 4.20 load-displacement (top) curves for various N_1

at pile tip was seen to increase with decreasing values of N_1 and this increase was concentrated only in the nonlinear portion of the load-displacement curves. In contrast, Fig. 4.20 shows that the displacement at pile top decreases lower values of N_1 and this trend has been observed throughout. Again, the curves for N_1 equal to 20 and 40 converge into one.

Quite amusing it may seem but it can be explained and this phenomenon is expected too. When the number of elements along the pile shaft is decreased, i.e., the vertical dimension of these elements are increased, then not only the size of soil elements are increased but also the size of elements of the pile itself are increased as they are also adjacent to interface elements. As the size of pile elements are increased, the pile becomes stiffer due to larger distances between Gauss points, and the elastic deflection of pile becomes less; producing more displacement in soil below it. Moreover, the displacement in pile elements are mainly elastic displacement as the pile is assumed to be made of linear elastic material (concrete in this case). Thus, the effect of the increased size of pile elements is expected to be observed in the linear portion of the load-displacement curves which is also evident from Fig. 4.20.

It can be stated that the use of the value of N_1 equal to 20 is adequate for all practical purposes as increased number does not bring any difference. However, if the number of elements in the region within twice the diameter of pile tip (N_2) is increased as it would be the case in the next section, then the selection of N_1 may have to be reviewed giving due consideration to aspect ratio. Keeping this view in mind, a study has been done with a increased value of N_2. For this increased value of N_2 (N_2=4), the effect of increase in the value of N_1 on the load-displacement response has been shown in Fig. 4.21. This figure shows that, with increased N_2, the load-displacement curves for increasing value of N_1 produce some deviation from each other and they do not form a single line as was the case for N_2 equal to 2. But once again, the deviations or improvements in the value of N_1 above 20 are insignificant from practical point of view. As the increase in the value of N_1 increases the running time, such an increase is not obligatory.

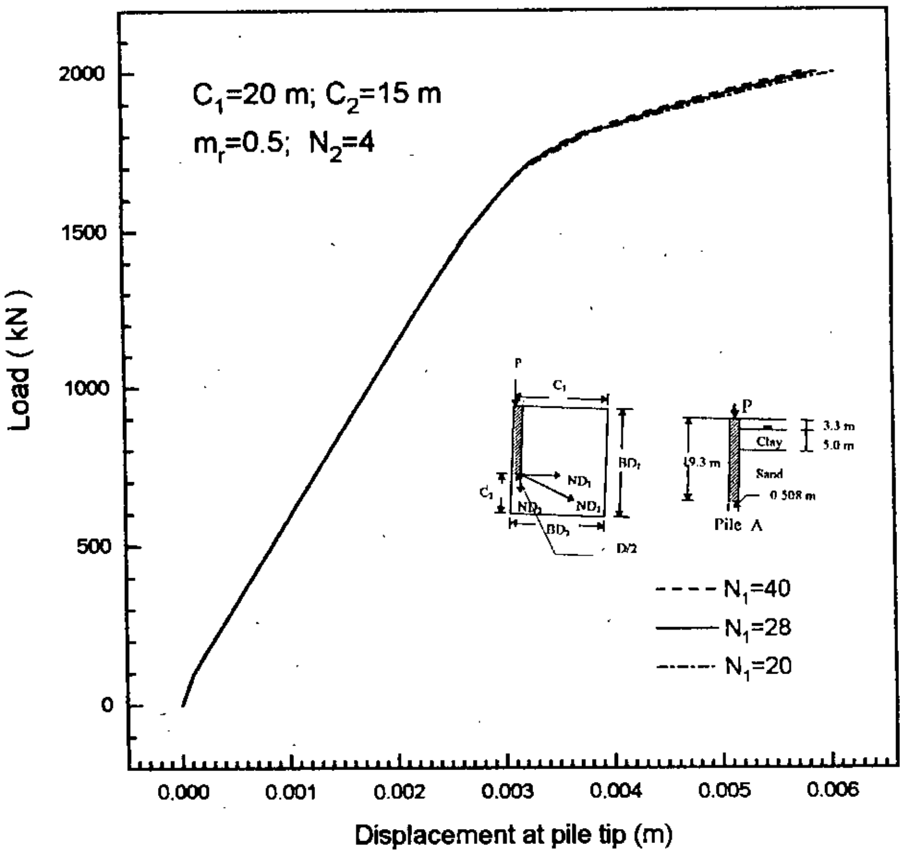

Fig. 4.21 Load-displacement curves for various N_1 (when N_2=4)

From all these extensive analyses, it can be concluded that the value of N_1 may be set at 20 (i.e. H/2D as put in the present case).

4.2.7 Determination of N_2

Much importance should be given to the dimension of elements near the pile tip as this is the highly stressed zone of a pile. The radial extent of this high stress zone, for which element dimensions should be smaller, has been fixed at twice the diameter of the pile (2D) in any direction from pile tip as shown in Fig. 4.1. The role of the number of elements (or the size of elements) in this zone have been investigated in this section. The other parameters used here are presented in Table 4.7 along with different values of N_2.

Table 4.7 Parameters used in analysis for fixing N_2

m_r (m/element)	C_1 (m)	C_2 (m)	L_i	N_1	N_2	T_i (m)
0.5	20	15	L_1	20	2 3 4	0.05

Three different values of N_2 have been investigated in this study. Much larger numbers are not used due to the problem associated with aspect ratio of these elements. Figure 4.22 shows the effect of varying N_2 on load-displacement behaviour. It can be seen form the plot that an increase in the value of N_2 predicts more deflections, as expected. But the plots do tend to come together for greater values of N_2. The use of value of N_2 greater than 4 is expected to produce no benefit and they would make the aspect ratio of elements along pile much greater than they should be. Therefore, the number of elements within 2D distance from pile tip has been selected to be 4 i.e. the dimension of these elements are equal to D/2.

In order to investigate whether the high-stressed zone with denser mesh should be extended below the pile tip beyond 2D, a study has been undertaken. In addition to the

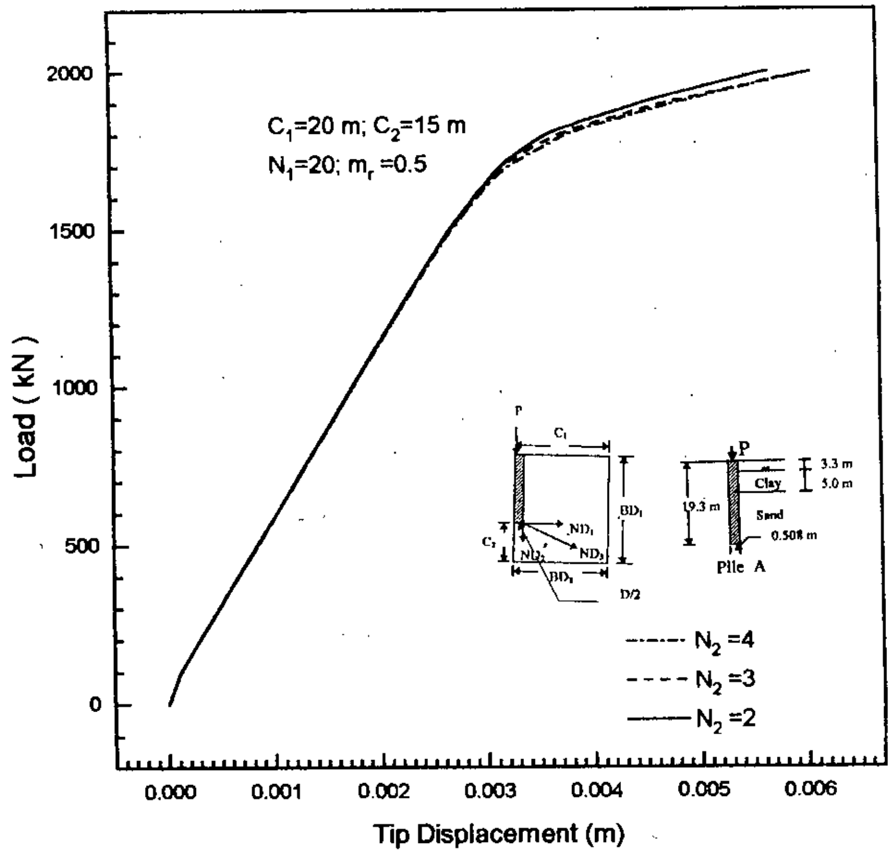

Fig. 4.22 Load-displacement curves for various N_2

previously studied case (case 1 in Fig. 4.23), a re-run by varying the vertical extent of critical zone from 2D to 3D (case 2 in Fig. 4.23) has been performed.

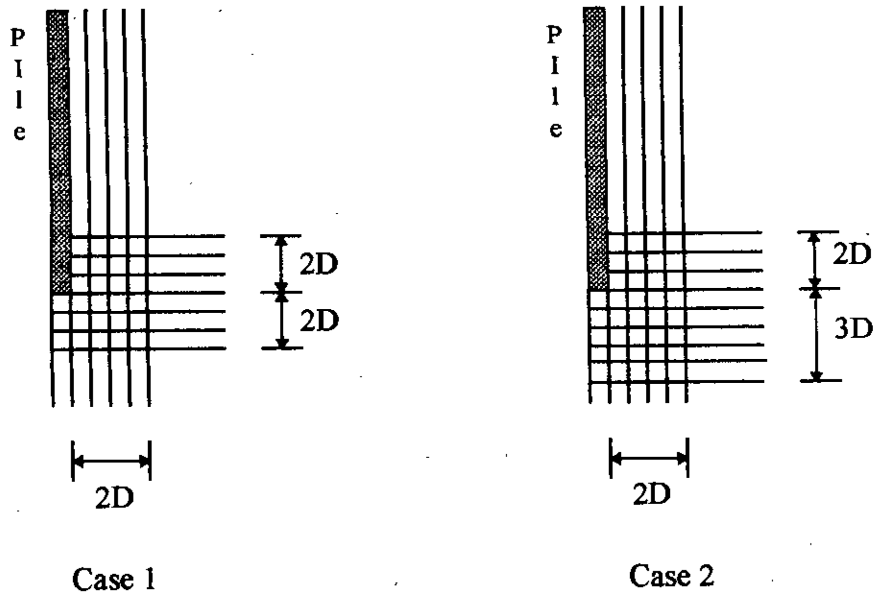

Fig 4.23 Different extent of high-stressed zone

The load- displacement responses for both cases 1 and 2 (shown in Fig. 4.24) do not show much difference. Hence, the use of N_2 equal to 4, i.e. the size of elements in high- stressed zone equal to D/2 is acceptable.

4.2.8 Determination of T_i

The selection of thickness of interface element, T_i, is just as important as selecting the soil parameters in any soil-structure interaction problem. Again, the proponents of interface element have prescribed the dimension for these special elements for accurate analysis. For the small thickness interface element proposed by Desai et. al (1984) which has been incorporated in this study, the dimension of interface elements should be such that T_i /b ratio remains within 0.1 to 0.01. Therefore, one does not have much

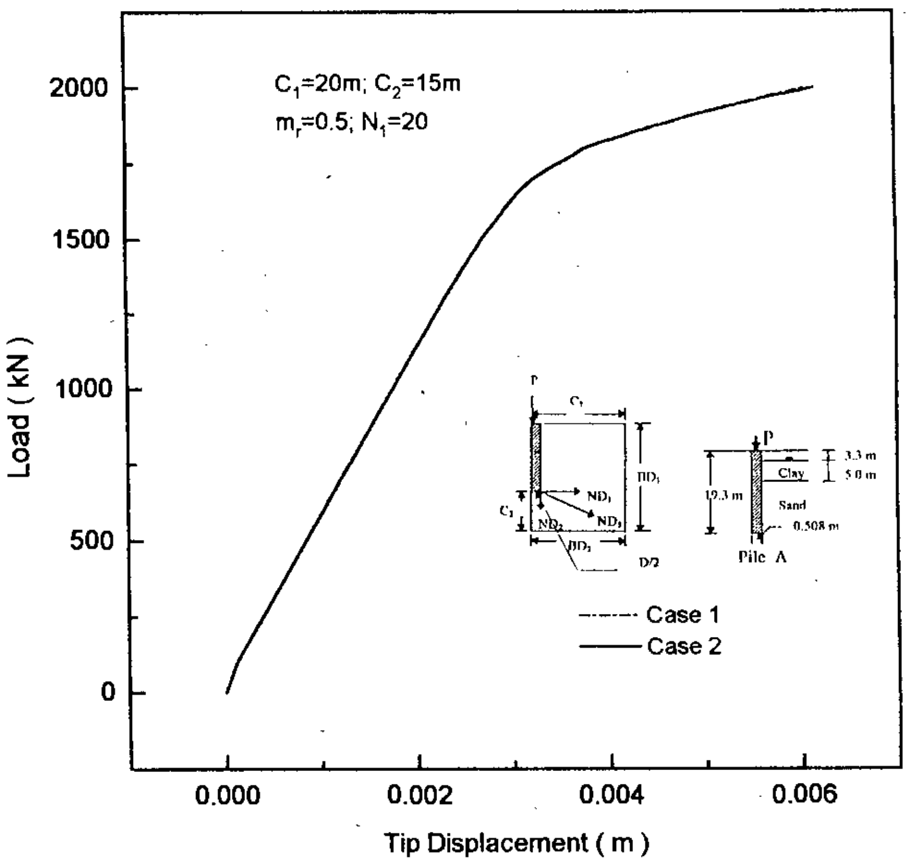

Fig 4.24 Load-displacement response for various cases of high-stressed zone

liberty in selecting T_i. The value of T_i used in this section along with all other parameters are shown in Table 4.8.

Table 4.8 Parameters used in analysis for fixing T_i

m_r (m/element)	C_1 (m)	C_2 (m)	L_i	N_1	N_2	T_i (m)
0.5	20	15	L_1	20	4	0.05 0.025 0.0125

The effect of varying interface element thickness on the load-displacement behaviour has been shown in Fig. 4.25. This load-displacement plot shows that a great deal of deviation of behaviour occurs for T_i equal to 0.025 and 0.0125 with respect to T_i equal to 0.05. However, the curves for the value of T_i equal to 0.025 and 0.0125 almost come together.

It should be kept in mind that the smallest dimension of elements adjacent to interface elements is D/2 (i.e. 0.25 m in this case) and the greatest being H/2D i.e. nearly equal to 1 m. The T_i value of 0.05 m make the (T_i /b) ratio for elements near pile tip equal to 0.2 which is slightly greater than what it should be. Hence, the subsequent inaccuracy. But for T_i equal to 0.025, the (T_i /b) ratio is 0.1, which is just about right and for T_i equal to 0.0125, it is equal to 0.05 which is well above than necessary.

Therefore, it can be concluded that the use of interface thickness keeping (T_i /b) ratio within specified limit is good enough while other values not abiding by this constraint should be avoided. But as long as the (T_i /b) ratio is within 0.1 to 0.01, there is no need to go for much fineness than necessary as these would not make much difference to the analysis. Thus, the thickness of interface element may be selected at 0.025 m (which is equal to one tenth of the dimension of adjacent smallest elements). Accordingly, the value of T_i in this study has been fixed at 1/10(D/2) i.e. D/20.

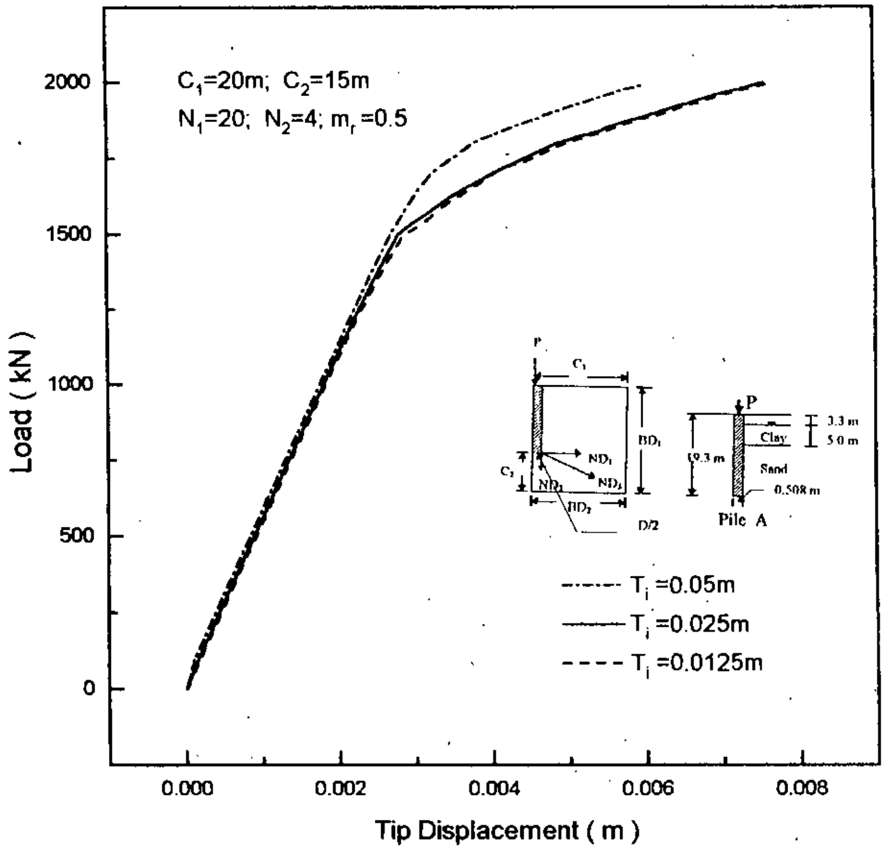

Fig4.25 Load-displacement curves for various T_i

4.2.9 The Final Mesh Configuration

The studies described in the previous sections lead to the selection of mesh configurations, as applicable to piles cast in Dhaka soil. Although during the present study, data available from Senakallayan Bhaban site have been used, the findings may be readily applied to other Dhaka city sites, as slight change in material properties from site to site in Dhaka may not affect the end result significantly. The findings, however, are applicable to relatively long pile (H/D > 20). These parameters which have been selected for the final use are presented in the non-dimensional form in Table 4.9 and also have been shown in Fig. 4.26.

Table 4.9 Final parameters of mesh configuration

m_r (m/element)	C_1 (m)	C_2 (m)	L_i	N_1	N_2	T_i (m)
D	H	0.75H	L_7	H/(2D)	4 (Size=D/2)	(1/10)(D/2)

In the subsequent studies, the finally chosen mesh configuration has been used for comparing the physical load-test data, available from three different sites in Dhaka, with its numerical counterpart. These analyses are expected to validate the present soil-structure system. Although in the previous analysis drained condition of soil was modelled, in order to converge to a satisfactory mesh configuration quickly, as Dhaka soil comprises both clay and sand layers, consolidation analysis with appropriate time increment would mimic the system more realistically. Thus, consolidation analysis would be carried out in the subsequent analyses following the mesh configuration fixed earlier in this chapter.

4.3 COMPARISON OF PHYSICAL AND ANALYTICAL LOAD-TESTS ON PILES

After extensive study for selecting the mesh configuration is performed and a rational mesh configuration is chosen, it is time for cross checking the parameters obtained

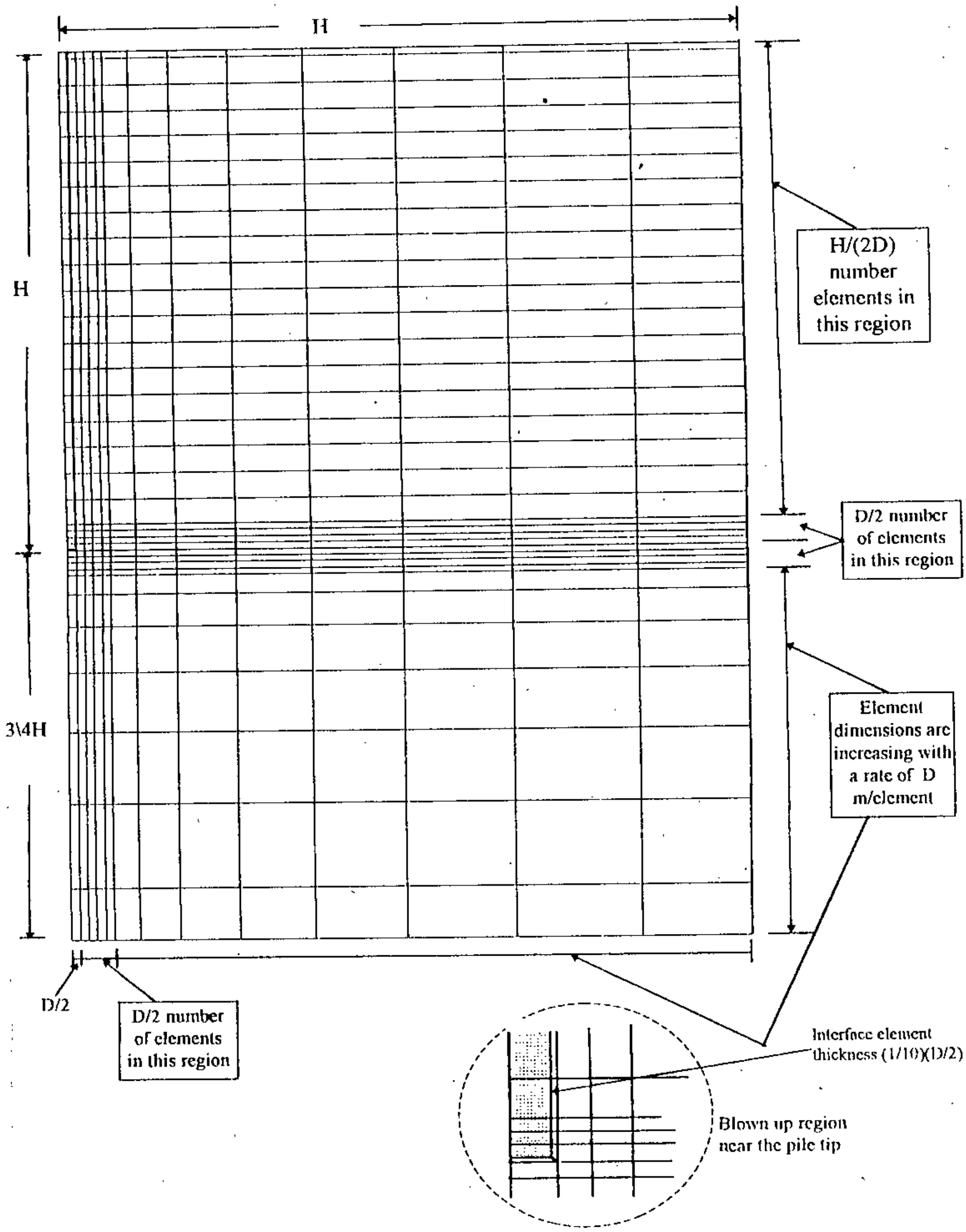

Fig. 4.26 The final mesh configuration in non-dimensional form

with various available pile load test results. It should be kept in mind that all the material properties and element types used in every example have been obtained in the way suggested in chapter 3; while the non-dimensional critical mesh dimensions suggested in chapter 4 have been used for configuring the mesh.

4.3.1 Pile A

The load- displacement response of Pile A cast in Senakallayan Bhaban site has already been shown in Fig. 3.6. The analytical load-displacement response for Pile A is quite satisfactory and it follows the trend of experimental curve rationally. From engineering point of view, the extra displacement predicted by this model is insignificant and was expected as it has already been argued in chapter 3.

4.3.2 Pile B

Now, a new pile load test data has been put to test against the soil-structure system developed for piles. The site concerned is at Kalabagan, Dhaka (IES, 1994) and the present pile would be designated as Pile B throughout the text. Soil exploration i.e. bore log chart with gradation curve, unconfined compression test and $(\log_{10}\sigma_v, e)$ curve and of course, the pile load-test data were available for Pile B.

Pile B is of 15.25 m height and 0.458 m diameter. The various material parameters needed as input to the FE model are presented in Tables 4.10, 4.11, 4.12, 4.13, 4.14, and Fig. 4.27.

Table 4.10 Soil parameters for Clay layer (Pile B)

Depth (m)	Soil Type	Zone number	κ	λ	e_{cs}	M	ν	γ_{bulk} (kN/m^3)	K_X (m/s)	K_Y (m/s)
0.0-3.0	Clay above W.T	6	0.015	0.075	0.81	0.898	0.25	13.5	8E-10	5.3E-10
3.0-5.25	Clay below W.T.	1	0.015	0.075	0.81	0.898	0.25	19.0	8E-10	5.3E-10

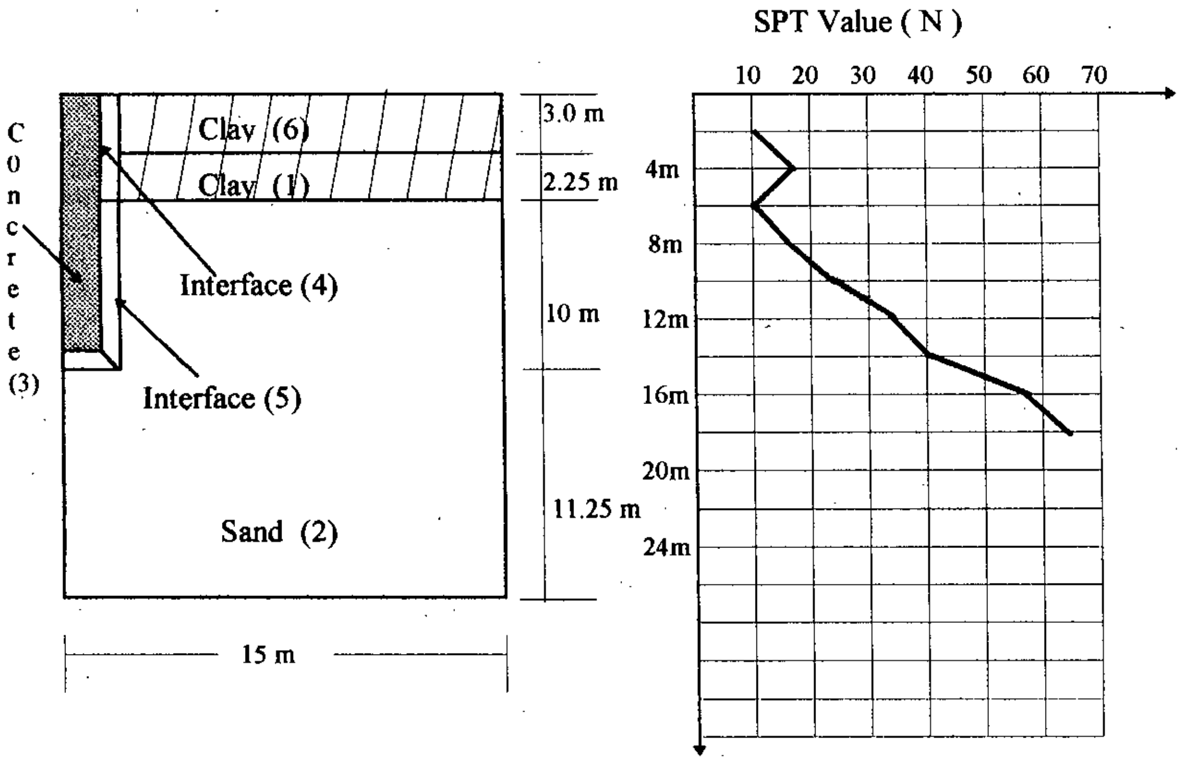

Fig 4.27 Soil Profile with SPT values and Zone numbers used for Pile B

Table 4.11 Soil parameters for Sand layer (Pile B)

Depth (m)	Zone Number	E_o (kN/m^2)	ν	C (kN/m^2)	ϕ (degree)	Y_o (m)	γ_{bulk} (kN/m^3)	K_x (m/s)	K_y (m/s)	Rate m_l (kN/m^2)/m
5.25-25.25	2	45.0E3	0.25	0	35	20.25	19.5	5E-4	3E-4	3.5E3

Table 4.12 Interface element parameters (Pile B)

Depth (m)	Zone Number	C (kN/m^2)	ϕ (degree)	K_n (kN/m^2)	G_s (kN/m^2)	G_{res} (kN/m^2)
0-5.25	4	5	23	23.34 E4	1.01 E4	10
5.25-15.25	5	0	35	54.9 E4	2.1 E4	10

Table 4.13 Parameters for Pile Material (Pile B)

E (kN/m^2)	Zone Number	ν	γ_{bulk} (kN/m^3)
30 E6	3	0.20	23.5

Table 4.14 In Situ Stresses for different in situ layers (Pile B)

Depth (m)	σ_v' (kN/m^2)	σ_h' (kN/m^2)	U_o (kN/m^2)	P_c' (kN/m^2)
0-3.0	40.50	24.675	0.0	40.32
3.0-5.25	60.75	37.013	22.5	60.48
5.25-25.25	250.75	121.604	222.50	00.00

Table 4.15 Parameters of mesh configuration (Pile B)

m_r m/element	C_1 (m)	C_2 (m)	N_1	N_2	T_i (m)
0.5	15	11.25	20	4	0.025

A consolidation analysis has been performed for Pile B with the same time increment as was the case during the actual pile load-test. The load-displacement response predicted by this model for Pile B is presented in Fig. 4.28. It shows clearly that the predicted curve simulate the real behaviour satisfactorily.

As for Pile A, the predicted displacement is slightly greater than the actual value. But, as long as it is on the safer side and the trend of the predicted values follows the real one well, the response can be considered as passable. Besides, the load at which nonlinearity commences, which, in return may be taken as a basis for pile design, has been predicted quite accurately.

In order to substantiate further the use of mesh configuration based on earlier findings, variation of stress-norm the variation of stress norm (σ_{sn}) with radial distance from pile and with depth below the pile tip have been studied and given in Figs. 4.29 and 4.30 respectively. These plots show clearly that the selection of C_1 equal to 15 m (H) and C_2 equal to 11.25m (3/4H) are acceptable as the values of σ_{sn} die out almost completely for these distances.

Besides, the nature of the curves in high stress zone i.e. near the pile tip (see Fig. 4.29 and 4.30) are smooth enough to show that the selection of m_r equal to 0.5 m (D) is also satisfactory. It should be remembered that the curves were not smooth in high stress zone when the mesh configuration were coarser (see Figs. 4.13 and 4.14).

Although, the selection of value for N_1, and N_2 could not be verified from these two plots, it is expected that they have also been appropriately chosen as these parameters were found to be not sensitive enough within certain limit as shown earlier in Figs. 4.21 and 4.22. One does not have much freedom in selecting interface element thickness as this has been prescribed by Desai et. al (1984). So, justification of the selection of T_i has also not been investigated separately.

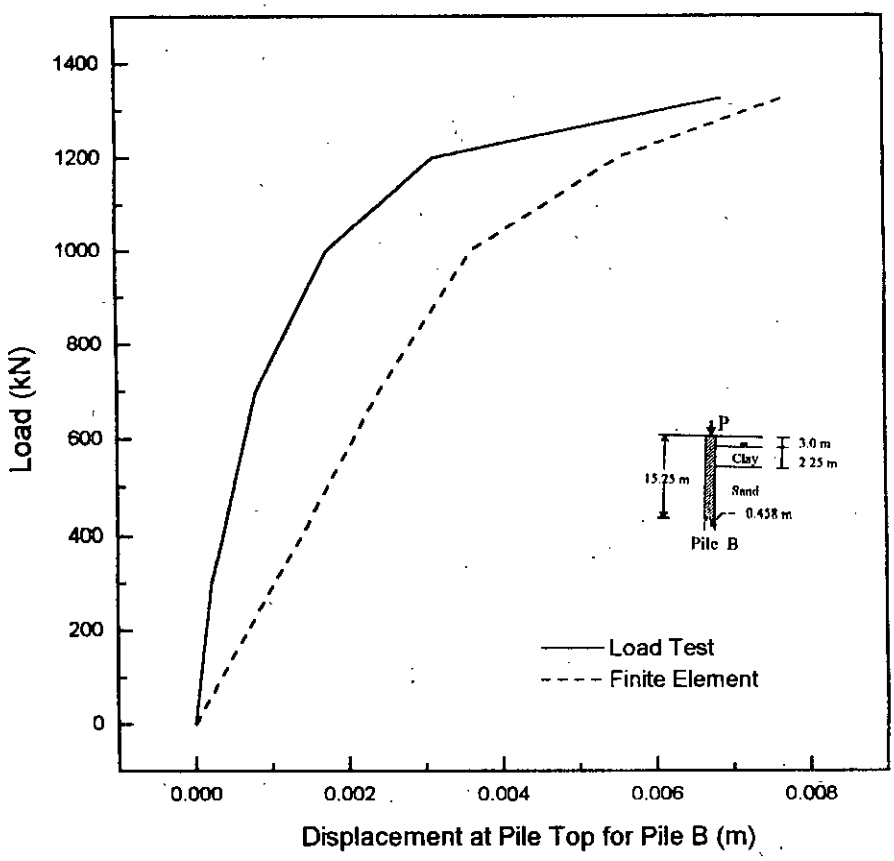

Fig 4.28 Load-displacement curves for Pile B

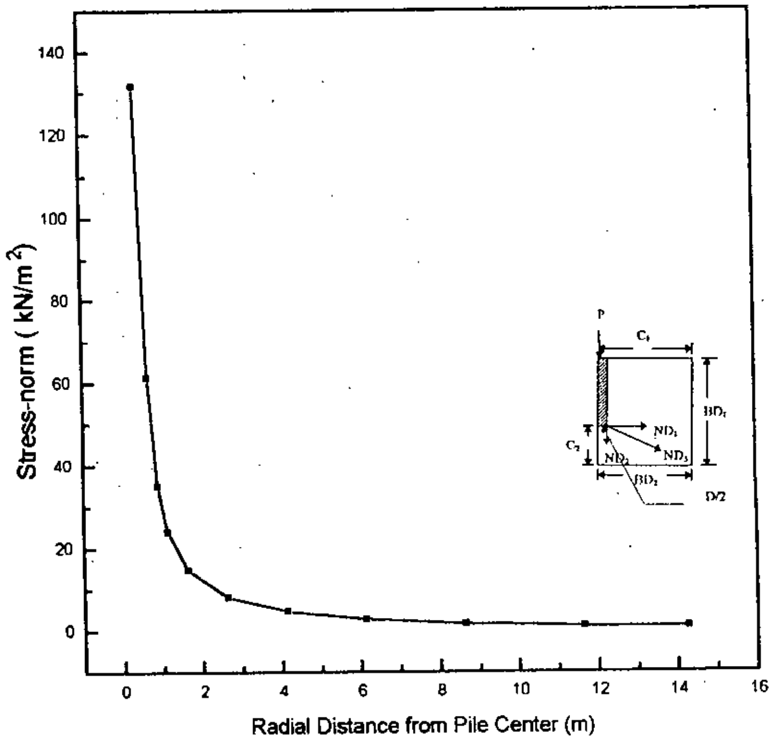

Fig 4.29 Variation of stress-norm along ND_1 for Pile B

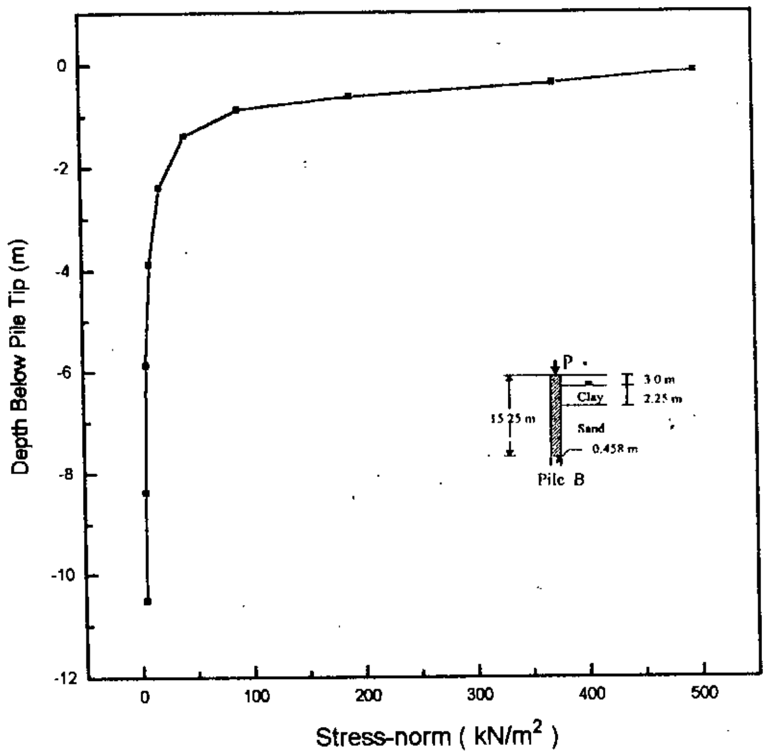

Fig4.30 Variation of stress-norm along ND_2 for Pile B

4.3.3 Pile C

The third pile is a bored pile cast at Green road, Dhaka (UBE, 1995) and designated as Pile C in this study. Pile C is only 11m in length and 0.432 m in diameter. All the parameters have been selected, once again, in light of chapter 3 and Article 4.2 as was done for Pile A and B. The necessary values of all parameters including material properties and mesh configuration properties are given in Tables 4.16, 4.17, 4.18, 4.19, 4.20, 4.21 and in Fig. 4.31

Table 4.16 Soil parameters for Clay layer (Pile C)

Depth (m)	Soil Type	Zone number	κ	λ	e_{cs}	M	ν	γ_{bulk} (kN/m^3)	K_x (m/s)	K_y (m/s)
0-3.0	Clay above W.T	6	8.75E-3	0.035	0.93	0.898	0.25	13.5	8E-10	5.3E-10
3.0-5.5	Clay below W.T.	1	8.75E-3	0.035	0.93	0.898	0.25	19.0	8E-10	5.3E-10

Table 4.17 Soil parameters for Sand layer (Pile C)

Depth (m)	Zone Number	E_o (kN/m^2)	ν	C	ϕ (degree)	Y_o (m)	γ_{bulk} (kN/m^3)	K_x (m/s)	K_y (m/s)	Rate m (kN/m^2)/m
5.5-19.25	2	35.0E3	0.25	0	35	14.25	19.5	5E-4	3E-4	3.5E3

Table 4.18 Interface element parameters (Pile C)

Depth (m)	Zone Number	C (kN/m^2)	ϕ (degree)	K_n (kN/m^2)	G_s (kN/m^2)	G_{res} (kN/m^2)
0-5.5	4	5	23	23.34 E4	1.01 E4	10
5.5-11	5	0	35	48.31 E4	1.86 E4	10

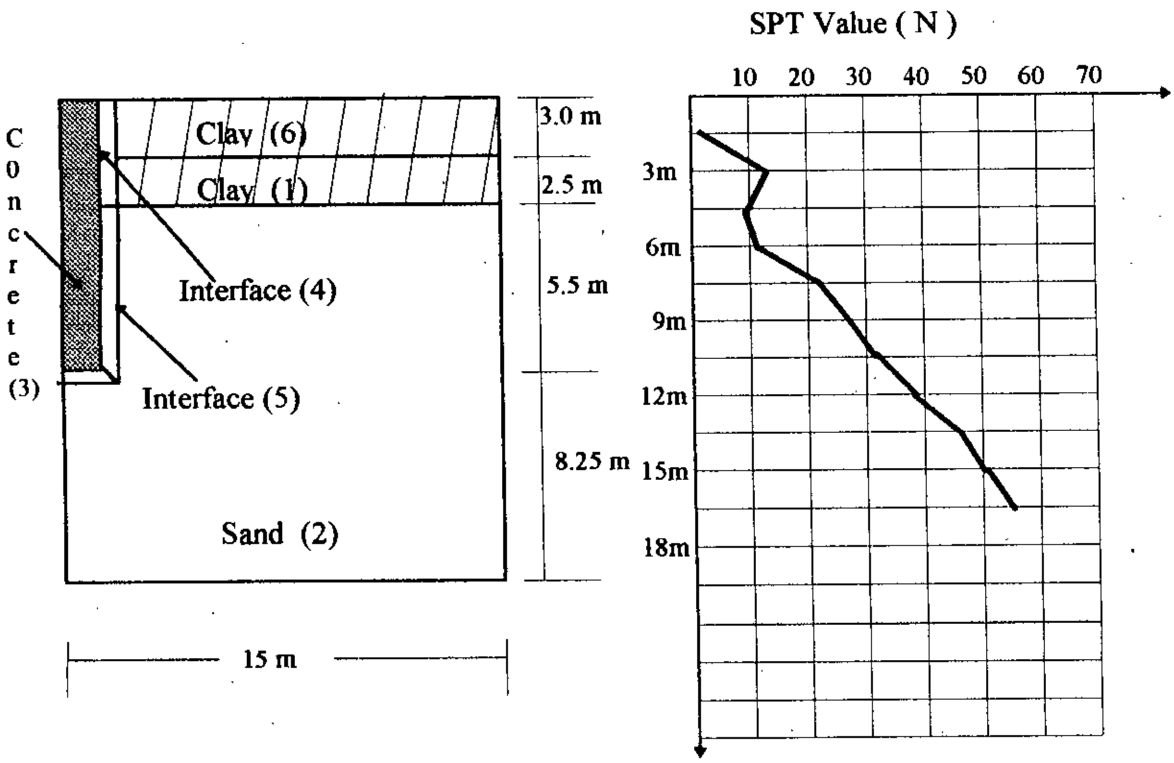

Fig 4.31 Soil Profile with SPT values and Zone numbers used for Pile C

Table 4.19 Parameters for Pile Material (Pile C)

E (kN/m^2)	Zone Number	ν	γ_{bulk} (kN/m^3)
30 E6	3	0.20	23.5

Table 4.20 In Situ Stresses for different layers (Pile C)

Depth (m)	σ_v' (kN/m^2)	σ_h' (kN/m^2)	U_o (kN/m^2)	P_c' (kN/m^2)
0-3.0	40.50	24.675	0.0	40.32
3.0-5.5	63.00	38.384	25.0	62.72
5.5-19.25	193.63	93.900	162.50	00.00

Table 4.21 Parameters of mesh configuration (Pile C)

m_r (m / element)	C_1 (m)	C_2 (m)	N_1	N_2	T_i (m)
0.5	11	8.25	13	4	0.025

For Pile C, the load-displacement response is given in Fig. 4.32. The curve shows that the predicted response is satisfactory. Figures 4.33 and 4.34, which show the variation of σ_{sn} with radial distance from pile center and depth below pile tip, manifest once again that the selection of the values for C_1, C_2 and m_r are also rational. Other mesh parameters are expected to match well too as they are not very sensitive.

4.4 REMARKS

Finally, if one tries to draw a bottom line of all these comparative studies, it can be stated that these studies can act as guidelines for selecting reasonable values of critical mesh parameters in any soil-structure interaction problem. Although the mesh

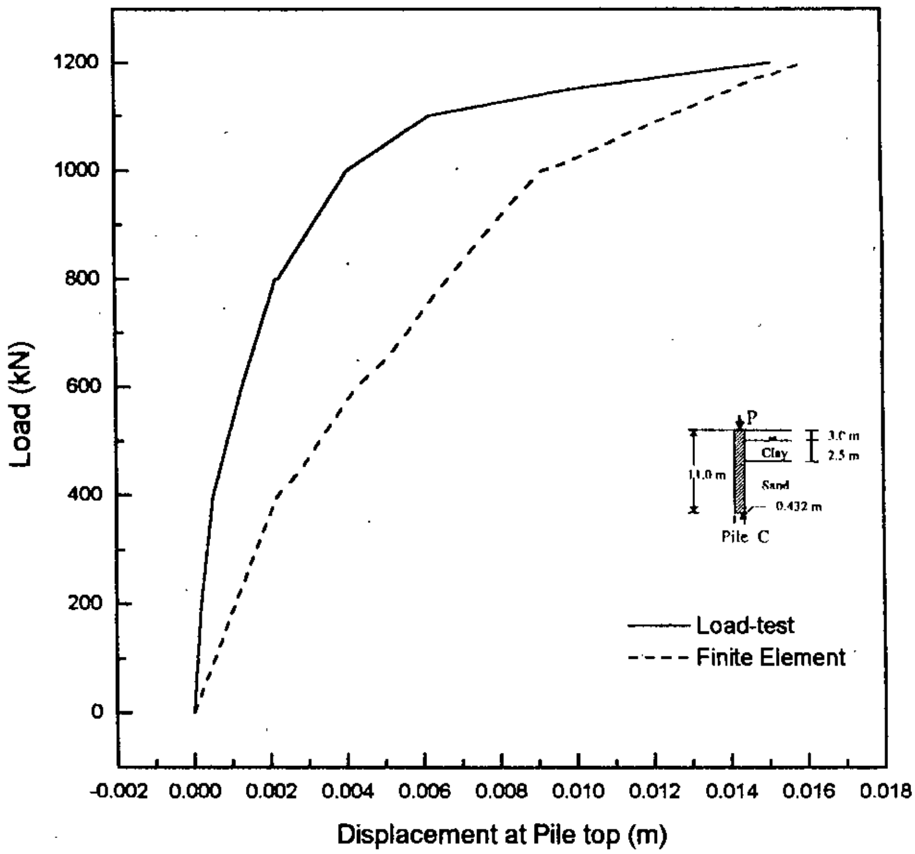

Fig 4.32 Load-displacement curves for Pile C

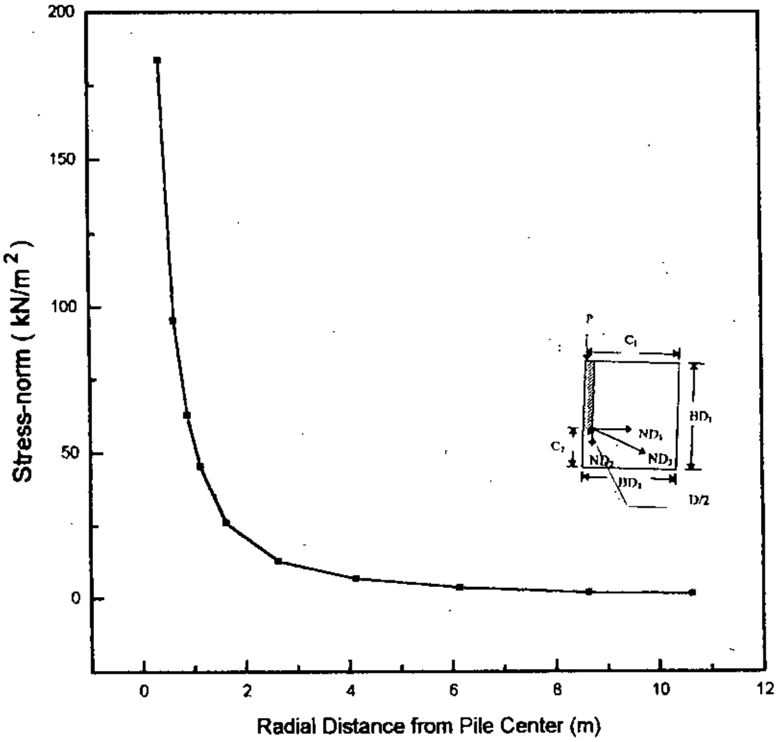

Fig 4.33 Variation of stress-norm along ND_1 for Pile C

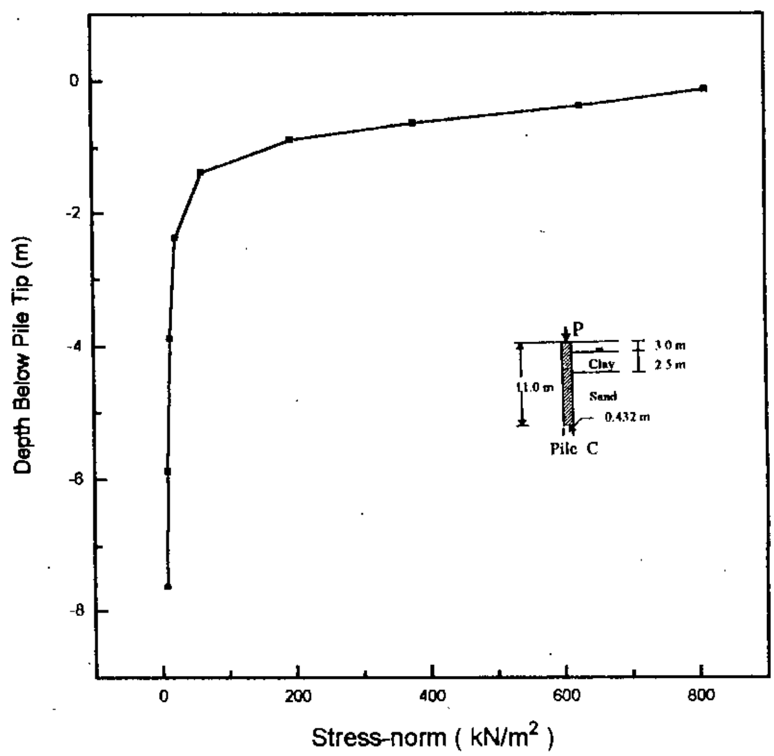

Fig4.34 Variation of stress-norm along ND_2 for Pile C

configuration in this study has been fixed for the case of pile-soil system, the methodology may well be applied to other soil-structure interaction problems.

CHAPTER 5

REALISTIC DESIGN OF PILE FOUNDATION VIA SOIL-STRUCTURE INTERACTION ANALYSIS

5.1 INTRODUCTION

It is a common practice in any finite element analysis to undertake a sensitivity analysis regarding various material parameters used. The omnipresent problem of unavailability of reliable and adequate soil parameters in any soil structure interaction problem also stresses for sensitivity analysis of some kind. The predicted response from any finite element analysis are expected to vary considerably with variation of some parameters, while some other parameters may not be much sensitive. The understanding derived from these relative sensitiveness would surely help in determining the level of emphasis that should be given in selection of various parameters.

This chapter aims at determining the level of sensitivity of various soil parameters and pile dimensions on the predicted response. The failure load capacity of single pile is investigated specially as this is the main criteria in designing a pile foundation. In doing so, some trends of failure load with variation of different parameters are observed and these trends are used subsequently in formulating a new design rationale for the failure load capacity of axially loaded single pile.

Many methods and formulae are available in determining the failure load capacity of single pile. But they seldom give comparable design capacities. A review of some well established methods for determining single pile capacity are presented below for evaluating their relative merits and demerits when compared with the rationale introduced in this study.

5.2 ULTIMATE LOAD CAPACITY OF PILES

The net ultimate load capacity, P_u, of a single pile is generally accepted to be equal to the sum of the ultimate shaft and base resistance, less the weight of the pile; as given below:

$$P_u = P_{su} + P_{bu} - W \tag{5.1}$$

where, P_{su} = ultimate shaft resistance

P_{bu} = ultimate base resistance

W = weight of pile

Theoretically, Eq. 5.1 is straight forward. But its successful use to make a prediction of capacity which closely compares with a load test is a rare event. This discrepancy is mainly due to the problem in determining *in-situ* parameters of soil, lateral and vertical variabilities of soil properties, effects of installation and complexities of pile soil interaction.

It is an implicit assumption of Eq. (5.1) that the shaft and base resistance are not interdependent. This assumption can not be strictly correct, but it is correct enough for practical purposes for all normally proportional piles and piers. A study of load-settlement and load transfer curves from a number of load tests indicates that the amount of slip to develop maximum skin or shaft resistance is of the order of 5 to 10 mm [Whitaker and Cooke (1966), Coyle and Reese (1966), AISI (1975)] and is relatively independent of pile diameter and embedment length, but may depend upon soil parameters. Mobilization of ultimate base resistance requires a tip displacement on the order of 10 percent of the tip diameter (D) for driven piles and upto 30 percent of tip diameter for bored piles (Bowles, 1982). So, it is highly probable that in the usual range of working loads, shaft resistance is the principal mechanism in all but the softest soils.

Now, the shaft resistance P_{su} can be expressed using the Coulomb expression for shear stress as follows:

$$P_{su} = \int_0^H C_p(C_a + \sigma_v K_h \tan\phi_a)dz \qquad (5.2)$$

where, C_P = Pile perimeter

H = Length of pile shaft

The ultimate base resistance can be evaluated from bearing capacity theory as

$$P_{bu} = A_b\left(C\,N_c + \sigma_{vb}\,N_q + 0.5\,\gamma\,N_\gamma\right) \qquad (5.3)$$

where A_b = area of pile tip and

N_c, N_q and N_γ are bearing capacity factors.

It should be kept in mind that if the undrained or short term ultimate load capacity is to be computed, the soil parameters C, ϕ , C_a and γ should be the values appropriate to undrained conditions, and σ_v , σ_{vb} should be the total stresses. If the long-term or drained load capacity is required, the soil parameters should be drained values, and σ'_v , σ'_{vb} the effective vertical stresses.

5.2.1 The Shaft Resistance

The shaft or skin resistance of piles can be evaluated by integration of the pile-soil shear strength over the surface area of the shaft which has been shown in Eq. 5.2.

The undrained soil-pile adhesion, C_a, varies considerably with many factors, including pile type, soil type and method of installation. Many attempts have been made to correlate C_a with undrained cohesion C_u, notably Tomlinson (1957, 1970), Morgan and Paulos (1968), McCelland (1972,1974).

For driven piles a number of methods are available. Method suggested by McCelland (1974) and by Tomlinson (1970) are widely used in determining C_a for driven piles.

But for bored piles, the available data on C_a / C_u is not as extensive as for driven piles, and much of the data that is available is related to London-clay. Table 5.1 gives a summary of adhesion factors, one of which is expressed in terms of remoulded strength, C_r, as well as C_u. Results obtained from Skempton (1959) and Meyerhof and Murdock (1953) suggest that an upper limit of C_a is 96 kPa.

Table 5.1 Adhesion factors for bored piles in clay

Soil Type	Adhesion Factor	Value	Reference
London clay	C_a/C_u	0.25-0.7 Average,0.45	Golder and Leonard (1954) Tomlinson (1957) Skempton (1959)
Sensitive clay	C_a/C_r	1	Golder (1957)
Highly expansive clay	C_a/C_u	0.5	Mohan and Chandra (1961)

For piles in clayey soil, Burland (1973) discusses appropriate values of the combined parameter β ($\beta = K_h \tan\phi_a'$) and demonstrated that a lower limit for this factor for normally consolidated clay can be given as

$$\beta = (1 - \sin\phi')\tan\phi' \qquad (5.4)$$

Meyerhof (1976) also represents data that suggest similar values of β; however, there is some data to suggest that β decreases with increasing pile length. Meyerhof also suggests that K_h value for driven piles in stiff clay is about 1.5 times K_o, while K_h for bored piles is about half the value for driven piles. For overconsolidated soils, K_o can be estimated as

$$K_0 = (1 - \sin\phi')\sqrt{OCR} \qquad (5.5)$$

where OCR = over consolidation ratio.

For sand, the values of $K_h \tan\phi_a'$ can be evaluated on the basis of test results of Vesic (1967) as shown in Fig. 5.1(a). But for bored or jacked piles in sand, the values of $K_h \tan\phi_a'$ in Fig. 5.1(a) are considered to be too large and it is suggested that the values derived form the data of Meyerhof (1976) are more appropriate for design. These values have been shown in fig. 5.1(b).

For driven piles $\phi = 3/4\ \phi'_1 + 10$

For bored piles $\phi = \phi'_1$

Where ϕ'_1 = angle of internal friction prior to installation of piles

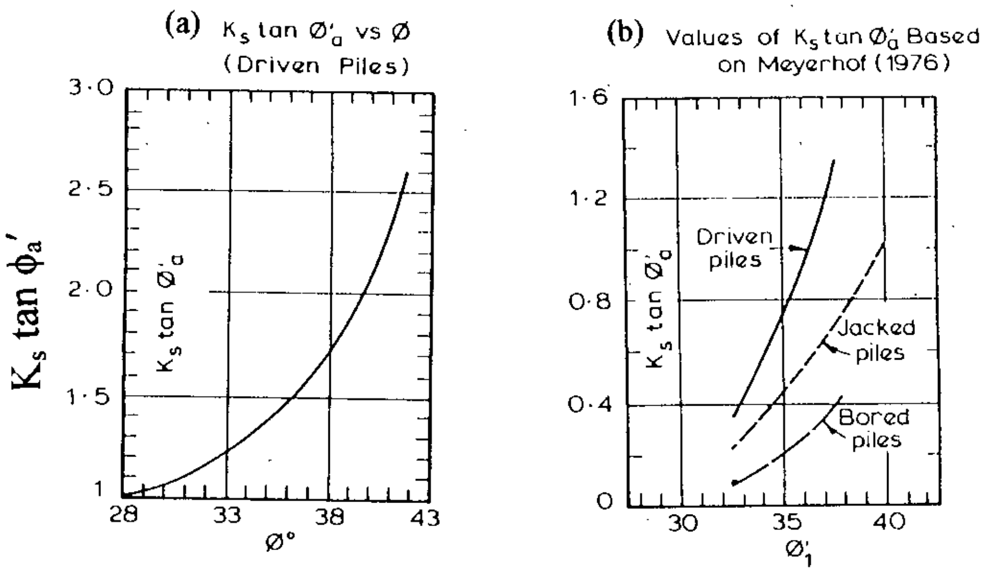

Fig 5.1 Values of $K_h \tan \phi_a'$ for piles in sand

Conventional methods of pile design assume that the vertical stresses σ_v and σ_{vh} in Eq. 5.2 and 5.3 are the effective vertical stresses caused by overburden pressure. However, extensive research by Vesic (1967) and Kerisel (1961) has revealed that the unit shaft and base resistance of a pile do not necessarily increase linearly with depth, but instead reach almost constant values beyond a certain depth. In light of this understanding, an idealized distribution of effective vertical stress σ'_v with depth adjacent to a pile is presented in Fig. 5.2(a) as suggested by Vesic (1967). Here, σ'_v is assumed to be equal to the overburden pressure to some critical depth, Z_c, beyond which σ'_v remains constant.

Now, Zc can be evaluated from relative density or angle of internal friction ϕ' as shown in Fig. 5.2(b). Besides all these, Sowers (1970) proposed values for K_h which are shown in Table 5.2.

Table 5.2 Earth pressure coefficient (K_h) for use in pile design (Sowers, 1970)

Type of sand	Pile placement method	Value of K_h
Loose	Jetted	0.5-0.75
(D_R< 50%)	Drilled	0.75-1.5
	Driven	2.0-3.0
Dense	Jetted	0.5-1.0
(D_R>85%)	Drilled	1.0-2.0
	Driven	3.0-5.0

Potyondy (1961) determined both ϕ and ϕ_a for sand using direct shear test in the laboratory. Using various construction materials and sands at different densities, he proposed the following coefficients (without factor of safety) for shaft resistance of piles.

$$f_\phi = \phi_a / \phi \quad (5.6a)$$

$$f_c = C_a / C \quad (5.6b)$$

$$f_{c,max} = C_{a,max} / C_{max} \quad (5.6c)$$

The values for f_ϕ , f_C and $f_{C,max}$ are presented in Table 5.3

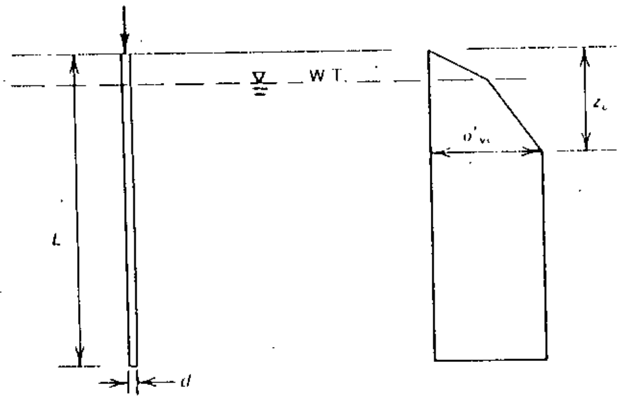

(a)

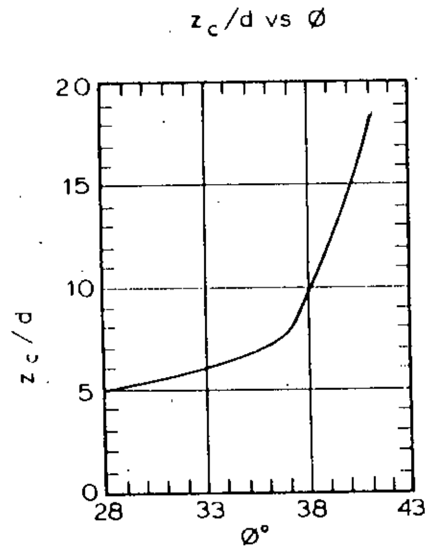

(b)

Fig. 5.2 (a) Simplified distribution of vertical stress adjacent to piles in sand (Vesic, 1967)

(b) Values Z_c/D for piles in sand

Table 5.3 Proposed coefficients of skin friction between soils and constructed materials (potyondy, 1961)

Construction material			Sand		Cohesionless silt			Cohesive granular soil		Clay		
			$0.06 < D < 2.0$ mm		$0.002 < D < 0.06$			50% Clay + 50% sand		$D \leq 0.06$ mm		
			Dry	Saturated	Dry	Saturated		Consistency index: 1.0–0.5		Consistency index: 1.0–0.73		
Surface finish of construction material			Dense		Dense	Loose	Dense					
			f_ϕ	f_ϕ	f_ϕ	f_ϕ	f_ϕ	f_ϕ	f_c	f_ϕ	f_c	$f_{c,max}$
Steel	Smooth	Polished	0.54	0.64	0.79	0.40	0.68	0.40	...	0.50	0.25	0.50
	Rough	Rusted	0.76	0.80	0.95	0.48	0.75	0.65	0.35	0.50	0.50	0.80
Wood		Parallel to grain	0.76	0.85	0.92	0.55	0.87	0.80	0.20	0.60	0.4	0.85
		At right angles to grain	0.88	0.89	0.98	0.63	0.95	0.90	0.40	0.70	0.50	0.85
Concrete	Smooth	Made in iron form	0.76	0.80	0.92	0.50	0.87	0.84	0.42	0.68	0.40	1.00
	Grained	Made in wood form	0.88	0.88	0.98	0.62	0.96	0.90	0.58	0.80	0.50	1.00
	Rough	Made on adjusted ground	0.98	0.90	1.00	0.79	1.00	0.95	0.80	0.95	0.60	1.00

5.2.2 Base Resistance

As most of the piles in Dhaka are bored, and since all the piles considered in this study have their bases or tips in the sand layer, Eq. 5.3 has to be modified for base resistance of sandy soils. For sands, the pile-soil adhesion C_a and the term C N_c can be taken as zero and the term $0.5\gamma N_\gamma$ can be neglected as being small in relation to the term involving N_q. Hence, the base resistance equation becomes:

$$P_{bu} = A_b \sigma'_{vb} N_q \tag{5.7}$$

Vesic (1967) suggested that σ'_{vb} should be equal to overburden pressure upto critical depth Z_c, and if the base of pile is situated beyond Zc, then σ'_{vb} would be equal to the overburden pressure at the level of Z_c (see Fig. 5.2).

Beresentsev (1961) proposed a factor α for calculating σ'_{vb} as follows:

$$\sigma'_{vb} = \alpha \gamma' H \tag{5.8}$$

Values of α are presented in Table 5.4.

Now; it is often quite difficult to determine the appropriate value of N_q. Figure 5.3 shows values of N_q obtained from several field test data and using different theories (Coyle and Castello, 1981).

Table 5.4 Reduction values (α) for overburden calculation (Berensentsez, 1961)

H\B	ϕ				
	26	**30**	**34**	**37**	**40**
5	0.75	0.77	0.81	0.83	0.85
10	0.62	0.67	0.73	0.76	0.79
15	0.55	0.61	0.68	0.73	0.77
20	0.49	0.57	0.65	0.71	0.75
≥ 25	0.44	0.53	0.63	0.70	0.74

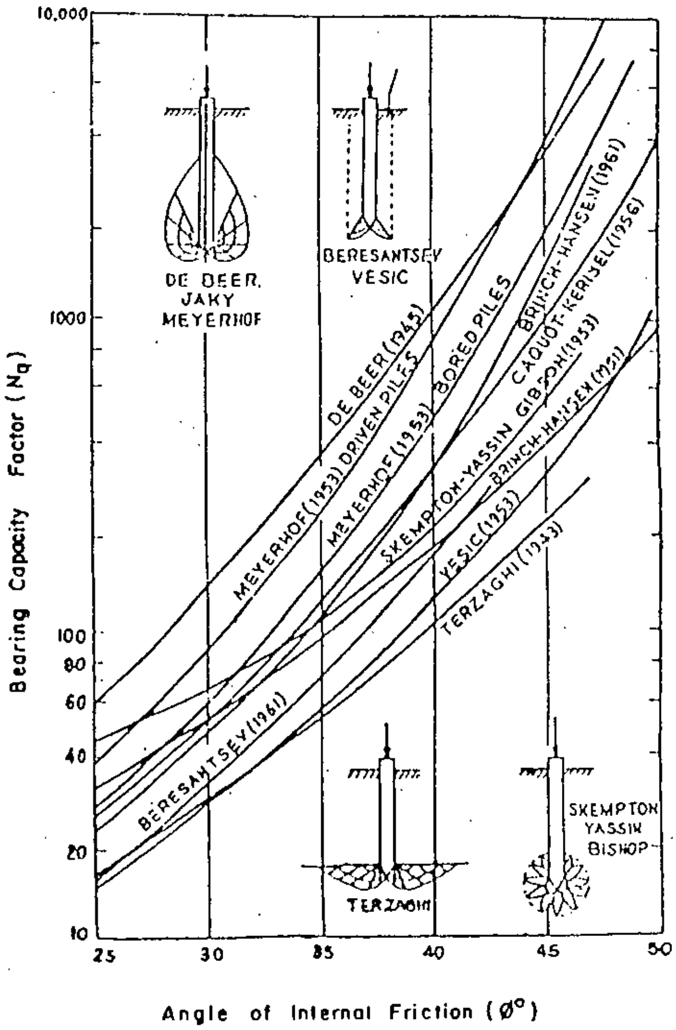

Fig. 5.3 Bearing capacity factor (N_q) proposed by various authors (Coyle and Castello, 1981)

As observed in Fig. 5.3, these values for N_q are erratic, obviously the theories on N_q are not in good agreement. This disagreement has been attributed to the incomplete understanding of the true failure mechanism. Consequently, in order to predict the actual failure pattern, various failure patterns and soil models have been proposed (Reissner, 1924); (Meyerhof 1959). Figure 5.3 represents (in addition to the N_q curves) some failure patterns as well.

Vesic (1967) has contributed significantly to the topic. His bearing capacity theory for deep foundations is logical and conservative. Figure 5.4 shows the curves for determining N_q and N_c as suggested by Vesic and this curve is usually recommended for determining N_q in pile design.

Meyerhof (1976) proposed the curves shown in Fig. 5.5 for determining the bearing capacity factors. When using these curves for obtaining N_q, the critical depth ratio (L_c/B) obtained from them should be compared with the actual depth ratio (L/B) of the pile (L= pile length, B = pile width). If it is found that the actual depth ratio is greater than the critical depth ratio, the total base resistance P_{bu} should be checked using Eq 5.9.

$$P_{bu} = A_b \sigma_{vb} N_q \leq A_b \left(50\, N_q\right) \tan\phi \quad \text{kN} \qquad (5.9)$$

Janbu (1976) proposed the following:

$$N_q = \left[\tan\phi + \sqrt{\left(1 + \tan^2\phi\right)}\right]^2 \exp(2\psi \tan\phi) \qquad (5.10)$$

where ψ is the angle shown in Fig. 5.6 and ψ may vary from 60° in soft soil to 105° in dense soil.

5.3 SENSITIVITY ANALYSIS

In this sensitivity study, a model pile is considered and the variation of failure load for this model pile with variation of different critical parameters are observed. The model

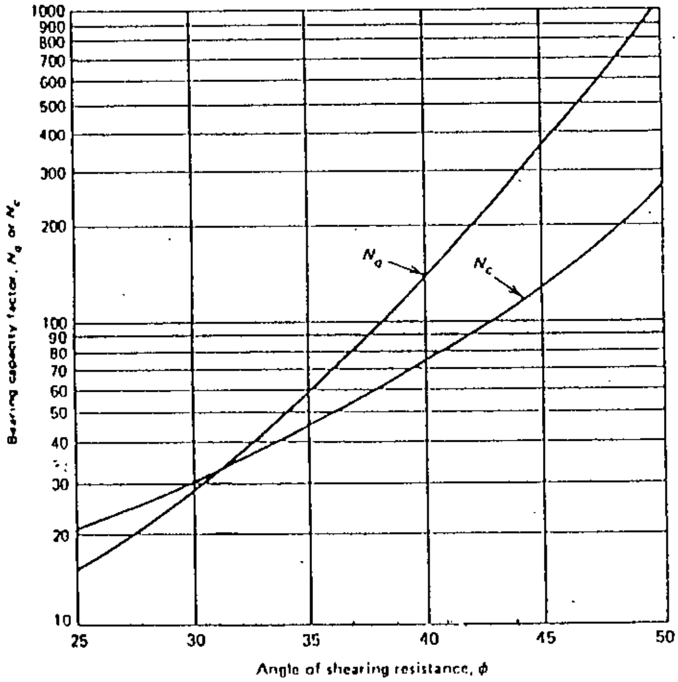

Fig. 5.4 Vesic's (1967) bearing capacity factors for deep foundation

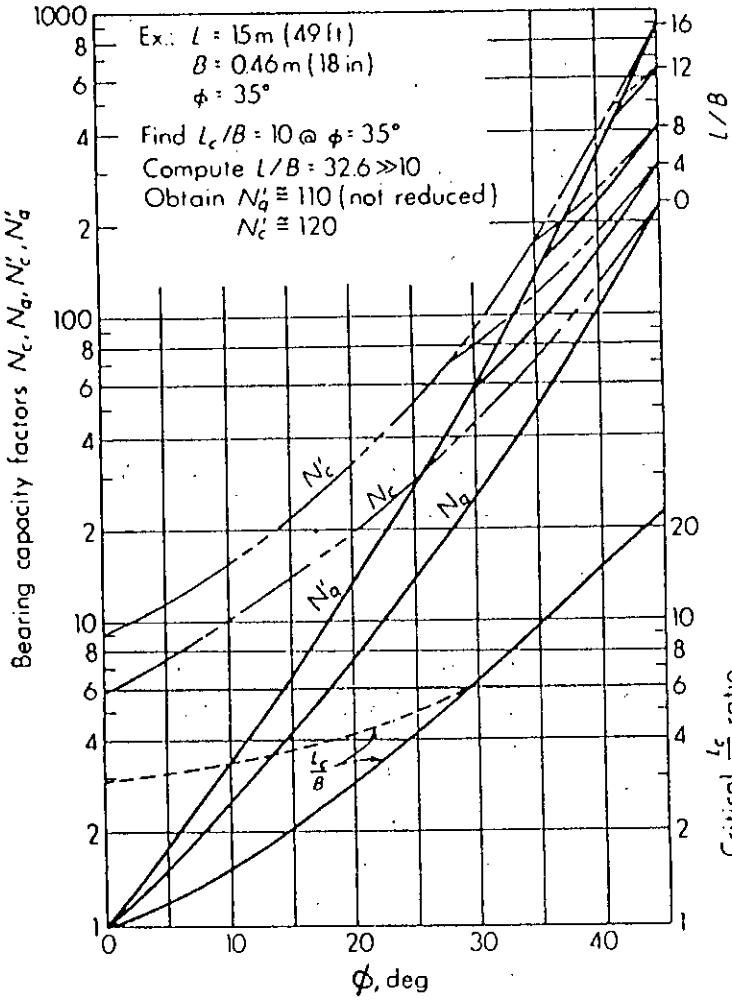

Fig. 5.5 Mayerhof,s (1967) bearing capacity factors for deep foundation

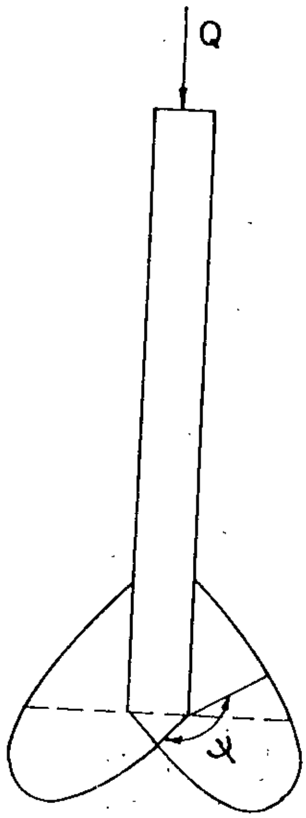

Fig. 5.6 Position of angle Ψ (Janbu, 1976)

pile, designated as Pile M, has the soil profile characteristics and pile dimensions similar to the Pile A, of the Senakallayan Bhaban site. The soil profile characteristics of Pile M have been shown in Fig. 3.1. All other parameters for pile M are shown in Tables 5.5, 5.6, 5.7,5.8 and 5.9.

Table 5.5 Soil parameters for Clay layer (Pile M)

Depth (m)	Soil Type	Zone number	κ	λ	e_{cs}	M	ν	γ_{bulk} (kN/m³)	K_x (m/s)	K_y (m/s)
0-3.3	Clay above W.T	6	0.0095	0.038	0.83	0.898	0.25	13.5	8.E-10	5.3E-10
3.3-8.3	Clay above W.T.	6	0.0095	0.038	0.83	0.898	0.25	19.0	8.E-10	5.3E-10

Table 5.6 Soil parameters for Sand layer (Pile M)

Depth (m)	Zone Number	E_o (kN/m²)	ν	C (kN/m²)	ϕ (degree)	Y_o (m)	γ_{bulk} (kN/m³)	K_x (m/s)	K_y (m/s)	Rate m_1 (kN/m²)/m
8.33-34.3	2	50E3	0.25	0	31	28.3	22.5	5.E-4	3.E-4	2.E3

Table 5.7 Interface element parameters (Pile M)

Depth (m)	Zone Number	C (kN/m²)	ϕ (degree)	K_n (kN/m²)	K_s (kN/m²)	G_{res} (kN/m²)
0-8.33	5	5	23	23.34 E4	1.01 E4	10
8.33-19.3	6	0	31	54.90 E4	2.1 E4	10

Table 5.8 Parameters for Pile Material

E (kN/m²)	Zone Number	ν	γ_{bulk} (kN/m³)
30 E6	3	0.20	23.5

Table 5.9. *In-situ* Stresses for different layers (Pile M)

Depth (m)	σ_v' (kN/m²)	σ_h' (kN/m²)	U_0 (kN/m²)	p_c' (kN/m²)
0-3.3	44.55	27.143	0.0	44.35
3.3-8.3	89.55	54.56	50.0	89.145
8.3-34.3	414.55	201.041	310.0	0.0

Now each critical parameters are varied keeping all other parameters same as Pile M. When parameters like pile height or diameter are varied, the overall configuration of mesh also have to be changed in accordance with the analysis performed in Chapter 3. The failure load obtained for each value of the parameter being varied are recorded and divided by the failure load of the model Pile M. These non dimensional failure load ratios are then plotted for various values of the varying parameters. Any trend that is apparent from this plot is formulated and subsequently used in formulating an all compassing empirical design rationale.

There are many methods available for determining failure load of piles using the load displacement curves obtained from pile load-test. But all of these methods usually lead to widely varying results. So, in this study, the failure load has been considered to be the load at which the load-displacement curve becomes non-linear from the initial linear portion of the curve. This failure load may be slightly conservative as the pile can sustain some more load beyond the first point of non-linearity. However this failure load is more realistic and rational because most of the piles remain in the linear portion of the load-displacement curve during their working life. The failure loads determined by these means has been designated as P while the failure load corresponding to the model Pile M has been designated as P_M throughout this study.

5.3.1 Sensitivity of Clay Parameters

Main parameters that are to be assigned in Modified Cam-clay model (MCC) are λ, κ, e_{cs}, M and γ. Besides, the adhesion C_a and angle of friction ϕ'_a also have to be assigned in the interface elements within the clay layer. Now, λ, κ and e_{cs} are interdependent as shown in Eq. 3.1, 3.2 and 2.8. Variation in values of λ changes the value of κ and e_{cs} accordingly. Therefore, only the sensitivity of failure load with the variation in λ, instead of κ is investigated which is shown in Fig. 5.7(a). In addition, the effect of e_{cs} on the failure load has also been investigated as shown in Fig. 5.7(b). Figuress 5.7(a) and 5.7 (b) show that for three widely varying values of λ and $e_{cs,}$ the failure loads do not show any significant change which signifies that failure load is not sensitive enough to the variation of λ, κ and e_{cs}.

Now, the slope of the CSL, M, is dependent on the angle of friction of clay as shown in Eq. 3.3. Hence, the variation of the angle of friction for clay, $\phi_{c,}$ is equivalent to the variation of M. Figure. 5.8(a) shows the load displacement responses with variation of ϕ_c. It can be seen from Fig. 5.8(a) that the failure load seems to be sensitive, although not considerably, to the variation of ϕ_c. Decreasing the value of ϕ_c increases the value of failure load, P, but the displacement responses do not change significantly with the variation of ϕ_c.

Figure 5.8(b) shows the effect of ϕ_c on the non-dimensional failure load factor P/P_M. If the best fitted curve through all the points are drawn, the trend of the curve can be expressed as a second degree polynomial as shown in Fig. 5.8(b).

The bulk unit weight of clay, $\gamma_{c,}$ represents the level of *in-situ* stresses in which the pile is subjected. Subsequently, γ_c determines the vertical overburden stress σ'_v and K_h for shaft resistance of piles. So the failure load, P, should be sensitive enough with the variation of γ_c. Figure 5.9(a) which shows the load displacement responses for various values of γ_c validate this too. The failure load P decreases considerably for lower values of γ_c. The variation of P/P_M follows a linear pattern as shown in Fig. 5.9(b). The equation of the best fit curve has also been shown in Fig. 5.9(b).

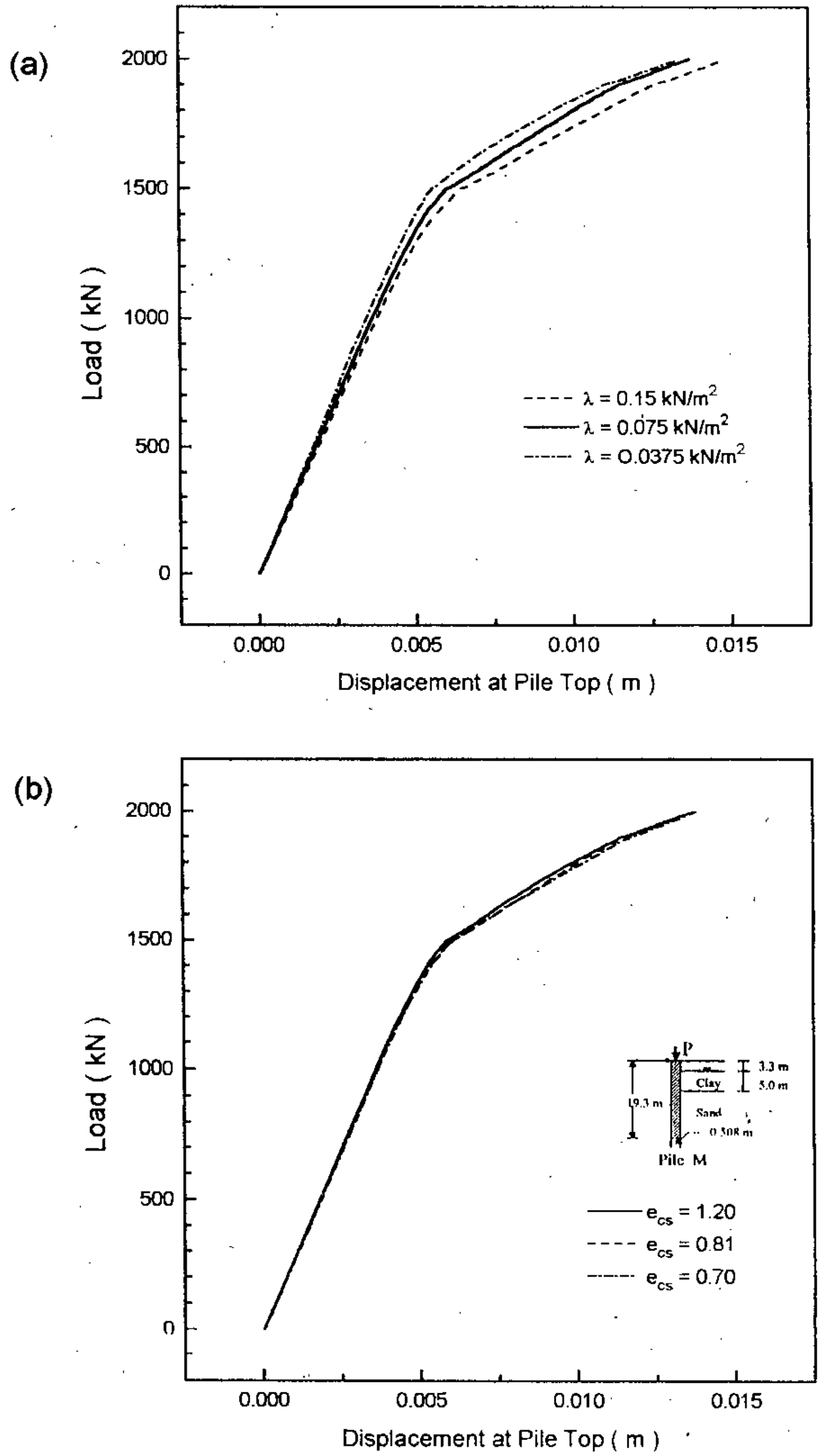

Fig. 5.7 Load-displacement responses of pile M for different values of (a) λ and (b) e_{cs}

(a)

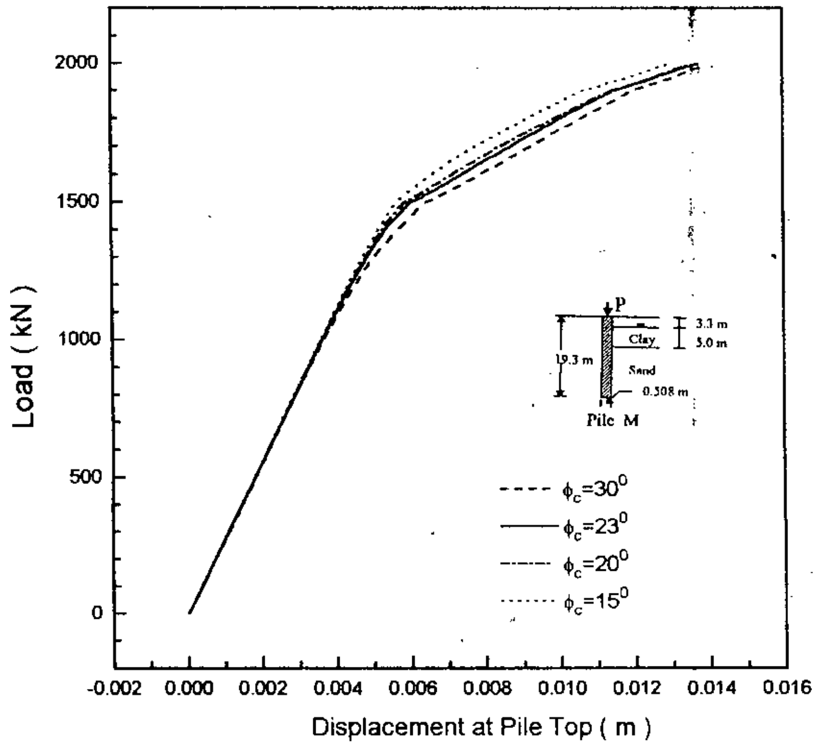

(b)

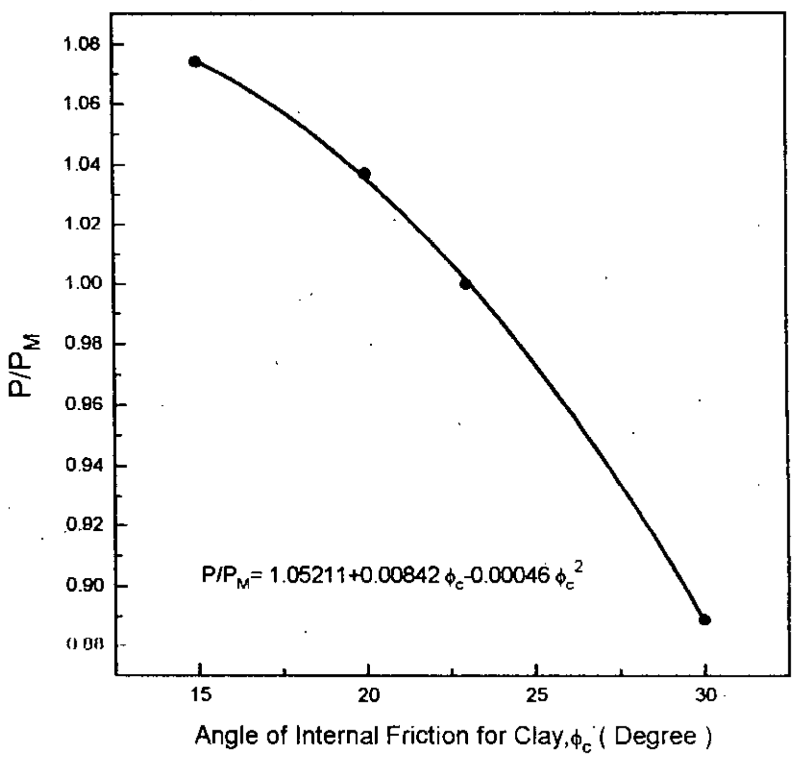

Fig 5.8 (a) Load-displacement responses, (b) Failure load factor of pile M for different values of ϕ_c

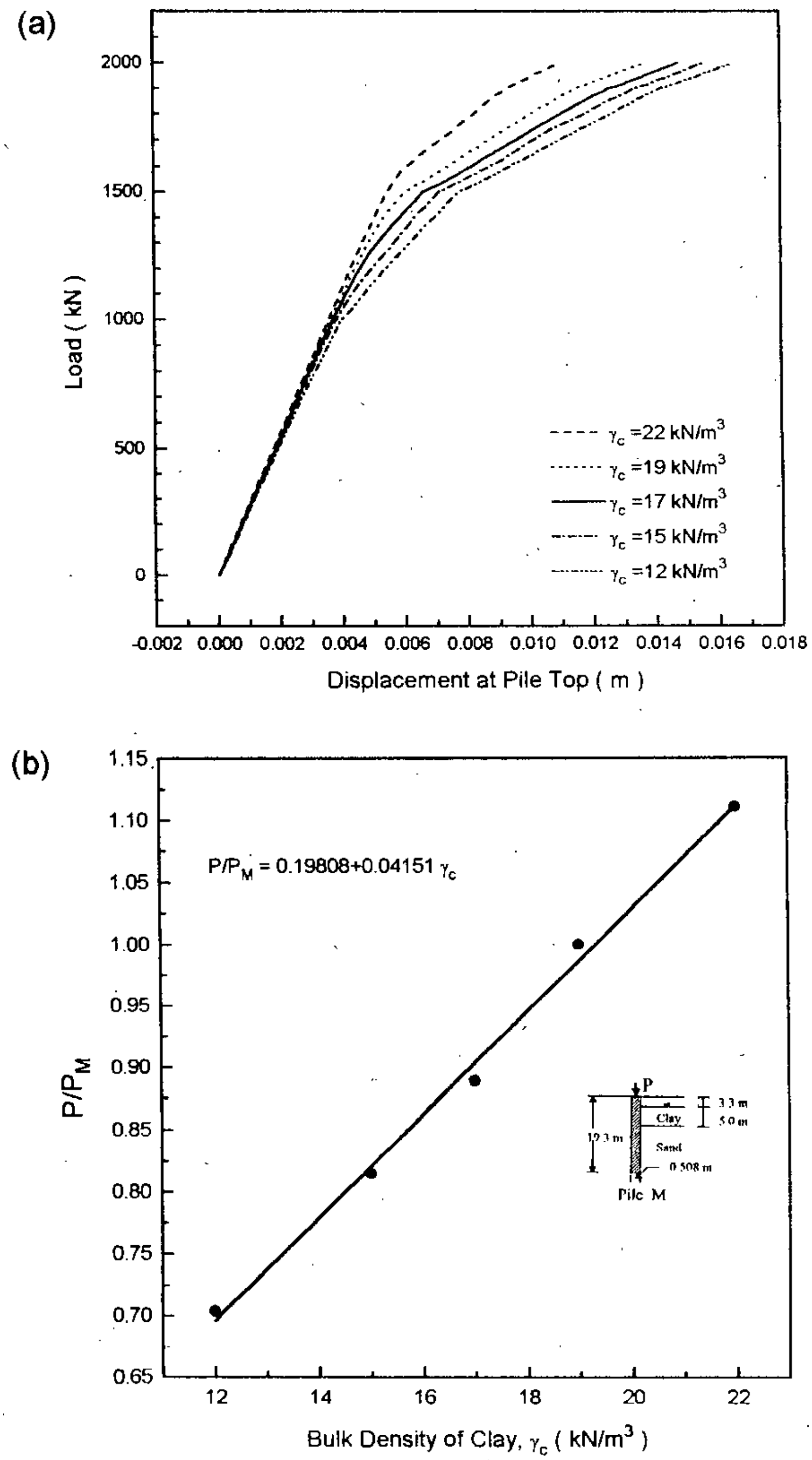

Fig. 5.9 (a) Load-displacement responses, (b) Failure load factor of pile M for different values of γ_c

The load-displacement responses for different values of adhesion, C_a, are shown in Fig. 5.10. It shows that the failure load is indifferent to the variation of C_a when within reasonable limit for Dhaka clay. Thus, the failure load can be considered to be not sensitive to the variation of cohesion or adhesion of clay as long as they are within the range applicable to Dhaka clay.

Lastly, the effect of the variation in the depth of clay layer, DCL to the load-displacement response is investigated and is shown in Fig. 5.11(a). The range of clay layer depth that are investigated has been chosen in line with the usual depth of clay layers observed in Dhaka soil. Figure 5.11(a) depicts that the displacement at the pile top increases with increase in DCL but the failure load decreases with increasing value of DCL. This tendency of decreasing failure load is visible clearly when P/P_M is plotted with different DCL in Fig. 5.11(a). The factor P/P_M decreases with increasing rate for higher values of DCL with a pattern that could be expressed as the equation of the best-fitted curve shown in Fig. 5.11(b).

5.3.2 Sensitivity of Sand Parameters

In Dhaka soil, beneath the clay layer, there is mainly sandy soil upto 30-35 m depth. For a reasonably long pile in Dhaka, the main portion of resistance is expected to be supplied by friction and base resistance of the sand layer. Hence, the parameters for sand are expected to affect the failure load significantly. Main parameters of sand that are to be assigned to input data of the FE model are E, C, ϕ, and γ. For sand, drained or long-term failure loads usually have to be considered for design. The value of cohesion, C, is usually considered to be zero for drained condition in sand. So, the effect of the variation of C on the failure load has not been investigated in this study.

The sand layer has been considered as an Elastic-perfectly-plastic material with increasing modulus of Elasticity with depth. So, the predicted load-displacement curve is expected to be sensitive to the variation of elastic modulus, E, for sand layer. In Fig. 5.12, the load-displacement responses for four different values of E are shown. Here, the E values shown are the average values of E for the sand layer. Fig. 5.12 shows an

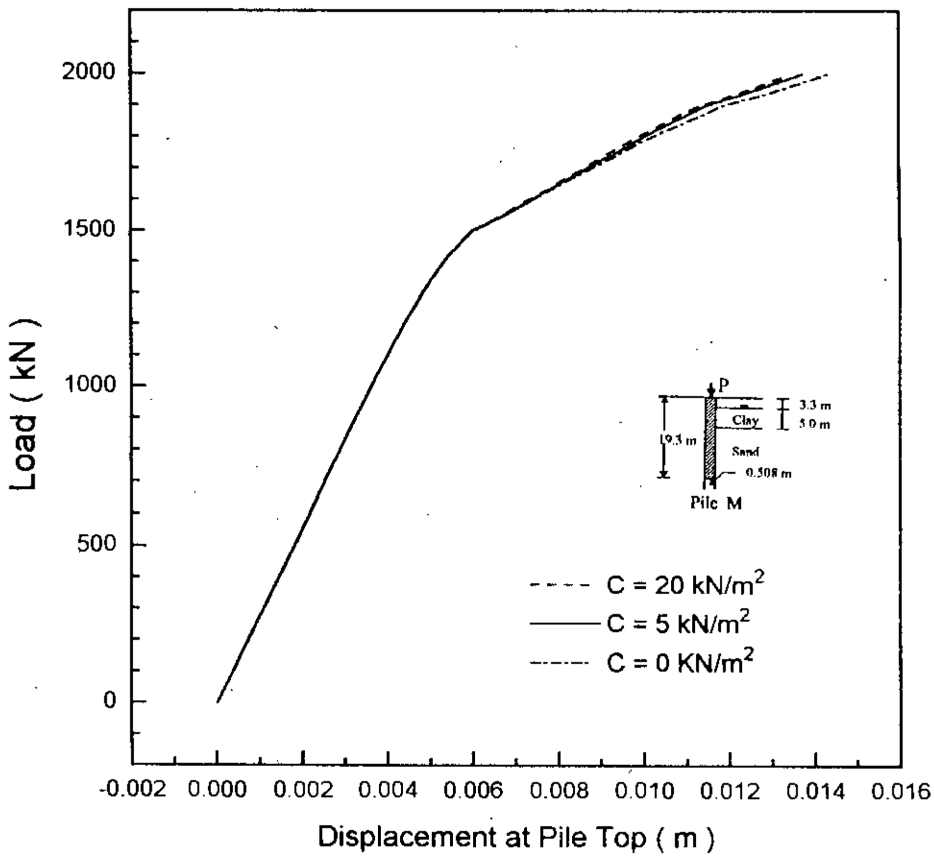

Fig. 5.10 Load-displacement responses of pile M for various values of C

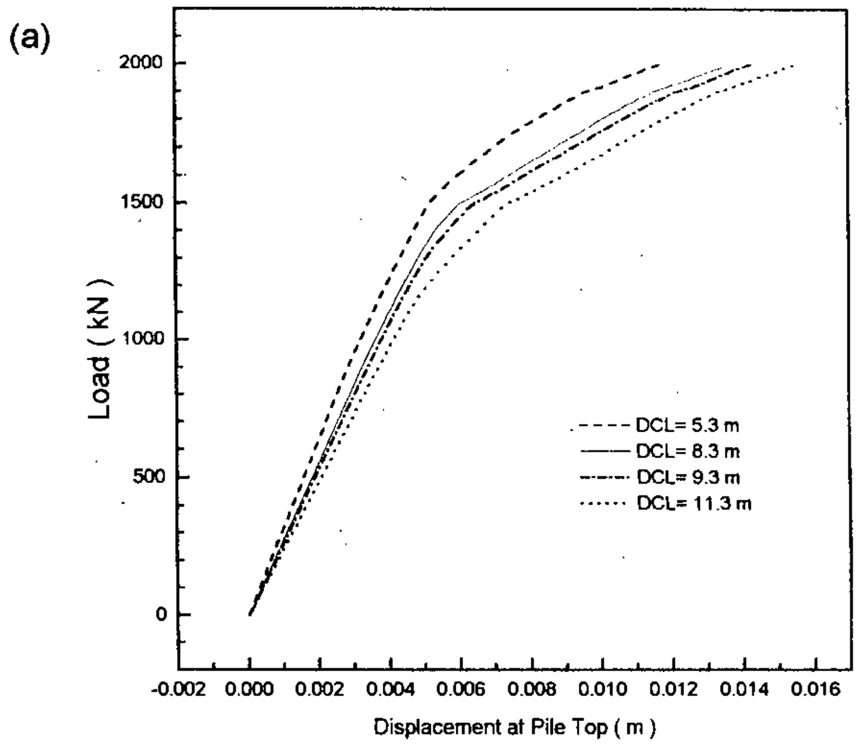

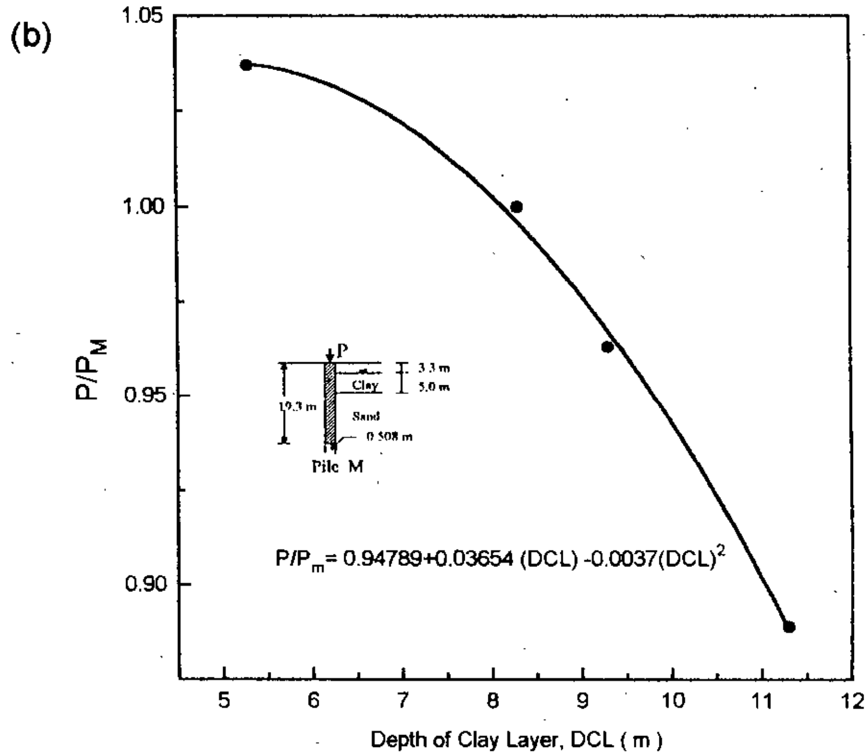

Fig. 5.11(a) Load-displacement responses, (b) Failure load factor of pile M for different values of DCL

interesting trend, the displacement prediction seems to be sensitive to the variation of E while the failure load does not show any significant change with varying E. In Elastic-perfectly-plastic model, the soil fails when it reaches the plastic zone and the slope of initial elastic region of stress-strain curve i.e., E does not affect the failure load in the way as it does the displacement. Therefore, quite expectedly, the variation in E values have not been reflected in the failure load predictions.

It should be noted that most of the methods for calculating pile capacity in sand are mainly dependent on ϕ of sand (see Art. 5.2). The bearing capacity factor N_q increases in logarithmic scale with change in values of ϕ [Fig.5.4, Vesic (1967)]. When the load-displacement responses for various values of ϕ are investigated, using the FE program in this study, as shown in Fig. 5.13(a), it is observed that the failure load P is quite sensitive to the variation of ϕ values. One thing worth noting here is that when the stress-strain curve shows nonlinearity i.e. at the point of failure load P, as defined in this study the main mode of pile load transfer is by friction or shaft resistance. Only a very insignificant amount of load is carried by base resistance (Fig. 3.9). As a result, the bearing capacity factors N_q which is responsible for base resistance in piles may vary logarithmically with variation in ϕ values; but the shaft resistance is not that much sensitive to the variation of ϕ. Figure 5.13(a) appears to be showing the same kind of trend with the variation of ϕ as would be expected in case of shaft resistance.

If the failure loads P are divided by the failure load of model pile P_M and plotted against corresponding values of ϕ as shown in Fig. 5.13(b), the relationship between P/P_M and ϕ appears to be a second degree polynomial. The equation of the best-fitted line has been shown in Fig. 5.13(b).

Fig. 5.14(a) shows the effect of variation in bulk density of sand, γ_s, to the load-displacement responses. With increasing values of γ_s, the *in-situ* stresses increases and consequently the failure loads also increase. But, the effect of the variation of γ_s to the displacement at the pile top is not much prominent. However, the trend of P/P_M values

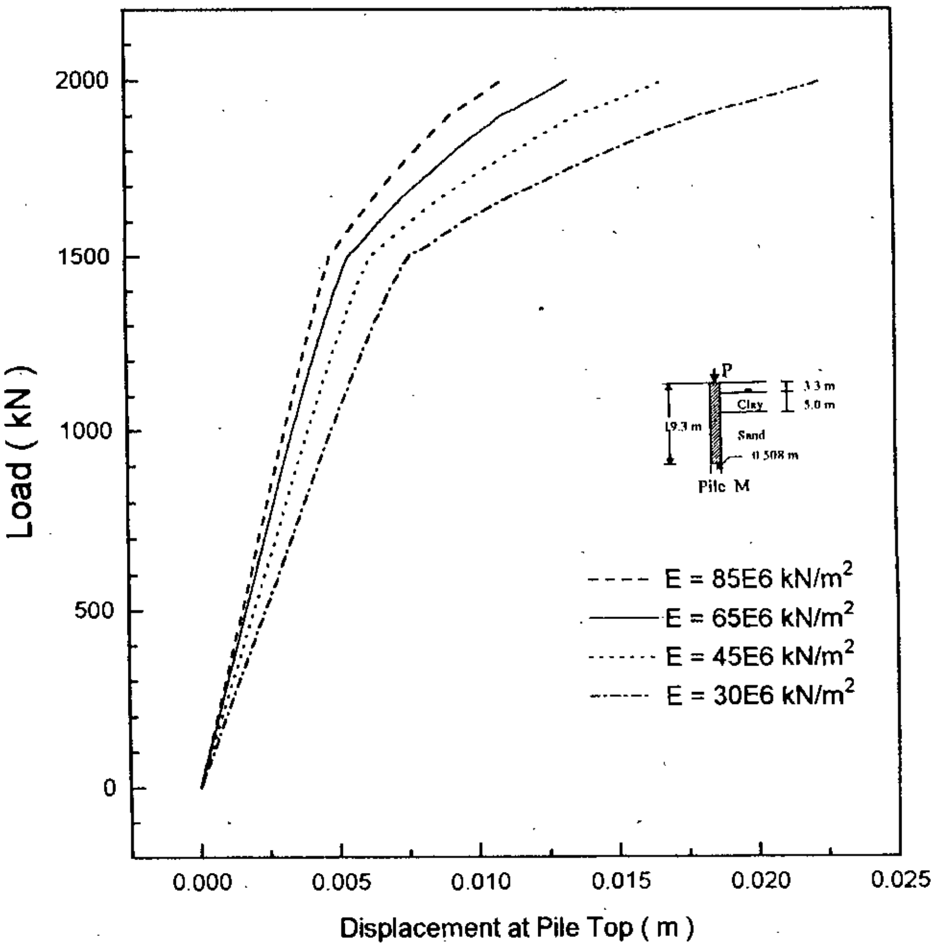

Fig. 5.12 Load-displacement responses of pile M for various E

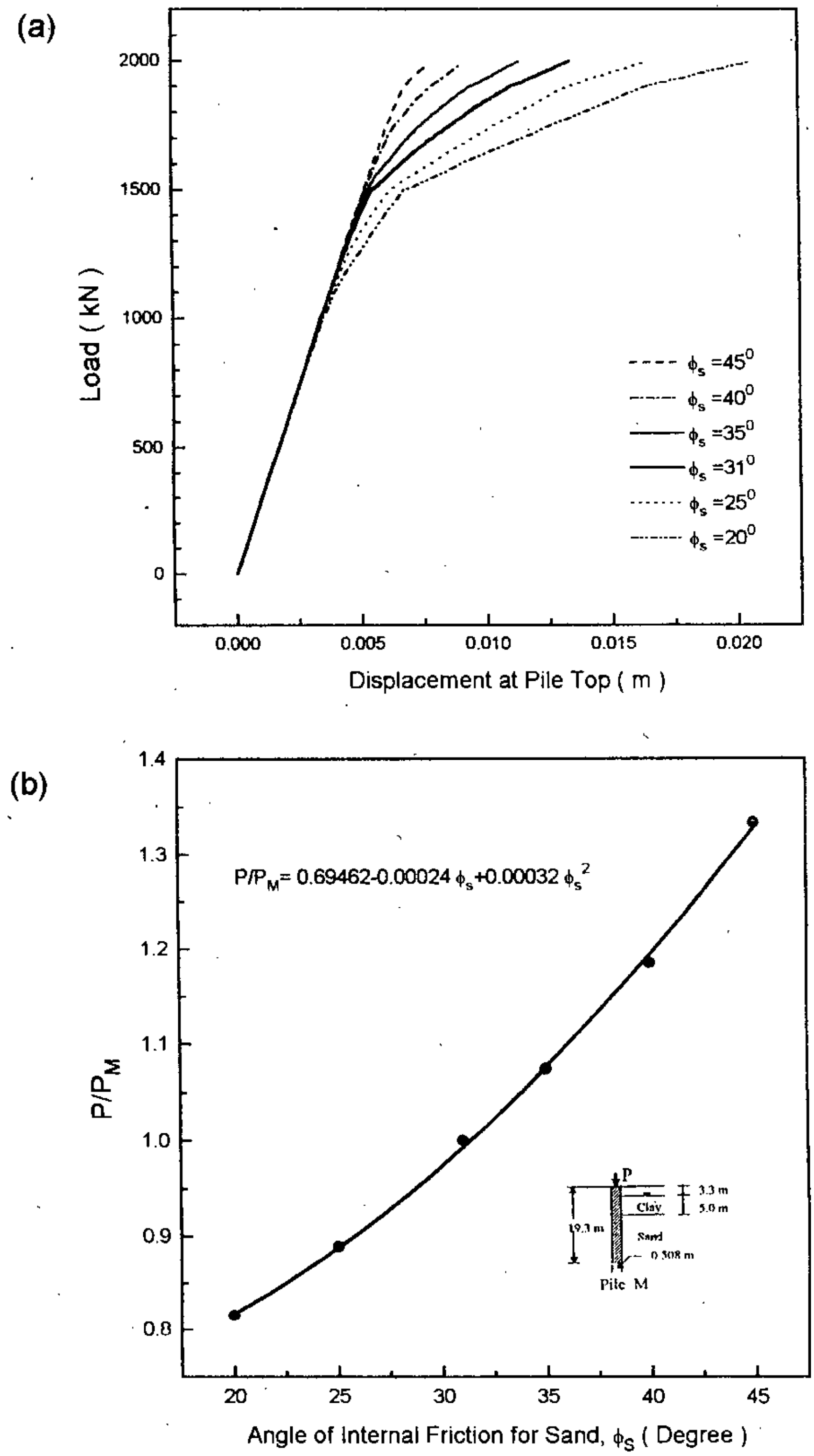

Fig. 5.13 (a) Load-displacement responses, (b) Failure load factor of pile M for different values of ϕ_s

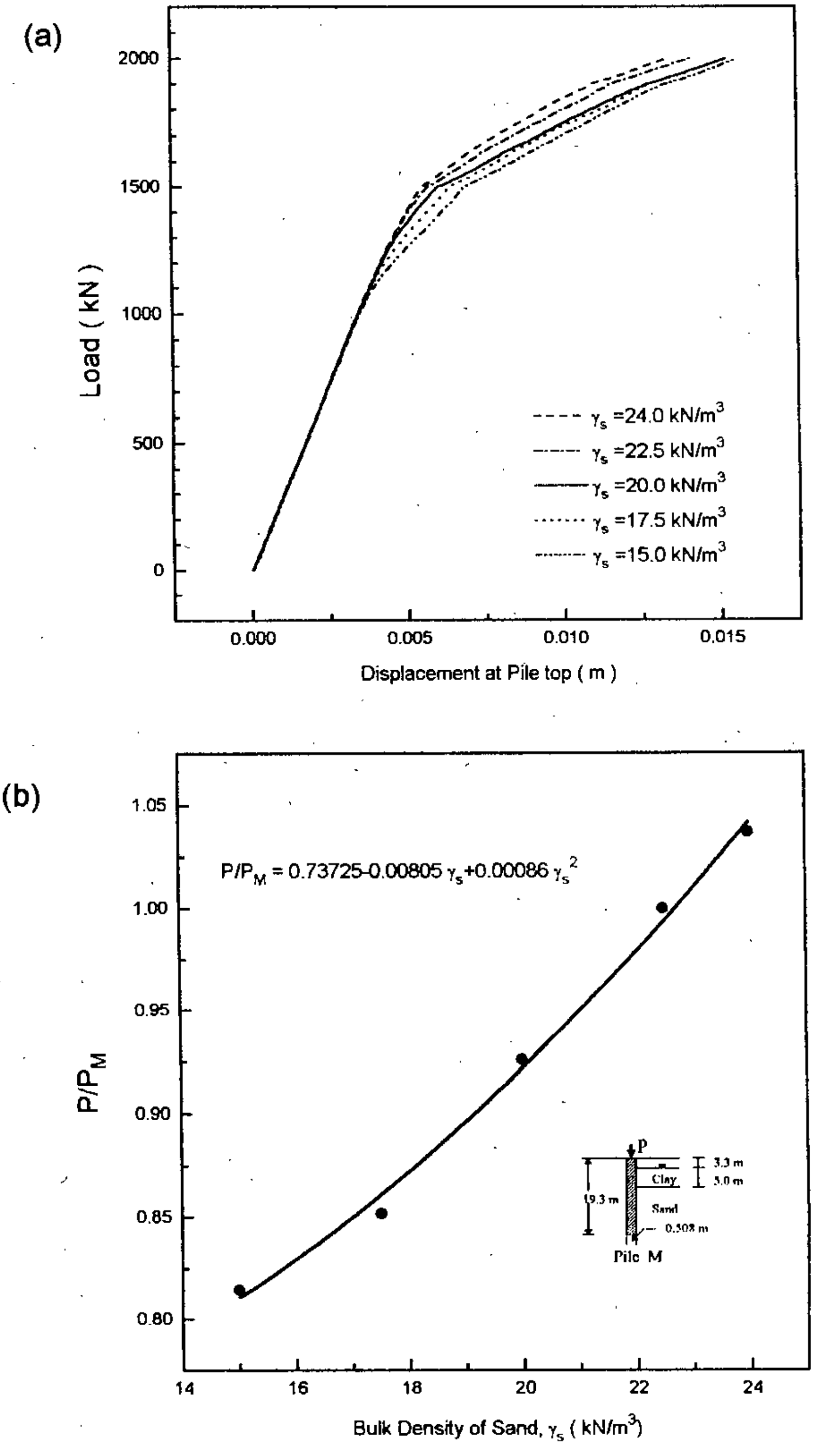

Fig. 5.14 (a) Load-displacement responses, (b) failure load factor of pile M for different values of γ_s

for different values of γ_S, plotted in Fig. 5.14(b) shows nonlinear (increasing) pattern with increasing values of γ_S. The equation of the best-fitted parabolic line is also shown in Fig. 5.14(b).

5.3.3 Sensitivity of Pile Dimensions

There are two dimensions of piles, namely the length (H) and the diameter (D) of the pile, which are expected to affect the failure load significantly and would be the main yard-stick for the desired design rationale. Figure 5.15(a) shows the load-displacement responses for different values of H. It is clear from Fig. 5.15(a) that the failure load varies significantly with variation in pile length H. The failure load P varies from values as high as 1800 kN to values as low as 400 kN with a decrease in pile length, within the range investigated. The displacement at the pile top also varies considerably.

From the change in P/ P_M with variation of H in Fig. 5.15(b), it can be observed that the failure load increases at an increasing rate for higher values of H. The curve is a second degree polynomial whose equation has also been shown in Fig. 5.15(b).

The variation in the diameter of pile, D, is also expected to play a very prominent role in changing the failure loads. The load-displacement response for various D values are shown in Fig. 5.16(a). Like H, the increase in the diameter of pile, D, produces higher values of failure load. However the influence of variation in D is much less pronounced than its H counterpart. Figure 5.16(b) shows that the failure load ratio, P/P_M assumes approximately a linear relation with variation in the diameter of pile.

5.4 A PROPOSED DESIGN RATIONALE

There are several methods available for calculating the pile capacity. But they rarely predict result which are close to the actual pile load test results. Besides, most of these formulae assume linear stress-strain relationship of soil, many of them are empirical in nature and heavily depends on SPT values. Despite all such short-comings and approximations some of these methods are used on a regular basis. Conservative

(a)

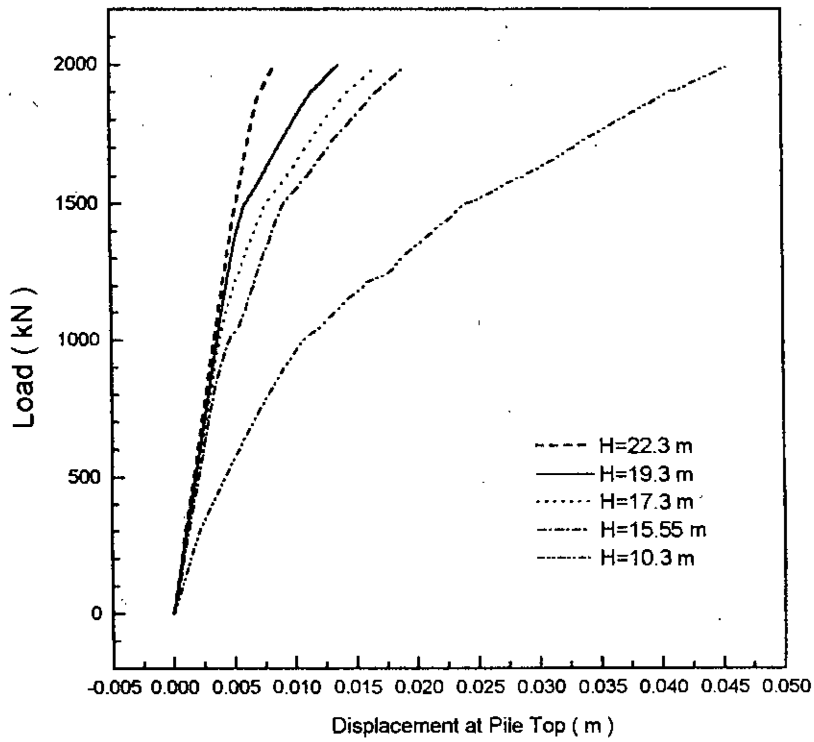

(b)

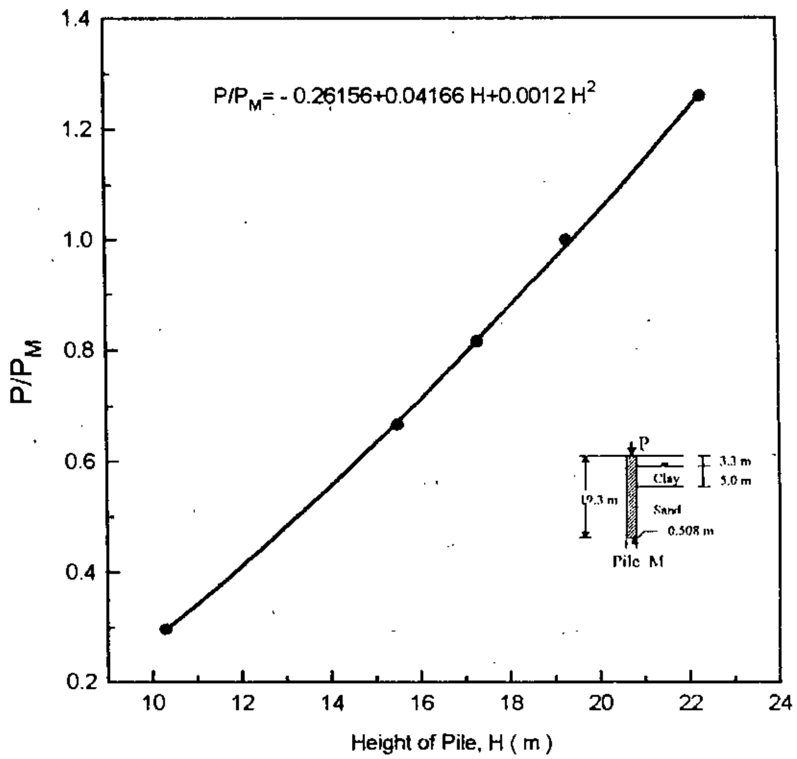

Fig. 5.15 (a) Load-displacement responses, (b) Failure load factor of pile M for different values of H

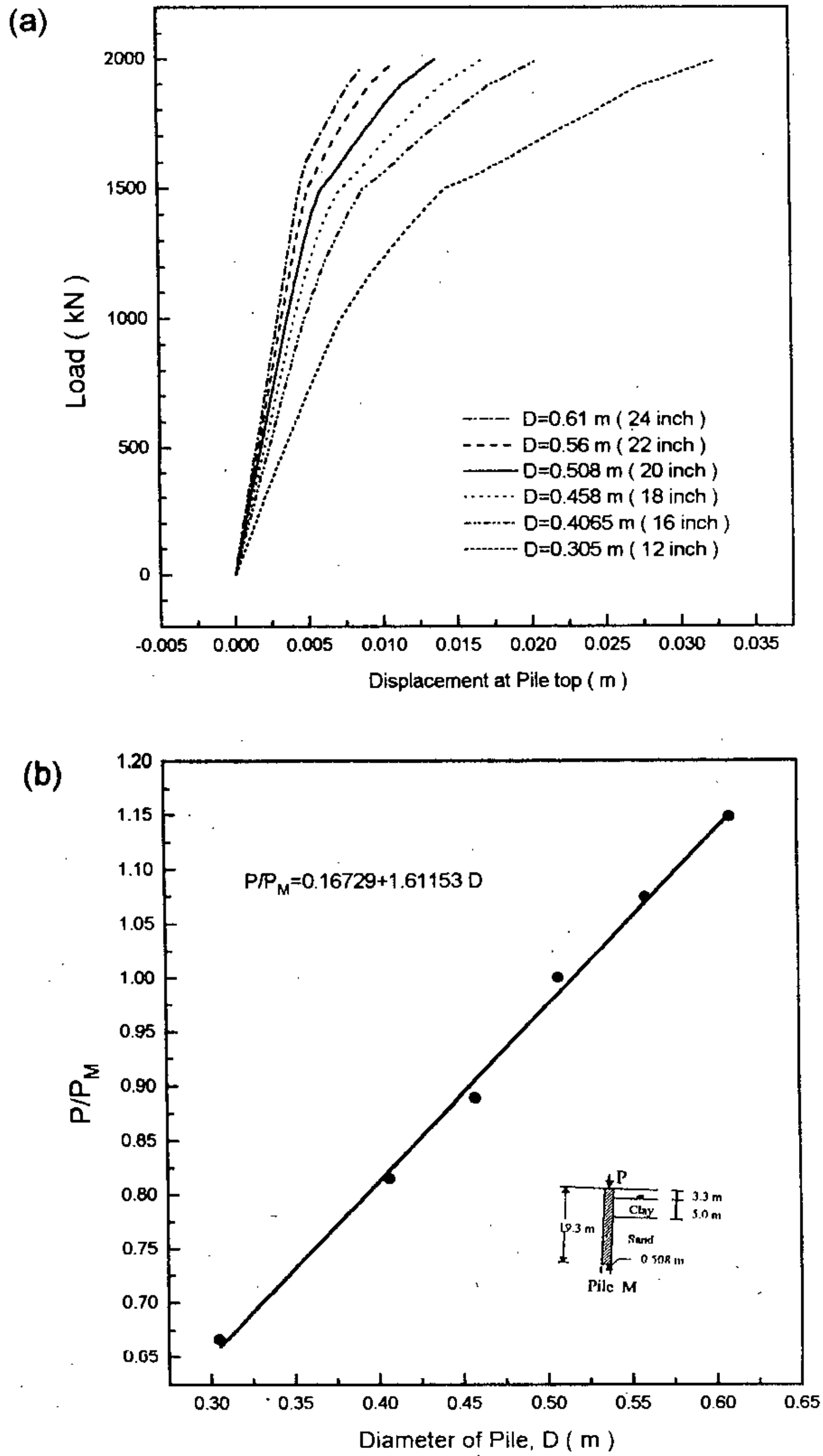

Fig. 5.16 (a) Load-displacement responses, (b) Failure load factor of pile M for different values of D

design approach combined with high factor of safety can be attributed to such successes.

With the advancement of the finite element techniques, it is now possible to analyze virtually any type of pile using the FE methods. But for determining only the failure load capacity of a single pile, use of FE method seems too elaborate and time consuming to be applied in each and every case. A straight forward method of analysis which enables one to carry out the design easily but with acceptable accuracy is preferable.

Usually, the factor of safety used for various methods for obtaining pile capacity is of the order of 2.5-2.75. Now, if it is possible to formulate explicit expressions for conservative estimation of pile capacity within the limit of even 5% to 10% accuracy, it will greatly reduce the effort necessary in calculation and will speed up the design process. In light of this understanding, an empirical formula for calculation of pile capacity is suggested in the present study.

Expression for pile capacity has been formulated in terms of various soil parameters and pile dimensions. These expressions are valid within a certain range of variation of corresponding parameters. Efforts have been made to cover the usual range found in Dhaka soil.

The expressions are explicit and of empirical in nature. Therefore, care must be taken to use proper units of corresponding parameters. The valid range of different parameters and their units are shown in Table 5.10.

One limitation of the proposed formula is that it has been formulated especially for Dhaka soil i.e. having mainly two layers, one is clay and the other is sand below it. The clay layer has been assumed, albeit approximately, to possess uniform properties while the sand layer has modulus of elasticity increasing with depth. In reality, there may be more than two layers of soil and some layers with sandy-clay, silty-clay or clayey-sand properties. But it should be kept in mind that this assumption of two distinct layer is expected to predict results not far different from the results that could be obtained by modelling Dhaka soil as a multi-layered continuum.

Table 5.10 Range of various parameters to be used in the proposed design rationale.

Parameters		Unit	**Range**
Clay	ϕ_c	Degree	15-30
	γ_c	kN/m^3	14-22
	DCL	m	5.0-11.5
Sand	ϕ_s	Degree	28-40
	γ_s	kN/m^3	15.0-22.5
Pile material	H	m	10-22
	D	m	0.4-0.61

With the above limitations and assumptions, the proposed equations are presented below:

$$P = K \cdot F_{c\phi} \cdot F_{c\gamma} \cdot F_{DCL} \cdot F_{s\phi} \cdot F_{s\gamma} \cdot F_H \cdot F_D \qquad (5.11)$$

Here

P = failure load, i.e. load capacity of a axially loaded pile (kN)

$K = 1282$

$F_{c\phi} = 1.05211 + 0.00842\,\phi_c - 0.00046\,(\phi_c)^2$

$F_{c\gamma} = 0.19808 + 0.04151\,\gamma_c$

$F_{DCL} = 0.94789 + 0.03654\,DCL - 0.0037\,(DCL)^2$

$F_{s\phi} = 0.69462 - 0.00024\,\phi_s + 0.00032\,(\phi_s)^2$

$F_{s\gamma} = 0.73725 - 0.00805\,\gamma_s + 0.00086\,(\gamma_s)^2$

$F_H = -0.26156 + 0.04166\,H + 0.0012\,(H)^2$

$F_D = 0.16729 + 1.61153\,D$

The use of the above equation is straight forward. The design capacity of pile can readily be calculated once the necessary soil parameters and pile dimensions are known.

5.4.1 Validation of the Proposed Method

To show the acceptability of the proposed values given by Eq. (5.11), they are compared with the corresponding values obtained from finite element analysis using CRISP and also with a traditional design method (Appendix C). For the purpose of comparison, four examples have been used where parameters are selected arbitrarily within the scope of the equations. In addition to that, three actual pile load-test data used in this study have also been considered for comparison purpose. The values of all the necessary parameters are listed in Table 5.11.

Table 5.11 Example piles for comparison

Example	ϕ_c	γ_c	DCL	ϕ_s	γ_s	H	D
1	25	22	7.3	37	20.0	12.3	0.40
2	20	16	9.3	40	18.0	18.3	0.50
3	25	18	8.3	33	17.0	20.3	0.55
4	17	14	10.3	29	20.0	22.3	0.60
Pile A	23	19	8.3	31	19.5	19.3	0.508
Pile B	23	19	5.25	35	19.5	15.25	0.46
Pile C	23	19	5.5	35	19.5	11.0	0.432

Table 5.12 The single pile capacity by different methods.

Example	Proposed Equation	FE Model (CRISP)	Traditional method
1	515	520	1150
2	1015	1000	1950
3	1240	1200	1120
4	1250	1250	1020
Pile A	1160	1200	1110
Pile B	765	800	1100
Pile C	380	400	680

Table 5.12 list the values of pile capacities given by the proposed equation for the above seven examples. The corresponding results from FE analysis are also presented along with the pile capacities using conventional design equations (see Appendix C for a sample calculation pertaining to design example.)

In the traditional method, the skin resistance has been calculated using Burland (1973) equation, Vesic's critical depth plot and Meyerhof's K_h tanϕ plot (see Art. 5.2.1) and the base resistance has been calculated using Meyerhof's method (see Art. 5.2.2). It can be stated from Table 5.12 that the proposed equations predict results very close to the results predicted by finite element methods. Now, the load capacities obtained from the traditional method show some variation form the capacities obtained from the proposed method. It should be kept in mind that the traditional methods calculate the ultimate load capacity of a pile which is only effective when both the shaft and base resistance reach their limiting capacities. The allowable pile capacity, i.e., the design pile capacity should be obtained by dividing the ultimate capacity with factor of safety ranging from 2.5 to 4 or more (Bowles, 1989). In this connection it may be recalled that for capacity determination, a large number of different equations are used, any two of which seldom give the same computed capacities (Bowles, 1989). Keeping this in mind, while calculating pile capacities using conventional mathod, only those traditional design equations have been carefully together which have gained wide acceptibility.

On the contrary, the load capacities obtained from the proposed method are the failure load (i.e.onset of nolinearity)capacities which are equivalent to design capacities and can be used as design loads. When viewed in this angle, it becomes apparent that the proposed method predicts results comparable to the traditional methods.

It can be seen from Table 5.12 that for higher values of ϕ_s, the ultimate capacities obtained from the traditioncal method are relatively greater than the proposed failure load capacities as compared to the capacities obtained using lower values of ϕ_s. In fact, for lower values of ϕ_s, the traditional procedure predicts results even slightly lesser than the proposed method. If one delves into the traditional methods, it becomes clear that the base resistance of pile in sand is very much dependent on ϕ_s values. For relatively larger values of ϕ_s, the base resistance increases in a logarithmic scale and becomes many times of the shaft resistance. As a result, when the load in which both the shaft and base resistance reach their limiting state would be applied, the displacement of the pile becomes much greater than allowable. Thus the ultimate capacities cannot be realized in reality using conventional mathods.. In this regard Paulos and Davis (1980) uttered some caution, "the use of high value of ϕ for very dense sands (say, $\phi_s \geq 40^{\circ}$) simultaneously for the shaft and base, should be treated with caution, since the full base resistance may well only be mobilized after a movement sufficient for the operative value of ϕ along the shaft to be significantly less than the peak".

Thus, the usual design methods can not take into account such factors as slippage and predict results somewhat farfetched than the reality. However, the proposed methods and FE methods can lead to reasonable (design) pile capacities as it uses interface elements, specially developed to cater for the slippage.

5.5 REMARKS

The predicted responses obtained for the pile-soil system from the present FE model have been found to be sensitive to parameters like the angle of friction of soil, density of soil, depth of clay layer and pile dimensions. In addition to that the predicted responses tend to follow general trends with the variation of these parameters. Efforts have been made in this study to formulate these trends and subsequently propose a empirical method which can replace the need for running the FE program for each and every case. When the proposed method has been tested against the FE model and a traditional pile design method, it has been found that the proposed method works satisfactorily. Although the method has been proposed for pile-soil system, it is expected that design parameters for any other soil-structure interaction problems could be obtained using the methodology presented in this study.

CHAPTER 6

LOAD-DISPLACEMENT RESPONSE OF SQUARE FOOTINGS

6.1 INTRODUCTION

After making an extensive study on pile-soil system in the previous chapters, attempts have been made in this chapter to use the FE model to predict the load-displacement behaviour of square footings in Dhaka soil. Square footings have been analyzed in this study as axisymmetric case. In doing so square footings have been idealized as circular footings having the same equivalent area as their square footing counterpart. Although this idealization is expected not to change the responses of square footing significantly, it simplifies the analysis to a great extent. In contrast to axisymmetric idealization, if a plain-strain idealization would have been adopted, the dimension of the model footing in the transverse plane would have assumed an infinite length. This would have invariably turned a square footing into a strip footing. Thus, use of axisymmetric modelling has been considered to be adequate, although not as an alternative to a fully three-dimensional study, which is beyond the scope of the present work. Again, the axisymmetric idealization of square footing simulates the mode of load transfer from column to footing and from footing to soil in a way comparable to the mode experienced in case of square footings.

As in the case of piles, the soil and footing elements have been analyzed in this study as linear strain quadrilateral with displacement unknown (type 4) and interface of footing and soil as the 6 noded interface elements with displacement unknown (see Fig. 6.1). The clay has been considered to follow Modified Cam-clay (MCC) constitutive law, while sand layer follows elastic-perfectly-plastic material properties. Drained analysis, instead of undrained or consolidation analysis, has been performed during the study of footing-soil interaction. Actually, a consolidation analysis with larger time span might have predicted the responses more realistically. On the other hand, if consolidation analysis is allowed to undergo for longer time period, then the displacement prediction from consolidation analysis converge to the displacement prediction from drained analysis. Thus, the drained analysis usually predicts higher displacements, which are not far different from the displacement predicted by consolidation analysis with sufficiently long time period. As a result, the drained analysis has been performed in this study and thus, the escalating running time cost that would have been incurred in case of consolidation analysis has been averted.

It is expected that the studies to be described here will lead to displacement predictions for footings on Dhaka clay under various conditions. Once displacements of all the footings are known, relative displacements among various footings can be determined. These relative displacements may be given as inputs to frame analysis in order to arrive at more realistic prognosis.

6.2 MESH CONFIGURATION

After performing parametric studies to fix the mesh configuration for a footing-soil system following with the methodology presented in Chapter 4 and considering the mesh configurations for footing presented by Dewaikar and Prajapati (1992) and Kaliakin and Li (1995), a representative mesh configuration has been chosen for footing-soil system in this study. The mesh configuration has been shown in Fig. 6.1.

To validate the mesh configuration, the variation of the stress norm, σ_{SN} with both radial distance and depth from the footing bottom have been investigated for a footing having 3 m diameter and 2.5 m depth. Figure 6.2(a) shows the variation of σ_{SN} with radial distance, while Fig. 6.2(b) shows the variation of σ_{SN} with depth below the footing. It is clear from Figs. 6.2(a) and 6.2(b) that σ_{SN} die down reasonably for the mesh boundaries considered.

Besides, the shear stress contour for the above mentioned footing has been plotted and shown in Fig. 6.3. It shows that the stress zone is well within the mesh boundaries and high stress zone occurs near the bottom edge of the footing. Thus, the mesh

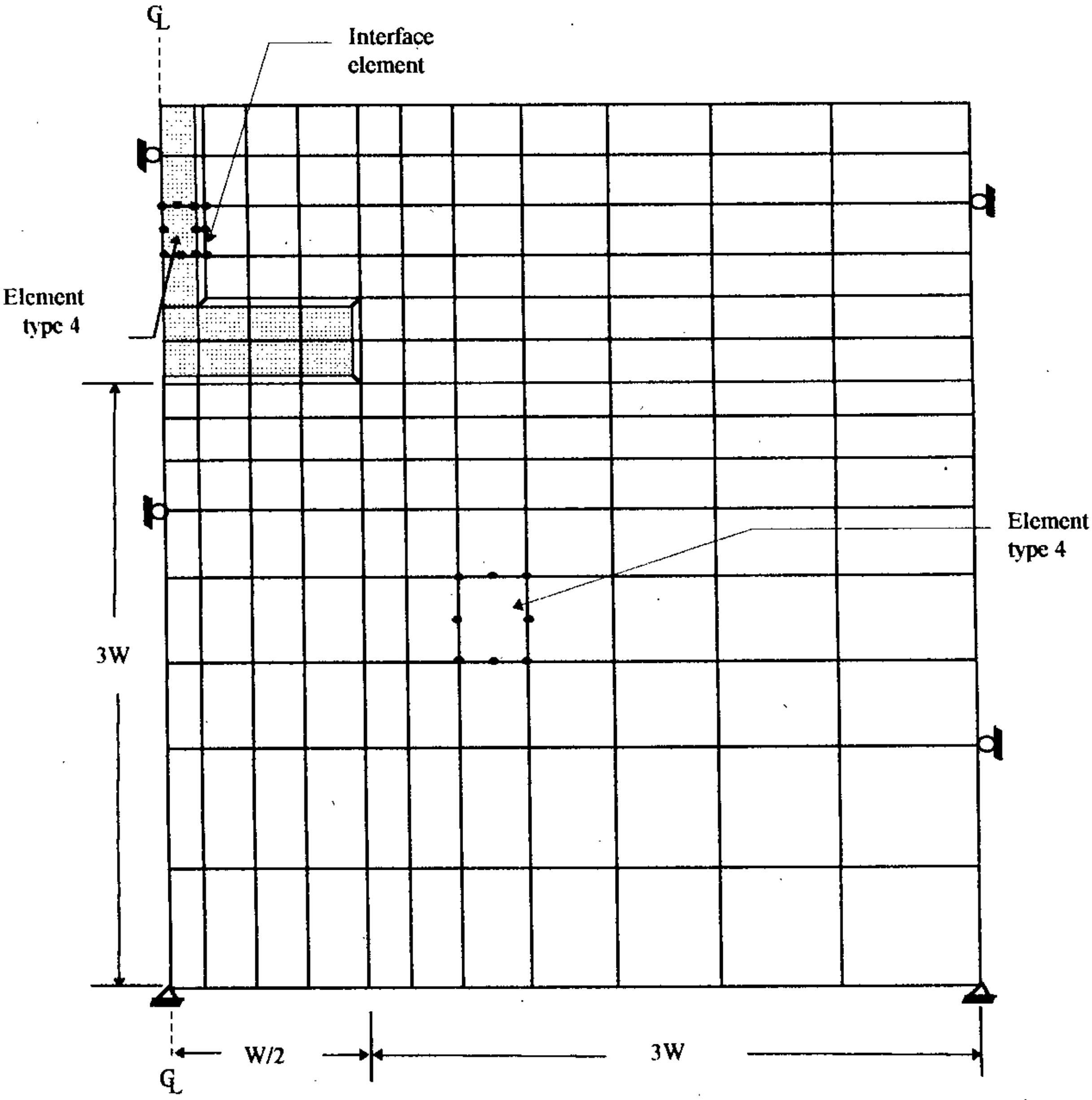

W = Diameter of the equivalent circular footing

Fig. 6.1 Typical mesh configuration for footing-soil system

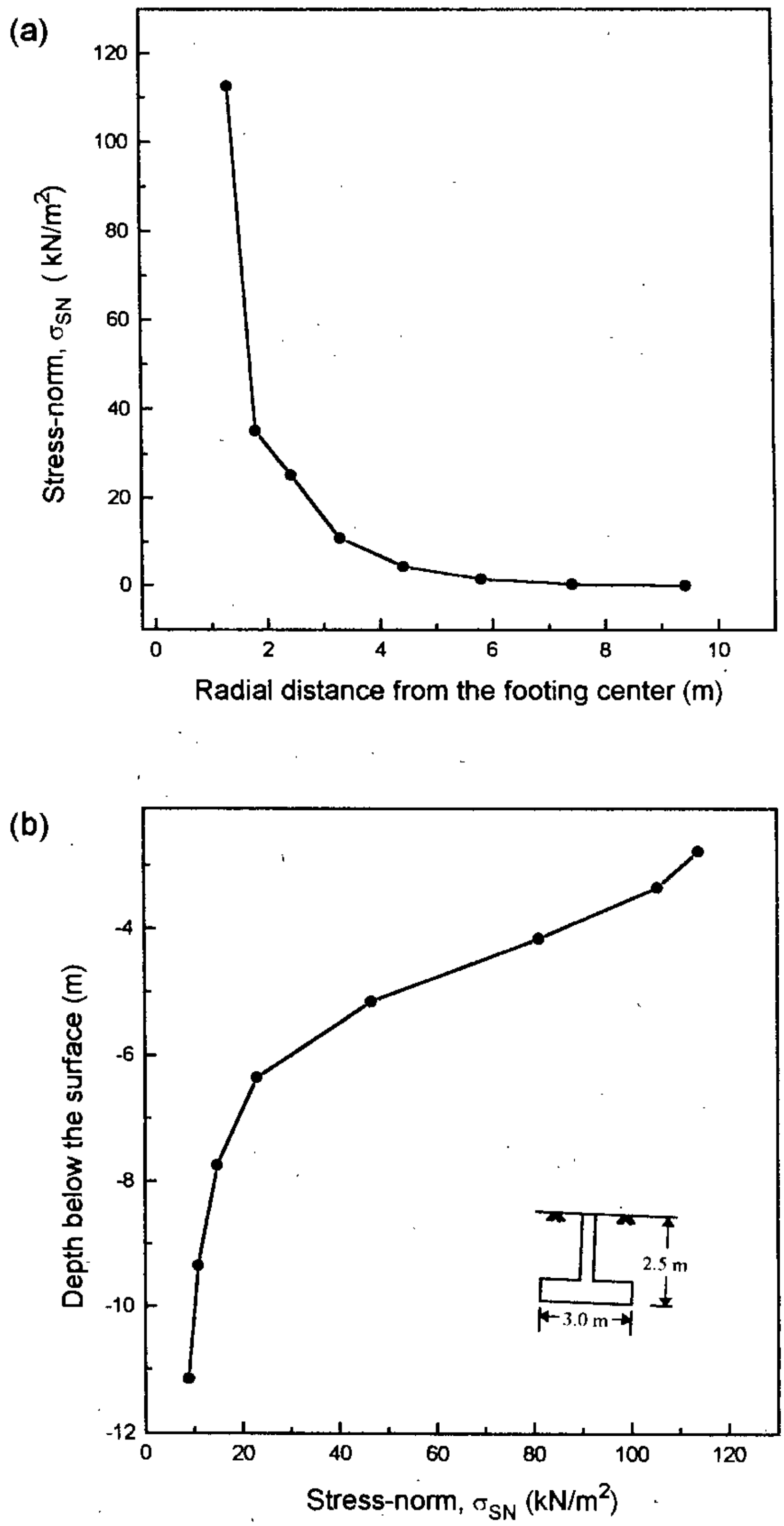

Fig. 6.2 Variation of stress-norm (a) along radial distance from footing center (b) along the depth below the footing

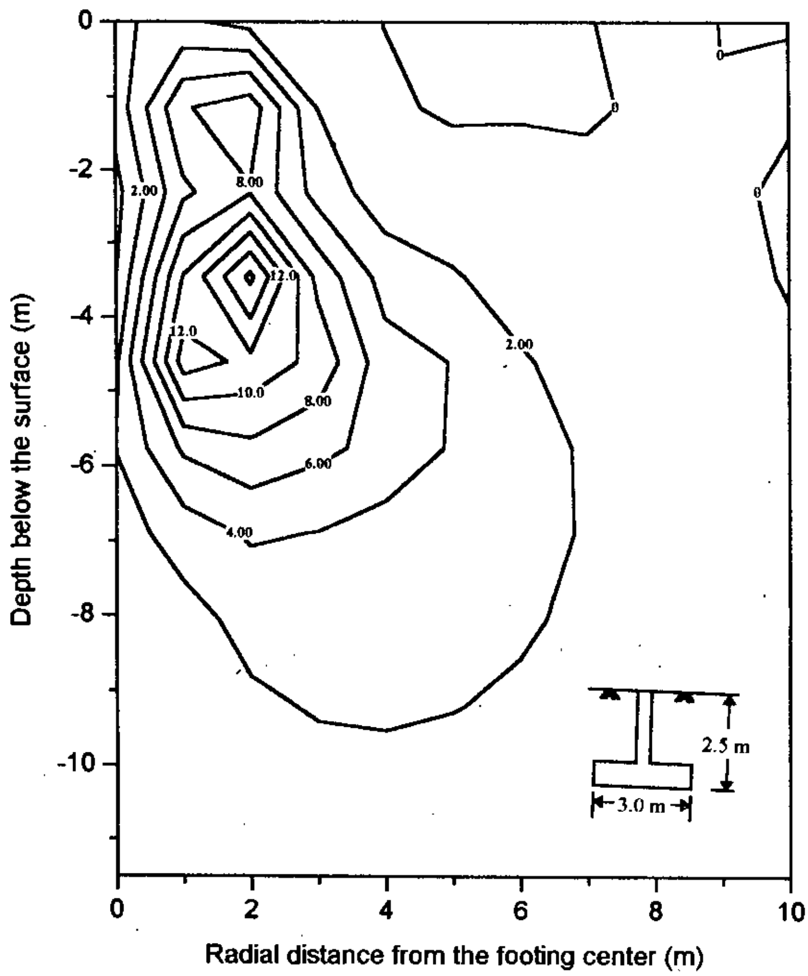

Fig.6.3 Shear stress contour for footing

configuration adopted which has finer mesh near the footing corner and reasonable extent of horizontal and vertical boundaries, appears to be an acceptable selection.

6.3 MATERIAL CHARACTERISTICS

As this study mainly aims at determining a design rationale to predict load-displacement behaviours of square footings buried in Dhaka soil, a representative soil profile of Dhaka soil has been considered. In doing so, the average values of different soil parameters have been selected by considering a number of soil investigation reports available for Dhaka soil. Although the soil conditions in some parts of Dhaka may differ slightly from the parameters considered in this study, it should be kept in mind that the soil parameters selected in this study represent average Dhaka soil conditions.. Moreover, this study is mainly concerned with proposing a methodology by which the load-displacement responses for any soil type can be formulated. The deviation of actual footing displacement from model footing displacement due to the use of average soil properties is expected to play a not so important role in the input to the design of superstructure, where in fact, relative displacement is expected to be input.

The representative soil profile considered in this study has been presented in Fig. 6.4. The figure shows that the water table has been assumed to be at a depth of 3 to 4 m from the soil surface. In the event the water table rises above this level, it is expected to reduce effective *in-situ* pressure slightly resulting in a slight increase in the footing displacement. Besides, the material properties of different material zones (See Fig. 6.4) have also been presented in Tables 6.1, 6.2, 6.3 and 6.4.

It should be observed that the interface elements in the back-filled clay layer have been given no shear resistance as has been suggested by Terzaghi (1943) in his shallow foundation theory.

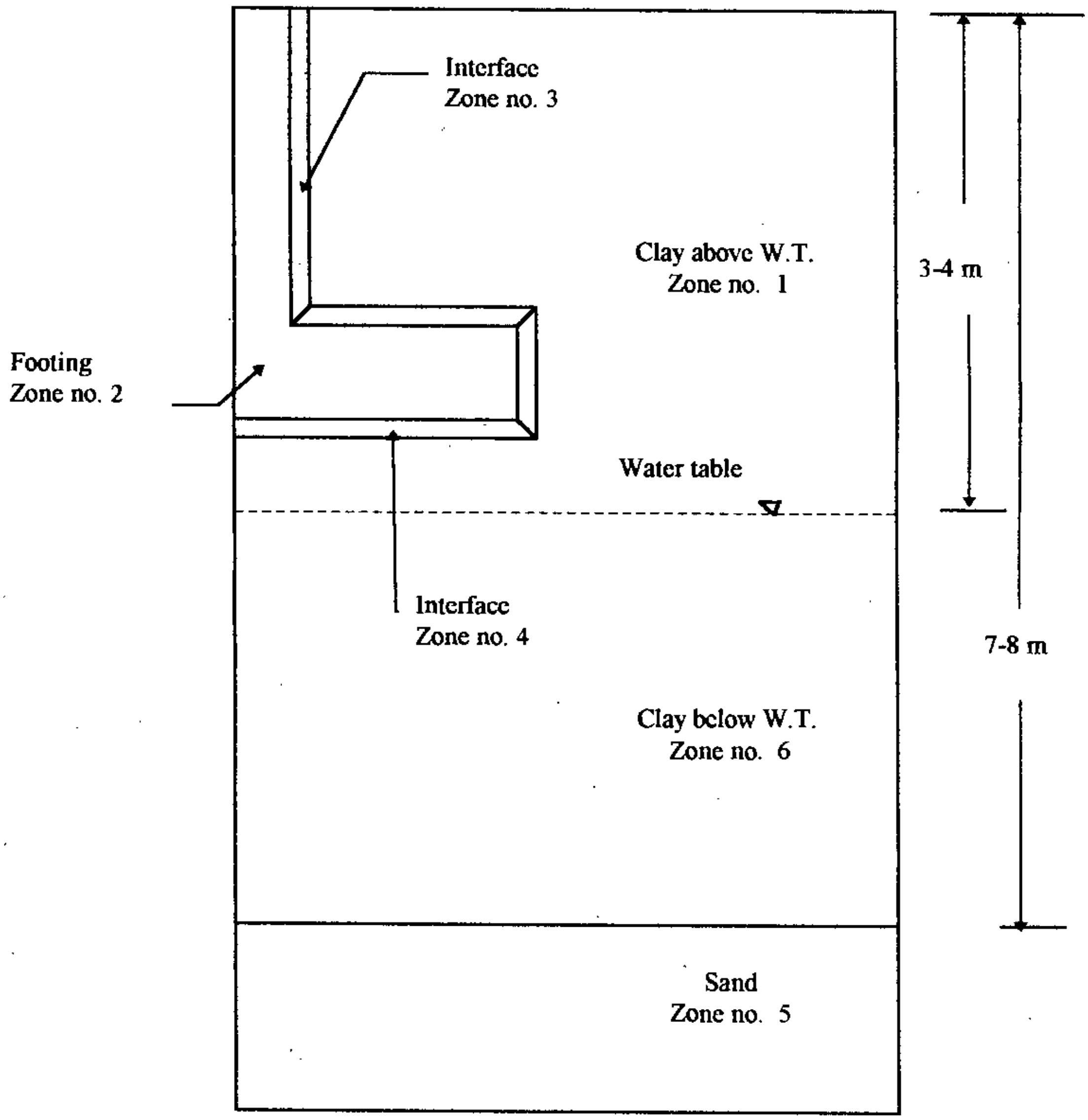

Fig. 6.4 Representative soil profile for Dhaka clay

Table 6.1 Parameters for representative clay layer of Dhaka

Soil Type	Zone number	κ	λ	e_{cs}	M	ν	γ_{bulk} (kN/m^3)
Clay above W.T	1	0.02125	0.085	1.08	0.898	0.25	14.5
Clay below W.T.	6	0.02125	0.085	1.08	0.898	0.25	19.5

Table 6.2 Parameters for representative sand layer of Dhaka

Zone Number	E_o (kN/m^2)	ν	C (kN/m^2)	ϕ (degree)	γ_{bulk} (kN/m^3)	Rate m_1 (kN/m^2)/m
5	50E3	0.25	0	31	20.0	2.0E3

Table 6.3 Interface element parameters for Dhaka clay

Zone Number	C (kN/m^2)	ϕ (degree)	K_n (kN/m^2)	G_s (kN/m^2)	G_{res} (kN/m^2)
3	5	23	23.34 E4	1.01 E4	10
4	0	0	23.34 E4	1.01 E4	10

Table 6.4 Parameters for footing material

E (kN/m^2)	Zone Number	ν	γ_{bulk} (kN/m^3)
30 E6	2	0.20	23.5

The *in-situ* stresses for different layers have to be calculated using Wroth's (1975) method considering overconsolidated clay for Dhaka (See Art.3.3.2 and Appendix A). From a number of consolidation tests i.e., ($\log_{10}\sigma_v$, e) plot for Dhaka, it has been observed that the overburden pressure on the surface of Dhaka clay has an average value of 50 kN/m^2. The *in-situ* stresses and p_c' have been calculated using this overburden pressure in this study. A complete input file for a typical footing has been presented in Appendix D.

6.4 LOAD-DISPLACEMENT RESPONSES

To investigated the effect of variation in the size of the footing or the depth of the footing embedment, a scheme has been followed in this study. Firstly, the depth of the

footing embedment has been kept constant (D_F = 2.5 m) and the load displacement responses for different sizes of footing have been investigated which are shown in Fig. 6.5(a). Next, keeping the size of the footing constant (S_F = 2.5), the depths are varied and the load-displacements responses for them are obtained and plotted in Fig. 6.5(b).

Now, efforts have been made to formulate a general trend of these load-displacement curves in this study. In doing so, a hyperbolic function in the form of Eq. 6.1 has been selected after many trials and considerations.

$$P = \frac{A\delta}{B+\delta} \qquad (6.1)$$

where P = load applied on the footing,

δ = displacement,

A and B are constants.

It has been found that Eq. 6.1 can trace the actual load-displacement curves reasonably well for significant distance even into the non-linear portion. Only, the portion of curves far away from the point of commencement of non-linearity may deviate considerably from the curves formulated using Eq. 6.1. Figure 6.6 shows a typical load displacement response of a particular footing along with the best fitted curve formulated using Eq. 6.1. It is clear from Fig. 6.6 that the best fitted curves using Eq. 6.1 simulate the actual tried of load-displacement curves satisfactorily.

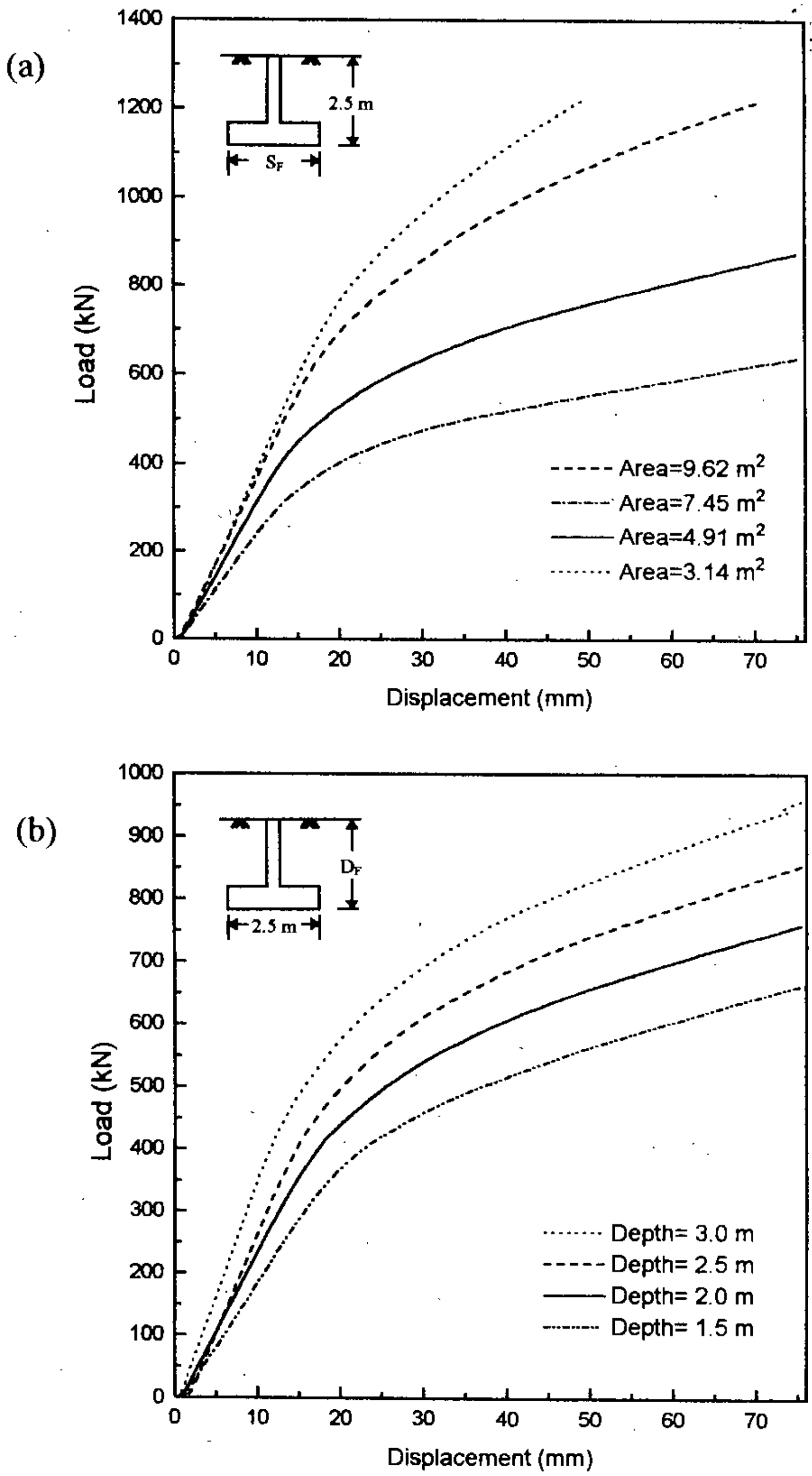

Fig.6.5 Load displacement responses for different (a) areas and (b) depths of footing

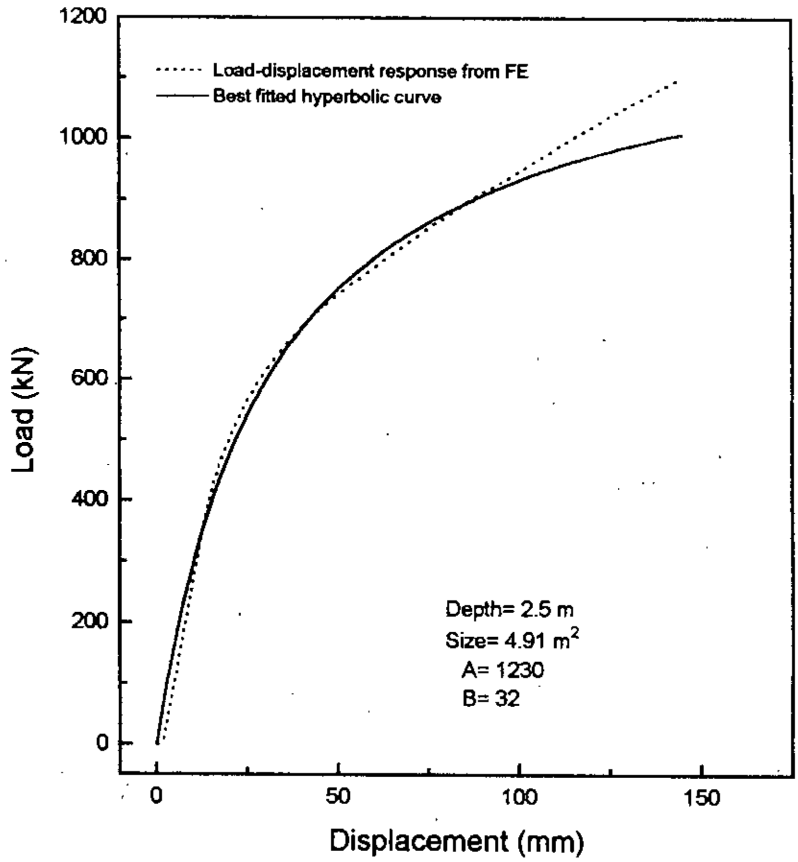

Fig. 6.6 Load-displacement response of a particular footing alongwith the best fitted hyperbolic curve.

Accordingly, every load-displacement curves shown in Fig. 6.5(a) and (b) have been formulated as a hyperbolic function (Eq. 6.1) and different values of constants A and B for various depths and sizes have been found out are presented in Table 6.1..

Table 6.1 Values of constants A and B for different sizes and depths of footing

Size of footing (m^2)	Depth of embedment (m)	A	B
3.14	2.5	810	22
4.91		1230	30
7.45		1850	36
9.62		2275	42
4.91	1.5	1050	42
	2.0	1130	35
	2.5	1230	30
	3.0	1280	26

Now, the variation of constants A and B with different values of sizes of footing have been shown in Figs. 6.7(a) and 6.7(b). Figure 6.7(a) shows that the constant A increases linearly with higher sizes. The equation of the best fitted straight lines has also been shown in Fig. 6.7(a). Similarly, the variation of constant B assumes a parabolic trend for higher sizes as shown in Fig. 6.7(b) which also includes the equation of the best fitted second degree polynomial.

In the same way, the trend followed by the constants A and B with variation in depths of embedment have been investigated in Figs. 6.8(a) and 6.8(b). Figures 6.8(a) and 6.8(b) also include the equations of the best fitted curves.

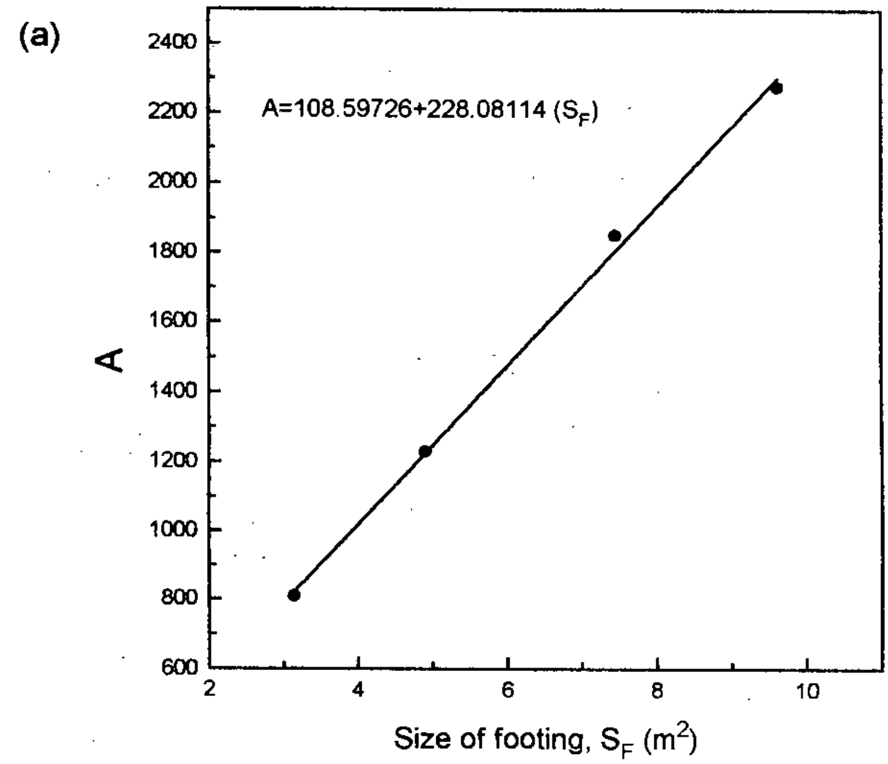

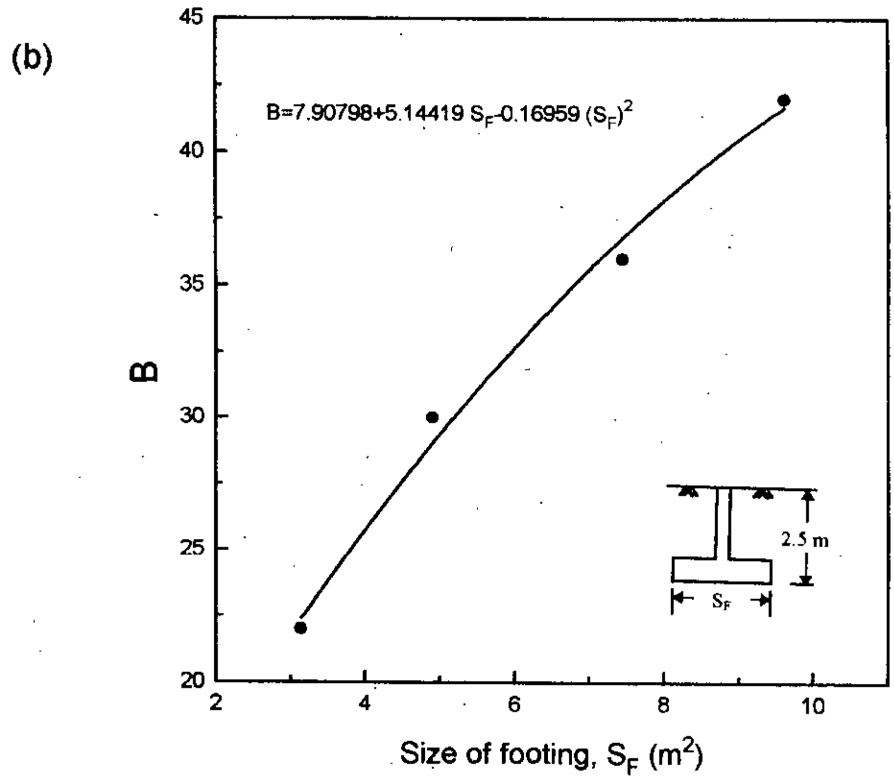

Fig. 6.7 Variation of constants (a) A and (b) B for different sizes of footing

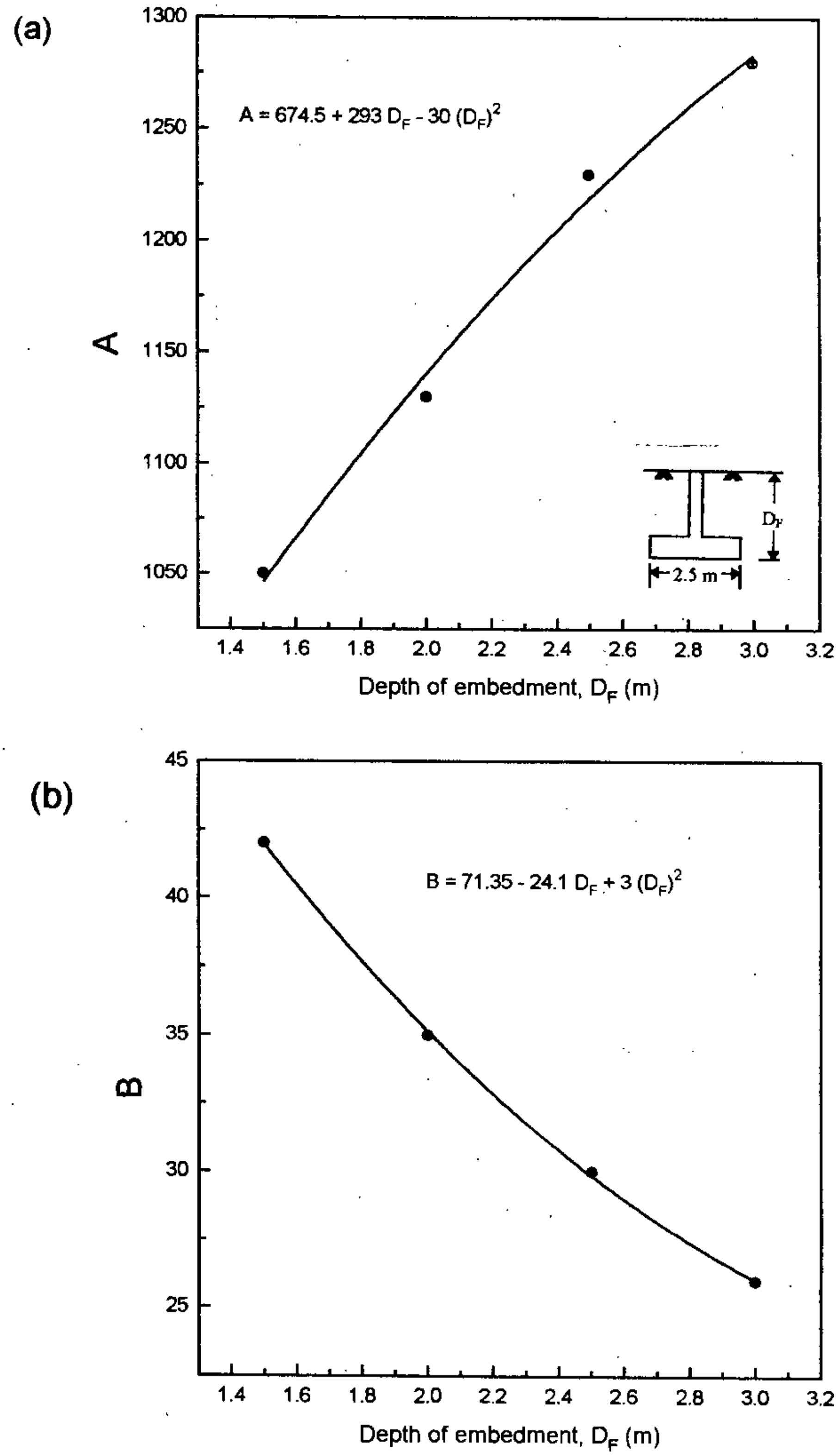

Fig. 6.8 Variation of constants (a) A and (b) B for different embedment depths of footing

6.5 A PROPOSED LOAD-DISPLACEMENT RATIONALE FOR SQUARE FOOTING IN DHAKA

As the constants of Eq. (6.1) appear to follow some defined trend with variation of depths and sizes of footings in Dhaka soil, an empirical equation can be introduced following the procedure described in Chapter 5 for piles. The ensuing empirical equation has been presented below as Eq. 6.2.

$$P = \frac{\left(\frac{A_S A_D}{K_A}\right)\delta}{\left(\frac{B_S B_D}{K_B} + \delta\right)} \text{ kN} \qquad (6.2)$$

Where

$$K_A = 1230 \quad \text{and} \quad K_B = 30$$

$$A_S = 108.60 + 228.08\,(S_F) \qquad (6.3)$$

$$B_S = 7.91 + 5.14\,(S_F) - 0.17\,(S_F)^2 \qquad (6.4)$$

$$A_D = 674.50 + 293.00\,(D_F) - 30.00\,(D_F)^2 \qquad (6.5)$$

$$B_D = 71.35 - 24.10\,(D_F) + 3.00\,(D_F)^2 \qquad (6.6)$$

It should be kept in mind that Eq. (6.2) is empirical in nature and valid for a certain range of footing dimensions. So proper consideration should be given to the units used and the range for which it is expected to work satisfactorily. Table 6.2 presents the units and the range of S_F and D_F applicable to Eq. 6.2.

Table 6.2 Units and range of sizes and depths of footings for Eq. 6.2.

	Unit	Range
Depth	m	15.0-3.00
Size	m^2	3.15-9.62

6.6 VALIDATION OF THE PROPOSED METHOD

To show the acceptability of the proposed equation, the load-displacement behaviours predicted by Eq. 6.2 have been compared with the corresponding load-displacement behaviours obtained from finite element analysis using the presently used FE model (CRISP). For the purpose of comparison, three examples are used whose parameters have been selected arbitrarily within the range of the equations. The values of necessary parameters for these examples are listed in Table 6.3.

Table 6.3 Example footing sizes and depths of embedment

	Size (S_F) (m^2)	**Depth of embedment (D_F) (m)**	**Equation of load-displacement curve from Eq.6.2**
Example 1	4.15	2.25	$P = 1015\,\delta/(28.35+\delta)$
Example 2	5.94	2.75	$P = 1490\,\delta/(30.00+\delta)$
example 3	6.61	3	$P = 1686\,\delta/(30.00+\delta)$

For these examples, values for constants A and B have been calculated using Eqs. 6.3, 6.4, 6.5 and 6.6. Now, using these values, a load-displacement equation for each example has been obtained, using Eq. 6.2 and shown in Table 6.3. In addition to that, finite element analysis has been performed separately for each of the example footing cases, and load-displacement responses obtained from these analyses have been compared with the proposed equations. Figure 6.9 show the load-displacement curves obtained from both CRISP and the proposed method in a single plot for all the three examples studied. It is clear from Fig. 6.9 that the load-displacement curves obtained from the proposed method and the load-displacement responses obtained from CRISP are almost same. Very insignificant deviations which are apparent from Fig. 6.9 can be neglected as far as practicality is concerned. Thus, it can be stated that the proposed

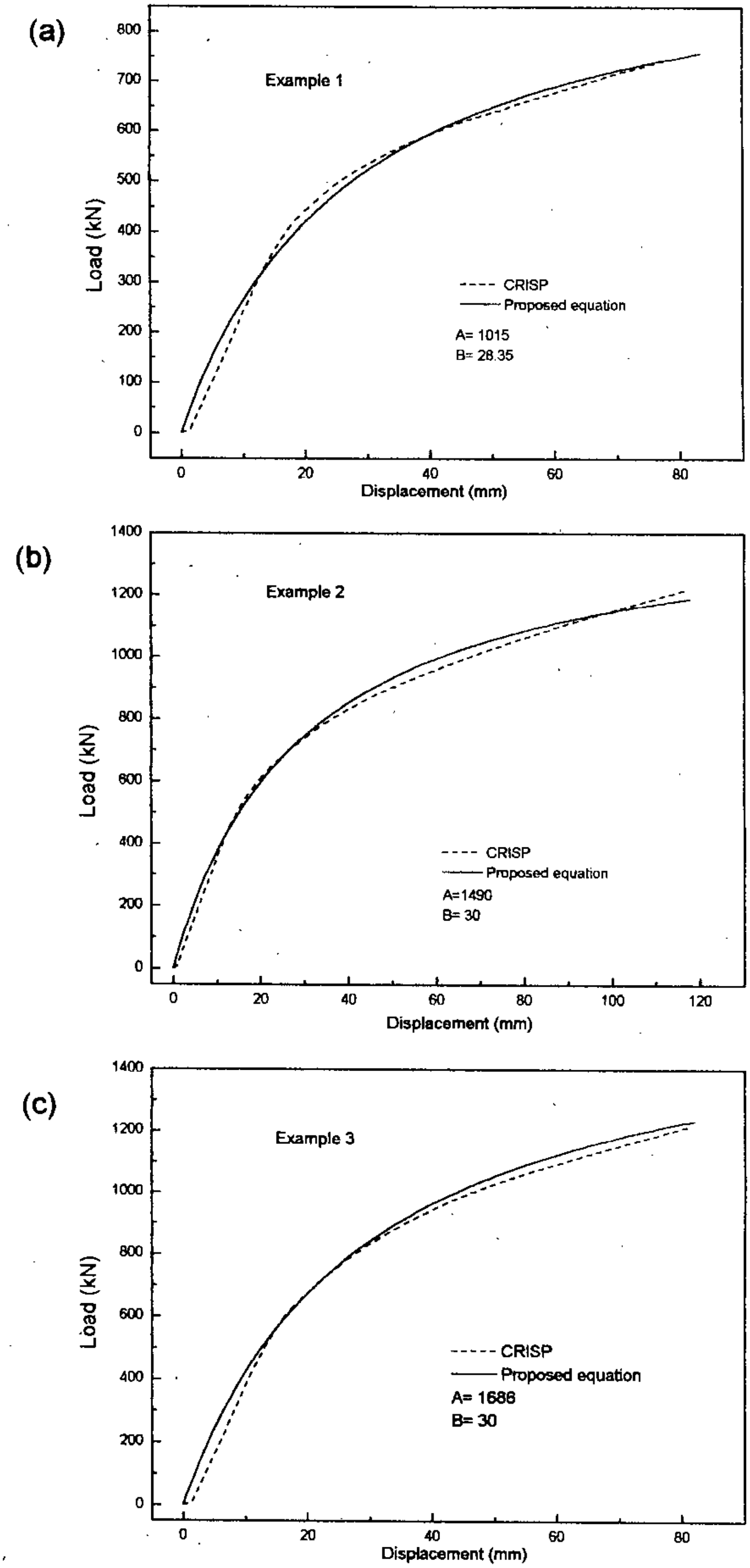

Fig.6.9 Load-displacement responses predicted by the proposed equation and FE for example (a) 1, (b) 2 and (c) 3

empirical equation based on soil-structure interaction study simulates the load-displacement responses satisfactorily for square footings embedded in Dhaka soil.

One thing should be kept in mind that this empirical method can not be applied readily to any site in Dhaka as the site concerned may have different local soil characteristics, which may be widely different from the representative soil characteristics considered in this study for Dhaka soil. But, if the soil conditions of the site are more-or-less comparable to the representative soil properties considered in this study (most of the sites in Dhaka are expected to fall within this status), the proposed method can be applied as a design aid for calculating approximate displacements for any loading on the footing. Besides, designers are mainly concerned with the differential displacements of different footings and this method can be an handy tool for calculating differential settlements of different footings with various sizes and depths at a site in Dhaka. Moreover, this study presents a methodology by which an empirical method can be developed for any locality, provided that extensive statistical analyses are carried out for obtaining representative soil parameters applicable to the locality.

6.7 REMARKS

The aim of this study was to introduce a methodology for obtaining an empirical method to formulate a load-displacement equation for square footings embedded in Dhaka soil. In view of this, representative parameters of Dhaka soil have been considered from a number of soil investigation reports and eventually, a rationale for obtaining the load-displacement equation has been introduced in this study. The proposed equation has been compared with the results obtained from FE method (CRISP). It has been found that the proposed equation simulates the FE solution with reasonable accuracy.

CHAPTER 7

CONCLUSIONS AND RECOMMENDATIONS FOR FUTURE RESEARCH

7.1 CONCLUSIONS

In this study, a soil-structure interaction system has been developed, for the study of various soil-structure systems, with special reference to Dhaka-soil conditions. An existing finite element code, CRISP, has been used after incorporating interface element into its computer code. After an extensive and systematic study using the model thus developed, the following conclusions can be drawn from the preceding chapters:

(a) Realistic input specification of various soil and structural parameters are very important for the model to simulate any soil-structure system properly. In this respect, the guidelines proposed and implemented for mimicking various structure-soil systems have been found to be very effective. Special care should be taken in specifying *in-situ* stresses in soil prior to the installation of the structural member in order to simulate real field behaviour.

(b) While studying the interaction of pile-soil system, it has been revealed that the horizontal and vertical extent of soil to be included in the finite element idealization has a pronounced effect on the predicted response of the system . In this study specific non-dimensional guidelines have been suggested and subsequently tested for obtaining reasonable mesh configurations. The proposed methodology may be suitably adopted to other structure-soil systems.

(c) Satisfactory performance of the finite element model is affected by the thickness of the interface element. It has been found that for a width-to-breadth ratio (t/b) of 0.1 for the interface element, effect is minimal.

(d) Prior to the final analysis of the soil-structure system, the loading rate has to be determined individually for the case concerned. The methodology suggested in this study may be adopted for such a selection.

(e) In case of consolidation analysis, it was observed that the excess pore water pressure did not dissipate much for the time span considered in case of pile load-testing in the field. Besides, the excess pore water pressure development has found to occur mainly near the pile. The pore pressure assumes the *in-situ* value at some distance away from it..

(f) The onset of nonlinearity of concrete pile -soil system has been found to be sensitive to the variation of parameters like the unit weight of soil, depth of clay layer, the angle of friction of soil and, of course, the pile size. On the other hand, the responses have been found not to be very sensitive to the variation of cohesion, critical void ratio and the slopes of the virgin compression and swelling lines. Although the displacement predictions were affected by the variation in the value of the initial tangent modulus of structural and soil elements, the failure load of deep (pile) foundations remained independent of such variations.

(g) The design rationale suggested in this study for designing pile foundations has been found to match the finite element predictions satisfactorily. Although some deviations from the results obtained from a traditional design method were observed, the reasons for this deviation could be explained. The satisfactory performance of the suggested rationale encourages the use of the proposed design equation, albeit approximately, in the design of pile foundations in lieu of full fledged interaction analysis.

(h) The load-displacement relationship of square footings, admittedly on the basis of presently conducted limited parametric study, has been found to be related by a hyperbolic functions; the ensuing load-displacement equation traced the finite element predictions faithfully.

7.2 RECOMMENDATIONS

The following recommendations for future study can be made from the present research:

(a) In the present study, three dimensional problems were simplified as axisymmetric problems. In the future, three dimensional analysis may be performed to simulate the real life situation more realistically.

(b) Finite element analysis can be performed on different types of soil-structure problems such as battered piles, hollow piles, mats, culverts, different types of footings, retaining walls, piles in groups etc. and the methodology proposed here may be adopted for obtaining design equation for such a system. Beside, structures can be subjected to different types of loading conditions like inclined loads, moments etc.

(c) Consolidation analysis can be performed on soil-structure interaction systems to observe the effects of consolidation under cyclic loading, dynamic loading as well as unloading.

(d) The existing finite element program can be modified to incorporate iterative solution technique.

REFERENCES

AISI (1975), Steel Pile Load Test Data, American Iron and Steel Institute, Washington, D.C., 84 .

Ameen, F. (1985), Geotechnical Characteristics of Dhaka Clay, M.Sc. Engg. Thesis, Department of Civil Engineering, Bangladesh University of Engineering and Technology, Dhaka.

Berezantzev, V.G., Khristoforov, V., and Golubkov, V. (1961), Load Bearing Capacity and Deformation of Piled Foundations, Proc. 5th Int. Conf. S.M. & F.E., vol. 2; 11-15.

Bowles, J.E. (1989), Foundation Analysis and Design, McGraw-Hill International Book Company, Fourth Edition , New York.

Britto, A.M. and Gunn, M.J. (1987), Critical State Soil Mechanics Via. Finite Elements, John Wiley & Sons Limited, New York.

Burland, J.B. (1973), Shaft Friction of Piles in Clay - A Simple Fundamental Approach, Ground Engg., vol. 6, no. 3, May; 30-42.

Clough, G.W. and Duncan, J.M. (1969), Finite Element Analysis of Port Allen and Old River Locks, Report No. TE-69-13, Univ. of California, Berkeley.

Coyle, H..M. and Reese, L.C. (1966), Load Transfer for Axially Loaded Piles in Clay, J.S.M.F.P., ASCE, vol. 92, SM2; 1-26.

Coyle, H..M., and Castello, R.R. (1981), New Design Correlations for Piles in Sand, JGED, ASCE, vol. 107, GT7, July; 965-986.

Crawford, C.B. and Burn, K.N. (1962), Settlement Studies on the Mt. Sinai Hospital, Engineering Journal of Canada, Ottawa, vol. 45, No. 12, December.

D'Appolonia, D.J., et al. (1970), Closure: Settlement of Spread Footings on Sand, JSMFD, ASCE, vol. 96, SM2; 754-762.

Desai, C.S., Zaman M..M., Lightner, J.G. and Siriwardane, H.J. (1984), Thin-layer Elements for Interfaces and Joints, Int. Jnl. for Numerical and Analytical Methods in Geomechancis, V.8; 19-43.

Dewaikar, D.M. and Prajapati, A.H. (1992), Geomechancis Today, Proc. Indian Geotechnical Conf., Calcutta, 18-20; 133-136.

Ghaboussi, J., Wilson, E.L. and Isenberg, J. (1973), Finite Element for Rock Joints and Interfaces, J.Struct. Eng. Div. Proc. Asce, V. 99, SM10.

Golder, H.Q. (1957), A Note on- Piles in Sensitive Clays, Geot., vol. 7; 192-195.

Golder, H.Q., and Leonard, M.W. (1954), Some Tests on Bored Piles in London Clay, Geot., vol. 4; 32-41.

Goodman, R.E. and John, C. (1977), Finite Element Analysis for Discontinuous Rocks, Chapter 4 of Desai, C.S. and Christian, J.T. (1977).

Goodman, R.E., Taylor R.L and Brekke T.L. (1968), A Model for Mechanics of Jointed Rock, J. Struct. Eng. Div. Proc. ASCE, V. 94, SM3.

Herrmann, L.R. (1978), Finite Element Analysis of Contact Problems, J.Eng. Mech. Div., Proc. ASCE, V. 104, EM5.

Icon Engineering Services (IES), (1994), H-79/F Airport Road, Banani, Dhaka, Report on- Geotechnical Investigation for Construction of Multistoried Building, Property Pair at Kalabagan, Dhaka.

Iwasaki, T. and Tatsuoka, F. (1977), Effects of Grain Size and Grading Dynamic Shear Modulus of Sands, Soils and Foundations, J.S.M.F.E, vol. 17, no. 3; 20-35.

Janbu, N. (1976), Static Bearing Capacity of Friction Piles, Proc. 6th European Conf. on SMFE, vol.1.2; 479-488.

Jeyatheran, K. (1996), Application of CRISP in Embankments, Excavations and Piles, Presented at a Short Course on Numerical Analysis in Geotechnical Engineering, Held at AIT, 12-16 February, 1996.

Kaliakin, V.N. and Li, J. (1995), Insight into Deficiencies Associated with Commonly used Zero-thickness Interface Elements, Comp. and Geomech. vol. 17; 225-252.

Kamal Uddin, M. (1990), Compressibility and Shear Strength of Remoulded Dhaka Clay.

Karim, M. R. (1985), An Investigation of the Behaviour of Soil-steel Structure, M.Sc. Engg. Thesis, Department of Civil Engineering, Bangladesh University of Engineering and Technology, Dhaka.

Katona, M.G., Smith, J.M., Odello, R.S. and Allgood, J.R. (1976), CANDE - A Modern Approach for Structural Design and Analysis of Buried Culverts, Report No. FHWA-RD-77-5, Naval Civil Engineering Laboratory.

Katona, M.G. (1981), A Simple Contact Friction Interface Element with Applications to Buried Culvert, Proc. Symp. on Impl. of Computer Procedure and Stress-strain Laws in Geotechnical Engineering, Chicago, Illinois, V.1.

Kerisel, J. (1961), Foundations Profondes en Milieu Sableux, Proc. 5th Int. Conf. S.M. & F.E., vol. 2; 73-83.

Kinoshita, M., Kotsovos, M.D. and Pavlovic, M.N. (1994), Behaviour of Concrete under Passive Confinement, Proc. JSCE, J. Materials. Conc. Struct. Pavements, No. 502, vol. 25; 131-142.

McClelland, B. (1972), Design and Performance of Deep Foundations, Proc. Spec. Conf. on Perf. of Earth and Earth-supp. Structs., ASCE, vol. 2; 111.

McClelland, B. (1974), Design of Deep Penetration Piles for Ocean Structures, Jnl. Geot. Eng. div., ASCE, vol. 100, no. GT7; 704-747.

Meyerhof, G.G. (1959), Compaction of Sands and Bearing Capacity of Piles, J.S.M.F.D., ASCE, vol. 85: SM6; 1-29.

Meyerhof, G.G. (1976), Bearing Capacity and Settlement of Pile Foundations, Jnl. Geot. Eng. div., ASCE, vol. 102, no. GT3:;195-228.

Meyerhof, G.G. and Murdock L.J. (1953), An Investigation of the Bearing Capacity of Some Bored and Driven Piles in London Clay, Geot., vol. 3; 267.

Mohan, D. and Chandra, S. (1961), Frictional Resistance of Bored Piles in Expansive Clays, Geot., vol. 11; 291.

Morgan, J.R. and Poulos, H.G. (1968), Settlement and Stability of Deep Foundations- in Soil Mechanics Selected Topics, ed. by I.K. Lee., Sydney, Aust: Butterworths; 528-609.

Morshed, J. (1991), Prediction of Load Deformation Behaviour of Axially Loaded Piles in Sand, M.Sc. Engg. Thesis, Department of Civil Engineering, Bangladesh University of Engineering and Technology, Dhaka.

Naylor, D. J. (1975), Non-linear Finite Element Models for Soil, PhD Thesis, University College of Swansea.

Nazneen, S. (1986), Structure-soil Interaction in Framed Buildings with Orthotropic Wall Infills, M.Sc. Engg. Thesis, Department of Civil Engineering, Bangladesh University of Engineering and Technology, Dhaka.

Potyondy, J.G. (1961), Skin Friction between Various Soils and Construction Materials, Geotechnique, vol. 11, 339-353.

Poulos, H.G. and Davis, E.H. (1980), Pile Foundation Analysis and Design, The Univ. of Sydney, John Wiley & Sons, Inc. Toranto, Canada.

Reese, L. C., Touma, F.T. and O'Neill, M.W. (1976), Behaviour of Drilled Piers under Axial Loading, Jnl. Geot. Eng. Div., ASCE, vol.102, GT5;493-510.
Reissner, H. (1924), Zum Erddruckproblem, Proc. 1st Int. Conf. Applied Mech., Delft. (Holland).

Seraj, S. M. (1986), Structure-soil Interaction in Buried Rigid Culvert, M.Sc. Engg. Thesis, Department of Civil Engineering, Bangladesh University of Engineering and Technology, Dhaka.

Siddique, A. and Safiullah, A.M.M. (1995), Permeability Characteristics of Dhaka Clay, Journal of the Civil Engineering Division, IEB, vol.23/CE, no.1.

Siddique, S.A. (1988), Experimental and Numerical Studies of Model Pile Behavior in Sand, M.Sc. thesis, BUET, Dhaka, Bangladesh.

Skempton, A.W. (1959), Cast-In-Situ Bored Piles in London Clay, Geot., vol. 9; 198.

Sowers, G.B. and Sowers, G.F. (1970), Introductory Soil Mechanics and Foundations, 3rd ed. New York, Macmillan.

Subsoil Engineers (SSB), (1982), 39 New Elephant Road, Dhaka, Report on -Soil Investigation for Proposed 20 Storied Commercial Building at 195, Motijheel Commercial Area, Dhaka.

Terzaghi, K. (1943), Theoretical Soil Mechanics, John Wiley & Sons, Inc., New York.

Tomlinson, M.J. (1957), The Adhesion of Piles Driven in Clay Soils, Proc. 4th Int. Conf. S.M. & F.E. vol. 2; 66-71.

Tomlinson, M.J. (1970), Some Effects of Pile Driving on Skin Friction, Conf. on Beh. of Piles, Inst. Civ. Engrs., London; 59-66.

Unique Boring & Engineering (UBE), (1995), 34 Green Road, Nowab Mansion (3rd Floor) Dhaka, Reprot on -Geotechnical Investigation for Construction of Multistoried Building, Shinepukur Holdings Ltd. at Green Road, Dhaka.

Vesic, A.S. (1967), A Study of Bearing Cpacity of Deep Foundations, Final Rep., Proj. B-189, School fo Civil Eng., Georgia Inst. of Tech., Atlanta, Ga.

Whitaker, T. and Cooke, R.W. (1966), An Investigation of the Shaft and Base Resistance of Large Bored Piles in London Clay, Proc. Symp. on Large Bored Piles; 7-49.

Wong, K.S. (1977), SSTIP-Soil Structure Interaction Program with Interface Elements, Univ. of California, Berkeley.

Wroth, C.P. (1975), In-situ Measurement of Initial Stresses and Deformation Characteristics, Proc. of the Specialty Conf. in In-situ Measurement of Soil Properties, ASCE, Rayleigh, North Carolina, June; 181-230.

Yasin, S.J.M. (1990), Effect of Particle Characteristics on the Strength and Volume Change Behaviour of Selected Granular Deposits of Bangladesh, M.Sc. Engg. Thesis, Department of Civil Engineering, Bangladesh University of Engineering and Technology, Dhaka.

Zienkiewicz, O.C. (1977), The Finite Element Method, 3rd ed., McGraw-Hill Book Company, New York; 787.

Zienkiewicz, O.C., Humpheson, C. and Lewis, R.W. (1975), Associated and Non-associated Visco-Plasticity and Plasticity in Soil Mechanics, Geotechnique, 25; 671-689.

Zienkiewicz, O.C., Valliappan, S., Dullage, C. and Stagg, K.G. (1970), Analysis of Non-linear Problems in Rock mechanics with Particular Reference to Jointed Rock Systems, Proc. of 2nd Conf. of Intl. Soc. for Rock Mech., Belgrade.

Appendix A

Wroth's method for calculating *in-situ* stresses.

Suppose Fig. A1 represent a layer in soil.

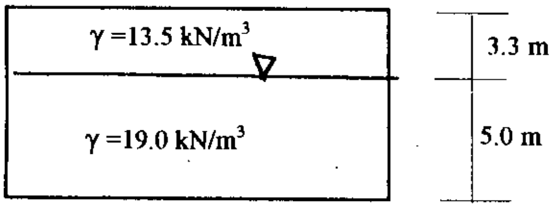

Fig A1

1. Calculation σ_v' from the bulk density of the soil and the position of the water table. Now, σ_v' for the Fig. A1 can be calculated as below:

$$\sigma_v' = 3.3 \times 13.5 + 5 \times 9 - 5 \times 10 = 89.55 \text{ kN/m}^2$$

2. Calculation of over consolidation pressure (σ_{vm}') from oedometer test. In this study, the Dhaka clay has been assumed to be normally consolidated. So, $\sigma_{vm}' = \sigma_v'$ = 89.55 kN/m^2 for the case shown in Fig. A1

3. Use of Jaky's relation to calculate K_{nc} and K_0 and hence horizontal effective stress acting when the maximum vertical effective stress (σ_{vm}') was present. Jaky's relation is

$$K_{nc} = 1 - \text{Sin}\phi' \qquad \text{(A1)}$$

$$K_0 = \text{OCR} \times K_{nc} - \frac{\nu'}{1-\nu'}(\text{OCR}-1) \qquad \text{(A2)}$$

As the soil used in this study is normally consolidated with OCR = 1, so $K_0 = K_{nc} = 1 - \text{Sin}\,\phi$ and $\sigma_h' = K_0 \sigma_v'$). For Fig 2.5.6., $\sigma_h' = (1 - \text{Sin}\,\phi) \times 89.55 = 54.56$ kN/m^2

4. Calculation of values of p' and q corresponding to the stress found in 3 using Eq. A3 and Eq. A4.

$$p' = \frac{\sigma'_v + 2\sigma'_h}{3} \tag{A3}$$

$$q = \sigma'_v - \sigma'_h \tag{A4}$$

In case of Fig. A1, $p' = 69.88$ kN/m^2 and $q = 34.991$ kN/m^2

5. Substitution of values for p' and q into the equation of yield locus (Eq. A5) to calculate the value of p_c'.

$$q^2 + M^2 (p')^2 = M^2 p' p'_c \tag{A5}$$

For the case shown in Fig. A1, p_c' is found to be 89.15 if M is equal to 0.898.

Appendix B
Input file of geometry specificatin of Pile A

```
PILE A
999
515 466 4 5 2 5
0 0
1 1 1 1 1 1 1 0 0 0
0 0 0 0
1 0.000 34.300
2 0.000 34.000
3 0.000 33.000
4 0.000 32.000
5 0.000 31.000
6 0.000 30.000
7 0.000 29.000
8 0.000 28.000
9 0.000 27.000
10 0.000 26.000
11 0.000 25.000
12 0.000 24.000
13 0.000 23.000
14 0.000 22.000
15 0.000 21.000
16 0.000 20.000
17 0.000 19.000
18 0.000 18.000
19 0.000 17.000
20 0.000 16.000
21 0.000 15.750
22 0.000 15.500
23 0.000 15.250
24 0.000 15.000
25 0.000 14.975
26 0.000 14.750
27 0.000 14.500
28 0.000 14.250
29 0.000 14.000
30 0.000 13.250
31 0.000 12.000
32 0.000 10.250
33 0.000 8.000
34 0.000 5.250
35 0.000 2.000
36 0.000 0.000
37 0.254 34.300
38 0.254 34.000
39 0.254 33.000
40 0.254 32.000
41 0.254 31.000
42 0.254 30.000
43 0.254 29.000
44 0.254 28.000
45 0.254 27.000
46 0.254 26.000
47 0.254 25.000
48 0.254 24.000
49 0.254 23.000
50 0.254 22.000
51 0.254 21.000
52 0.254 20.000
53 0.254 19.000
54 0.254 18.000
55 0.254 17.000
56 0.254 16.000
57 0.254 15.750
58 0.254 15.500
59 0.254 15.250
60 0.254 15.000
61 0.279 34.300
62 0.279 34.000
63 0.279 33.000
64 0.279 32.000
65 0.279 31.000
66 0.279 30.000
67 0.279 29.000
68 0.279 28.000
69 0.279 27.000
70 0.279 26.000
71 0.279 25.000
72 0.279 24.000
73 0.279 23.000
74 0.279 22.000
75 0.279 21.000
76 0.279 20.000
77 0.279 19.000
78 0.279 18.000
79 0.279 17.000
80 0.279 16.000
81 0.279 15.750
82 0.279 15.500
83 0.279 15.250
84 0.279 14.975
85 0.279 14.750
86 0.279 14.500
87 0.279 14.250
88 0.279 14.000
89 0.279 13.250
90 0.279 12.000
91 0.279 10.250
92 0.279 8.000
93 0.279 5.250
94 0.279 2.000
95 0.279 0.000
96 0.529 34.300
97 0.529 34.000
98 0.529 33.000
99 0.529 32.000
100 0.529 31.000
101 0.529 30.000
102 0.529 29.000
103 0.529 28.000
104 0.529 27.000
105 0.529 26.000
106 0.529 25.000
107 0.529 24.000
108 0.529 23.000
109 0.529 22.000
110 0.529 21.000
111 0.529 20.000
112 0.529 19.000
113 0.529 18.000
114 0.529 17.000
115 0.529 16.000
116 0.529 15.750
117 0.529 15.500
118 0.529 15.250
119 0.529 14.975
120 0.529 14.750
121 0.529 14.500
122 0.529 14.250
123 0.529 14.000
124 0.529 13.250
125 0.529 12.000
126 0.529 10.250
127 0.529 8.000
128 0.529 5.250
129 0.529 2.000
130 0.529 0.000
131 0.779 34.300
132 0.779 34.000
133 0.779 33.000
134 0.779 32.000
135 0.779 31.000
136 0.779 30.000
137 0.779 29.000
138 0.779 28.000
139 0.779 27.000
140 0.779 26.000
141 0.779 25.000
142 0.779 24.000
143 0.779 23.000
144 0.779 22.000
145 0.779 21.000
146 0.779 20.000
147 0.779 19.000
148 0.779 18.000
149 0.779 17.000
150 0.779 16.000
151 0.779 15.750
152 0.779 15.500
153 0.779 15.250
154 0.779 14.975
155 0.779 14.750
156 0.779 14.500
157 0.779 14.250
158 0.779 14.000
159 0.779 13.250
160 0.779 12.000
161 0.779 10.250
162 0.779 8.000
163 0.779 5.250
164 0.779 2.000
165 0.779 0.000
166 1.029 34.300
167 1.029 34.000
168 1.029 33.000
169 1.029 32.000
170 1.029 31.000
171 1.029 30.000
172 1.029 29.000
173 1.029 28.000
174 1.029 27.000
175 1.029 26.000
176 1.029 25.000
177 1.029 24.000
178 1.029 23.000
179 1.029 22.000
180 1.029 21.000
181 1.029 20.000
182 1.029 19.000
183 1.029 18.000
184 1.029 17.000
185 1.029 16.000
186 1.029 15.750
187 1.029 15.500
188 1.029 15.250
189 1.029 14.975
190 1.029 14.750
191 1.029 14.500
192 1.029 14.250
193 1.029 14.000
194 1.029 13.250
195 1.029 12.000
196 1.029 10.250
197 1.029 8.000
198 1.029 5.250
199 1.029 2.000
200 1.029 0.000
201 1.279 34.300
202 1.279 34.000
203 1.279 33.000
204 1.279 32.000
205 1.279 31.000
206 1.279 30.000
207 1.279 29.000
208 1.279 28.000
209 1.279 27.000
210 1.279 26.000
211 1.279 25.000
212 1.279 24.000
213 1.279 23.000
214 1.279 22.000
215 1.279 21.000
216 1.279 20.000
217 1.279 19.000
218 1.279 18.000
219 1.279 17.000
220 1.279 16.000
221 1.279 15.750
222 1.279 15.500
223 1.279 15.250
224 1.279 14.975
225 1.279 14.750
226 1.279 14.500
227 1.279 14.250
228 1.279 14.000
229 1.279 13.250
230 1.279 12.000
231 1.279 10.250
232 1.279 8.000
233 1.279 5.250
234 1.279 2.000
235 1.279 0.000
236 2.029 34.300
237 2.029 34.000
238 2.029 33.000
239 2.029 32.000
240 2.029 31.000
241 2.029 30.000
242 2.029 29.000
243 2.029 28.000
244 2.029 27.000
245 2.029 26.000
246 2.029 25.000
247 2.029 24.000
248 2.029 23.000
249 2.029 22.000
250 2.029 21.000
251 2.029 20.000
252 2.029 19.000
253 2.029 18.000
254 2.029 17.000
255 2.029 16.000
256 2.029 15.750
257 2.029 15.500
258 2.029 15.250
```

Appendix B

Input file of geometry specificatin of Pile A

```
259 2.029 14.975
260 2.029 14.750
261 2.029 14.500
262 2.029 14.250
263 2.029 14.000
264 2.029 13.250
265 2.029 12.000
266 2.029 10.250
267 2.029 8.000
268 2.029 5.250
269 2.029 2.000
270 2.029 0.000
271 3.279 34.300
272 3.279 34.000
273 3.279 33.000
274 3.279 32.000
275 3.279 31.000
276 3.279 30.000
277 3.279 29.000
278 3.279 28.000
279 3.279 27.000
280 3.279 26.000
281 3.279 25.000
282 3.279 24.000
283 3.279 23.000
284 3.279 22.000
285 3.279 21.000
286 3.279 20.000
287 3.279 19.000
288 3.279 18.000
289 3.279 17.000
290 3.279 16.000
291 3.279 15.750
292 3.279 15.500
293 3.279 15.250
294 3.279 14.975
295 3.279 14.750
296 3.279 14.500
297 3.279 14.250
298 3.279 14.000
299 3.279 13.250
300 3.279 12.000
301 3.279 10.250
302 3.279 8.000
303 3.279 5.250
304 3.279 2.000
305 3.279 0.000
306 5.029 34.300
307 5.029 34.000
308 5.029 33.000
309 5.029 32.000
310 5.029 31.000
311 5.029 30.000
312 5.029 29.000
313 5.029 28.000
314 5.029 27.000
315 5.029 26.000
316 5.029 25.000
317 5.029 24.000
318 5.029 23.000
319 5.029 22.000
320 5.029 21.000
321 5.029 20.000
322 5.029 19.000
323 5.029 18.000
324 5.029 17.000
325 5.029 16.000
326 5.029 15.750
327 5.029 15.500
328 5.029 15.250
329 5.029 14.975
330 5.029 14.750
331 5.029 14.500
332 5.029 14.250
333 5.029 14.000
334 5.029 13.250
335 5.029 12.000
336 5.029 10.250
337 5.029 8.000
338 5.029 5.250
339 5.029 2.000
340 5.029 0.000
341 7.279 34.300
342 7.279 34.000
343 7.279 33.000
344 7.279 32.000
345 7.279 31.000
346 7.279 30.000
347 7.279 29.000
348 7.279 28.000
349 7.279 27.000
350 7.279 26.000
351 7.279 25.000
352 7.279 24.000
353 7.279 23.000
354 7.279 22.000
355 7.279 21.000
356 7.279 20.000
357 7.279 19.000
358 7.279 18.000
359 7.279 17.000
360 7.279 16.000
361 7.279 15.750
362 7.279 15.500
363 7.279 15.250
364 7.279 14.975
365 7.279 14.750
366 7.279 14.500
367 7.279 14.250
368 7.279 14.000
369 7.279 13.250
370 7.279 12.000
371 7.279 10.250
372 7.279 8.000
373 7.279 5.250
374 7.279 2.000
375 7.279 0.000
376 10.029 34.300
377 10.029 34.000
378 10.029 33.000
379 10.029 32.000
380 10.029 31.000
381 10.029 30.000
382 10.029 29.000
383 10.029 28.000
384 10.029 27.000
385 10.029 26.000
386 10.029 25.000
387 10.029 24.000
388 10.029 23.000
389 10.029 22.000
390 10.029 21.000
391 10.029 20.000
392 10.029 19.000
393 10.029 18.000
394 10.029 17.000
395 10.029 16.000
396 10.029 15.750
397 10.029 15.500
398 10.029 15.250
399 10.029 14.975
400 10.029 14.750
401 10.029 14.500
402 10.029 14.250
403 10.029 14.000
404 10.029 13.250
405 10.029 12.000
406 10.029 10.250
407 10.029 8.000
408 10.029 5.250
409 10.029 2.000
410 10.029 0.000
411 13.279 34.300
412 13.279 34.000
413 13.279 33.000
414 13.279 32.000
415 13.279 31.000
416 13.279 30.000
417 13.279 29.000
418 13.279 28.000
419 13.279 27.000
420 13.279 26.000
421 13.279 25.000
422 13.279 24.000
423 13.279 23.000
424 13.279 22.000
425 13.279 21.000
426 13.279 20.000
427 13.279 19.000
428 13.279 18.000
429 13.279 17.000
430 13.279 16.000
431 13.279 15.750
432 13.279 15.500
433 13.279 15.250
434 13.279 14.975
435 13.279 14.750
436 13.279 14.500
437 13.279 14.250
438 13.279 14.000
439 13.279 13.250
440 13.279 12.000
441 13.279 10.250
442 13.279 8.000
443 13.279 5.250
444 13.279 2.000
445 13.279 0.000
446 17.029 34.300
447 17.029 34.000
448 17.029 33.000
449 17.029 32.000
450 17.029 31.000
451 17.029 30.000
452 17.029 29.000
453 17.029 28.000
454 17.029 27.000
455 17.029 26.000
456 17.029 25.000
457 17.029 24.000
458 17.029 23.000
459 17.029 22.000
460 17.029 21.000
461 17.029 20.000
462 17.029 19.000
463 17.029 18.000
464 17.029 17.000
465 17.029 16.000
466 17.029 15.750
467 17.029 15.500
468 17.029 15.250
469 17.029 14.975
470 17.029 14.750
471 17.029 14.500
472 17.029 14.250
473 17.029 14.000
474 17.029 13.250
475 17.029 12.000
476 17.029 10.250
477 17.029 8.000
478 17.029 5.250
479 17.029 2.000
480 17.029 0.000
481 20.279 34.300
482 20.279 34.000
483 20.279 33.000
484 20.279 32.000
485 20.279 31.000
486 20.279 30.000
487 20.279 29.000
488 20.279 28.000
489 20.279 27.000
490 20.279 26.000
491 20.279 25.000
492 20.279 24.000
493 20.279 23.000
494 20.279 22.000
495 20.279 21.000
496 20.279 20.000
497 20.279 19.000
498 20.279 18.000
499 20.279 17.000
500 20.279 16.000
501 20.279 15.750
502 20.279 15.500
503 20.279 15.250
504 20.279 14.975
505 20.279 14.750
506 20.279 14.500
507 20.279 14.250
508 20.279 14.000
509 20.279 13.250
510 20.279 12.000
511 20.279 10.250
512 20.279 8.000
513 20.279 5.250
514 20.279 2.000
515 20.279 0.000
0
1 4 3 1 2 38 37
2 4 3 2 3 39 38
3 4 3 3 4 40 39
4 4 3 4 5 41 40
5 4 3 5 6 42 41
6 4 3 6 7 43 42
7 4 3 7 8 44 43
8 4 3 8 9 45 44
9 4 3 9 10 46 45
10 4 3 10 11 47 46
11 4 3 11 12 48 47
12 4 3 12 13 49 48
13 4 3 13 14 50 49
14 4 3 14 15 51 50
15 4 3 15 16 52 51
16 4 3 16 17 53 52
17 4 3 17 18 54 53
18 4 3 18 19 55 54
19 4 3 19 20 56 55
20 4 3 20 21 57 56
21 4 3 21 22 58 57
22 4 3 22 23 59 58
23 4 3 23 24 60 59
24 13 5 25 84 60 24
25 5 2 25 26 85 84
26 5 2 26 27 86 85
```

Appendix B

Input file of geometry specificatin of Pile A

```
27 5 2 27 28 87 86
28 5 2 28 29 88 87
29 5 2 29 30 89 88
30 5 2 30 31 90 89
31 5 2 31 32 91 90
32 5 2 32 33 92 91
33 5 2 33 34 93 92
34 5 2 34 35 94 93
35 5 2 35 36 95 94
36 13 4 37 38 62 61
37 13 4 38 39 63 62
38 13 4 39 40 64 63
39 13 4 40 41 65 64
40 13 4 41 42 66 65
41 13 4 42 43 67 66
42 13 4 43 44 68 67
43 13 4 44 45 69 68
44 13 4 45 46 70 69
45 13 5 46 47 71 70
46 13 5 47 48 72 71
47 13 5 48 49 73 72
48 13 5 49 50 74 73
49 13 5 50 51 75 74
50 13 5 51 52 76 75
51 13 5 52 53 77 76
52 13 5 53 54 78 77
53 13 5 54 55 79 78
54 13 5 55 56 80 79
55 13 5 56 57 81 80
56 13 5 57 58 82 81
57 13 5 58 59 83 82
58 13 5 59 60 84 83
59 5 6 61 62 97 96
60 5 6 62 63 98 97
61 5 6 63 64 99 98
62 5 6 64 65 100 99
63 5 1 65 66 101 100
64 5 1 66 67 102 101
65 5 1 67 68 103 102
66 5 1 68 69 104 103
67 5 1 69 70 105 104
68 5 2 70 71 106 105
69 5 2 71 72 107 106
70 5 2 72 73 108 107
71 5 2 73 74 109 108
72 5 2 74 75 110 109
73 5 2 75 76 111 110
74 5 2 76 77 112 111
75 5 2 77 78 113 112
76 5 2 78 79 114 113
77 5 2 79 80 115 114
78 5 2 80 81 116 115
79 5 2 81 82 117 116
80 5 2 82 83 118 117
81 5 2 83 84 119 118
82 5 2 84 85 120 119
83 5 2 85 86 121 120
84 5 2 86 87 122 121
85 5 2 87 88 123 122
86 5 2 88 89 124 123
87 5 2 89 90 125 124
88 5 2 90 91 126 125
89 5 2 91 92 127 126
90 5 2 92 93 128 127
91 5 2 93 94 129 128
92 5 2 94 95 130 129
93 5 6 96 97 132 131
94 5 6 97 98 133 132
95 5 6 98 99 134 133
96 5 6 99 100 135 134
97 5 1 100 101 136 135
98 5 1 101 102 137 136
99 5 1 102 103 138 137
100 5 1 103 104 139 138
101 5 1 104 105 140 139
102 5 2 105 106 141 140
103 5 2 106 107 142 141
104 5 2 107 108 143 142
105 5 2 108 109 144 143
106 5 2 109 110 145 144
107 5 2 110 111 146 145
108 5 2 111 112 147 146
109 5 2 112 113 148 147
110 5 2 113 114 149 148
111 5 2 114 115 150 149
112 5 2 115 116 151 150
113 5 2 116 117 152 151
114 5 2 117 118 153 152
115 5 2 118 119 154 153
116 5 2 119 120 155 154
117 5 2 120 121 156 155
118 5 2 121 122 157 156
119 5 2 122 123 158 157
120 5 2 123 124 159 158
121 5 2 124 125 160 159
122 5 2 125 126 161 160
123 5 2 126 127 162 161
124 5 2 127 128 163 162
125 5 2 128 129 164 163
126 5 2 129 130 165 164
127 5 6 131 132 167 166
128 5 6 132 133 168 167
129 5 6 133 134 169 168
130 5 6 134 135 170 169
131 5 1 135 136 171 170
132 5 1 136 137 172 171
133 5 1 137 138 173 172
134 5 1 138 139 174 173
135 5 1 139 140 175 174
136 5 2 140 141 176 175
137 5 2 141 142 177 176
138 5 2 142 143 178 177
139 5 2 143 144 179 178
140 5 2 144 145 180 179
141 5 2 145 146 181 180
142 5 2 146 147 182 181
143 5 2 147 148 183 182
144 5 2 148 149 184 183
145 5 2 149 150 185 184
146 5 2 150 151 186 185
147 5 2 151 152 187 186
148 5 2 152 153 188 187
149 5 2 153 154 189 188
150 5 2 154 155 190 189
151 5 2 155 156 191 190
152 5 2 156 157 192 191
153 5 2 157 158 193 192
154 5 2 158 159 194 193
155 5 2 159 160 195 194
156 5 2 160 161 196 195
157 5 2 161 162 197 196
158 5 2 162 163 198 197
159 5 2 163 164 199 198
160 5 2 164 165 200 199
161 5 6 166 167 202 201
162 5 6 167 168 203 202
163 5 6 168 169 204 203
164 5 6 169 170 205 204
165 5 1 170 171 206 205
166 5 1 171 172 207 206
167 5 1 172 173 208 207
168 5 1 173 174 209 208
169 5 1 174 175 210 209
170 5 2 175 176 211 210
171 5 2 176 177 212 211
172 5 2 177 178 213 212
173 5 2 178 179 214 213
174 5 2 179 180 215 214
175 5 2 180 181 216 215
176 5 2 181 182 217 216
177 5 2 182 183 218 217
178 5 2 183 184 219 218
179 5 2 184 185 220 219
180 5 2 185 186 221 220
181 5 2 186 187 222 221
182 5 2 187 188 223 222
183 5 2 188 189 224 223
184 5 2 189 190 225 224
185 5 2 190 191 226 225
186 5 2 191 192 227 226
187 5 2 192 193 228 227
188 5 2 193 194 229 228
189 5 2 194 195 230 229
190 5 2 195 196 231 230
191 5 2 196 197 232 231
192 5 2 197 198 233 232
193 5 2 198 199 234 233
194 5 2 199 200 235 234
195 5 6 201 202 237 236
196 5 6 202 203 238 237
197 5 6 203 204 239 238
198 5 6 204 205 240 239
199 5 1 205 206 241 240
200 5 1 206 207 242 241
201 5 1 207 208 243 242
202 5 1 208 209 244 243
203 5 1 209 210 245 244
204 5 2 210 211 246 245
205 5 2 211 212 247 246
206 5 2 212 213 248 247
207 5 2 213 214 249 248
208 5 2 214 215 250 249
209 5 2 215 216 251 250
210 5 2 216 217 252 251
211 5 2 217 218 253 252
212 5 2 218 219 254 253
213 5 2 219 220 255 254
214 5 2 220 221 256 255
215 5 2 221 222 257 256
216 5 2 222 223 258 257
217 5 2 223 224 259 258
218 5 2 224 225 260 259
219 5 2 225 226 261 260
220 5 2 226 227 262 261
221 5 2 227 228 263 262
222 5 2 228 229 264 263
223 5 2 229 230 265 264
224 5 2 230 231 266 265
225 5 2 231 232 267 266
226 5 2 232 233 268 267
227 5 2 233 234 269 268
228 5 2 234 235 270 269
229 5 6 236 237 272 271
230 5 6 237 238 273 272
231 5 6 238 239 274 273
232 5 6 239 240 275 274
233 5 1 240 241 276 275
234 5 1 241 242 277 276
235 5 1 242 243 278 277
236 5 1 243 244 279 278
237 5 1 244 245 280 279
238 5 2 245 246 281 280
239 5 2 246 247 282 281
240 5 2 247 248 283 282
241 5 2 248 249 284 283
242 5 2 249 250 285 284
243 5 2 250 251 286 285
244 5 2 251 252 287 286
245 5 2 252 253 288 287
246 5 2 253 254 289 288
247 5 2 254 255 290 289
248 5 2 255 256 291 290
249 5 2 256 257 292 291
250 5 2 257 258 293 292
251 5 2 258 259 294 293
252 5 2 259 260 295 294
253 5 2 260 261 296 295
254 5 2 261 262 297 296
255 5 2 262 263 298 297
256 5 2 263 264 299 298
257 5 2 264 265 300 299
258 5 2 265 266 301 300
259 5 2 266 267 302 301
260 5 2 267 268 303 302
261 5 2 268 269 304 303
262 5 2 269 270 305 304
263 5 6 271 272 307 306
264 5 6 272 273 308 307
265 5 6 273 274 309 308
266 5 6 274 275 310 309
267 5 1 275 276 311 310
268 5 1 276 277 312 311
269 5 1 277 278 313 312
270 5 1 278 279 314 313
271 5 1 279 280 315 314
272 5 2 280 281 316 315
273 5 2 281 282 317 316
274 5 2 282 283 318 317
275 5 2 283 284 319 318
276 5 2 284 285 320 319
277 5 2 285 286 321 320
278 5 2 286 287 322 321
279 5 2 287 288 323 322
280 5 2 288 289 324 323
281 5 2 289 290 325 324
282 5 2 290 291 326 325
283 5 2 291 292 327 326
284 5 2 292 293 328 327
285 5 2 293 294 329 328
286 5 2 294 295 330 329
287 5 2 295 296 331 330
288 5 2 296 297 332 331
289 5 2 297 298 333 332
290 5 2 298 299 334 333
291 5 2 299 300 335 334
292 5 2 300 301 336 335
293 5 2 301 302 337 336
294 5 2 302 303 338 337
295 5 2 303 304 339 338
296 5 2 304 305 340 339
297 5 6 306 307 342 341
298 5 6 307 308 343 342
299 5 6 308 309 344 343
300 5 6 309 310 345 344
301 5 1 310 311 346 345
302 5 1 311 312 347 346
303 5 1 312 313 348 347
304 5 1 313 314 349 348
305 5 1 314 315 350 349
306 5 2 315 316 351 350
307 5 2 316 317 352 351
308 5 2 317 318 353 352
309 5 2 318 319 354 353
310 5 2 319 320 355 354
```

Appendix B

Input file of geometry specificatin of Pile A

```
311 5 2 320 321 356 355
312 5 2 321 322 357 356
313 5 2 322 323 358 357
314 5 2 323 324 359 358
315 5 2 324 325 360 359
316 5 2 325 326 361 360
317 5 2 326 327 362 361
318 5 2 327 328 363 362
319 5 2 328 329 364 363
320 5 2 329 330 365 364
321 5 2 330 331 366 365
322 5 2 331 332 367 366
323 5 2 332 333 368 367
324 5 2 333 334 369 368
325 5 2 334 335 370 369
326 5 2 335 336 371 370
327 5 2 336 337 372 371
328 5 2 337 338 373 372
329 5 2 338 339 374 373
330 5 2 339 340 375 374
331 5 6 341 342 377 376
332 5 6 342 343 378 377
333 5 6 343 344 379 378
334 5 6 344 345 380 379
335 5 1 345 346 381 380
336 5 1 346 347 382 381
337 5 1 347 348 383 382
338 5 1 348 349 384 383
339 5 1 349 350 385 384
340 5 2 350 351 386 385
341 5 2 351 352 387 386
342 5 2 352 353 388 387
343 5 2 353 354 389 388
344 5 2 354 355 390 389
345 5 2 355 356 391 390
346 5 2 356 357 392 391
347 5 2 357 358 393 392
348 5 2 358 359 394 393
349 5 2 359 360 395 394
350 5 2 360 361 396 395
351 5 2 361 362 397 396
352 5 2 362 363 398 397
353 5 2 363 364 399 398
354 5 2 364 365 400 399
355 5 2 365 366 401 400
356 5 2 366 367 402 401
357 5 2 367 368 403 402
358 5 2 368 369 404 403
359 5 2 369 370 405 404
360 5 2 370 371 406 405
361 5 2 371 372 407 406
362 5 2 372 373 408 407
363 5 2 373 374 409 408
364 5 2 374 375 410 409
365 5 6 376 377 412 411
366 5 6 377 378 413 412
367 5 6 378 379 414 413
368 5 6 379 380 415 414
369 5 1 380 381 416 415
370 5 1 381 382 417 416
371 5 1 382 383 418 417
372 5 1 383 384 419 418
373 5 1 384 385 420 419
374 5 2 385 386 421 420
375 5 2 386 387 422 421
376 5 2 387 388 423 422
377 5 2 388 389 424 423
378 5 2 389 390 425 424
379 5 2 390 391 426 425
380 5 2 391 392 427 426
381 5 2 392 393 428 427
382 5 2 393 394 429 428
383 5 2 394 395 430 429
384 5 2 395 396 431 430
385 5 2 396 397 432 431
386 5 2 397 398 433 432
387 5 2 398 399 434 433
388 5 2 399 400 435 434
389 5 2 400 401 436 435
390 5 2 401 402 437 436
391 5 2 402 403 438 437
392 5 2 403 404 439 438
393 5 2 404 405 440 439
394 5 2 405 406 441 440
395 5 2 406 407 442 441
396 5 2 407 408 443 442
397 5 2 408 409 444 443
398 5 2 409 410 445 444
399 5 6 411 412 447 446
400 5 6 412 413 448 447
401 5 6 413 414 449 448
402 5 6 414 415 450 449
403 5 1 415 416 451 450
404 5 1 416 417 452 451
405 5 1 417 418 453 452
406 5 1 418 419 454 453
407 5 1 419 420 455 454
408 5 2 420 421 456 455
409 5 2 421 422 457 456
410 5 2 422 423 458 457
411 5 2 423 424 459 458
412 5 2 424 425 460 459
413 5 2 425 426 461 460
414 5 2 426 427 462 461
415 5 2 427 428 463 462
416 5 2 428 429 464 463
417 5 2 429 430 465 464
418 5 2 430 431 466 465
419 5 2 431 432 467 466
420 5 2 432 433 468 467
421 5 2 433 434 469 468
422 5 2 434 435 470 469
423 5 2 435 436 471 470
424 5 2 436 437 472 471
425 5 2 437 438 473 472
426 5 2 438 439 474 473
427 5 2 439 440 475 474
428 5 2 440 441 476 475
429 5 2 441 442 477 476
430 5 2 442 443 478 477
431 5 2 443 444 479 478
432 5 2 444 445 480 479
433 5 6 446 447 482 481
434 5 6 447 448 483 482
435 5 6 448 449 484 483
436 5 6 449 450 485 484
437 5 1 450 451 486 485
438 5 1 451 452 487 486
439 5 1 452 453 488 487
440 5 1 453 454 489 488
441 5 1 454 455 490 489
442 5 2 455 456 491 490
443 5 2 456 457 492 491
444 5 2 457 458 493 492
445 5 2 458 459 494 493
446 5 2 459 460 495 494
447 5 2 460 461 496 495
448 5 2 461 462 497 496
449 5 2 462 463 498 497
450 5 2 463 464 499 498
451 5 2 464 465 500 499
452 5 2 465 466 501 500
453 5 2 466 467 502 501
454 5 2 467 468 503 502
455 5 2 468 469 504 503
456 5 2 469 470 505 504
457 5 2 470 471 506 505
458 5 2 471 472 507 506
459 5 2 472 473 508 507
460 5 2 473 474 509 508
461 5 2 474 475 510 509
462 5 2 475 476 511 510
463 5 2 476 477 512 511
464 5 2 477 478 513 512
465 5 2 478 479 514 513
466 5 2 479 480 515 514
```

Appendix B

Input file of main portion for Pile A

```
Pile A
999
1 6 33 1 157 0 0 1 0
0 0 0 1 100 0 0 1 466
3
1 3 8
1 3 0.01875 0.075 0.81 0.898 0.25 0 10.0 19 8.E-10 5.3E-10 0 0
2 5 50.0E3 0.25 00.0 31.0 28.3 4 10.0 19.5 5.E-4 3.3E-4 2000.0 0.0
3 1 30.0E6 30.0E6 0.2 0.2 12.5E6 0 10.0 23.5 0 0 0 0
4 8 5.0 23.0 23.35E4 1.0135E4 10.0 .025 0 0.0 0 0 0 0
5 8 0.0 31.0 54.9E4 2.1E4 10.0 .025 0 0.0 0 0 0 0
6 3 0.01875 0.075 0.81 0.898 0.25 0 10.0 13.5 8.E-10 5.3E-10 0 0
1 4
1 34.3 0.0 0.0 0.0 0.0 0.0 0.0 0.0
2 31 27.14293 44.55 27.14293 0.0 0.0 0.0 44.35
3 26 54.56003 89.55 54.56003 0.0 50 0.0 89.145
4 0.0 163.215 336.55 163.215 0.0 310 0.0 0.0
0 82 1
1 1 2 1 1 0.0 0.0 0.0
2 2 3 1 1 0.0 0.0 0.0
3 3 4 1 1 0.0 0.0 0.0
4 4 5 1 1 0.0 0.0 0.0
5 5 6 1 1 0.0 0.0 0.0
6 6 7 1 1 0.0 0.0 0.0
7 7 8 1 1 0.0 0.0 0.0
8 8 9 1 1 0.0 0.0 0.0
9 9 10 1 1 0.0 0.0 0.0
10 10 11 1 1 0.0 0.0 0.0
11 11 12 1 1 0.0 0.0 0.0
12 12 13 1 1 0.0 0.0 0.0
13 13 14 1 1 0.0 0.0 0.0
14 14 15 1 1 0.0 0.0 0.0
15 15 16 1 1 0.0 0.0 0.0
16 16 17 1 1 0.0 0.0 0.0
17 17 18 1 1 0.0 0.0 0.0
18 18 19 1 1 0.0 0.0 0.0
19 19 20 1 1 0.0 0.0 0.0
20 20 21 1 1 0.0 0.0 0.0
21 21 22 1 1 0.0 0.0 0.0
22 22 23 1 1 0.0 0.0 0.0
23 23 24 1 1 0.0 0.0 0.0
24 24 25 1 1 0.0 0.0 0.0
25 25 26 1 1 0.0 0.0 0.0
26 26 27 1 1 0.0 0.0 0.0
27 27 28 1 1 0.0 0.0 0.0
28 28 29 1 1 0.0 0.0 0.0
29 29 30 1 1 0.0 0.0 0.0
30 30 31 1 1 0.0 0.0 0.0
31 31 32 1 1 0.0 0.0 0.0
32 32 33 1 1 0.0 0.0 0.0
33 33 34 1 1 0.0 0.0 0.0
```

Appendix B

Input file of main portion for Pile A

```
34 34 35 1 1 0.0 0.0 0.0
35 35 36 1 1 0.0 0.0 0.0
35 36 95 2 1 0.0 0.0 0.0
92 95 130 2 1 0.0 0.0 0.0
126 130 165 2 1 0.0 0.0 0.0
160 165 200 2 1 0.0 0.0 0.0
194 200 235 2 1 0.0 0.0 0.0
228 235 270 2 1 0.0 0.0 0.0
262 270 305 2 1 0.0 0.0 0.0
296 305 340 2 1 0.0 0.0 0.0
330 340 375 2 1 0.0 0.0 0.0
364 375 410 2 1 0.0 0.0 0.0
398 410 445 2 1 0.0 0.0 0.0
432 445 480 2 1 0.0 0.0 0.0
466 480 515 2 1 0.0 0.0 0.0
466 515 514 1 1 0.0 0.0 0.0
465 514 513 1 1 0.0 0.0 0.0
464 513 512 1 1 0.0 0.0 0.0
463 512 511 1 1 0.0 0.0 0.0
462 511 510 1 1 0.0 0.0 0.0
461 510 509 1 1 0.0 0.0 0.0
460 509 508 1 1 0.0 0.0 0.0
459 508 507 1 1 0.0 0.0 0.0
458 507 506 1 1 0.0 0.0 0.0
457 506 505 1 1 0.0 0.0 0.0
456 505 504 1 1 0.0 0.0 0.0
455 504 503 1 1 0.0 0.0 0.0
454 503 502 1 1 0.0 0.0 0.0
453 502 501 1 1 0.0 0.0 0.0
452 501 500 1 1 0.0 0.0 0.0
451 500 499 1 1 0.0 0.0 0.0
450 499 498 1 1 0.0 0.0 0.0
449 498 497 1 1 0.0 0.0 0.0
448 497 496 1 1 0.0 0.0 0.0
447 496 495 1 1 0.0 0.0 0.0
446 495 494 1 1 0.0 0.0 0.0
445 494 493 1 1 0.0 0.0 0.0
444 493 492 1 1 0.0 0.0 0.0
443 492 491 1 1 0.0 0.0 0.0
442 491 490 1 1 0.0 0.0 0.0
441 490 489 1 1 0.0 0.0 0.0
440 489 488 1 1 0.0 0.0 0.0
439 488 487 1 1 0.0 0.0 0.0
438 487 486 1 1 0.0 0.0 0.0
437 486 485 1 1 0.0 0.0 0.0
436 485 484 1 1 0.0 0.0 0.0
435 484 483 1 1 0.0 0.0 0.0
434 483 482 1 1 0.0 0.0 0.0
433 482 481 1 1 0.0 0.0 0.0
1 1 2 0 -1 0 0 0 00011 0 2.0 0 0.
1 1 37 0.0 690.20 0.0 690.20 0.0 690.20
```

Appendix B

Input file of main portion for Pile A

```
2 3 7 0 0 0 14 0 00011 0 7200. 1 0.
600. 600. 1200. 1800. 3000.
1 1 37 3 2 0.0 0.0 0.0
36 37 61 3 2 0.0 0.0 0.0
59 61 96 3 2 0.0 0.0 0.0
93 96 131 3 2 0.0 0.0 0.0
127 131 166 3 2 0.0 0.0 0.0
161 166 201 3 2 0.0 0.0 0.0
195 201 236 3 2 0.0 0.0 0.0
229 236 271 3 2 0.0 0.0 0.0
263 271 306 3 2 0.0 0.0 0.0
297 306 341 3 2 0.0 0.0 0.0
331 341 376 3 2 0.0 0.0 0.0
365 376 411 3 2 0.0 0.0 0.0
399 411 446 3 2 0.0 0.0 0.0
433 446 481 3 2 0.0 0.0 0.0
3 8 9 0 -1 0 0 0 00011 0 2.0 0 0.
1 1 37 0.0 690.20 0.0 690.20 0.0 690.20
4 10 14 0 0 0 0 0 00011 0 7200. 1 0.
600. 600. 1200. 1800. 3000.
5 15 16 0 -1 0 0 0 00011 0 2.0 0 0.
1 1 37 0.0 690.20 0.0 690.20 0.0 690.20
6 17 21 0 0 0 0 0 00011 0 7200. 1 0.
600. 600. 1200. 1800. 3000.
7 22 23 0 -1 0 0 0 00011 0 2.0 0 0.
1 1 37 0.0 690.20 0.0 690.20 0.0 690.20
8 24 28 0 0 0 0 0 00011 0 7200. 1 0.
600. 600. 1200. 1800. 3000.
9 29 30 0 -1 0 0 0 00011 0 2.0 0 0.
1 1 37 0.0 690.20 0.0 690.20 0.0 690.20
10 31 35 0 0 0 0 0 00011 0 7200. 1 0.
600. 600. 1200. 1800. 3000.
11 36 37 0 -1 0 0 0 00011 0 2.0 0 0.
1 1 37 0.0 690.20 0.0 690.20 0.0 690.20
12 38 42 0 0 0 0 0 00011 0 7200. 1 0.
600. 600. 1200. 1800. 3000.
13 43 44 0 -1 0 0 0 00011 0 2.0 0 0.
1 1 37 0.0 690.20 0.0 690.20 0.0 690.20
14 45 49 0 0 0 0 0 00011 0 7200. 1 0.
600. 600. 1200. 1800. 3000.
15 50 51 0 -1 0 0 0 00011 0 2.0 0 0.
1 1 37 0.0 690.20 0.0 690.20 0.0 690.20
16 52 56 0 0 0 0 0 00011 0 7200. 1 0.
600. 600. 1200. 1800. 3000.
17 57 58 0 -1 0 0 0 00011 0 2.0 0 0.
1 1 37 0.0 690.20 0.0 690.20 0.0 690.20
18 59 63 0 0 0 0 0 00011 0 7200. 1 0.
600. 600. 1200. 1800. 3000.
19 64 65 0 -1 0 0 0 00011 0 2.0 0 0.
1 1 37 0.0 690.20 0.0 690.20 0.0 690.20
20 66 70 0 0 0 0 0 00011 0 7200. 1 0.
```

Appendix B

Input file of main portion for Pile A

```
600. 600. 1200. 1800. 3000.
21 71 72 0 -1 0 0 0 00011 0 2.0 0 0.
1 1 37 0.0 690.20 0.0 690.20 0.0 690.20
22 73 77 0 0 0 0 0 00011 0 7200. 1 0.
600. 600. 1200. 1800. 3000.
23 78 87 0 -1 0 0 0 00011 0 2.0 0 0.
1 1 37 0.0 690.20 0.0 690.20 0.0 690.20
24 88 92 0 0 0 0 0 00011 0 7200. 1 0.
600. 600. 1200. 1800. 3000.
25 93 102 0 -1 0 0 0 00011 0 2.0 0 0.
1 1 37 0.0 690.20 0.0 690.20 0.0 690.20
26 103 107 0 0 0 0 0 00011 0 7200. 1 0.
600. 600. 1200. 1800. 3000.
27 108 117 0 -1 0 0 0 00011 0 2.0 0 0.
1 1 37 0.0 690.20 0.0 690.20 0.0 690.20
28 118 122 0 0 0 0 0 00011 0 7200. 1 0.
600. 600. 1200. 1800. 3000.
29 123 132 0 -1 0 0 0 00011 0 2.0 0 0.
1 1 37 0.0 345.10 0.0 345.10 0.0 345.10
30 133 137 0 0 0 0 0 00011 0 7200. 1 0.
600. 600. 1200. 1800. 3000.
31 138 147 0 0 0 0 0 00011 0 36000. 0 0.
32 148 153 0 0 0 0 0 00011 0 43200. 0 0.
33 154 157 0 0 0 0 0 00011 0 57600. 0 0.
```

Appendix C

Calculation of ultimate load carrying capacity of axially loaded single pile

The soil characteristics of example 3 of chapter 6 has been considered as the pile-soil problem here. The necessary parameters and the soil profile is presented below.

$\phi_c = 23^0$; $\gamma_c = 19$ kN/m^3 ; DCL = 5.25 m; $\phi_s = 35^0$; $\gamma_s = 19.5$ kN/m^3;
H = 15.25 m; D = 0.46 m

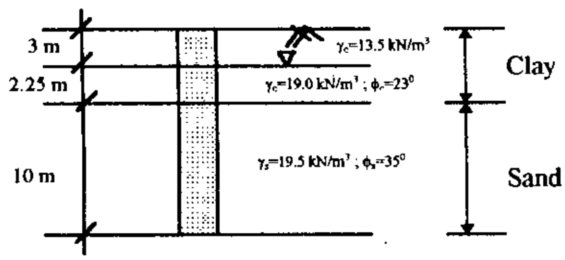

Fig. C_1

For clay, the shaft resistance is calculated using Eq. 5.2.

Here, Burland (1973) equation has been used to obtain K_h (K_h=1-sinϕ).

$$\text{Now,}\quad P_{su} = \int_0^H C_p\left(C_a + \sigma_v K_h \tan\phi_a\right)dz$$

$$= (2\pi \times 0.23)[\ (5+40.5 \times 0.2586)/2 \times 3 + (5 +(40.5+60.75)/2 \times 0.2586) \times 2.25]$$

$$= 103 \text{ kN}$$

Now, the critical depth Z_c for sand layer (from Fig. 5.2, Vesic, 1967) has been found to be equal to 2.75 m. Besides, K_h tanϕ' value of sand has been obtained from Fig. 5.1(b).

$$\text{Now,}\quad P_{su}\ (\text{sand}) = (2\pi \times 0.23)[\ (60.75+86.875)/2 \times 0.2 \times 2.75 + 86.875 \times 0.2 \times 7.25]$$

$$= 241 \text{ kN}$$

The base capacity of pile has been obtained using Eq. 5.9 and Fig. 5.5 (Meyerhof, 1976)

$$P_{bu} = A_b \sigma'_{vb} N_q \quad \le A_b \left(50 N_q\right) \tan\phi$$

$$= \pi \, (0.23)^2 \times 50 \;\; \times 130 \;\; \times \tan 35^0$$

$$= 756 \text{ kN}$$

Thus, Total $P = {}_{Psu}(\text{clay}) + {}_{Psu}(\text{sand}) + P_{bu}(\text{sand}) = 1100$ kN

Appendix D
Input file of the geometry specification of sqare footing

```
FOOTING
999
194 167 4 4 2 5
0 0
1 1 1 1 1 1 1 0 0 0
0 0 0 0
1 0.000 9.450
2 0.000 9.013
3 0.000 8.575
4 0.000 8.138
5 0.000 7.700
6 0.000 7.450
7 0.000 7.200
8 0.000 7.175
9 0.000 7.000
10 0.000 6.600
11 0.000 6.000
12 0.000 5.200
13 0.000 4.200
14 0.000 3.000
15 0.000 1.600
16 0.000 0.000
17 0.250 9.450
18 0.250 9.013
19 0.250 8.575
20 0.250 8.138
21 0.250 7.700
22 0.250 7.450
23 0.250 7.200
24 0.250 7.175
25 0.250 7.000
26 0.250 6.600
27 0.250 6.000
28 0.250 5.200
29 0.250 4.200
30 0.250 3.000
31 0.250 1.600
32 0.250 0.000
33 0.275 9.450
34 0.275 9.013
35 0.275 8.575
36 0.275 8.138
37 0.275 7.725
38 0.550 9.450
39 0.550 9.013
40 0.550 8.575
41 0.550 8.138
42 0.550 7.725
43 0.550 7.700
44 0.550 7.450
45 0.550 7.200
46 0.550 7.175
47 0.550 7.000
48 0.550 6.600
49 0.550 6.000
50 0.550 5.200
51 0.550 4.200
52 0.550 3.000
53 0.550 1.600
54 0.550 0.000
55 0.850 9.450
56 0.850 9.013
57 0.850 8.575
58 0.850 8.138
59 0.850 7.725
60 0.850 7.700
61 0.850 7.450
62 0.850 7.200
63 0.850 7.175
64 0.850 7.000
65 0.850 6.600
66 0.850 6.000
67 0.850 5.200
68 0.850 4.200
69 0.850 3.000
70 0.850 1.600
71 0.850 0.000
72 1.125 7.700
73 1.125 7.450
74 1.125 7.200
75 1.150 9.450
76 1.150 9.013
77 1.150 8.575
78 1.150 8.138
79 1.150 7.725
80 1.150 7.450
81 1.150 7.175
82 1.150 7.000
83 1.150 6.600
84 1.150 6.000
85 1.150 5.200
86 1.150 4.200
87 1.150 3.000
88 1.150 1.600
89 1.150 0.000
90 1.400 9.450
91 1.400 9.013
92 1.400 8.575
93 1.400 8.138
94 1.400 7.725
95 1.400 7.450
96 1.400 7.175
97 1.400 7.000
98 1.400 6.600
99 1.400 6.000
100 1.400 5.200
101 1.400 4.200
102 1.400 3.000
103 1.400 1.600
104 1.400 0.000
105 1.900 9.450
106 1.900 9.013
107 1.900 8.575
108 1.900 8.138
109 1.900 7.725
110 1.900 7.450
111 1.900 7.175
112 1.900 7.000
113 1.900 6.600
114 1.900 6.000
115 1.900 5.200
116 1.900 4.200
117 1.900 3.000
118 1.900 1.600
119 1.900 0.000
120 2.650 9.450
121 2.650 9.013
122 2.650 8.575
123 2.650 8.138
124 2.650 7.725
125 2.650 7.450
126 2.650 7.175
127 2.650 7.000
128 2.650 6.600
129 2.650 6.000
130 2.650 5.200
131 2.650 4.200
132 2.650 3.000
133 2.650 1.600
134 2.650 0.000
135 3.650 9.450
136 3.650 9.013
137 3.650 8.575
138 3.650 8.138
139 3.650 7.725
140 3.650 7.450
141 3.650 7.175
142 3.650 7.000
143 3.650 6.600
144 3.650 6.000
145 3.650 5.200
146 3.650 4.200
147 3.650 3.000
148 3.650 1.600
149 3.650 0.000
150 4.900 9.450
151 4.900 9.013
152 4.900 8.575
153 4.900 8.138
154 4.900 7.725
155 4.900 7.450
156 4.900 7.175
157 4.900 7.000
158 4.900 6.600
159 4.900 6.000
160 4.900 5.200
161 4.900 4.200
162 4.900 3.000
```

Appendix D

Input file of the geometry specification of sqare footing

```
163 4.900 1.600
164 4.900 0.000
165 6.400 9.450
166 6.400 9.013
167 6.400 8.575
168 6.400 8.138
169 6.400 7.725
170 6.400 7.450
171 6.400 7.175
172 6.400 7.000
173 6.400 6.600
174 6.400 6.000
175 6.400 5.200
176 6.400 4.200
177 6.400 3.000
178 6.400 1.600
179 6.400 0.000
180 8.150 9.450
181 8.150 9.013
182 8.150 8.575
183 8.150 8.138
184 8.150 7.725
185 8.150 7.450
186 8.150 7.175
187 8.150 7.000
188 8.150 6.600
189 8.150 6.000
190 8.150 5.200
191 8.150 4.200
192 8.150 3.000
193 8.150 1.600
194 8.150 0.000
0
1 4 2 1 2 18 17
2 4 2 2 3 19 18
3 4 2 3 4 20 19
4 4 2 4 5 21 20
5 4 2 5 6 22 21
6 4 2 6 7 23 22
7 13 3 8 24 23 7
8 4 1 8 9 25 24
9 4 1 9 10 26 25
10 4 1 10 11 27 26
11 4 6 11 12 28 27
12 4 6 12 13 29 28
13 4 6 13 14 30 29
14 4 6 14 15 31 30
15 4 5 15 16 32 31
16 13 4 17 18 34 33
17 13 4 18 19 35 34
18 13 4 19 20 36 35
19 13 4 20 21 37 36
20 4 1 33 34 39 38
21 4 1 34 35 40 39
22 4 1 35 36 41 40
23 4 1 36 37 42 41
24 13 3 21 43 42 37
25 4 2 21 22 44 43
26 4 2 22 23 45 44
27 13 3 24 46 45 23
28 4 1 24 25 47 46
29 4 1 25 26 48 47
30 4 1 26 27 49 48
31 4 6 27 28 50 49
32 4 6 28 29 51 50
33 4 6 29 30 52 51
34 4 6 30 31 53 52
35 4 5 31 32 54 53
36 4 1 38 39 56 55
37 4 1 39 40 57 56
38 4 1 40 41 58 57
39 4 1 41 42 59 58
40 13 3 43 60 59 42
41 4 2 43 44 61 60
42 4 2 44 45 62 61
43 13 3 46 63 62 45
44 4 1 46 47 64 63
45 4 1 47 48 65 64
46 4 1 48 49 66 65
47 4 6 49 50 67 66
48 4 6 50 51 68 67
49 4 6 51 52 69 68
50 4 6 52 53 70 69
51 4 5 53 54 71 70
52 4 1 55 56 76 75
53 4 1 56 57 77 76
54 4 1 57 58 78 77
55 4 1 58 59 79 78
56 13 3 60 72 79 59
57 4 2 60 61 73 72
58 13 3 72 73 80 79
59 4 2 61 62 74 73
60 13 3 63 81 74 62
61 13 3 73 74 81 80
62 4 1 63 64 82 81
63 4 1 64 65 83 82
64 4 1 65 66 84 83
65 4 6 66 67 85 84
66 4 6 67 68 86 85
67 4 6 68 69 87 86
68 4 6 69 70 88 87
69 4 5 70 71 89 88
70 4 1 75 76 91 90
71 4 1 76 77 92 91
72 4 1 77 78 93 92
73 4 1 78 79 94 93
74 4 1 79 80 95 94
75 4 1 80 81 96 95
76 4 1 81 82 97 96
77 4 1 82 83 98 97
78 4 1 83 84 99 98
79 4 6 84 85 100 99
80 4 6 85 86 101 100
81 4 6 86 87 102 101
82 4 6 87 88 103 102
83 4 5 88 89 104 103
84 4 1 90 91 106 105
85 4 1 91 92 107 106
86 4 1 92 93 108 107
87 4 1 93 94 109 108
88 4 1 94 95 110 109
89 4 1 95 96 111 110
90 4 1 96 97 112 111
91 4 1 97 98 113 112
92 4 1 98 99 114 113
93 4 6 99 100 115 114
94 4 6 100 101 116 115
95 4 6 101 102 117 116
96 4 6 102 103 118 117
97 4 5 103 104 119 118
98 4 1 105 106 121 120
99 4 1 106 107 122 121
100 4 1 107 108 123 122
101 4 1 108 109 124 123
102 4 1 109 110 125 124
103 4 1 110 111 126 125
104 4 1 111 112 127 126
105 4 1 112 113 128 127
106 4 1 113 114 129 128
107 4 6 114 115 130 129
108 4 6 115 116 131 130
109 4 6 116 117 132 131
110 4 6 117 118 133 132
111 4 5 118 119 134 133
112 4 1 120 121 136 135
113 4 1 121 122 137 136
114 4 1 122 123 138 137
115 4 1 123 124 139 138
116 4 1 124 125 140 139
117 4 1 125 126 141 140
118 4 1 126 127 142 141
119 4 1 127 128 143 142
120 4 1 128 129 144 143
121 4 6 129 130 145 144
122 4 6 130 131 146 145
123 4 6 131 132 147 146
124 4 6 132 133 148 147
125 4 5 133 134 149 148
126 4 1 135 136 151 150
127 4 1 136 137 152 151
128 4 1 137 138 153 152
129 4 1 138 139 154 153
130 4 1 139 140 155 154
131 4 1 140 141 156 155
132 4 1 141 142 157 156
133 4 1 142 143 158 157
134 4 1 143 144 159 158
135 4 6 144 145 160 159
```

Appendix D

Input file of the geometry specification of sqare footing

136	4	6	145	146	161	160
137	4	6	146	147	162	161
138	4	6	147	148	163	162
139	4	5	148	149	164	163
140	4	1	150	151	166	165
141	4	1	151	152	167	166
142	4	1	152	153	168	167
143	4	1	153	154	169	168
144	4	1	154	155	170	169
145	4	1	155	156	171	170
146	4	1	156	157	172	171
147	4	1	157	158	173	172
148	4	1	158	159	174	173
149	4	6	159	160	175	174
150	4	6	160	161	176	175
151	4	6	161	162	177	176
152	4	6	162	163	178	177
153	4	5	163	164	179	178
154	4	1	165	166	181	180
155	4	1	166	167	182	181
156	4	1	167	168	183	182
157	4	1	168	169	184	183
158	4	1	169	170	185	184
159	4	1	170	171	186	185
160	4	1	171	172	187	186
161	4	1	172	173	188	187
162	4	1	173	174	189	188
163	4	6	174	175	190	189
164	4	6	175	176	191	190
165	4	6	176	177	192	191
166	4	6	177	178	193	192
167	4	5	178	179	194	193

Appendix D
Input file of main part specification for footing

```
FOOTING21
 999
1 6 7 1 199 0 0 1 0
0 0 0 1 194 0 0 1 167
3
1 3 8
1 3 0.02125  0.085 1.08  .898  0.25 0 0 14.5  0 0 0 0
2 1 30.0E6 30.0E6 0.2 0.2 12.5E6 0 0 23.5 0 0 0 0
3 8 5.0 23.0  23.35E4  1.0135E4  10.0 .025  0  0.0 0 0 0 0
4 8 0.0 0.0  23.35E4  1.0135E4  10.0 .025  0  0.0 0 0 0 0
5 5 50.0E3 0.25 00.0 31.0  1.60  4 0  20.0  0 0 0.0 0.0
6 3 0.02125  0.085 1.08  .898  0.25 0 0 19.5  0 0 0 0
1 5
1  9.45  0.0  0.0  0.0 0.0 0.0 0.0  49.78
2  7.2  34.0  32.625  34.0 0.0  0.0  0.0  82.0
3  6.0  45.95  50.025  45.95 0.0  0.0  0.0  99.0
4  1.6  68.76  89.625  68.76 0.0  44.00  0.0  138.275
5  0.0  51.23  105.625  51.23 0.0  60.0  0.0  0.0
0  40  1
 1  1  2  1 1 0.0 0.0 0.0
 2  2  3  1 1 0.0 0.0 0.0
 3  3  4  1 1 0.0 0.0 0.0
 4  4  5  1 1 0.0 0.0 0.0
 5  5  6  1 1 0.0 0.0 0.0
 6  6  7  1 1 0.0 0.0 0.0
 7  7  8  1 1 0.0 0.0 0.0
 8  8  9  1 1 0.0 0.0 0.0
 9  9  10  1 1 0.0 0.0 0.0
 10  10  11  1 1 0.0 0.0 0.0
 11  11  12  1 1 0.0 0.0 0.0
 12  12  13  1 1 0.0 0.0 0.0
 13  13  14  1 1 0.0 0.0 0.0
 14  14  15  1 1 0.0 0.0 0.0
 15  15  16  1 1 0.0 0.0 0.0
 15  16  32  2 1 0.0 0.0 0.0
 35  32  54  2 1 0.0 0.0 0.0
 51  54  71  2 1 0.0 0.0 0.0
 69  71  89  2 1 0.0 0.0 0.0
 83  89  104  2 1 0.0 0.0 0.0
 97  104  119  2 1 0.0 0.0 0.0
 111  119  134  2 1 0.0 0.0 0.0
 125  134  149  2 1 0.0 0.0 0.0
 139  149  164  2 1 0.0 0.0 0.0
 153  164  179  2 1 0.0 0.0 0.0
 167  179  194  2 1 0.0 0.0 0.0
 167  194  193  1 1 0.0 0.0 0.0
 166  193  192  1 1 0.0 0.0 0.0
 165  192  191  1 1 0.0 0.0 0.0
 164  191  190  1 1 0.0 0.0 0.0
 163  190  189  1 1 0.0 0.0 0.0
```

Appendix D

Input file of main part specification for footing

```
162  189  188  1 1 0.0 0.0 0.0
161  188  187  1 1 0.0 0.0 0.0
160  187  186  1 1 0.0 0.0 0.0
159  186  185  1 1 0.0 0.0 0.0
158  185  184  1 1 0.0 0.0 0.0
157  184  183  1 1 0.0 0.0 0.0
156  183  182  1 1 0.0 0.0 0.0
155  182  181  1 1 0.0 0.0 0.0
154  181  180  1 1 0.0 0.0 0.0
1 1 1 0 -1 0 0 0  00011 0 0.0 0 0.
1 1  17  0.0  0.0  0.0  0.0  0.0  0.0
2 2 6 0 -1 0 0 0  00001 0 0.0 0 0.
1 1  17  0.0  153.  0.0  153.  0.0  153.
3 7 19 0 -1 0 0 0  00001 0 0.0 0 0.
1 1  17  0.0  1989.  0.0  1989.  0.0  1989.
4 20 39 0 -1 0 0 0  00001 0 0.0 0 0.
1 1  17  0.0  1020.  0.0  1020.  0.0  1020.
5 40 119 0 -1 0 0 0  00001 0 0.0 0 0.
1 1  17  0.0  2040.  0.0  2040.  0.0  2040.
6 120 198 0 -1 0 0 0  00001 0 0.0 0 0.
1 1  17  0.0  1007.25  0.0  1007.25  0.0  1007.25
7 199 199 0 -1 0 0 0  00011 0 0.0 0 0.
1 1  17  0.0  12.75  0.0  12.75  0.0  12.75
```